The Effects of Heat and Explosions on Forensic DNA Analyses

Thesis submitted for the degree of Doctor of Philosophy at the University of Leicester

by
Marwan El Khoury

Department of Genetics and Genome Biology

March 2019

UNIVERSITY OF LEICESTER

The Effects of Heat and Explosions on Forensic DNA Analyses

Marwan El Khoury

Abstract

This project explores the effects of high temperatures and explosions on DNA samples of forensic value. It aims to determine the conditions under which biomaterials may degrade in accidental disasters, crime involving fire, and bombings, and how degradation affects interpretation. The experiments were designed to reflect situations requiring victim and suspect identification, and so involved testing various human samples including blood and saliva stains. Some samples were heated under laboratory conditions, while others were attached to pipe bombs and detonated outdoors with the assistance of US Police bomb enforcement officers. A sensitive mitochondrial DNA multiplex system was devised, and successfully used to detect DNA degradation prior to more costly analyses. Capillary electrophoresis-based STR typing and Massively Parallel Sequencing were compared in terms of their performance on degraded DNA. Treatment at 180 °C for 30 minutes was required to induce the first signs of DNA degradation in dried blood and saliva stains, reflected by reduced post-PCR DNA detection or drop-out of longer amplicons. There were no interpretable DNA products when heat treatment increased to 200 °C. Similar degraded DNA effects were observed in 27% of stains placed on and within smokeless-powder-charged pipe bombs, but no sign of degradation was observed with the more energetic C4 explosive, probably because of the shorter duration of heat exposure.

DNA degradation poses challenges to the interpretation of retrieved genetic data. These challenges were investigated both in real profiles from heat-treated samples, and in simulated data. In addition, a real case of an unidentified male victim (the Blazing Car Murder 1931) was analysed. The combination of real and simulated data provided realistic scenarios, but also allowed control of parameters which affect evidential strength such as population size and diversity, through lowering of the likelihood ratio and increasing the number of random matches in a database.

Acknowledgements

This project was made possible through the collaboration between the University of Leicester, notably Prof. Lisa Smith, and the European Commission's seventh Framework Programme, Marie Curie Actions. I am first and foremost grateful for this opportunity of a lifetime, the training provided, and the resulting PhD-level research.

I would not have embarked on this dream project, had it not been for the trust of the interviewing team at the University of Leicester back in 2014 comprised of Dr. Jon Wetton, Prof. Mark Jobling, Dr. Celia May, Prof. Lisa Smith, and Prof. Robert Hillman.

To Dr. Jon Wetton, my primary supervisor and the major backbone of this project: thank you for elevating the level of this work by providing crucial advice, foreseeing challenges before they even arose, and exerting continuous scientific rigour and meticulousness.

Prof. Mark Jobling, our principal investigator, thank you for combining extreme scientific brilliance with a caring and understanding personality, as well as rare management skills.

Thank you both for seeing and encouraging me to explore my own capabilities, for your patience, and finally for helping to steer this boat (through calm and stormy waters) to the dock.

This dissertation is the proud conclusion of my work as part of the INTREPID Forensics team, of which I would like to thank every member for being such a cohesive and fun group of friends.

A special acknowledgement in this regard to the most precious neighbour Silke Jensen, and also to Alex Smyth, the transatlantic pioneer who facilitated collaboration with US law enforcement agencies. I take the opportunity to express my gratitude to Sgt. Brian Wangler, Dep. Sheriff Harvey Hildreth, Sgt. Ryan Ertman, Lt. Matthew White, their respective Police Forces, as well as the FBI.

My experience in the United States would not have been the same without my Secondment at Penn State University. Prof. Mitchell Holland's mentorship and inspiring leadership provided me with the magic potion to boost this project with challenging experiments and analyses. Thank you, Prof. Mitchell, for extending me every possible form of generosity, and for allowing me to see clearly why we love what we do. I take this chance to expand my gratitude to your welcoming and dedicated team: Dr. Charity Holland, Dr. Jennifer McElhoe, Elena Zavala, Jamie Gallimore, Emily Demchak, and Rachel Bonds.

Throughout these four years at the University of Leicester's Department of Genetics and Genome Biology, I was surrounded by good friends and devoted scientists.
All my appreciation to Dr. Chiara Batini, Dr. Pille Hallast, and all members of the G2 lab for creating the most welcoming atmosphere since my first day at work, for being available on and off-campus and for allowing me to discover different tastes and angles of the city of Leicester; Dr. Richard Badge and Prof. Mark Ryder for checking my work's progress at every milestone, for asking the right questions, and providing crucial advice; and finally Dr. Nicholas Eastley for helping me collect samples as a medical doctor and a certified phlebotomist.

Externally. I would like to thank Lorenzo Gaborini for inspiring me to use R after I saw his beautiful graphs at the Summer School of Criminal Justice in Switzerland, and for

accepting to share his knowledge. Dr. Ghassan Baliki, for your precious friendship, but also for having taken my R knowledge to another level, favouring basic understanding and sound methodology over fancy graphics.

To my Family, my core: thank you for the unconditional support system that you continuously provide through the ups and downs. A special mention my mother Gisèle who flew to the UK to stay by my side when I felt poorly; my father Dr. Elie and my sister Rana for being available in heart and mind.

To Olivia whom I married in the second year of this project. Thank you for accepting me in your life, for coming to Leicester, for accompanying me to Penn State, and for your contribution in making these four years undoubtedly the most important of my academic, professional, and personal life.

To Sasha.

Table of Contents

CHAPTER 1 INTRODUCTION **1**

1.1 THE PRINCIPLE OF EXCHANGE: "EVERY CONTACT LEAVES A TRACE" 1
1.2 THE PRINCIPLE OF INDIVIDUALITY: "EVERYTHING IS UNIQUE" 2
1.3 THE CRIME SCENE 5
1.3.1 Decay and transformation *6*
1.3.2 Contamination *7*
1.3.3 The collection procedure *8*
1.3.4 The laboratory *9*
1.4 HUMAN IDENTIFICATION 10
1.4.1 Identification through genetics *10*
1.4.2 Non-autosomal markers in forensic DNA analysis *14*
1.4.3 Low-template and degraded DNA *17*
1.4.4 Forensic implications and proposed solutions *23*
1.5 AIMS AND OBJECTIVES 31

CHAPTER 2 MATERIALS AND METHODS **33**

2.1 MATERIALS 33
2.1.1 Samples and Ethical Approvals *33*
2.1.2 Instruments and Apparatus *33*
2.1.3 Reagents and Enzymes *34*
2.1.4 Plasticware and Membranes *35*
2.1.5 Oligonucleotides *35*
2.1.6 Software *36*
2.2 METHODS 37
2.2.1 Sample Preparation and Collection *37*
2.2.2 DNA extraction *38*
2.2.3 Quantification of DNA samples *38*
2.2.4 Agarose gel electrophoresis *38*
2.2.5 Purifying PCR products for sequencing *39*
2.2.6 Sequencing reactions *39*
2.2.7 Y-STR typing *39*
2.2.8 Autosomal STR typing *40*
2.2.9 Mitochondrial DNA Multiplexes *40*
2.2.10 ForenSeq® MPS analysis *41*
2.2.11 Anti-Contamination Precautions *42*
2.2.12 Data Analysis *43*

CHAPTER 3 THE EFFECTS OF HIGH TEMPERATURE ON FORENSIC DNA ANALYSIS **44**

3.1 INTRODUCTION 44
3.1.1 The effects of "extremely" high temperatures on DNA *46*
3.1.2 Which heat treatment would be of interest? *49*
3.2 AIMS AND OBJECTIVES 51
3.3 MATERIALS AND METHODS 52
3.3.1 Sample Collection *52*
3.3.2 Recovery and DNA Extraction *53*
3.3.3 Quantification *54*
3.3.4 Degradation assessment *57*
3.3.5 Forensic Typing/Sequencing *57*
3.4 RESULTS 60
3.4.1 Quantification *60*
3.4.2 Degradation Assessment *62*
3.4.3 Typing Results - Biological Stains Temperature Treatments *64*
3.4.4 Massively Parallel Sequencing-Based Technique: Autosomal/Y-STRs and Identity SNPs *70*

3.5 Discussion 74
3.5.1 Methodology 74
3.5.2 Significance of results 76

CHAPTER 4 THE EFFECTS OF EXPLOSIONS ON FORENSIC DNA ANALYSIS 78

4.1 Introduction 78
4.2 Aims and Objectives 88
4.3 Materials and Methods 89
4.3.1 Introductory Briefing 89
4.3.2 Sample preparation and bomb assembly 89
4.3.3 Detonation and Collection of Items 92
4.3.4 Extraction 94
4.3.5 Real-Time PCR Quantification 94
4.3.6 DNA Typing/Sequencing 95
4.4 Results 95
4.4.1 Sample Recovery 95
4.4.2 Quantification Results 99
4.4.3 Degradation assessment 103
4.4.4 DNA Typing/Sequencing 106
4.5 Discussion 113
4.5.1 Experimental Design - Strengths and Limitations 113
4.5.2 Distinguishing Between Explosions and Accompanying Fires 116
4.5.3 Significance of Results 117
4.5.4 Improvements from First to Second Explosion Experiment 118
4.5.5 Difference in the effects of High and Low Explosives 120

CHAPTER 5 IMPLICATIONS OF DEGRADED DNA ON THE WEIGHT OF EVIDENCE 124

5.1 Introduction 124
5.2 Aims and Objectives 134
5.3 Materials and Methods 135
5.3.1 Autosomal STRs and SNPs - Interpretation 135
5.3.2 Haploid Markers 137
5.4 Results 145
5.4.1 Heat-Induced Dropouts 145
5.4.2 Simulated Dropouts 147
5.4.3 Mitochondrial - The Blazing Car Murder 154
5.5 Discussion 157
5.5.1 The Likelihood Ratio in Forensic Science 157
5.5.2 The Different Types of Markers 158

CHAPTER 6 DISCUSSION AND FUTURE DIRECTIONS 164

6.1 Sample Type Choice 166
6.1.1 Identification of Victims 166
6.1.2 Identification of Perpetrators 168
6.2 Explaining the Damage 169
6.3 Future Directions 173
6.3.1 Overcoming Real Casework Difficulties 173
6.3.2 Miscoding Lesions and DNA Repair 174

7 BIBLIOGRAPHY 177

Web Resources 192

8 APPENDIX 193

8.1 Implications of Heat Induced Dropouts 193
8.2 Electropherograms Examples 197

List of Figures

Figure 1.1 Identification and individualisation. 3
Figure 1.2 Intravariability and intervariability 4
Figure 1.3 Persistence of DNA at crime scenes. 7
Figure 1.4 Timeline of key developments in forensic genetics. 10
Figure 1.5 Capillary Electrophoresis. 13
Figure 1.6 Electropherogram, autosomal STR profile. 14
Figure 1.7 Electropherogram, Y-STR profile. 16
Figure 1.8 Post-mortem DNA damage. 20
Figure 1.9 Pipe bomb fragmentation. 23
Figure 1.10 PCR cycle number increase and associated risks in analysis of low-template DNA. 24
Figure 1.11 PCR replications of low-template DNA. 25
Figure 1.12 Stochastic Effects. 26
Figure 1.13 miniSTR multiplex kit. 28
Figure 1.14 Summary of the commonly used forensic DNA markers. 30
Figure 3.1 Grenfell tower fire incident. 48
Figure 3.2 INTREPID Forensics training on fire investigation- University of Leicester. 49
Figure 3.3 Amplification threshold (Ct) increasing with temperature treatment. 50
Figure 3.4 DNA concentration decreasing with temperature treatment. 51
Figure 3.5 Biological v. technical replicates. 56
Figure 3.6 Sensitivity of the mitochondrial DNA multiplex. 57
Figure 3.7 Sample concentrations (ng/µL) determined by Qubit® fluorometry. 61
Figure 3.8 DNA concentrations derived from the four stain groups at volume 30 µL. 62
Figure 3.9 The effects of temperature on autosomal STR typing. 66
Figure 3.10 The effects of temperature on Y-STR typing. 66
Figure 3.11 Electropherograms after autosomal and Y-STR typing. 67
Figure 3.12 The effect of temperature on smaller volumes - autosomal STRs. 69
Figure 3.13 The effect of temperature on smaller volumes - Y-STRs. 70
Figure 3.14 Depth of Coverage affected by temperature- autosomal STRs. 72
Figure 3.15 Depth of Coverage affected by temperature- Y-STRs. 72
Figure 3.16 Depth of Coverage affected by temperature- iSNPs. 73
Figure 3.17 4 °C v. 180 °C stains on the Universal Analysis Software (UAS). 73
Figure 4.1 Assassination with Vehicle-Bound Improvised Explosive Device (VB-IED). 78
Figure 4.2 Time to explosion and duration. 82
Figure 4.3 Explosive containers and energetic charges - statistics. 86
Figure 4.4 Bomb: weapon of choice in terrorism. 87
Figure 4.5 Preparing pipe bomb associated samples. 91
Figure 4.6 Pipes and their associated samples. 91
Figure 4.7 On-site preparation of a DBSP charged pipe bomb. 93
Figure 4.8 Placing the pipe bomb. 93
Figure 4.9 Bombs search and recovery areas- USA. 94
Figure 4.10 Post-blast recovered items associated with DBSP-pipe 1 (P1- brass). 96
Figure 4.11 Post-recovery items associated with DBSP-pipe 2 (P2- copper). 97
Figure 4.12 Post-recovery items associated with DBSP-pipe 3 (P3- brass). 97
Figure 4.13 Post-recovery items associated with C4-pipes four and five. 98
Figure 4.14 RT-PCR DNA concentrations after the explosions. 100
Figure 4.15 Significance testing between sample type and DNA concentration. 102
Figure 4.16 Divergence for normal distribution. 103
Figure 4.17 Degradation Indices- controls v. exploded stains. 104
Figure 4.18 mtDNA multiplex results applied to C4-exploded stains. 105
Figure 4.19 mtDNA multiplex results applied to DBSP-exploded stains. 105
Figure 4.20 Electropherogram- stain exploded with C4 pipe. 107
Figure 4.21 The effect of C4 explosions on CE-based STR typing. 108
Figure 4.22 Unexploded v. C4 exploded stains on the Universal Analysis Software (UAS). 108

Figure 4.23 The effects of C4 explosions on Massively Parallel Sequencing. 109
Figure 4.24 The effects of DBSP explosions on CE-based STR typing. 112
Figure 4.25 Electropherogram - partial Y profile from DBSP exploded stain. 113
Figure 4.26 Currently used Improvised Explosive Devices. 116
Figure 4.27 Vnukovo Airlines Flight 2801 crash. 117
Figure 4.28 Stepwise frames of DBSP explosion. 122
Figure 4.29 Stepwise frames of C4 explosion. 122
Figure 5.1 Y haplotype matching probability per number of meiosis. 132
Figure 5.2 Similarity matrix of Y haplotypes. 138
Figure 5.3 Similarity matrix (broader view)-. 139
Figure 5.4 Victim's FFPE prostate tissue-. 141
Figure 5.5 Victim's partial NGM profile. 142
Figure 5.6 Sanger sequence of the victim's control region. 142
Figure 5.7 LR comparison between CE and MPS. 146
Figure 5.8 Combining the LR from autosomal STRs with that from SNPs. 146
Figure 5.9 Dropouts effects on King's College Database. 147
Figure 5.10 Effects of dropouts on UoL's database. 147
Figure 5.11 Effects of dropouts on the similarity matrix from UoL's database. 149
Figure 5.12 Effects of dropouts on the MALAN simulated population. 150
Figure 5.13 Pedigree illustration of population one- number of matches. 151
Figure 5.14 Pedigree illustration of population two- number of matches. 153
Figure 5.15 Matches in the pedigree v. matches in the live population. 154
Figure 6.1 Skeletal decomposition. 168
Figure 6.2 Thermal scission of the C-N sugar base bonds. 171
Figure 8.1 NGMSElect® electropherogram for a blood stain at 4 °C. 197
Figure 8.2 PowerPlex® Y23 electropherogram for a blood stain at 4 °C. 197
Figure 8.3 NGMSElect® electropherogram for a blood stain at 180 °C. 198
Figure 8.4 PowerPlex® Y23 Electropherogram for a blood stain at 180 °C. 198
Figure 8.5 PowerPlex® Fusion 6C Electropherogram for a blood stain exposed to a C4 explosion. 199
Figure 8.6 PowerPlex® Y23 Electropherogram for a blood stain that was exposed to a DBSP explosion. 199
Figure 8.7 PowerPlex® Y23 Electropherogram for a touch DNA sample. 200

List of Tables

Table 1.1 Different types of STRs (Gill et al. 1997). 12
Table 1.2 Different types of DNA markers for identification purposes. 27
Table 2.1Mitochondrial DNA multiplex. 40
Table 2.2 HVSI and HVSII assay. 41
Table 3.1 Temperature dependent decay rates of mitochondrial DNA from bones. 45
Table 3.2 Partial profiles from the Texas Waco investigation. 47
Table 3.3 Heating oven's technical specifications. 53
Table 3.4 List of biological stains included in the Qubit® quantification. 54
Table 3.5 List of biological stains included in the Real-Time PCR quantification. 55
Table 3.6 List of blood stains of decreased volumes that were also DNA quantified via Real-Time PCR. 56
Table 3.7 Stain types, donor origin, stain volume, temperature treatment and number of samples tested in the NGMSElect® autosomal STRs multiplex assay. 58
Table 3.8 Stain types, donor origin, stain volume, temperature treatment and number of samples tested in the PowerPlex® Y23 multiplex assay. 59
Table 3.9 Stain types, donor origin, temperature treatment and number of samples tested in the ForenSeq®/ MiSeq FGx®. 60
Table 3.10 Samples that were initially quantified at less 0.2 ng/µL through qPCR. 60
Table 4.1 Duration of exposure to explosions. 83
Table 4.2 Dimensions and charge of DBSP-charged pipe bombs in Colorado 90
Table 4.3 Dimensions and charge of C4 charged pipe bombs in Penn State. 92
Table 4.4 Post-blast items recovery- DBSP. 98
Table 4.5 Post-blast items recovery- C4. 99
Table 4.6 Significance testing between pipe material and DNA concentration. 101
Table 4.7 Partial profiles from DBSP exploded stains through autosomal STR typing. 110
Table 4.8 Partial profiles from DBSP exploded stains through Y-STR typing. 111
Table 4.9 Climatic conditions at the time of the bomb experiments. 121
Table 5.1 Samples used for the autosomal STR and SNP interpretation. 135
Table 5.2 Mutation rates per Y-STR marker - MALAN partial profiles. 140
Table 5.3 Blazing car victim's mtDNA results. 156

Chapter 1 Introduction

1.1 The principle of exchange: "Every contact leaves a trace"

In 1920, medical practitioner Edmond Locard wrote the following: "The truth is that none can act with the intensity required for a crime without leaving multiple marks of their passage. [...]. There are two orders of clues that I want to show here: the perpetrators leave their passage marks on the scene, but also and in a reverse action, their bodies and clothes carry the clues of their past locations or movements" (Locard 1920). Locard's principle is often simplified in the form "every contact leaves a trace", which raises the notion of transfer that is central to the field and this project in particular. For example, an individual is expected to transfer material upon touching an object with his or her bare hands. Two types of marks can result simultaneously from this process:

1- Biological traces in the form of epithelial cells.

2- Latent fingerprints, in the form of lipids and sweat.

In a criminal investigation context, these marks become physical evidence if detected, recovered and judged relevant. This means *de facto* that the marks should persist on the object until recovery. The persistence is conditioned by a wide range of factors such as the delay between transfer and detection/collection, the characteristics of the donor and the substrate, the intensity of the contact and the environment in which the mark has been transferred and persists (Olsen 1978). The phenomena of transfer and persistence of the mark represent the core around which this project will be built.

Interestingly, the "intensity" of a crime, which Locard describes as the cause behind the inevitable presence of clues, can distort or destroy the clues themselves when extremely high in magnitude. A direct example for this is the distortion phenomenon that is

observed when latent fingerprints are created by an uneven distribution of pressures when transferred onto the substrate (Champod et al. 2004). In a less direct but nevertheless sensible correlation, a bomb maker would leave biological traces on the device that would then be destroyed by the blast's extreme conditions. The predominant type of mark that is expected to have transferred on the device during construction is a small amount of touch cells which by default are shed in a random inconsistent manner and result often in a low-template DNA sample (Lowe et al. 2002).

1.2 The principle of individuality: "Everything is unique"

Biochemist Paul Kirk stated the following in 1963: "Identity is defined by all philosophical authorities as uniqueness. A thing can be identical only with itself, never with any other object, since all objects in the universe are unique" (Kirk 1963). It is the principle of individuality that makes it possible for the source, i.e. persons or objects behind the mark, to be identified. However, Kirk distinguishes between the identification, which he sees as scientifically attainable through a laboratory exam and a statistical interpretation, and the individualisation, which he considers to be an ideal goal in forensic science. Figure 1.1 illustrates this distinction through an investigative process that starts with a large population of suspects that narrows down to a smaller group of individuals after the evaluation of a scientific result, without necessarily singling out only one individual.

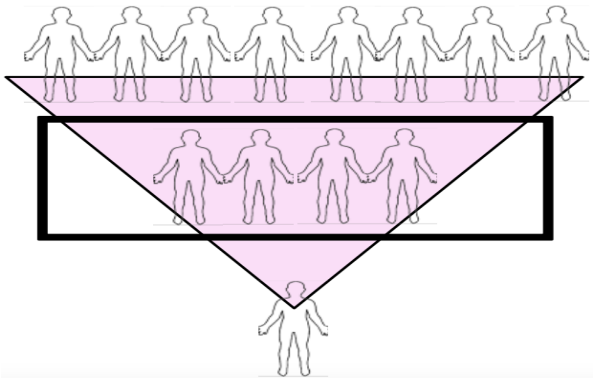

Figure 1.1 Identification and individualisation.

The work of identification does not always lead to *individualisation* but to a narrowing down to a list of suspects.

If "all objects in the universe are unique" then all fingerprint or DNA profile replicates are different from their originals. Therefore, physical evidence is not unique to its source but only to itself. What allows the identification then, is a high enough degree of correspondence between the mark and its reference combined with the absence of inexplicable differences.

Unavoidable subjective quantitative terms such as "high enough", place statistics and probability at the heart of forensic interpretation, and a necessary prelude to decision-making (Aitken et al. 2010). An example of a statistical analysis that is useful in this respect is the determination of intra- and inter-variability of a population of marks of a specific type. For example, the comparison between DNA profiles that are generated from the same donor (intra-variability) followed by the comparison of profiles that are generated from different individuals (inter-variability) gives an idea about the discriminating power of DNA as an identifying mark (Figure 1.2): the less the overlap in scores obtained for the two types of comparisons, the higher the discriminating power.

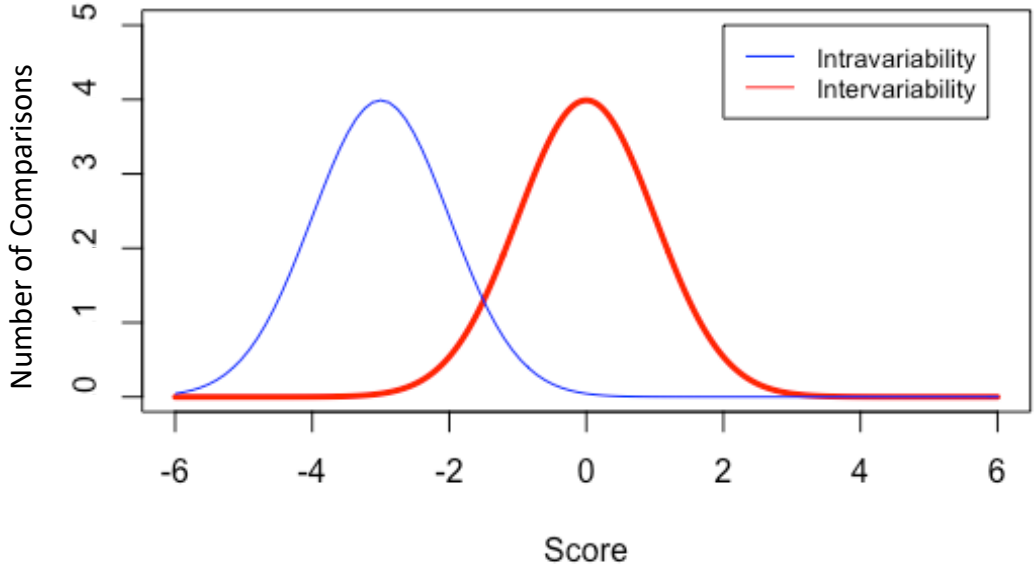

Figure 1.2 Intravariability and intervariability

This figure simulates hypothetical comparisons between same donors of forensic marks (Intravariability), such as latent fingerprints or DNA profiles, and comparisons between different donors (Intervariability) plotted against their comparison scores. The comparison scores are hypothesized as being numerical and ranging between [-6; 6]. Incorrect identification decisions can occur in the area of overlap in scores between same and different donor comparisons (score between -3 and 0). Figure created by the author for demonstrative purposes using hypothetical values.

Not only is uncertainty inherent to all sciences (if not to everything in the universe), but also and more specifically the aim of forensic science is to reconstruct past events, which essentially requires measures of beliefs. Probability is a good way of reasoning in these conditions. The real value of science in the investigation is the appreciation of scientific observations in the light of the two mutually exclusive propositions brought forward by the prosecution and the defence. The Bayesian approach in forensic interpretation calculates the Likelihood Ratio (LR) between the probabilities of the scientific observation given that one or the other proposition was true, within a framework of given circumstances (Berger et al. 2011b).

We consider in the following a basic interpretation example of a DNA analysis using the Bayesian approach:

Let **'E'** represent a match between two DNA profiles that were respectively generated from a collected sample (questioned source) and a reference sample (known source). '**Hp'** is the prosecution's hypothesis proposing that the collected sample comes from the known source. '**Hd'** is the defence's hypothesis proposing that the collected sample comes from someone else. Finally, '***i'*** represents the framework of given circumstances.

The likelihood ratio '**LR**' is calculated through the following odds ratio that is derived from Bayes theorem:

$$LR = \frac{\mathbf{P(E \mid Hp, i)}}{\mathbf{P(E \mid Hd, i)}}$$

The numerator represents the probability '**P**' of the match '**E**', given that the collected sample comes from the known suspected source (**Hp)**, within the framework of given circumstances (***i***). The denominator represents the probability '**P**' of the match '**E**', given that the collected sample comes from someone else (**Hd**), within the same framework of given circumstances (***i***). It is important to stress that the forensic scientist cannot express beliefs around the propositions themselves, but on the scientific observations if one or the other of these propositions were true.

We have seen that the likelihood ratio is dependent on the given circumstances, and these include where, how and why was the mark collected, stored and analysed. The following sections will explore the workspaces in which the forensic scientist operates while keeping record of the chain of evidence.

1.3 The Crime Scene

The crime scene (CS) is theoretically every potential place containing a mark that is relevant to the case in question. The CS is likely to be the opposite of a controlled, clean and protected space that contains only the items of interest. In fact, it is often chaotic and requires disentangling of the relevant from the irrelevant (Kind 1987). This is determined by specific questions such as the identity of perpetrators and victims. The

CS can also be a hostile place not to be accessed before safety clearance, as in cases of fire or explosion that will be explored during this project.

From what is described about the state of a typical CS, one can deduce the factors that reduce the marks' persistence, thus leading to an irreversible loss of information. These risks are present from the moment the marks were transferred, and they depend on factors that are discussed in Sections 1.3.1 and 1.3.2. The loss of information can be in the form of decay, transformation or contamination.

1.3.1 Decay and transformation

Although distinct in nature, both decay and transformation affect the original structure of the mark and frequently occur in tandem; these factors affect CS DNA samples as well as other traces. Raymond et al. (2009) showed a significant decrease over time of DNA recovery from outdoor surfaces (Figure 1.3). The abnormal spikes in DNA recovery from the laboratory at weeks one and two were explained by an uneven distribution of biological cells between samples during their preparations, accentuated by the sample's increased visibility (white stain) after few days, which facilitated the task of collecting all of the biomaterial. The time at which a criminal event happened, which is a fundamental question in forensic science (Weyermann and Ribaux 2012), could be inferred from the mark's quality and quantity. It is true that ageing ultimately leads to the loss of information, but it does not act on its own. In fact, all environmental factors play key roles in this matter. Extremely high temperatures for example are expected to increase drastically the rate at which decay and transformation of the evidence occur.

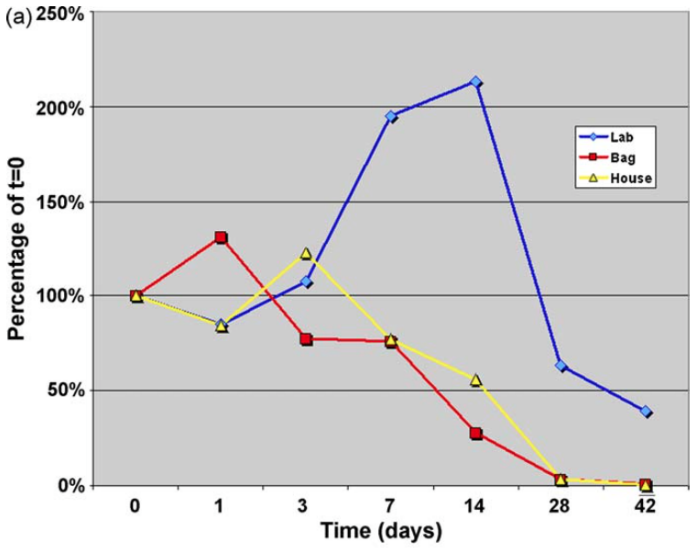

Figure 1.3 Persistence of DNA at crime scenes.

Recovery of DNA from swabbed surfaces (lab, bag, window frames) at various times up to six weeks, presented as a percentage of the amount recovered at t=0 (Raymond et al. 2009).

1.3.2 Contamination

Contamination is detrimental to the information without necessarily affecting the original structure of the mark. It is unavoidable when it originates from elements that were brought by the event itself or from elements that were already present at the CS. However, the post-event contamination can be minimised via a rapid initial response followed by CS security, while still prioritising the control of dangerous situations and the medical assistance to affected individuals (TGWGCSI, USA 2012). The consequences of contamination vary greatly from one situation to another. Overlapping latent fingerprints, for example, slow down further analyses as the overpopulation of ridge impressions might obscure important details (Bradshaw et al. 2012). When necessary, this visual perception issue can be overcome with a number of proposed techniques such as mass spectrometry. However, another problem remains in the selection of the marks that are relevant to the case from those which were 'innocently' deposited on the same surface.

A more serious consequence can arise when biological traces of different sources are mixed together as this can have an adverse effect on the final interpretation of the

results. This is because DNA analysis often amplifies the signal of minute traces by passing necessarily through the polymerase chain reaction (PCR). Fortunately, the resulting PCR amplicons are proportional in quantity to the starting material; which allows a reliable deconvolution of some DNA mixture profiles between major and minor contributors (Bleka et al. 2016). This is helpful in situations where the mark of interest is rich in DNA, such as a pool of blood that is contaminated by a poor mark, for example the saliva of a different individual. The major problems happen in situations where the mark of interest is expected to be so poor in DNA that it becomes impossible to distinguish it from other biological contaminants.

As for contaminants that are of a different nature than the mark itself: these can either destroy it, for example the dilution of both biological traces and latent fingerprints by water; or impede future analysis, like bacteria, dust particles and pollen that have been reported to inhibit PCR (Wilson 1997). A pre-processing clean-up of all items containing such elements is therefore recommended. Moreover, silica-based column extraction, as selected for this project, has been demonstrated to efficiently attenuate PCR inhibition without affecting the final yield (Alaeddini 2012).

1.3.3 The collection procedure

If the item that carries the biological mark is moveable, it can be collected and packaged individually after *in situ* documentation. Paper bags are chosen over plastic ones, since moisture condenses in plastic and favours DNA degradation (Cătălin et al. 2011). This is also why all liquid stains must be air-dried before packaging. Additionally, the contact between the biological trace and the bag's inner walls must be avoided. Evidence cardboard boxes have been specially designed to overcome the above-mentioned practical difficulties - the object is internally fixed with minimal contact and air-dried whilst packaged (Coquoz and Taroni 2013).

At-scene sampling must be considered when the biological mark is located on a fixed substrate; or when it has been judged to be sensible by the Scene of Crimes Officer

(SOCO). A number of at-scene collection techniques exist and can be selected depending on the situation at hand. Apart from some readily detectable blood and semen stains, most biological traces are invisible and therefore only collected under the assumption that they exist in specific locations. This automatically raises the additional necessity to collect around the suspected area in order to authenticate the localised transfer by testing for blanks. SOCOs have regularly used adhesive tapes to collect all sorts of microscopic traces from immoveable large objects or from victims present in the CS (Barash et al. 2010). The method consists of applying the tape to the suspected area before protecting it with a plastic or acetate paper. Most biological traces however are collected using swabs (Van Oorschot et al. 2010). "Double swabbing", which consists of applying a wet swab followed by a dry one, is considered today's optimal method for the collection of cellular material and has been used in this work (Pang and Cheung 2007). Both swabs are then combined in downstream applications to maximise the yield. Finally, both swabs and tapes perform poorly when biological traces are inside crevices or below a textile's surface. Wet vacuums such as the M-VAC system have been reported to be efficient alternatives in these specific situations (Hedman et al. 2015).

1.3.4 The laboratory

The detection and collection of marks, including taping and swabbing, are not restricted to the CS as they are also essential laboratory activities. Such tasks can begin upon the reception of exhibits and once the priorities have been established. Relevant marks that are detectable and sufficient in quantity and quality are prioritised for analysis. Less weight is given however to those invisible marks that fail quality/quantity tests, unless the seriousness of the case is extremely high and the potential of finding other evidence is low. These are in fact the cases of interest for this work, where the perpetrator's poor marks or the victims' scattered remains have been degraded by environmental extremes.

The laboratory conditions must therefore be exceptionally clean and well managed when it comes to DNA analysis. The separation of the pre- and post- PCR working environments and the dedication of special equipment and reagents for difficult procedures are envisioned for the continuity of this project. Full gear protective equipment that includes clean lab coats as well as disposable facemasks, hairnets and gloves will be all worn during the handling of sensitive samples. A clean space with restrictive access should be prepared for low-template DNA analysis (discussed below). The aim is to establish an in-house quality insurance program that would increase the possibilities of generating profiles with a measured error rate close to zero. The management system should comply with the ISO 17025.

1.4 Human identification

1.4.1 Identification through genetics

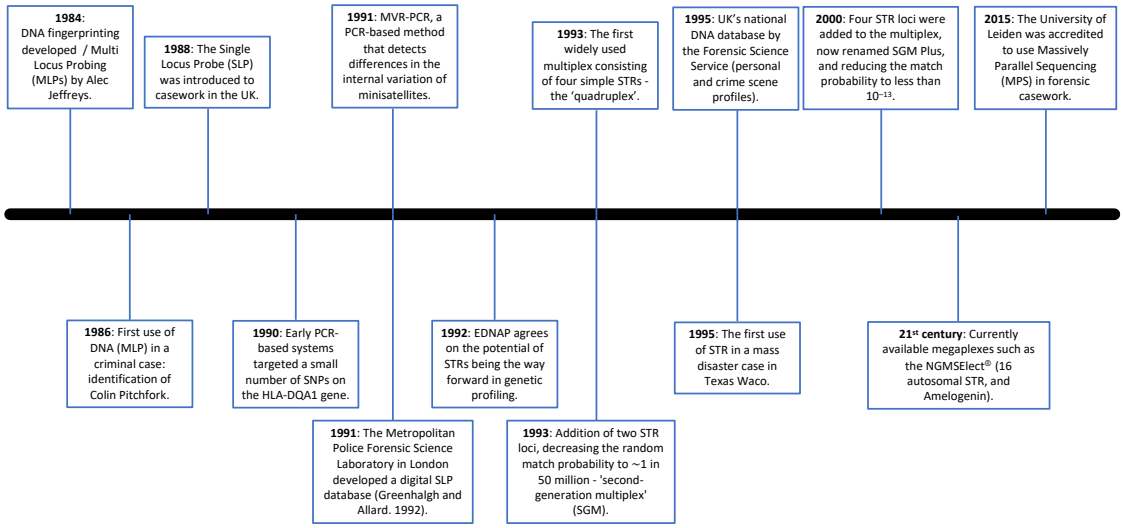

Figure 1.4 Timeline of key developments in forensic genetics.
Illustration listing the major advances in forensic genetics from the twentieth and the twenty-first century.

The first means of distinguishing among people through genetics was by grouping them according to (Landsteiner 1900) detection of the ABO blood polymorphisms. Its

application in forensic casework helped in straightforward exclusions but was less reliable in linking a biological sample to a person, because the frequencies of the different blood group types in a population were often high. Following further developments, the smallest random match probability (RMP) between two unrelated persons could reach the order of one in a thousand when a high-quality bloodstain was analysed with blood groups and polymorphic protein markers. Moreover, the characteristics of identification were susceptible to rapid degradation, and generally only available from blood (Jobling and Gill 2004).

A greater role for genetics in forensic science emerged with the discovery of DNA 'fingerprints' by Jeffreys in 1984 at the University of Leicester (Jeffreys et al. 1985). DNA fingerprinting utilises DNA probes comprising the conserved core sequence of a class of highly polymorphic minisatellites, or variable number of tandem repeat (VNTR) loci, to detect a number of such loci in restriction-digested genomic DNA separated by size on a Southern blot. Using the original DNA fingerprinting method, RMPs of $\sim 10^{-11}$ (with a single probe), or $\sim 10^{-19}$ (with two probes) were achievable (Jeffreys et al. 1985), and hence individual identification with the exception of monozygotic twins. This technique brought answers to criminal investigations, kinship studies, immigration disputes and the science of wildlife demography.

However, another approach was soon adopted after the discovery of PCR and the automation of sequencing by multi-channel capillary electrophoresis systems, thereby increasing sensitivity and reducing the time of analysis. Attention shifted from minisatellites with lengths of 1 - 40 kb (impossible to amplify via PCR and affected greatly by DNA degradation) to the characterisation and analysis of Short Tandem Repeats (STRs; also known as microsatellites; Edwards et al. 1991). Forensic STR markers are highly polymorphic and significantly shorter than minisatellite VNTRs, with each repeat unit being two to seven base pairs (bp) long, tandemly repeated typically 10 – 30 times, in an amplified fragment spanning over a range of 100 - 400 bp. Different types of markers are distinguished (Table 1.1) by their repeats' sequence

conformations (Urquhart et al. 1994). They can be simple, interrupted, compound or complex:

Table 1.1 Different types of STRs (Gill et al. 1997).

Type	Example of repeat unit pattern	Example
Simple repeats	$(ATTT)_n$	HUMFES
Simple with non-consensus repeats	$(TCAT)_nCAT(TCAT)_m$	HUMTH01
Compound repeat sequences with non-consensus repeats	$(TCAT)_n(TCTG)_m(TCTA)_p$	HUMVWFA31
Complex repeat sequences	$(TCTA)_n(TCTG)_m$ $(TCTA)_pTA(TCTA)_q$ $TCA(TCTA)_rTCCATA(TCTA)_sTA.$-TCTA.TC	D21S11

n-s: integer values

The first STR analyses targeted four autosomal markers (the Quadruplex kit comprised markers TH01, FES/FPS, vWA and F13A1) and had a relatively high RMP of 10^{-4}. Consequently, it was combined in forensic reports with a simpler form of DNA 'fingerprint' called single-locus profiling (SLP) which detected minisatellite loci one at a time (Jobling and Gill 2004). As soon as additional autosomal STR markers were added to the previous four, thereby decreasing the RMP to 5×10^{-7}, only the STR profile was reported. The power of discrimination increased with the addition of STRs selected on the basis of relatively high mutation rates, independent chromosomal re-assortment and recombination. The independent inheritance of the analysed STRs allows the multiplication of allele frequencies in estimating the RMP (the 'product rule'). The RMP of recent autosomal STR multiplex kits such as GlobalFiler®, which contains 21 markers, is as low as 10^{-25}, thus providing individual identification. Nonetheless, interpretation must take into consideration monozygotic twins, close relatives and sub-population effects, necessitating a conservative approach to the reporting of results (Balding and Nichols 1994).

Separation of STR PCR fragments is via capillary electrophoresis (Figure 1.5), and detection via fluorescent labelling of one of each primer pair at its 5′ end. Current devices allow 6-colour detection, which, together with size-range differences, facilitates the distinction of one STR from another.

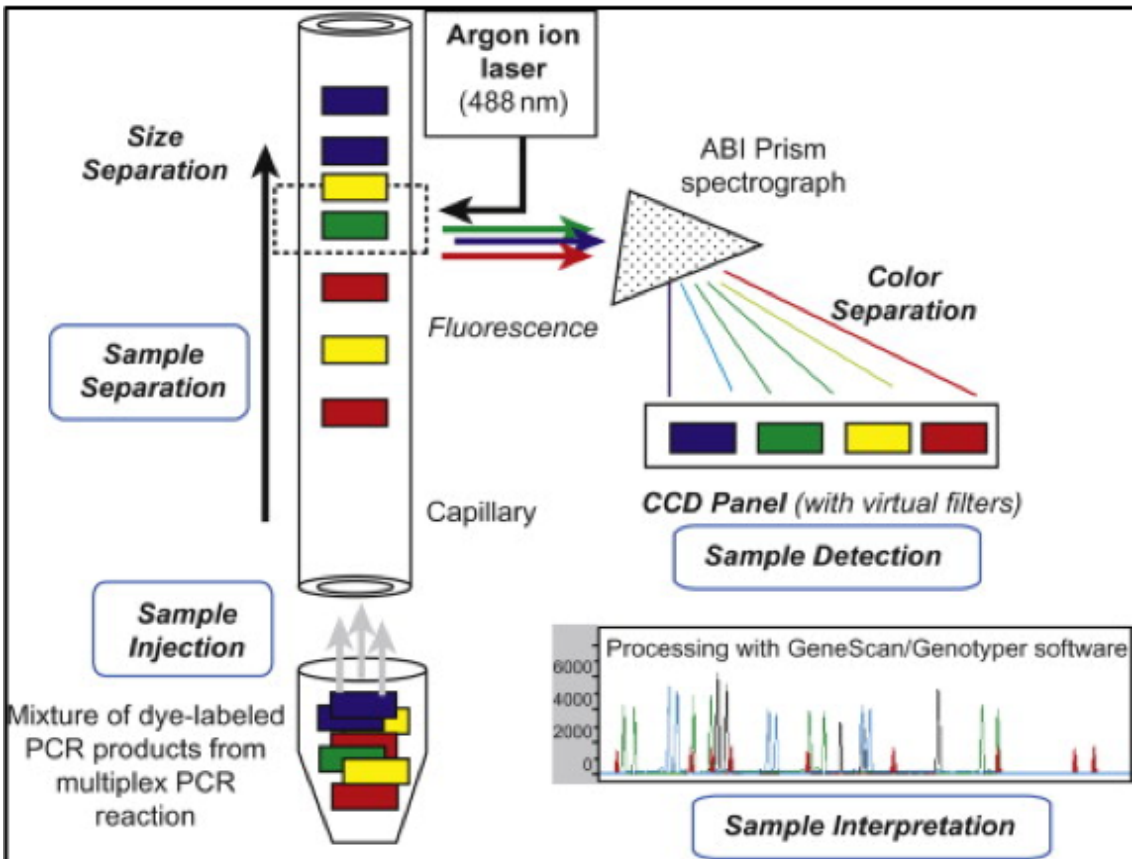

Figure 1.5 Capillary Electrophoresis.

The capillary electrophoresis (CE) method used for the separation and detection of STR alleles. PCR products are fluorescently labelled with different coloured dyes (four in this example), and fragments are then separated out by fragment size and then detected by an argon laser. The laser excitation emits visible light detected by a camera that is recorded on a computer as a profile (Butler 2011). In practice, a dye-labelled size standard is also included in each capillary.

STR-based DNA profiles are detected and interpreted in the forms of electropherograms – graphs of relative fluorescent intensity against molecular weight in bp. Alleles are observed as peaks and assigned automatically using software. An example is shown in Figure 1.6.

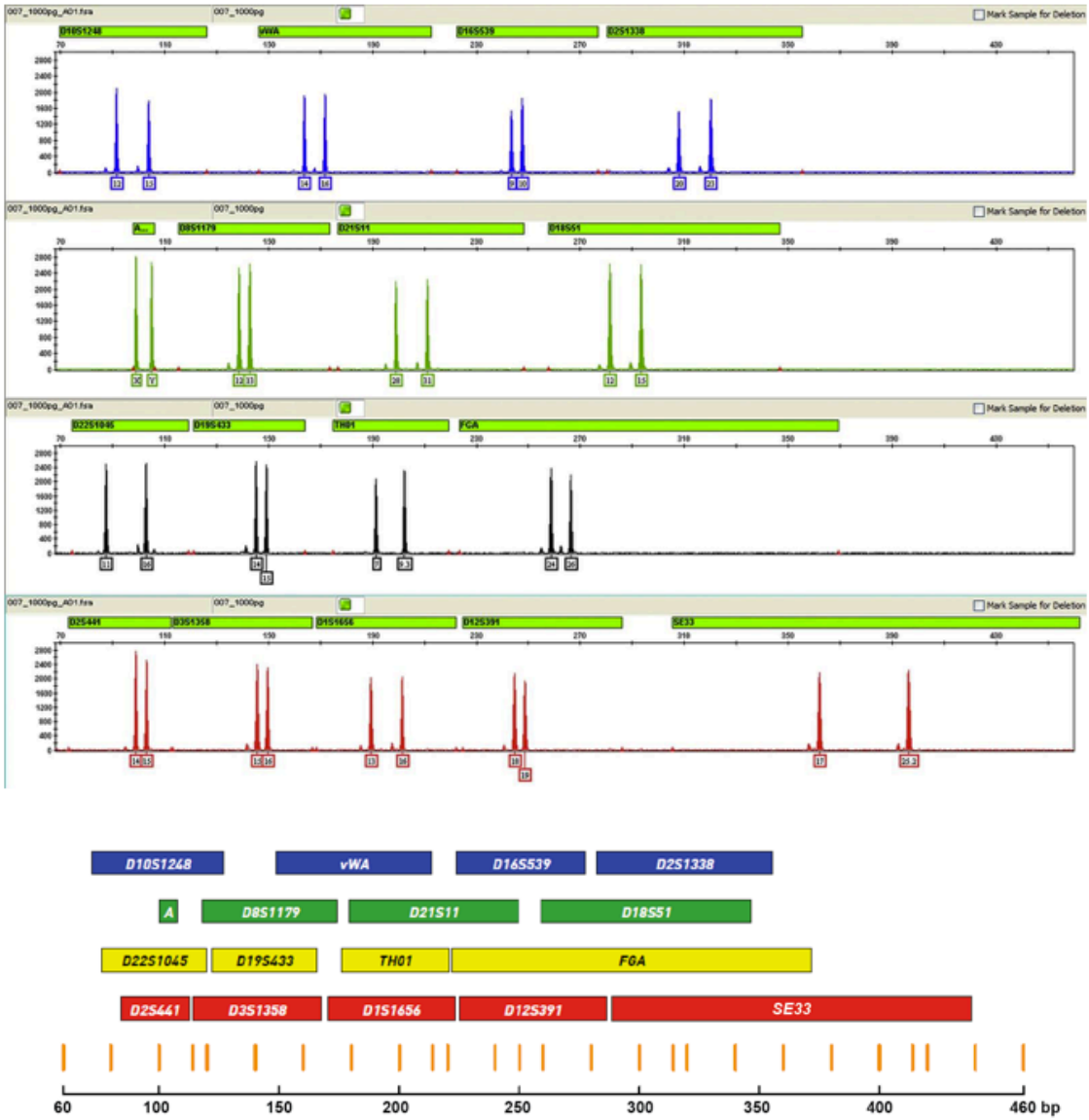

Figure 1.6 Electropherogram, autosomal STR profile.

An electropherogram showing a 16-locus autosomal STR profile produced with the NGMSElect® kit, and schematic representation of the size ranges of markers in the kit. The y-axis in the electropherogram is in relative fluorescence units, and the x-axis in base-pairs. Colours in the schematic size-range diagram correspond to fluorescent dye colours; orange dye labels the size standard (bottom); A – amelogenin. Image redrawn from ThermoFisher.com (thermofisher.com/order/catalog/product/4457889#/4457889).

1.4.2 Non-autosomal markers in forensic DNA analysis

Most multiplex autosomal analyses also amplify a locus from the human sex chromosomes, part of the XY-homologous amelogenin gene, which has sizes differing by 6 bp between the X and Y copies. Its sex-test characteristic is useful as it can narrow down the suspect population to only men or women for a profile from a single

contributor and helps in confirming a mixture profile if contributors differ in sex (excluding rare cases of sex-chromosomal aneuploidy or translocations between the X and Y chromosomes). Sometimes however, notably in cases of male aggression toward women, a high female to low male biological sample can hinder the detection of the male's autosomal alleles. Normally in such cases, differential extraction selective for DNA present in spermatozoa is attempted, which if successful allows downstream profiling of the males' autosomal STRs when sperm has been collected (Gill et al. 1985).

However, sperm is far from being the only trace to search for even in cases of sexual assault, and differential extraction is not applicable to other biological fluids or touch cells. The alternative approach is to analyse the highly polymorphic STRs that have been characterised on the male-specific region of the Y chromosome. Not only can this help identify the male in a male/female mixture, it also allows the resolution of mixtures containing two or more male individuals (Prinz and Sansone 2001). Another advantage in criminal investigations is that men commit most offences: perpetrators were reported to be males in around three-quarters of violent incidents (78%) in March 2017 in England and Wales (Office for National Statistics 2017b). For the same year, sexual offence perpetrators were reported to be males 99% of the times (Office for National Statistics 2017a).

However, the Y chromosomes male specificity is a double-edged sword. In the absence of recombination, mutation is the sole source of discriminating characteristics of Y-STR analysis (the product rule cannot be used), which reduces its identification power significantly. A typical Y-STR profile of 11 markers has a RMP of approximately 3×10^{-2} that could be reduced to 3.56×10^{-4} with the addition of 12 markers in the PowerPlex® Y23 kit (Figure 1.7; Purps et al. 2014). Most importantly, individualisation is impossible to achieve as all descendants of the same paternal lineage are expected to have matching haplotypes, unless a large enough number of rapidly mutating Y-STRs are included in the analysis which may generate a novel haplotype in an individual through *de novo* mutation.

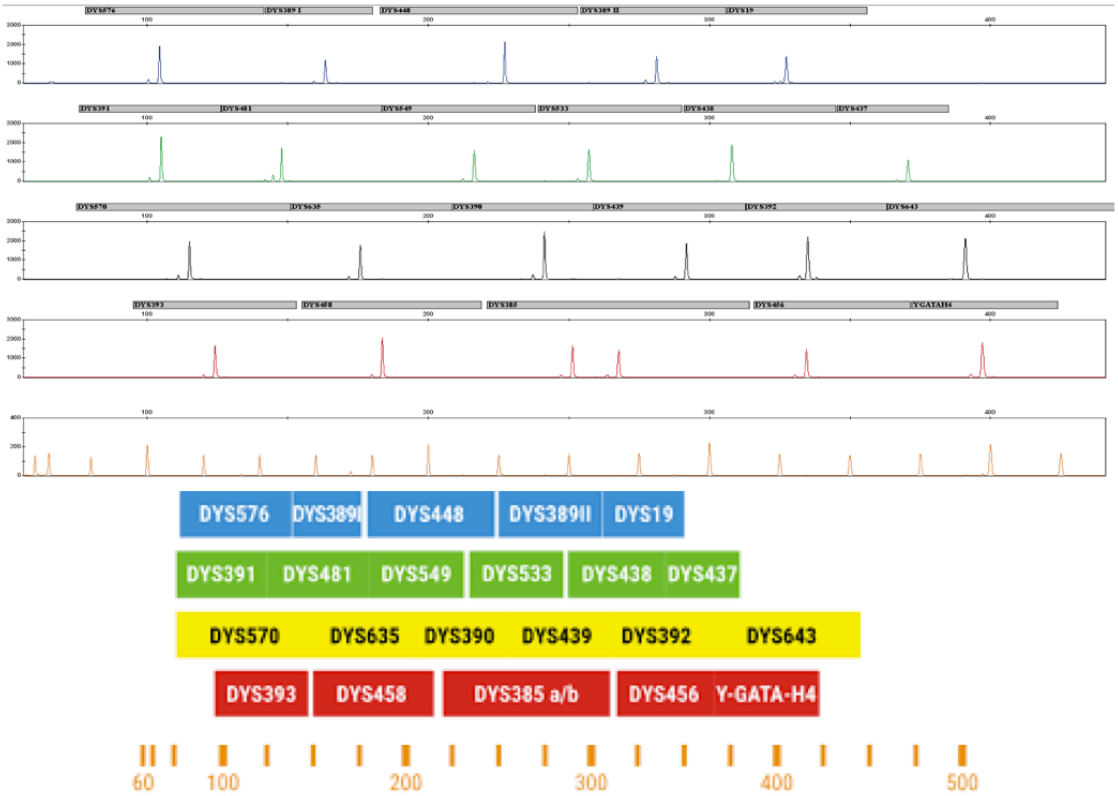

Figure 1.7 Electropherogram, Y-STR profile.

An electropherogram showing a 23-locus Y-STR profile produced with the Promega PPY23 kit, and schematic representation of the size ranges of markers in the kit. The y-axis in the electropherogram is in relative fluorescent units, and the x-axis in base-pairs. Colours in the schematic size-range diagram correspond to fluorescent dye colours. Image from Promega.com.

As well as the paternally-inherited Y chromosome, the maternally inherited mitochondrial DNA (mtDNA) has important applications in forensic DNA analysis. Unlike the Y, it is carried by both sexes, but passes down only from mothers to offspring because of its relative abundance in eggs compared to sperm, and an apparent mechanism for the elimination of paternal mitochondria after fertilisation (Sato and Sato 2012). MtDNA is small (~16.5 kb) compared to nuclear chromosomes, and therefore presents relatively limited scope for variation, which is seen as single-nucleotide changes rather than tandem-repeat variation and is detected by DNA sequencing. Like Y-chromosome haplotypes within paternal lineages, mtDNA haplotypes are shared among individuals sharing matrilineal descent. Thus, though

exclusions can be straightforward with mtDNA, matches need to be interpreted with care, and individualisation is impossible.

1.4.3 Low-template and degraded DNA

This project intends to test biological material that is most relevant to cases involving fires, explosions and mass disasters. The marks can be of various quantities ranging from a high number of recoverable cells from human soft and hard tissues to theoretically a single cell recovery. In between, 10^5 spermatozoa are counted per microlitre of sperm on average, while 10^3 to 10^4 leucocytes are counted in a microlitre of blood. Saliva is a poorer mark with an estimated amount of hundreds of squamous epithelial cells per microlitre (Coquoz and Taroni 2013). It is nonetheless still widely used as reference material, and successfully produces high-quality DNA profiles. Saliva can also be recovered from crime-scene items such as drinking vessels, cigarette butts, food, postage stamps, envelopes, and other material that may have come in contact with a person's mouth (Sweet and Hildebrand. 1999).

1.4.3.A Low-template DNA

Apart from the biological fluids cited above, shed material such as hair and touch cells could also be potential sources of genetic evidence. However, their low DNA content makes these samples more challenging. Hair has the advantage of being visually detectable, while touch cells are collected and analysed under the assumption that they are present in locations that were probably handled by the person of interest (e.g. suspect, victim). DNA yields have shown to increase when hairs or epidermal cells have been forcibly removed, rather than shed naturally, as for example when stuck inside sticky tape or when trapped underneath a victim's fingernails. However, only 10% and 26% respectively of hair and touch samples are reported to generate interpretable autosomal STR profiles (Castella and Mangin 2008; Coquoz and Taroni 2013).

Nevertheless, touch DNA can also be recovered and analysed from chemically enhanced fingerprints, such as those treated with ninhydrin or 1,8-diazafluoren-9-one (DFO) (Sewell et al. 2008). Success rates of autosomal STR profiling increase when targeted double swabbing is performed on a visible finger-mark (Templeton and Linacre 2014). Context-dependent decisions are expected to be made, when a relevant fingerprint is detected, in order to establish priorities between DNA analysis and fingerprint examination. Reliable genotyping of low-template DNA samples, as is expected from a swabbed fingerprint, was approached by the development of sensitive PCR-based methods that also rely on mathematical models to detect 'false alleles' (Taberlet et al. 1996).

1.4.3.B DNA degradation

Forensic DNA samples are also often of poor quality, a property typical to most marks when compared to their reference samples. Biological cells are particularly susceptible to degradation once they are deprived of their physiological conditions. This happens both when cells are transferred as a mark out of the organism onto a surface, and when the cells remain *in situ* in a dead organism. The lack of oxygen switches the central metabolism into a fermentative pathway that leads to the autolysis of cellular components. This includes DNA fragmentation into shorter strands (Haglund and Sorg 1997). The cell membranes' lysis aggravates the conditions further by exposing the cellular material to putrefaction, which is decomposition led by the activity of microorganisms. Putrefaction is detrimental to the genetic information first by causing more strand breaks due to additional release of nucleases, and then by contaminating the area with the microorganisms' DNA (Hummel and Herrmann 1994).

DNA degradation is not only limited to physical fragmentation but also includes consequent chemical modifications (Figure 1.8). The degree to which hydrolysis and oxidation affect the genetic information depends on the specific nucleotide site where the reaction occurs. For example, hydrolytic attacks on glycosidic sugar-base bonds can

lead to abasic sites by depurination. The same mechanism could be followed by single- and double-strand breaks in an alkaline environment (Lindahl and Nyberg 1972) or by DNA-protein and DNA-DNA crosslinks in an acidic environment (Freese and Cashel 1964). Exposing the sample to UV light also induces DNA-DNA crosslinks (Cadet et al. 2005). Oxidation mostly leads to the conversion of pyrimidines into hydantoins. Abasic sites, DNA fragmentation, crosslinks and the abovementioned oxidative transformations are types of damage that inhibit PCR (Hoss et al. 1996). Some chemical transformations are more consequent as they alter a DNA sequence without blocking downstream analysis. Fortunately, the rate at which such reactions occur is slow. For example, the transformation of a cytosine to a uracil by hydrolytic deamination is estimated to happen less than once every 30,000 years (Lindahl 1993).

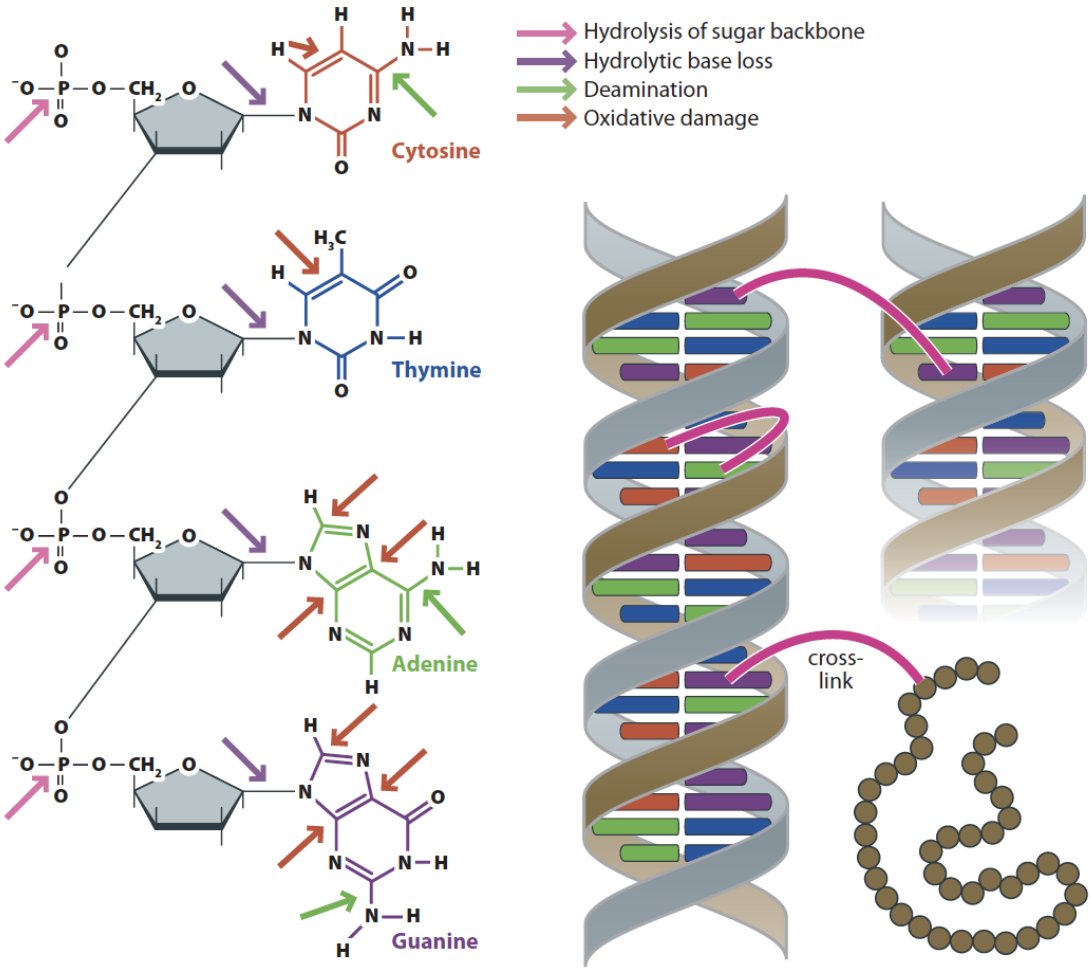

Figure 1.8 Post-mortem DNA damage.

DNA is prone to spontaneous damage and degradation, including hydrolytic and oxidative damage, and cross-linking between or within helices, as well as to proteins. Figure from Jobling et al. (2014).

DNA is a resistant macromolecule that can last for thousands of years. At 15 °C and under physiological pH, it takes up to 10,000 years to destroy an 800-bp DNA fragment by hydrolysis alone and up to 100,000 years to destroy all DNA in a human (Lindahl and Andersson 1972; Hofreiter et al. 2001). However, small environmental changes affect these rates significantly. All previously described damage requires a minimum amount of water and heat to occur. In general, any increase of either or both temperature and moisture would accelerate autolysis, putrefaction and chemical reactions. DNA has been shown to resist exposure to high temperatures by preserving more than 80% of its residual weight at temperatures that exceed 250 °C. Around 50%

of its residual weight was still detectable at 600 °C (Alongi et al. 2015), which is the approximate temperature at the epicentre of a live fire burning in oxygen. While Alongi et al. (2015) showed intumescent-like properties in DNA they did not test for the ability to retrieve identifying DNA profiles following exposure to such temperatures. Autosomal STRs and the Y-chromosome were successfully analysed from dental pulp that was exposed to 300 °C (Tsuchimochi et al. 2002).

It is worth mentioning that the tooth's crown protected by enamel, which is the body's hardest substance, and its root encased within a bony socket, offers DNA one of most protective environments against post-mortem degradation (Higgins and Austin 2013). Expectations are therefore lowered when the same analysis is applied to more vulnerable samples. However, it was still possible to generate interpretable autosomal STR profiles from 22% of touch cells samples that were deposited on 9 mm Luger brass-cased ammunition prior to firing (Montpetit and O'Donnell 2015). It remains to be investigated whether the failure of typing the remaining 78% of the samples was due to the low-template DNA from touch cells, or to the friction that occurs between the cartridge's external surface and the gun's ammunition chamber following gas expansions, or to the sudden rise in temperature upon firing. This temperature does not exceed 63 °C, when measured externally on the same type of ammunition, and reaches its peak at 1.2 milliseconds (Gashi et al. 2010).

The sudden increase in temperature and pressure when firing a gun is a result of the propellant's explosion after the internal striker hit the friction-sensitive primer. An explosion can be defined as an exothermic violent and expansive reaction of already existing or rapidly forming gases or vapours (Martin 2008). Explosions can be classified into deflagrations and detonations. The main differences between the two categories are the reaction's velocity and intensity. Deflagrations occur at subsonic speeds (typically below 100 m/s) and produce relatively low temperatures for a significant amount of time, as in the case of firing a gun (Heramb and McCord. 2002), while detonations occur at supersonic speeds (thousands of m/s) and cause a short

outburst of extremely high temperatures (thousands of °C). Most accidental explosions deflagrate, as they are the product of combustible gases that were pressurised then ignited. However, a shift from deflagration to detonation happens under certain conditions, such as partial confinement and physical barriers against the flames (Schultz et al. 1999). All unauthorised intentional explosions are usually classified as serious crimes due to the potential damage they are associated with. One of today's greatest security concerns is the use of improvised explosive devices (IEDs) against the public (Abdul-Karim et al. 2013). All IEDs involve a fusing mechanism, a casing, and an explosive mixture.t However heir lethality and design vary greatly. For example, homemade pipe bombs consist of readily available materials that may enclose a low explosive mixture such as black or smokeless powders (Figure 1.9), whereas military-grade explosive systems are usually more sophisticated and use high explosives such as 'Research Department Explosives' (RDX) (Gill et al. 2011). Under normal conditions, low explosives deflagrate whilst high explosives detonate. Autosomal STR analyses were performed on 195 casework samples consisting of non-exploded IED materials such as the tape ends of a strip and explosive wiring (presumably touched by one suspect of interest). DNA was detectable in 23 % of the samples, of which nine generated full profiles (Phetpeng et al. 2015). The Forensic Science Service in the U.K. (FSS) has exploited the same type of evidence that led to the prosecution of S. Hoey for the 1998 Omagh bombing. The court expressed concerns regarding "the recording and storage of items" and the reliability of low-level DNA testing (LCN – see following section) and the evidence was refused (R v Hoey 2007). However, a subsequent independent Government review initiated by the Forensic Science Regulator confirmed that the DNA test used was reliable and fit for purpose (Caddy et al. 2008).

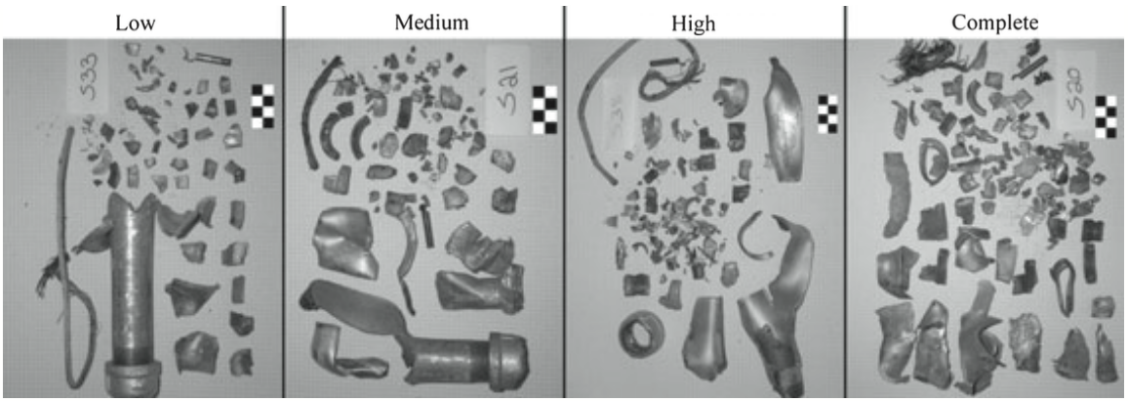

Figure 1.9 Pipe bomb fragmentation.

Different fragmentation patterns using the same low explosive which is a single base smokeless gunpowder (Foran et al. 2009).

1.4.4 Forensic implications and proposed solutions

Section 1.2.3 describes the suboptimal quantity and quality of forensic biological samples as being the two major obstacles for a successful identification through DNA. This section describes a set of analytical improvements, starting at the pre-PCR stage, in order to increase the chances of success.

1.4.4.A Analysis of Low-Template DNA

Although sensitivity of analysis increased after the adoption of multiplex PCR into forensic genetics, many low-template samples remain undetected. The FSS in the U.K. introduced Low Copy Number (LCN) analysis, which refers to the technique adopted when the starting material is less than 200 pg of DNA (given a 6-pg mass for a human genome, this represents <~30 copies) (Budowle et al. 2009). Modifications that were proposed included the increase of PCR cycles from 28 to 34 cycles, reducing the reaction volume, doubling the annealing time, increasing the injection time, and post-PCR purifications (Budowle et al. 2001; Caragine et al. 2009). While more than ten nanograms of input DNA may result in over-amplification leading to off-scale data even by the 28th cycle, low input (~10 to 100 pg) may result in dropouts which occur when an allele fails to be detected by the system. Increasing the number of cycles (31 to 34 cycles) reduces the likelihood of missing alleles, but it might also increase background noise in the form of allelic drop-in, which is when alleles unconnected to

the sample's source are detected by the system as a result of laboratory contamination. When typing a heterozygous locus and increasing the number of PCR cycles, one allele's peak height may be less than 60% of that of the other allele, resulting in what is called heterozygous imbalance (Figure 1.10). The peak height imbalance between two heterozygous alleles in the analysis of low-template DNA may be more severe putting the lower peak's authenticity in question.

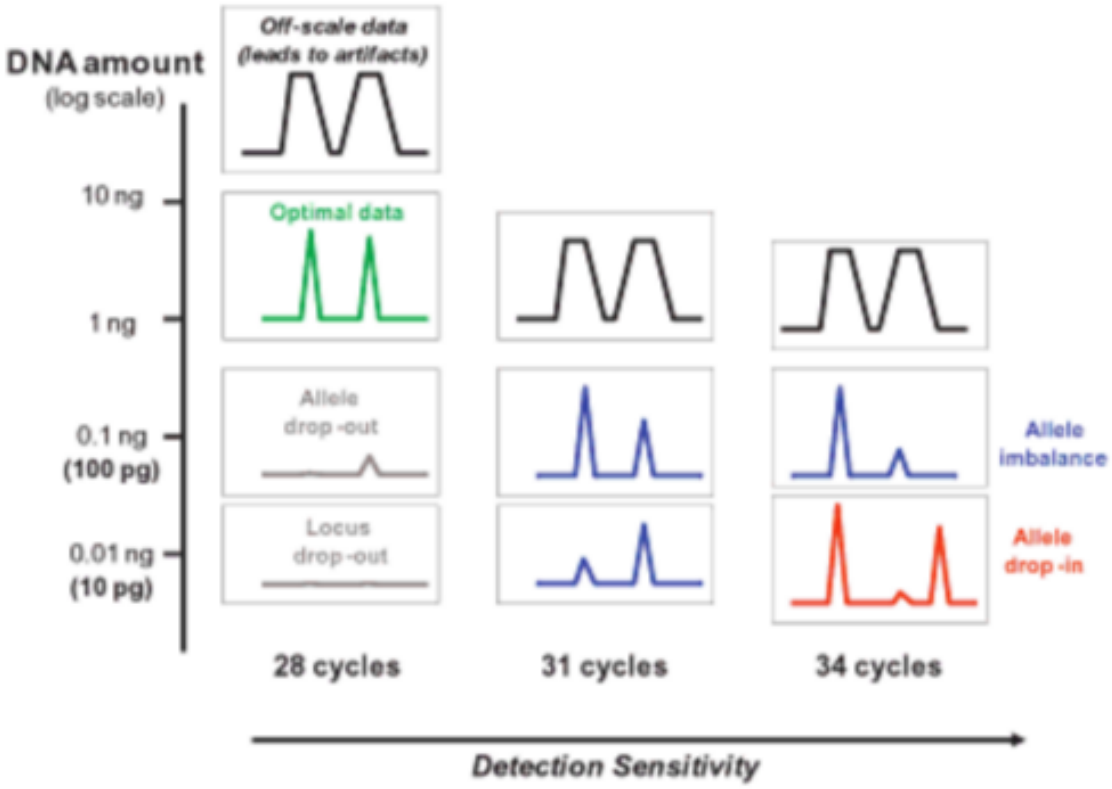

Figure 1.10 PCR cycle number increase and associated risks in analysis of low-template DNA.

This graph illustrates the possible consequences of having too low or too high DNA input after the amplification of a heterozygous locus at the 28th, 31st, and 34th PCR cycles. These are characterised by off-scale data, dropouts, heterozygous peak imbalance, and drop-ins. Image from Butler (2011).

Consequently, screening the data at the 28th cycle before running the six additional cycles may prove essential to prevent stochastic effects and off-scale data, which is when the PCR products exceed the linear dynamic range for detection by the instrument (Kloosterman and Kersbergen 2003). Stochastic effects can lead to ambiguities in the interpretation of LCN generated profiles, which necessitates the

replication of the PCR stage in order to reach a reliable consensus profile (Figure 1.11; Wetton et al. 2011). They can be manifested as signal losses which includes dropouts and heterozygous peak imbalances, or as gains of false signals which includes drop-ins and stutters (Figure 1.12). Stutters are artefactual peaks that are due to the polymerase slippage during PCR, and are usually one, two, or three repeats smaller than the cognate product. They are difficult to be excluded as artefacts when their peak heights is higher than the regular 5% to 10% of the nominal allele's peak height; a problem that is more likely occurring with low input DNA.

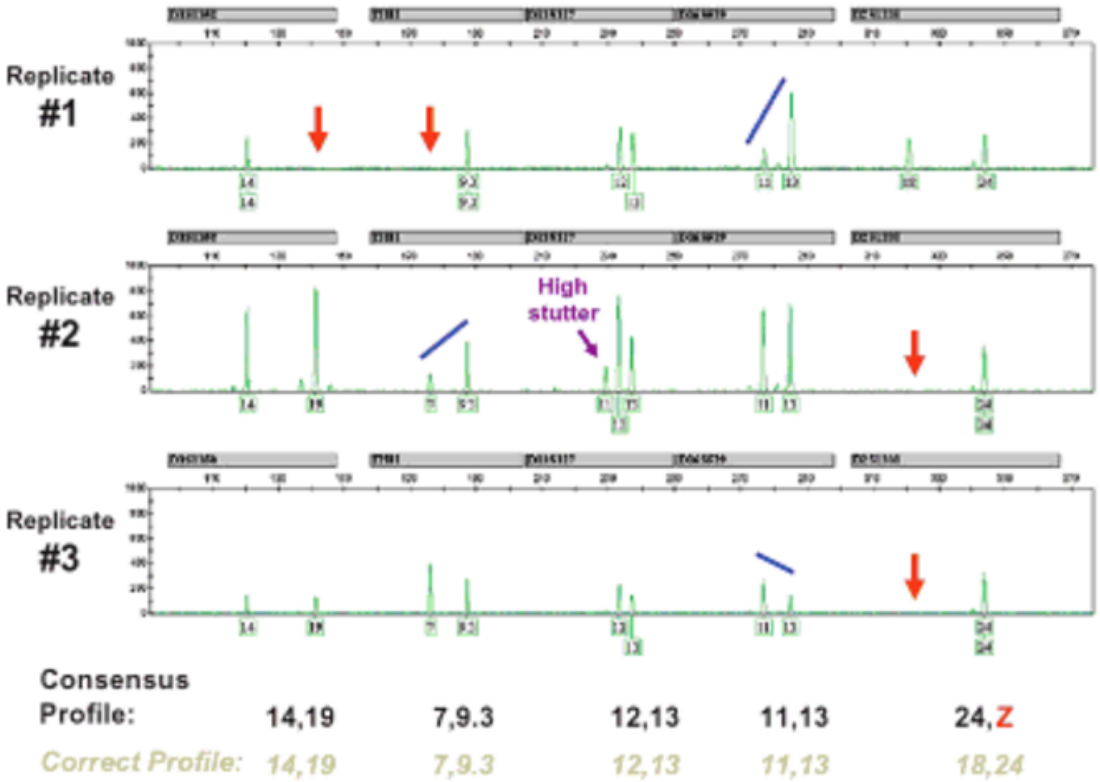

Figure 1.11 PCR replications of low-template DNA.

Three replicate PCR amplifications from the same DNA extract to reach a consensus profile. The second replicate succeeded in the detection of the otherwise dropped out allele 7 on locus TH01 but has also produced high stutter (higher than 10% of the nominal allele's peak height) and a heterozygous peak imbalance. These were resolved in the third replicate allowing for a consensus profile with one allele missing compared to the correct profile. Image from Butler (2011).

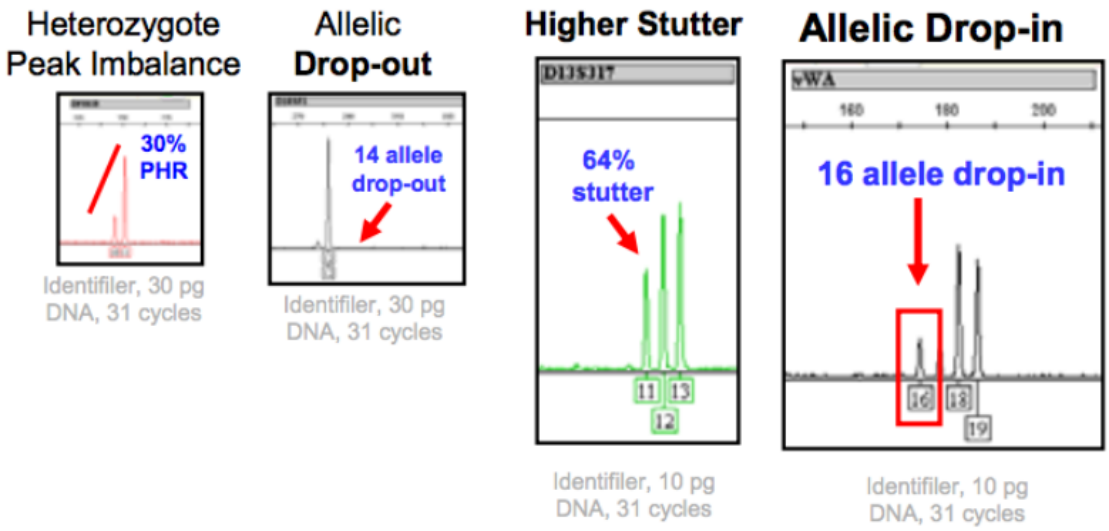

Figure 1.12 Stochastic Effects.

Different types of stochastic effects that may complicate the interpretation of profiles in challenging samples. From left to right: Heterozygous peak imbalance occurring when the peak heights ratio (PHR) exceeds the 60% major allele and 40% minor allele - allelic dropout caused the failure of the system to detect a true allele - high stutter, due to polymerase slippage and generally low peak heights for the true alleles - non-authentic alleles that are detected by the system as a result of contamination, otherwise known as drop-ins. Image from Butler (2011).

1.4.4.B Analysis of degraded DNA

PCR failures have been associated with targeting large DNA fragments (Whitaker et al. 1995). Whilst this conforms with the technological switch from minisatellite to STR analysis, heavily degraded DNA can still be broken into strands that are shorter than some STR markers. A straightforward approach to this issue is to further reduce the amplicons' sizes. 'Mini-STR' loci were created for this purpose by bringing the PCR primers closer to the repeat regions (Figure 1.13). Mini-STR assays performed well on degraded DNA and are highly recommended for such analysis (Gill et al. 2006).

Table 1.2 lists the different types of markers that can be targeted depending on the specific identification purpose and on the sample's quality. An alternative to STRs and Mini-STRs are single nucleotide polymorphisms (SNPs) that can be amplified in fragments less than 100 bp in size, which is smaller than most STR markers. It is, however, essential to analyse relatively large numbers of SNPs (50 to 100) to reach the

same evidential value that is achieved by a 10 to 16 STR profile. This is because SNPs are individually less polymorphic than multiallelic STRs (Gill et al. 2004). Another limitation is the difficulty in resolving mixtures, since most SNPs are biallelic. One way of overcoming this disadvantage is to target the rarer triallelic SNPs (Phillips et al. 2004). They are considered today more as complementary to STRs, rather than an alternative for identification (Butler 2011).

Table 1.2 Different types of DNA markers for identification purposes.

DNA targets	Target sequence length	Advantages for forensic applications	Disadvantages for forensic applications
Minisatellites including PCR-compatible loci e.g. D1S80	≈ 400 bp to 30,000 bp	Highly polymorphic	Low resistance to DNA degradation: large DNA targets, large input material requirement (difficult to PCR) Lengthy operational time
Traditional forensic STR	≈ 100 bp to 400 bp	Moderate resistance to DNA degradation: relatively small DNA targets Highly polymorphic	Polymorphism based only on target size
Mini-STR	≈ 50 bp to 280 bp	Higher resistance to DNA degradation: small DNA targets Highly polymorphic	Polymorphism based only on target size Fewer makers can be simultaneously detected by CE due to overlapping size ranges
SNP	Can usually be detected in amplicons less than 100 bp	High resistance to DNA degradation: small DNA targets Some specific SNPs can be used for geographic provenance prediction and phenotype prediction	Moderately polymorphic low discrimination per locus as typically biallelic

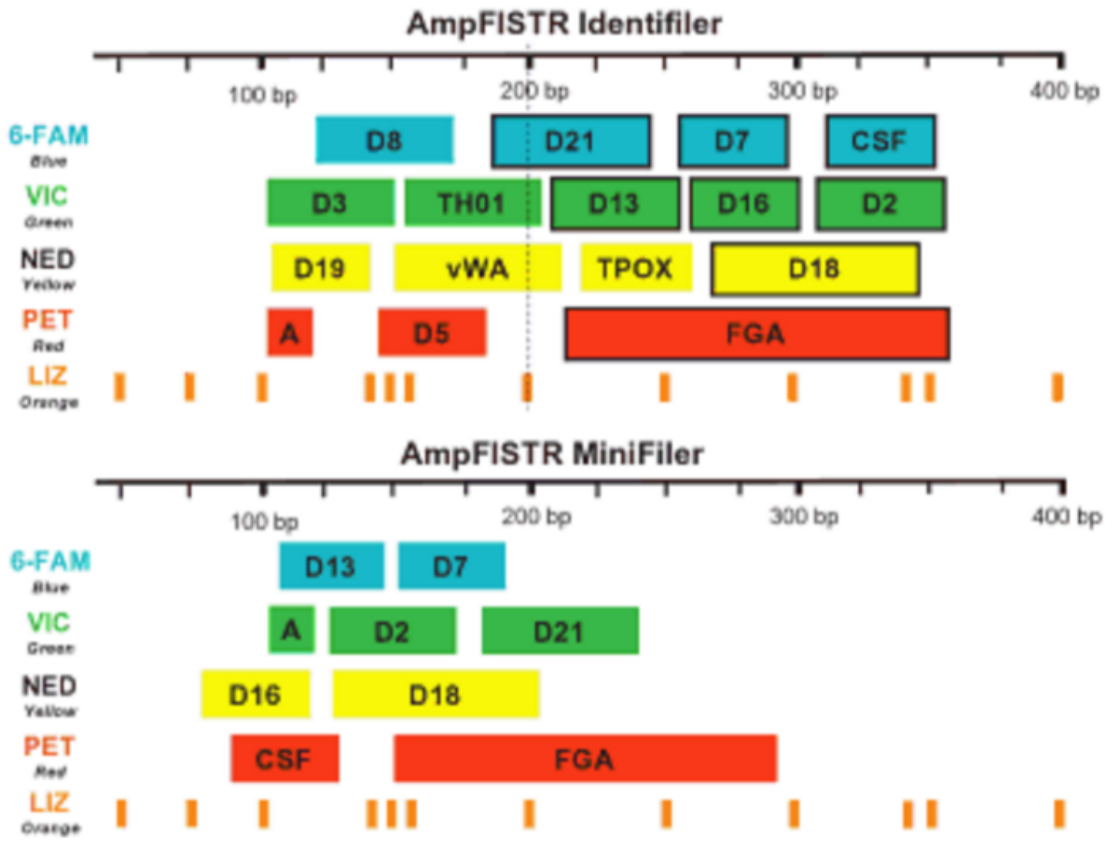

Figure 1.13 miniSTR multiplex kit.

An illustration showing reduction in amplicon sizes between standard STR and miniSTR multiplex kits (Butler 2011).

Among other ways of tackling degraded DNA is the use of a DNA polymerase combined with a "PreCR repair mix" that may allow repair and amplification of abasic, nicked and cross-linked DNA (Nelson 2009). One of the most efficient strategies to analyse both degraded and low-template DNA is to turn away from nuclear DNA and target the significantly more abundant mtDNA. While two copies of the nuclear genome are contained within a single cell, mtDNA is found in 200 to 1700 copies depending on the tissue type (Holland and Parsons 1999). This abundance increases the probability of detection in low-template DNA analysis and decreases the probability of loss through complete degradation. MtDNA analyses of challenging samples have improved rates of success. For example, 75% of mtDNA analyses from hair yield satisfying results (Pfeiffer et al. 1999). MtDNA sequencing from exploded pipe bombs allowed correct individual designations 50% of the time, and successfully classified

19% of bomb samples into groups that generated the same mitochondrial haplotype (Foran et al. 2009). As mentioned above, mtDNA is uniparentally inherited (though through the mother) without recombination. This reduces its power of identification, as only mutations that are shared down the maternal lineage contribute to its specificity. On the other hand, this also allows for efficient ancestry tracing and kinship evaluation. The mtDNA mutation rate exceeds that of nuclear DNA by at least 10-fold (Butler 2011). In some parts of the mtDNA genome, mutation rate is so high that sequences coming from the same individual can differ, especially at the sites that are most commonly mutated (mutation hotspots). Strict guidelines have been developed to overcome this issue, which is referred to as heteroplasmy (Scientific Working Group on DNA Analysis Methods (SWGDAM) 2015). Though heteroplasmy can cause problems through being mistaken for DNA mixture, shared heteroplasmy between samples can increase the evidential value when testing for maternal relationships (Ivanov et al. 1996). Figure 1.14 summarises the commonly used forensic DNA markers and their properties.

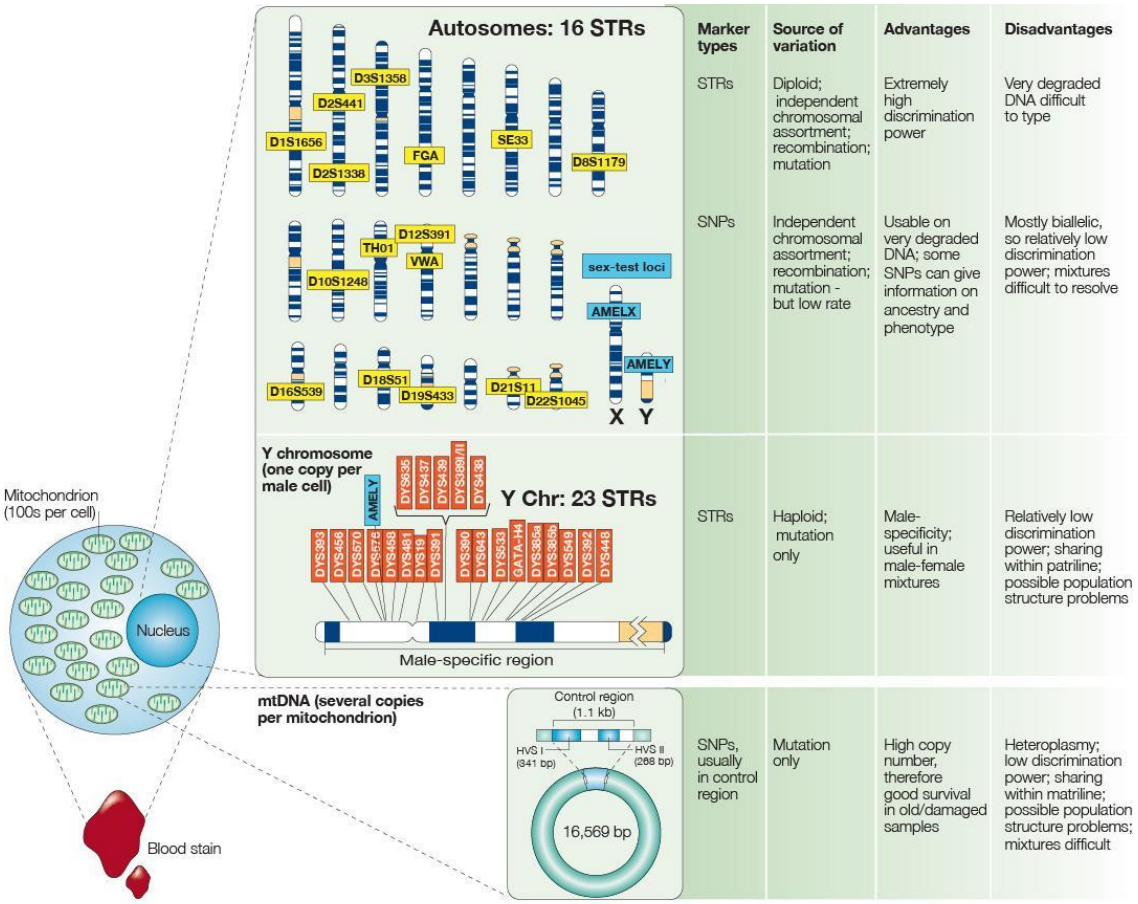

Figure 1.14 Summary of the commonly used forensic DNA markers.

Here, the autosomal STRs included in the NGM Select multiplex, and the Y-STRs of PPY23 are shown – both of these kits are used in this project. Figure adapted from Jobling and Gill 2004.

1.4.4.C The development of massively parallel sequencing approaches in forensic genetics

The desire for producing more genomic data faster and less expensively led to the development of new technologies, collectively known as Next Generation Sequencing (NGS), or, more informatively, Massively Parallel Sequencing (MPS). These methods have in common the property that millions or billions of sequencing reactions are carried out in parallel, and have greatly increased throughput, allowing whole human genomes to be sequenced rapidly and affordably (Goldfeder et al. 2017). Since the introduction of the first MPS platform in 2005 (Roche 454), developments have revolutionised genetic research and established the application of MPS to human

clinical diagnostics (Rehm et al. 2013). Ancient DNA analysts whose samples are also always degraded soon adopted the method and realised breakthroughs such as the complete Neanderthal mtDNA sequence (Green et al. 2010). In the forensic context, MPS allows the simultaneous sequence analysis of all the previously described markers in one experiment (autosomal and Y STRs/miniSTRs, mtDNA and SNPs) henceforth reaching maximal evidential value. Its power of identification also increases by revealing the internal sequence variations of alleles that otherwise would not be differentiated based only on their lengths (Børsting and Morling 2015). For example, this is the case for STR D21S11, which comprises four different alleles of equal size with varying repeat-block conformations (Butler 2011). Uncovering internal sequence variations could also help in resolving complex mixtures especially when combined with a quantitative analysis of allelic reads. Since detection of a locus is via its sequence only, there is no need to avoid overlapping lengths in fragments within a multiplex. This means that fragment sizes can be kept to a minimum, in order to maximise performance from degraded templates. The sensitivity of MPS-based technologies was shown to be comparable to that of post-PCR CE, with the generation of well-balanced complete 18-STR autosomal profiles starting with 250pg input DNA, and complete to nearly complete profiles starting with 62 pg (Zeng et al. 2015). The high coverage (number of sequences covering each nucleotide position) of MPS plays in favour of its reliability and reproducibility. Bioinformatics is a crucial support for MPS because of the amount of data produced (Butler 2011).

1.5 Aims and Objectives

This project intended to illustrate and measure the consequences of losing genetic information due to crimes or accidents that involve fires and/or explosions. Experiments were designed to mimic such conditions in order to identify temperatures that would degrade DNA in biological stains on one hand and the types of explosives that are most detrimental to the genetic material on the other. The loss of the genetic

information caused by such extreme conditions was assessed through typing and sequencing SNPs and STRs using Capillary Electrophoresis and Massively Parallel Sequencing. Consequences of resulting partial matches on the strength of evidence were then illustrated through a Bayesian approach, the simulation of allelic dropouts and its effects on DNA databases and the interpretation of Mitochondrial DNA evidence from real casework that involved fire as part of a homicide.

Chapter 2 Materials and Methods

2.1 Materials

2.1.1 Samples and Ethical Approvals

- The final version of ethical clearance allowing the collection and use of all this study's sample types was obtained on 16/04/2015, from the Ethics Committee at the University of Leicester (mek12-c7af).
- For the preliminary database, saliva was collected from 22 co-workers (13 males and nine females), aliquoted and stored in NDS buffer (EDTA, Tris base and N-lauroylsarcosine, pH=9).
- Buccal cotton swabs (Euroturbo, Deltalab) were collected from eighteen additional donors (13 males and five females) throughout the project whether to be added in the elimination database or for reference during the experiments that were carried up overseas.

2.1.2 Instruments and Apparatus

- Low Copy Number Hood
- Level-2 laminar-flow hood
- Airflow incubator, heat block and water bath
- Centrifuge and microcentrifuge
- Vortexer
- Analytical Balance
- UVC 500 Ultraviolet Crosslinker (Hoefer)
- Agarose gel tray, comb, tank, and power generator
- Qubit 2.0 fluorometer (Invitrogen)
- 7500 Fast Real-Time PCR thermal cycler (Applied Biosystems)
- Veriti® thermal cycler (Life Technology)
- DNA Engine Tetrad® 2 (Bio-Rad)
- Applied Biosystems® 3130xl Genetic Analyzer
- MiSeq 500 FGx Sequencer (Illumina)
- Electric convection oven (Heraeus® T 6030)
- Industrial digital thermometer (6802 II, Bestone Industrial LTD)

2.1.3 Reagents and Enzymes

- 11xPCR buffer (Tris HCl pH 8.8, Ammonium Sulphate, $MgCl_2$, 2-mercaptoethanol, EDTA pH 8.0, dATP, dCTP, dGTP, dTTP, BSA Ambion).
- Kits:
    - QIAamp® DNA Mini and Blood Mini (Qiagen)
    - Qubit® dsDNA HS Assay (Invitrogen)
    - Quantifiler® HP and Trio (Applied Biosystems)
    - AmpFLSTR® NGMSElect® (Applied Biosystems)
    - PowerPlex® Y23 (Promega)
    - PowerPlex® Fusion 6C (Promega)
    - ForenSeq® DNA Signature Prep (Verogen)
    - TruSeq® DNA PCR-Free LT Sample Prep Set A or B (Illumina)
    - PowerSeq® Systems, Auto/Y/Mito and Mito Nested System Prototypes (Promega)
    - GeneRead® Size Selection (Qiagen)
    - GeneRead® DNA Library Prep I (Qiagen)
    - MiSeq® Reagent kit v3 (600 cycles, Illumina)
- Molecular Biology Grade water (Sigma-Aldrich)
- Absolute Ethanol prepared at the University of Leicester (95%)
- Agarose (Sigma-Aldrich, powder form)
- Tris/Borate/EDTA buffer
- Ethidium Bromide (Sigma, 10 mg/mL)
- Proteinase K (20 mg/mL)
- EDTA
- N-lauroylsarcosinate
- Salmon Sperm DNA (Sigma, 1 µg/µL stock)
- TE buffer (10 mM Tris-HCL, pH 7.5: 0.1 mM EDTA)
- Low Copy Number extraction buffer (0.01% [w/v] SDS; 10 mM EDTA; 100 mM NaCl, pH 8.0)
- Non-acetylated BSA (Thermo Fisher)
- TaqMan® Universal Master Mix II, no UNG (Thermo Fisher)
- 2M NaOH (molecular biology-grade)

2.1.4 Plasticware and Membranes

- Amicon Centrifugal Filters (Ultra-0.5 and Ultra-4)
- Microcon filters (50 and 100)
- Tubes (0.2, 1.5, 1.7, 2, 25, 50 mL)
- DNA LoBind tubes (1.5 mL, Eppendorf)
- 96-well plates and septa
- Optical qPCR Seal (Thermo Fisher)
- 0.1–10, 1–200 and 100–1,000 µL pipette tips

2.1.5 Oligonucleotides

Oligonucleotide primers were synthesized by Sigma-Aldrich. Purification of oligonucleotides was by the desalting method.

- Mitochondrial DNA degradation assessment multiplex, designed at the University of Leicester:

Label	Sequence
mt804-F	(5′- CCCCACGGGAAACAGCAGTGAT- 3′)
mt900-R	(5′- CGGTGGCTGGCACGAAATTGAC- 3′)
mt2326-F	(5′- ACAATGGGGCTCACTCACCCAC- 3′)
mt2655-R	(5′- TGCTGTGTTGGCATCTGCTCGG- 3′)
mt12002-F	(5′- TCTCCTCCGCATAAGCCTGCGT- 3′)
mt12238-R	(5′- AGCTGAACCCTCGTGGAGCCAT- 3′)

- Mitochondrial DNA covering the HVSI and HVSII regions, designed at the University of Leicester:

Label	Sequence
Mt15999-F	(5′- CACCATTAGCACCCAAAGCT- 3′)
Mt409-R	(5′- CTGTTAAAAGTGCATACCGCC- 3′)

- Mitochondrial DNA Real-Time PCR, designed at Penn State University:

Label	Sequence

mtND1-F	(5′- CCCTAAAACCCGCCACATCT- 3′; IDT)
mtND1-R	(5′- GAGCGATGGTGAGAGCTAAGG T- 3′; IDT)
mtND1- MGB-NFQ probe	(5′- VIC-CCATCACCCTCTACATC-MGB-NFQ- 3′; Thermo Fisher)
mt8154 Fa	(5′- GGGTATACTACGGTCAATGCTCTGA- 3′; IDT)
mt8436 Ra	(5′- GTGATGAGGAATAGTGTAAGGAGTATGG- 3′; IDT)
mt8345- MGB-NFQ probe	(5′- FAM-CCAACACCTCTTTACAGTGAA-MGB-NFQ- 3′; Thermo Fisher)

2.1.6 Software

- Statistical treatment of data was done using **Microsoft® Excel** 2016 and **R**. All plots were made using **R** (R Core Team 2013).
- Primer design was performed using **MPprimer**: biocompute.bmi.ac.cn/MPprimer/ (Shen et al. 2010).
- The designed primers quality was assessed using **Autodimer**: nist.gov/dnaAnalysis/primerToolsPage.do.
- The specificity of the PCR reaction was tested using the Basic Local Alignment Search Tool (**BLAST,** https://blast.ncbi.nlm.nih.gov/Blast.cgitool).
- Potential non-specific primer binding locations were screened for using the University of California Santa Cruz (**UCSC**) **In-Silico PCR** (genome.ucsc.edu/cgi-bin/hgPcr).
- Reverse-complement was converted through: **bioinformatics.org**/sms/rev_comp.html.
- Real-Time PCR data were analysed using **High Resolution Melt (HRM)** Software v2.0 (Wittwer 2009).
- Mitochondrial DNA Sanger sequences were aligned to the revised Cambridge Reference Sequence (rCRS) and analysed using **CodonCode Aligner version 4.2.7** (**CodonCode** Corporation, www.codoncode.com)
- Y-STR profiles were analysed by **GeneMapper® ID** v4.0 (Life Technologies)
- Autosomal STRs profiles were analysed by **GeneMapper® ID-X** v1.5 (Life Technologies).

- Autosomal and Y-STRs as well as identity informative SNPs were analysed using the **Universal Analysis Software (UAS)** developed for the ForenSeq® DNA Signature Prep kit (Verogen).
- Autosomal and Y STRs from **PowerSeq®** (Promega) were analysed using **STRait razor** v2. 0 (Warshauer *et al.* 2015).
- A manual analysis of the **PowerSeq®** Mito Control Region (10-Plex) was performed through a **Linux** based terminal, followed by analysis on the **GeneMarker® HTS** (Holland *et al.* 2017).
    - Manual analysis:
        - Data QC and Pre-processing: initial data quality using **FastQC**, followed by the trimming/removal of poor-quality bases/reads and removal of adapter sequences using **Trimmomatic** (Bolger et al. 2014).
        - The reads were then aligned to the rCRS through the **Burrows-Wheeler Alignment tool** (**BWA,** http://bio-bwa.sourceforge.net/bwa.shtml) (Li and Durbin 2009), followed by BAM refinement using the **Genome Analysis Toolkit** (**GATK,** http://www.broadinstitute.org/gatk/) and **Picard** scripts (http://picard.sourceforge.net/command-line-overview.shtml), and Variant Calling/filtering using **SAMtools/VTOL's** (http://samtools.sourceforge.net/samtools.shtml, http://vcftools.sourceforge.net/).
        - The BAM files were visualized via **IGV 2.3** (https://software.broadinstitute.org/software/igv/)
        - The VCF files were generated from BAM files by **SAMtools Software 1.3.2** (http://samtools.sourceforge.net/)

2.2 Methods

2.2.1 Sample Preparation and Collection

The study had the relevant ethical clearance from the Ethics Committee at the University of Leicester (mek12-c7af obtained on 16/04/2015).

Discussion of Samples Choice

- Native human DNA samples were chosen rather than DNA extracts or animal tissue to match realistic scenarios as closely as possible.
- Although the double swab technique is commonly used (one wet swab followed by one dry swab), wet swabbing (200 µL) was preferred for dried stains over the double swab as the entire stain could be concentrated on one swab and submerged in the extraction reagents (AL buffer, proteinase K).
- Context dependent decisions are expected to be made when latent fingerprints are detected in order to establish priorities between DNA analysis and fingerprint examination.

2.2.2 DNA extraction

DNA was extracted from control samples from blood (2, 5, 10, and 30 µL) and saliva (200 µL) using the QIAamp® DNA Mini and Blood Mini commercial kit, following the manufacturer's recommended protocols.

DNA extractions from degraded samples were done via the QIAamp® DNA Investigator commercial kit, following the manufacturer's recommended protocols.

2.2.3 Quantification of DNA samples

DNA concentrations of control samples were determined by fluorescence, using the Qubit 2.0 Fluorometer, following the manufacturer's protocols.

For experimental samples, concentrations were determined using real-time PCR and the Quantifiler Trio kit (Thermo Fisher), according to manufacturer's protocols.

2.2.4 Agarose gel electrophoresis

0.8% (w/v) (for PCR products > 0.8 kb in size) or 1.6 – 1.8% (w/v) (for PCR products < 0.8 kb in size) agarose gel were prepared in 1× TBE containing 0.5 µg/ml EtBr. Gels were immersed in a TBE-filled gel running tank. ΦX174 and/or λ DNA markers were diluted in loading dye (10 mM EDTA pH 8.0, 1 mg/ml xylene cyanol FF, 1 mg/ml bromophenol blue) to give an amount of 50 ng of the 1078 bp band of ΦX174 and/or 9416 bp band of λ DNA when loading 6 µL of marker mixture. In cases requiring a ΦX174 and λ DNA-marker mix, both were mixed together in loading dye (each marker 1:1:2 loading dye:8 dH_2O) to give the same overall concentration of each marker. To

check PCR amplicons, finished gels were visualized under UV light (λ ~302 nm) and captured using the GeneGenius Gel Imaging System.

2.2.5 Purifying PCR products for sequencing

Each amplicon was excised from the gel using a blue-light trans-illuminator (Dark Reader™), and a Zymoclean™ Gel DNA Recovery Kit was used for purification using the manufacturer's protocol. To purify a batch of PCR amplicons, the E.Z.N.A.® Cycle-Pure Kit was used as per the manufacturer's protocol. Any product which failed to purify by this column kit was purified by gel excision. Purified DNA was finally diluted with dH_2O or 5 mM Tris-HCl to 10 ng/µL concentration.

2.2.6 Sequencing reactions

Purified PCR product was prepared for a sequencing reaction (total volume 20 µL/reaction) using the manufacturer's protocol and an input 20-30 ng/kb of purified DNA. The sequencing protocol was run using manufacturer's conditions. After the sequencing reaction, excess dye removal was performed by this protocol:

1) Add 2 µL of 2.2% (w/v) SDS and mix
2) Incubate in PCR machine: 98 °C-5 min, 25 °C-10 min
3) Use Performa® Gel Filtration Cartridge under the manufacturer's protocol

Finally, the ready reaction was then run on an Applied Biosystems 3700 Genetic Analyzer by the Protein and Nucleic Acid Laboratory of the University of Leicester (PNACL), and data returned via email.

2.2.7 Y-STR typing

23 Y-STRs (DYS576, DYS389I/II, DYS448, DYS19, DYS391, DYS481, DYS549, DYS533, DYS438, DYS437, DYS570, DYS635, DYS390, DYS439, DYS392, DYS643, DYS393, DYS458, DYS385a/b, DYS456 and Y-GATA-H4) were typed using the Promega PowerPlex® Y23 PCR reaction kit following the manufacturer's protocol. PCRs were prepared in a total volume of 25 µl/reaction. Genomic DNA was diluted to 1 ng/µl and 0.5 ng taken per reaction. When not using PCR product immediately, it was stored at -20 °C. One microlitre of PCR product was prepared to run on an Applied Biosystems 3130xl Genetic Analyzer capillary electrophoresis apparatus by adding 1 µl of CC5 Internal Lane Standard 500 Y23, 10 µl of Hi-Di™ formamide in each well according to the manufacturer's protocol. The ready-to-run product in 96-well plates was then denatured in a PCR machine at 95 °C for 3 minutes,

then immediately chilled on crushed ice or a freezer plate block or in an ice-water bath for 3 minutes. This process was done just prior to loading the instrument. The product was run through a 36 cm electrophoresis capillary filled with POP-4® polymer in the ABI 3130xl Genetic Analyzer, using an injection voltage of 1-3 kV; fluorescent emission was detected via a CCD camera. Following the run, the run data were analyzed using GeneMapper® ID v.4.0 Software.

2.2.8 Autosomal STR typing

The protocol for typing Autosomal STRs was similar to that described above, except the NGMSElect® kit (Thermo Fisher) was employed to analyze the STRs D3S1358, vWA, D16S539, D2S1338, D8S1179, D21S11, D18S51, D19S433, TH01, FGA, D10S1248, D22S1045, D2S441, D1S1656, D12S391, and SE33, plus the sex-test marker Amelogenin, following manufacturer's PCR protocols. The internal lane standard used was LIZ-500.

2.2.9 Mitochondrial DNA Multiplexes

Mitochondrial DNA degradation assessment multiplex, designed at the University of Leicester:

Table 2.1Mitochondrial DNA multiplex.

Reagents	Volume per sample (µL)	Final [C] per sample
11x PCR buffer	0.9	1x
dH_2O	7.82	NA
1 M Tris base	0.125	12.5 mM
20:1 Taq:Pfu polymerase mix	0.06	0.03 U/µL Taq, 0.0015 U/µL Pfu
10 µM primer pair 1 (F and R)	0.3 (x2)	3 µM
10 µM primer pair 2 (F and R)	0.3 (x2)	3 µM
10 µM primer pair 3 (F and R)	0.3 (x2)	3 µM
20 ng/µl genomic DNA	0.5	20 ng/µL (when possible)
Total PCR volume	11.205	NA

Table 2.2 HVSI and HVSII assay.

Reagents	Volume per sample (µL)	Final [C] per sample
11x PCR buffer	0.9	1x
dH_2O	7.82	NA
1 M Tris base	0.125	12.5 mM
20:1 Taq:Pfu polymerase	0.06	0.03 U/µL Taq, 0.0015 U/µL Pfu
10 µM primer pair (F & R)	0.3 (x2)	3 µM
20 ng/µL genomic DNA	0.5	20 ng/µL
Total PCR volume	10.005	NA

2.2.10 ForenSeq® MPS analysis

The ForenSeq® DNA Signature Prep Kit (Verogen) was used according to manufacturer's instructions to amplify the following markers, via DNA Primer Mix A:

Autosomal STRs: D1S1656, TPOX, D2S441, D2S1338, D3S1358 D4S2408, FGA, D5S818, CSF1PO, D6S1043, D7S820, D8S1179, D9S1122, D10S1248, TH01, vWA, D12S391, D13S317, PentaE, D16S539, D17S1301, D18S51, D19S433, D20S482, D21S11, PentaD, D22S1045

Y-STRs: DYF387S1, DYS19, DYS385a-b, DYS389I, DYS389II, DYS390, DYS391, DYS392, DYS437, DYS438, DYS439, DYS448, DYS460, DYS481, DYS505, DYS522, DYS533, DYS549, DYS570, DYS576, DYS612, DYS635, DYS643, Y-GATA-H4

X-STRs: DXS10074, DXS10103, DXS10135, DXS7132, DXS7423, DXS8378, HPRTB

Autosomal SNPs: rs10495407, rs1294331, rs1413212, rs1490413, rs560681, rs891700, rs1109037 rs12997453 rs876724, rs907100, rs993934, rs1355366, rs1357617, rs2399332, rs4364205, rs6444724, rs1979255, rs2046361, rs279844, rs6811238, rs13182883, rs159606, rs251934, rs338882, rs717302, rs13218440, rs1336071, rs214955, rs727811, rs321198, rs6955448, rs737681, rs917118, rs10092491, rs2056277, rs4606077, rs763869, rs1015250, rs10776839, rs1360288, rs1463729, rs7041158, rs3780962, rs735155, rs740598, rs826472, rs964681, rs10488710, rs1498553, rs2076848, rs901398, rs10773760, rs2107612, rs2111980,

rs2269355, rs2920816, rs1058083, rs1335873, rs1886510, rs354439, rs1454361, rs4530059, rs722290, rs873196, rs1528460, rs1821380, rs8037429, rs1382387, rs2342747, rs430046, rs729172, rs740910, rs8078417, rs938283, rs9905977, rs1024116, rs1493232, rs1736442, rs9951171, rs576261, rs719366, rs1005533, rs1031825, rs1523537, rs445251, rs221956, rs2830795, rs2831700, rs722098, rs914165, rs1028528, rs2040411, rs733164, rs987640.

Results were visualized and interpreted using the ForenSeq® Universal Analysis Software (UAS) v1.2.1, and the default settings.

2.2.11 Anti-Contamination Precautions

Much of the work undertaken as part of this research involved analyses that are often from a low copy number template. Precautions were taken throughout the study to minimize the probability of introducing contamination.

Elimination Database:

- The profiles were checked against a staff DNA database to detect any contamination introduced from individuals working in proximity.
- The autosomal and Y-STRs of all the relevant persons were typed and their mtDNA's control region sequenced as part of an elimination database to ensure that they did not inadvertently contaminated any samples.

Workspace Separation: Clean Room for Degraded DNA and LCN:

- Restricted access
- Personal protective equipment consisting of dedicated lab coat, face mask, hairnet, shoe protection, disposable gloves.

Controls:

- Positive and negative controls are used throughout each stage of the lab process to ensure that all methods are working as expected and any contamination, should it occur can be detected and traced to its source.
- Extraction blanks were included with each DNA extraction (1 blank per 23 extractions).

2.2.12 Data Analysis

Data analysis and statistical tests were carried out using the R programming language (R Core Team 2013), as was the production of graphs for figures.

Chapter 3 The Effects of High Temperature on Forensic DNA Analysis

3.1 Introduction

Temperature is defined as a measure of the average kinetic energy of a system's atoms and molecules (Sullivan and Edmondson 2008). It affects the quality and preservation of DNA in samples of biological origin. On one hand, warmth facilitates desiccation which in turn slows the decomposition of bodies and samples (DiMaio and DiMaio 2001; Fabre et al. 2017), and on the other it favours post-mortem or ex vivo decomposition processes (Bär et al. 1988) as high temperatures increase enzyme activity, chemical reaction rates and promote bacterial and fungal growth. As soon as an organism dies, it begins to decompose. The process starts with autolysis, where tissues are destroyed through the action of the body's own enzymes, and putrefaction, where endogenous and exogenous micro-organisms also break up the same tissue. By the time decomposition is visible to the naked eye, it had already affected the molecular level including the DNA (Parsons and Weedn 1997). The time since death, or Post-Mortem Interval (PMI), and environmental factors such as temperature, humidity, pH, and light are the main parameters that affect post-mortem decomposition (Mann et al. 1990).

High temperatures were found to accelerate the post-mortem decomposition of human bodies and subsequently that of DNA (Robins et al. 2001). An exception to this rule is encountered in the event of a natural mummification, where dry and hot climates lead to the histologic and cellular desiccation of the biomaterial and protect DNA from further degradation (Pääbo 1989). As the time since death or since the biomaterial exited a living organism lengthens, DNA degrades into smaller fragments resulting in the difficulty of reading long sequences (Cina et al. 1994). In the literature, this time interval was often combined with the sample's environing temperature. The discipline of forensic entomology measures the Accumulated Degree-Days (ADD), which is the temperature that was accumulated by the sample over the days, to estimate the PMI (Hall 2001). Because of the inverse relationship between DNA survivability and the PMI, Larkin et al. (2010) used ADD to estimate the survivability of DNA in pig muscles. Their study showed a sharp loss of the genetic material between 101 and 166

ADD, not considering other factors such as soil pH, relative humidity and light. Similarly, Allentoft et al. (2012) proposed a *post-mortem* DNA fragmentation theory through which the rate of DNA strand breaks- can be derived from the specimen's age, and its environing temperature. As shown in Table 3.1, the decay rates of DNA fragments of various lengths would then be directly linked to the ambient temperatures. Generally, the warmer it is, and the more time has passed between the sample deposition and its recovery, the more degraded DNA is expected to be. In addition to warmth, fluctuating temperatures were also found to be detrimental to DNA recovery (Matisoo-Smith and Horsburgh 2016). In this sense, Smith et al. (2003) concludes that the ability to successfully amplify DNA depends on the sample's *thermal age*, which is the mean temperature and the variation about this mean over time.

Table 3.1 Temperature dependent decay rates of mitochondrial DNA from bones.

Temperature	*Decay rate (k)* per site per year	Half-life (years) for 30 bp fragment length	Half-life (years) for 100 bp fragment length	Half-life (years), for 500 bp fragment length	Average fragment length (bp) at 10K years	Time (years) until average length = 1 bp
25 °C	4.5×10^{-5}	500	150	30	2	22,000
15 °C	7.6×10^{-6}	3,000	900	180	13	131,000
5 °C	1.1×10^{-6}	20,000	6,000	1,200	88	882,000
−5 °C	1.5×10^{-7}	158,000	47,000	9,500	683	6,830,000

Predictions of decay rates (k) of mtDNA in bone of various sizes at various temperatures. Damage rate (k) = 0.02 per site per year (2% of the bonds in the DNA backbone are broken. Reproduced from Allentoft et al. (2012).

The focus in this chapter is on temperatures that would compromise the quality of a biological sample in a matter of minutes, rather than DNA damage that occurs over the years. In other words, samples that experience shorter but more intense environmental insults.

One of the earliest studies of the impact of temperature on DNA analysis reported successful DNA "fingerprinting" of blood stains that had been incubated at 37 °C for several days, demonstrating that at least a proportion of Restriction Fragment Length Polymorphism (RFLP) targets several kilobases in length could survive this treatment

(McNally et al. 1989). However, Al-Kandari et al. (2016) reported a significant loss of quantifiable DNA from 50 µL of swabbed liquid blood and saliva, after 14 and 12 days of exposure at 37 °C and 55% humidity, respectively. Incubating human muscles (10 g) in water at 56 °C for 38 days resulted in an average amplifiable size of 200 bp (Maciejewska et al. 2012). The amplifiable fragment size distribution may, however, be biased, as double-strand breaks tend to occur within a pattern of cleavage in between nucleosomes, the protein structures around which ~200 bp of DNA are wrapped, and hence somewhat protected from degradation (McNevin et al. 2005). Two weeks of combined exposure to Texan summer temperatures (30-35 °C), solar radiation and atmospheric humidity, were not enough to prevent autosomal STR typing of 5-µL bloodstains (maximum amplicon length: 450 bp). It took four weeks for the first dropouts to show under the same conditions (Ambers et al. 2014). Outdoor crime scenes in the Arabian Peninsula can exceed 55 °C during the day (Al-Kandari et al. 2016). The effect of several days' exposure at this temperature on the collection efficiency of saliva, using a detergent-based buffer for swabbing and on subsequent DNA quantification from both saliva and blood, was tested by autosomal STR typing with a University of Central Lancashire designed quadruplex (Aloraer et al. 2015). Full quadruplex profiles were generated from dried saliva that was exposed to 50 °C for 48 h (maximum amplicon length ≅ 150 bp). However, there was no quantifiable DNA in either blood or saliva at days 14 and 17, respectively, after exposure to 55 °C and 41% humidity. These temperatures are representative of those that might be experienced by crime stains through natural climatic conditions; in the next section more extreme temperatures are considered.

3.1.1 The effects of "extremely" high temperatures on DNA

DNA degradation can be accelerated by higher temperatures as a result of criminal activity or disaster. One of the first applications of STR typing to Disaster Victim Identification followed the Texas Waco raid in 1993. Challenging search and recovery efforts led to the recovery of the remains of the 76 victims from the debris of a compound that was levelled by a fire and two explosions. The remains were highly fragmented and a Quadruplex plus Amelogenin assay was used to associate 61 human bones (2 g each) with the corresponding victims. Full profiles were obtained from 50 of these samples (82%), while six returned partial profiles (10%), and five did not provide

any genetic information (8%). The six partial profiles were characterised by loss of the larger amplicon(s) (Clayton et al. 1995; Graham 2006).

Table 3.2 Partial profiles from the Texas Waco investigation.

	Partial profiles						No result				
Sample type	Psoas muscle	L. fourth rib	L. fourth rib	Humerus	L. fourth rib	L. humerus	Rib	Rib	Humerus	Tibia	Muscle
Number of typed markers	4/5	3/5	2/5	1/5	2/5	3/5	0/5	0/5	0/5	0/5	0/5

Description (type of bone) and typing results obtained from the partial and failed profile during the Texas Waco investigation (Clayton et al. 1995).

The largest terrorist-related mass fatality incident in the history of the United States, known as the 9/11 attacks, occurred eight years after the Waco disaster. It presented one of the most challenging investigations as it subjected many of the victims' remains to temperatures above 1000 °C for a period of time. As a result, only 65% of the skeletal samples (8000 out of 13,000) produced interpretable STR profiles (Holland et al. 2003).

Nevertheless, other incidents involving fire or sources of high temperatures afforded a substantially higher genetic identification success. On November 20th 2000, a cable car caught fire in Kaprun, Austria, killing 155 persons and leaving their bodies badly burned with "cooked" internal organs. Everyone was genetically identified within 19 days post-incident, with 100% typing success from the victims' cardiac blood (Meyer 2003). Similarly, 92% of the skeletal remains from the American Airlines Flight 587 crash that occurred on November 12th 2001, produced interpretable STR profiles (Holland *et al. 20*03). More recently, on the morning of June 14th 2016, a fire broke out in a West London building known as the Grenfell Tower. The destructive fire that lasted for several hours, the co-mingling of remains, and the entrapment of whole families inside their flats precluded access to direct and indirect reference samples rendering the genetic identification of all victims an almost impossible task (Figure 3.1). Hronešová (2018) reported that DNA methods developed by the International

Commission on Missing Persons (ICMP) are being employed to identify the Grenfell Tower victims.

As part of their three years training, the INTREPID Forensics team practiced on fire investigations through a professionally simulated fire at the University of Leicester followed by a practical exercise to locate the origin and decipher the cause (Figure 3.2). As participants, we became familiar with the destructive nature of such events through the burning effects and the deposition of solid carbon (soot) on most items that would require identification.

Figure 3.1 Grenfell tower fire incident.

Photography showing the deadly blaze that engulfed the building (Victoria Jones/PA Images)

Figure 3.2 INTREPID Forensics training on fire investigation- University of Leicester.

Similarly to Figure 3.1, the simulated fire included burning flames (left image) and charred material (right image).

3.1.2 Which heat treatment would be of interest?

Spectroscopic analyses of heated DNA [50-900 °C, +10 °C/min.] demonstrated that the molecule's onset of thermal decomposition starts at 160 °C, with the largest weight loss occurring at 180 °C, and start of pyrolysis at 220-230 °C. However, about 50% of its residual weight was still detectable at 600 °C (50 to 600 °C +10 °C/min), which is significantly higher than the flame tips temperatures reported above (Alongi *et al.* 2015). As this study was mostly concerned with the molecule's structural changes and molecular weight loss, demonstrating its intumescent-like properties and hence its particular resistance to high temperatures, it did not test whether forensic DNA methods could be successfully applied after exposure to such high temperatures.
On the other hand, (Şakalar et al. 2012) discussed the effects of a wide range of temperatures on a crucial step in DNA analyses, which is PCR-amplification as measured by Real-Time quantitative PCR (qPCR). Moreover, the quantification test targeted the more sensitive (due to its higher copy number) mtDNA, at three different amplicon lengths (374, 290 and 183 bp), rather than the more degradation-prone nuclear DNA. Quantitative PCR reflects the amplifiabilty of DNA in a sample through the threshold cycle value (Ct) which is expected to increase as the concentration of intact DNA decreases with increasing the heat exposure. The steepest dip in DNA concentration was observed at temperature 120 °C for 30 minutes, while the sharpest rise in Ct occurred at 180 °C for the same amount of time (Figure 3.3). Remarkably, DNA was still detected at 150 °C but entirely lost at 200 °C (Figure 3.4). (Imaizumi et

al. 2014) reported compatible results, where short mtDNA fragments (128 bp) failed to amplify from compact bones after exposure to 200 °C for 30 minutes.

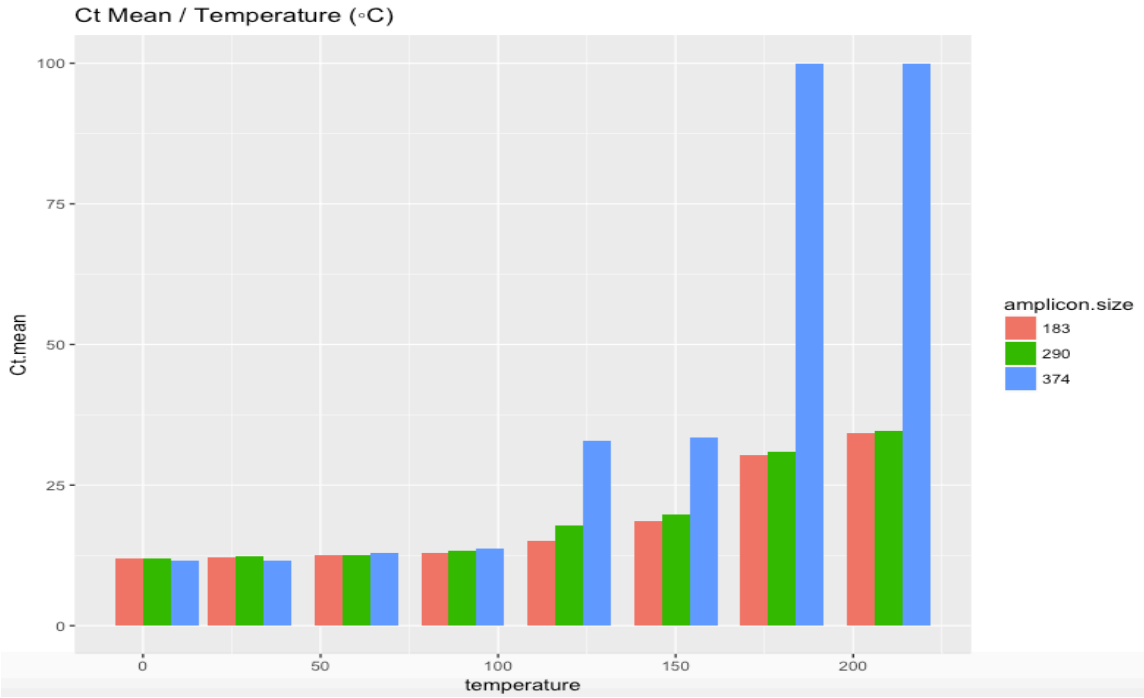

Figure 3.3 Amplification threshold (Ct) increasing with temperature treatment.

Histogram adapted from Şakalar et al. (2012) data showing the progressive increase in the mean amplification threshold (Ct) between the three mtDNA targets (183, 290 and 374 bp) with increasing temperature exposure for 30 minutes. A value of Ct=100 was assigned in case of no detection throughout the real-time PCR, indicating severe degradation. Triplicate amplifications were performed on seven dilution series for each target as standards.

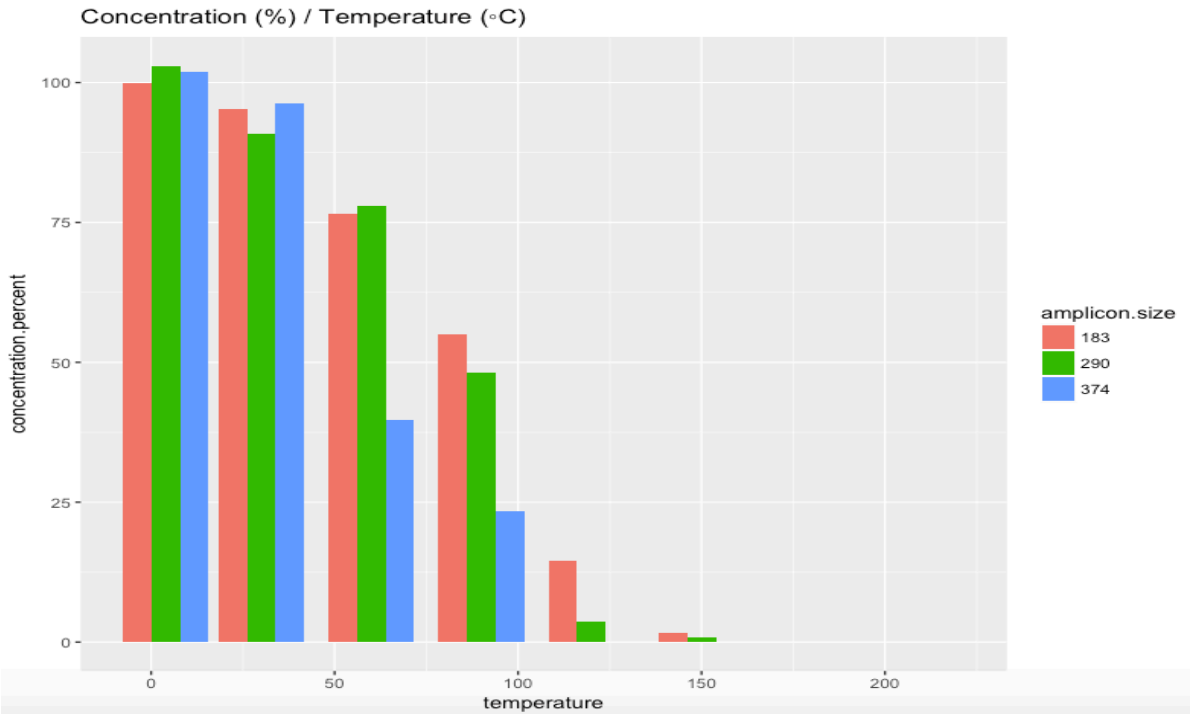

Figure 3.4 DNA concentration decreasing with temperature treatment.

Histogram adapted from Şakalar et al. (2012) data showing the progressive decline in the concentration percent (100% being 100 ng/µl), between the three mtDNA targets with increasing temperature exposure for 30 minutes. Same data as Figure 3.3.

3.2 Aims and Objectives

This chapter aimed at studying the effects of different temperature treatments on the DNA analyses from dried blood and saliva stains of specific volumes. To select experimental treatments, an exploratory approach was adopted starting with 140 °C for 30 minutes and ending with 200 °C for the same duration. One objective was to design a sensitive and robust mitochondrial DNA multiplex that assesses DNA degradation before subsequent typing. Another goal was to design an experiment that allows working with such samples and test the selected temperatures. This was followed by the swabbing of stains, DNA extraction, quantification, and typing using Capillary Electrophoresis-based methods and Massively Parallel Sequencing. The loss of genetic information was then assessed through the comparison of full profiles that were obtained from control samples, with partial profiles that resulted from degraded DNA samples. The last objective was to compare performances between Capillary Electrophoresis and Massively Parallel Sequencing.

3.3 Materials and Methods

3.3.1 Sample Collection

Three donors were selected based on their availability, a range of different ancestries (European, Middle-Eastern and Chinese) to maximise allele diversity, and the heterozygosity of their genotypes (two of them are heterozygous for all 17 autosomal STR loci). Heterozygotes are advantageous because they allow any drop-out to be easily recognised. Blood was withdrawn by a certified phlebotomist into EDTA-coated tubes and their saliva collected in 50-mL sterile tubes. The biological fluids were spread on glass microscope slides - initially 30 uL of blood or 200 uL of saliva - and left to dry to produce stains similar to those found in crime scenes. Bloodstains volume was then gradually reduced down to 2 uL to test the volume variation on DNA degradation. The donors provided written informed consent and all experiments were approved by the Ethical Review Board of Genetics at the University of Leicester (mek12-c7af)

3.3.1.A Heat Treatment

The stains were heated using a batch type cabinet-style convection heating/drying oven (Thermo Scientific Heraeus® T6030) with technical specifications described in Table 3.3. The 30-minute timer (s) was started after the samples were placed inside the oven and the desired temperature had been reached. The maximum time for the oven to regain the desired temperature after the door opening and closure was less than two minutes.

Table 3.3 Heating oven's technical specifications.

Temperature range: ambient to 300 °C
Spatial temperature deviation*: · ± 1.5 at 70 °C · ± 3 at 150 °C · ± 6 at 300 °C · ± 3 at 180 °C**
Temp. deviation over time: ⩽0.5 °C** *: The values stated apply to the unloaded oven in conjunction with the central wire mesh trays (measurement according to DIN 12880, Part 2), air flap closed. **: Value measured by the operator during the experiments.

3.3.1.B Temperature Measurements

A digital thermometer (with Thermocouple Sensors -50~1300 °C) was first tested by measuring the temperature of an ice bath against a mercury thermometer (0.1 °C ± 0.1). The sensor was then fixed on a glass microscope slide to mimic the stains' microenvironment and moved to establish temperatures at different times and in different locations inside the heating oven. A temperature difference of 20 °C was detected between the warmer base of the chamber (adjacent to the heat source) and the cooler middle rack placed inside the oven. All stains were placed on the middle rack once their assigned temperature was reached.

Four groups of stains were produced:

- Group 1(4 °C stains): Control stains kept at 4 °C.
- Group 2 (140 °C stains): heated at 140 °C for 30 minutes.
- Group 3 (180 °C stains): heated at 180 °C for 30 minutes.
- Group 4 (200 °C stains): heated at 200 °C for 30 minutes.

3.3.2 Recovery and DNA Extraction

The stains were recovered following a wet swabbing procedure: 200 µL of Molecular Biology Grade water (Sigma-Aldrich) were pipetted onto a sterile cotton swab prior to recovery of all visible parts of the stain into a 1.5-mL tube. DNA extraction was performed manually in a limited access pre-PCR environment using a silica adsorption method with two washes and a final elution volume in 100 µL (QIAGEN QIAamp® DNA Mini kit, DNA purification from swabs, spin protocol).

3.3.3 Quantification

3.3.3.A Fluorescence detection of double-stranded DNA

Extracts from the four groups of biological stains (n=70) were quantified by fluorescence detection on the Qubit® using the double-stranded (ds) DNA High Sensitivity (HS) kit (Thermo Fisher Scientific Inc 2016) Qubit®, Thermo Fisher Scientific Inc 2016). The assay has a linear detection range of 0.2–100 ng and is selective for dsDNA (90-98% accuracy) even in a solution predominated by single-stranded (ss) nucleic acid. The assay's accuracy and precision are reported in (Thermo Fisher Scientific Inc 2016). The samples' description is presented in Table 3.4.

Table 3.4 List of biological stains included in the Qubit® quantification.

Stain type	Donors	Temperature treatment			
Blood		4 °C	140 °C	180 °C	200 °C
	P02	5	0	8	2
	P09	4	3	5	5
	P22	4	2	4	4
Saliva	P02	2	2	2	2
	P09	2	2	2	2
	P22	2	2	2	2
Total	70 (46 blood + 24 saliva)				

3.3.3.B Real-Time PCR: Quantification of Nuclear DNA and Derivation of Degradation Index

Quantifiler Trio® Real-Time PCR was used to quantify DNA from the four groups of biological stains (n=57), to assess for PCR inhibition, and to generate sample specific degradation indices. The number of samples to quantify was influenced by the experimental costs and the plate size (n=96) knowing that a number of wells was dedicated to duplicated standards, samples, and negative controls. Where possible, the technical duplicates variability was compared to that of biological duplicates (see Figure 3.5). The assay is based on a TaqMan probe that keeps the fluorophore quenched until the 5´- 3´ exonuclease activity of the DNA polymerase (Holt et al.

2016) degrades the probe and separates the fluorophore from the quencher. The assay amplifies three different primate-specific nuclear DNA multi-copy targets: a 214-bp "large" locus (LH), an 80-bp small locus (SH), and a 75-bp male-specific locus (MH) whilst also amplifying an Internal PCR Control (IPC). PCR inhibition is suspected when the sample's IPC CT is larger than twice the standards' average ΔCT (Holt *et al* 2016). The Degradation Index is the ratio of SH:LH which, in degraded samples, is expected to be greater than one.

Table 3.5 List of biological stains included in the Real-Time PCR quantification.

Stain type and volume	Donors	Temperature treatment			
		4 °C	140 °C	180 °C	200 °C
Blood (30 µL)	P02	7	0	11	4
	P09	8	5	8	10
	P22	3	0	4	4
Saliva (30 µL)	P02	2	2	2	2
Total	57 (49 blood + 8 saliva)				

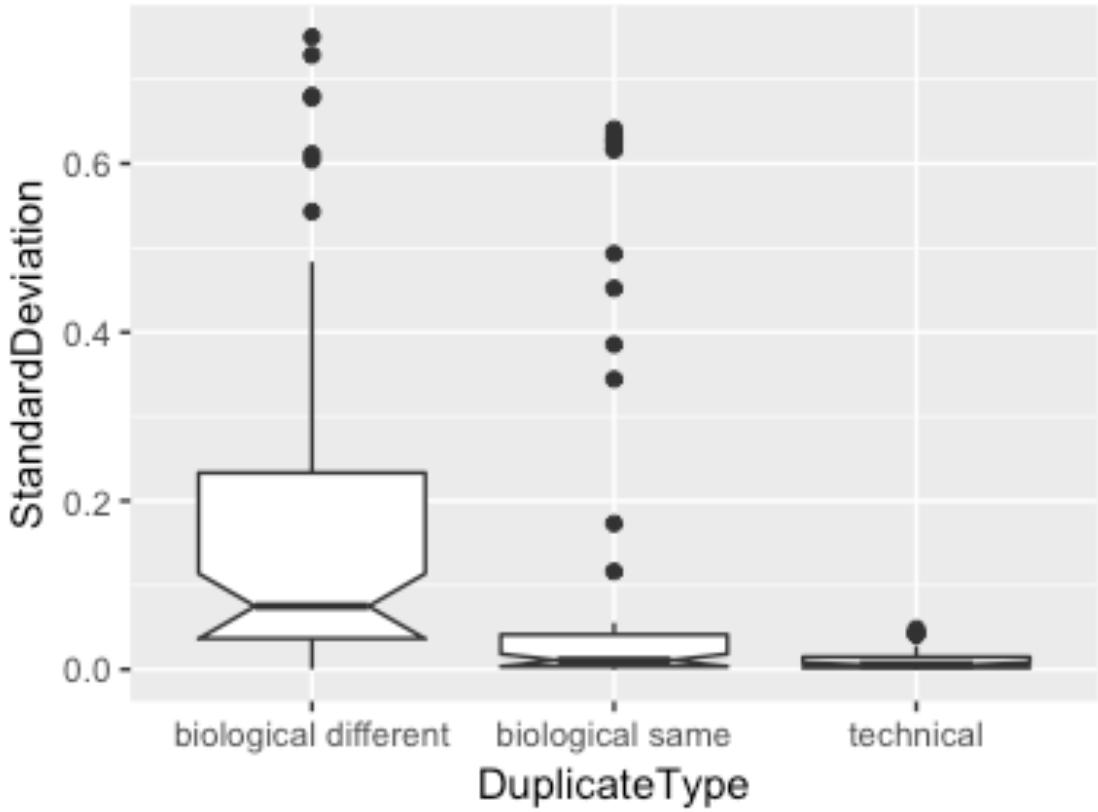

Figure 3.5 Biological v. technical replicates.

Standard deviations of technical and biological duplicates (64 standard deviations from each duplicate type were randomly selected in equal proportions from stains at 4 °C and at 180 °C). The technical duplicates are repeats from the same DNA extract/tube, while the biological duplicates are repeats from two different DNA extracts each coming from a stain of a similar type and volume. Biological duplicates are divided between same and different donors (Irizarry and Love 2014).

A serial decrease in blood stains volume from one donor was also DNA quantified, as described below (Table 3.6):

Table 3.6 List of blood stains of decreased volumes that were also DNA quantified via Real-Time PCR.

Stain type and volume	Donor	Temperature treatment	
		4 °C	180 °C
Blood (10, 5 and 2 µL)	P02	1	2
		1	2
		1	2
Total			9

3.3.4 Degradation assessment

A mitochondrial DNA multiplex assay was designed to assess amplification success of 837-bp (large), 330-bp (intermediate) and 97-bp (small) amplicons in a cost-efficient manner. The three targets were selected from the revised Cambridge Reference Sequence (rCRS) of the *Homo sapiens* complete mitochondrial genome (https://www.ncbi.nlm.nih.gov/nuccore/J01415.2?report=fasta). The targets do not overlap, and are located outside of the control region, thereby reducing the likelihood of polymorphic SNPs occurring within the primer annealing sites. The primers were designed on the MPprimer software (biocompute.bmi.ac.cn/MPprimer/) and their parameters verified through the NIST Online DNA Analysis tools (https://www-s.nist.gov/dnaAnalysis/primerToolsPage.do). The specificity of the reaction was tested using the Basic Local Alignment Search Tool (https://blast.ncbi.nlm.nih.gov/Blast.cgitool) and potential unintended primer binding locations were screened for by electronic PCR (genome.ucsc.edu/cgi-bin/hgPcr). The multiplex assay was capable of detecting mitochondrial amplicons at an untreated genomic DNA input equivalent to one diploid cell's content (≈6.6 pg, see Figure 3.6), as determined by serial dilution from a concentrated stock.

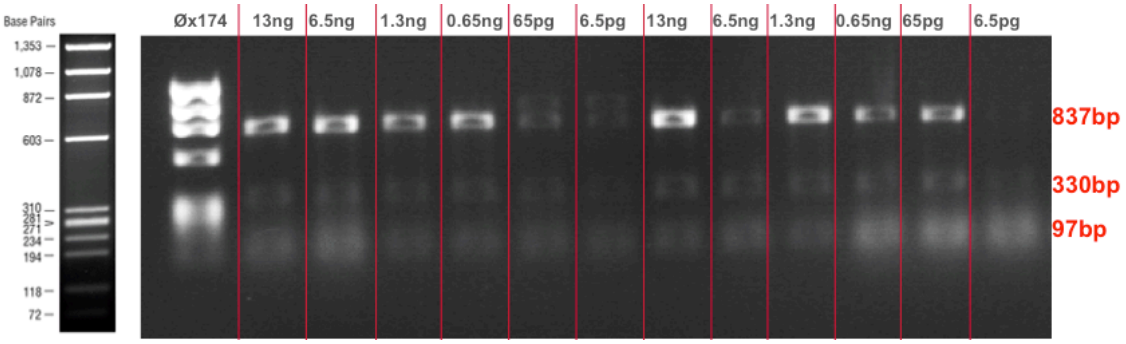

Figure 3.6 Sensitivity of the mitochondrial DNA multiplex.

Gel electrophoresis (2% Agarose in TBE) image illustrating the sensitivity of the method by showing the amplification of the three desired products at input DNA levels approaching one diploid cell input.

3.3.5 Forensic Typing/Sequencing

3.3.5.A Capillary Electrophoresis

DNA from the four groups of biological stains (n=47) were typed using a 23 Y-STR assay (PowerPlex® Y23, Promega). Of these samples, 31 were also typed using a 17

autosomal STR assay (AmpFLSTR NGMSElect®, Applied Biosystems). The number of samples typed through each assay was influenced by experimental costs and by an iterative process that depended on preliminary results. For example, testing the 140 °C stains was ceased once this temperature treatment showed full profiles of a quality that is comparable to their controls (n=6). On the other hand, saliva stains were soon replaced by blood stains once results between the two sample types did not show significant differences upon quantification and typing in relation to temperature exposure. The amplicon sizes within these two PCR/CE based assays range from 80 bp to 440 bp and were separated on an ABI 3130xl Genetic Analyzer. The resulting electropherograms were analysed using GeneMapper® v4 (for the Y data) and GeneMapper® ID-X v1.5 (for the autosomal data). The minimum thresholds used for reportable alleles was 50 rfu for homozygous loci and 25 rfu for heterozygous loci. Uncertainty of the smaller allele in case of heterozygous imbalance is reduced through the fact that the donors' profiles were known as part of this study's constructed database. Additionally, any peak height ratio larger than 7:3 for the same locus eliminated both alleles from further analyses. A detailed sample description is found in Tables 3.7 and 3.8.

Table 3.7 Stain types, donor origin, stain volume, temperature treatment and number of samples tested in the NGMSElect® autosomal STRs multiplex assay.

Stain type	Donors	Volume (µL)	Temperature treatment			
			4 °C	140 °C	180 °C	200 °C
Saliva	P02	30	1	2	2	2
Blood	P02	30	1	0	2	2
		10	1	0	2	0
		5	1	0	2	0
		2	1	0	2	0
	P09	30	2	2	3	3
	P22	30	1	0	1	1
Total						31

Table 3.8 Stain types, donor origin, stain volume, temperature treatment and number of samples tested in the PowerPlex® Y23 multiplex assay.

Stain type	Donors	Volume (µL)	Temperature treatment			
			4 °C	140 °C	180 °C	200 °C
Blood	P02	30	1	0	2	2
		10	1	0	2	0
		5	1	0	2	0
		2	1	0	2	0
	P09	30	2	2	3	3
	P22	30	1	0	1	1
Total						47

3.3.5.B Massively Parallel Sequencing

DNA Libraries from biological stains at 4, 180, and 200 °C (n=12, Table 3.9) were prepared using the ForenSeq® DNA Signature Prep kit (Plex A) and sequenced on the MiSeq FGx® machine. Stains treated at 140 °C were excluded from analysis as they did not produce partial profiles on CE-based typing. This system enables testing of 27 autosomal, 7 X-, and 24 Y-chromosome STR targets and a set of 94 identity informative SNPs (iSNPs). It relies on a PCR-based target enrichment before hybridization of adaptor tagged amplicons to complementary oligos for eventual sequencing by synthesis - base-by-base sequencing with imaging at each base incorporation. The results were analysed using Illumina's dedicated software (Universal Analysis Software-UAS). The X-STRs were excluded from the project for simplification purposes and comparability with the CE-based methods. The minimum thresholds used for reportable alleles were 29 reads for autosomal and Y-STRs (both homozygous and heterozygous loci), 14 reads for heterozygous identity informative SNPs and 20 reads for homozygous ones. These thresholds were developed by comparing results with known profiles included in the University of Leicester's database, and that were repeatedly typed using CE-based methods. Heterozygous imbalance was dealt with similarly to 3.3.5.A. As per the manufacturer's

recommendation, five microliters of 0.2 ng/µL input DNA totalling one nanogram was used where possible per sample. Table 3.10 lists the four samples that were quantified as less than 0.2 ng/µL.

Table 3.9 Stain types, donor origin, temperature treatment and number of samples tested in the ForenSeq®/ MiSeq FGx®.

Stain type	Donors	Temperature		
		4 °C	180 °C	200 °C
Blood	P09	1	2	1
	P22	1	2	1
Saliva	P02	1	2	1
Total				12

The volume was 30 µL for all stains-152 loci per profile

Table 3.10 Samples that were initially quantified at less 0.2 ng/µL through qPCR.

Sample name	Concentration (ng/µL) determined by Real-Time PCR	ForenSeq® run Input(ng)
P22 bloodstain at 4 °C	0.1	0.5
P22 bloodstain (a) at 180 °C	0 or < 0.01	<0.05
P22 bloodstain (b) at 180 °C	0 or < 0.01	<0.05

3.4 Results

3.4.1 Quantification

DNA concentrations of the various stain groups were obtained through fluorometry and qPCR. The Qubit® Fluorometry concentrations were plotted according to their temperature treatments (Figure 3.7) and show a generally declining trend from 4 °C to 200 °C, passing by 180 °C. The results show a reduction in quantifiable DNA from with increasing temperature, with most samples yielding below 500 pg/µL at 180 °C and values close to zero at 200 °C.

While the declining pattern is seen in the qPCR Long Human (LH, 214 bp) target concentration plot (Figure 3.8, left) the simultaneous quantification of the Small Human (SH, 80 bp) target sheds light on the sample's quality as the LH is significantly lower than SH in degraded samples because of strand breaks. This explains the few spikes of the SH concentration (Figure 3.8, right) that are observed for a number of 140 °C and 180 °C stains before totally declining back at 200 °C. Indeed, the stains at 180-200 °C that do not show a higher SH but rather extremely low LH and SH reflect the heavily degraded nature of samples where both long and short DNA targets were virtually eliminated.

The four outlier dots marked in red (Figure 3.8, left) represent SH concentrations from two blood stains from a single donor. Although they were treated at 180 °C for 30 minutes, they manifested less degradation compared to their counterparts that were similarly treated. Possible explanations for this discrepancy in DNA damage will be visited in the discussion.

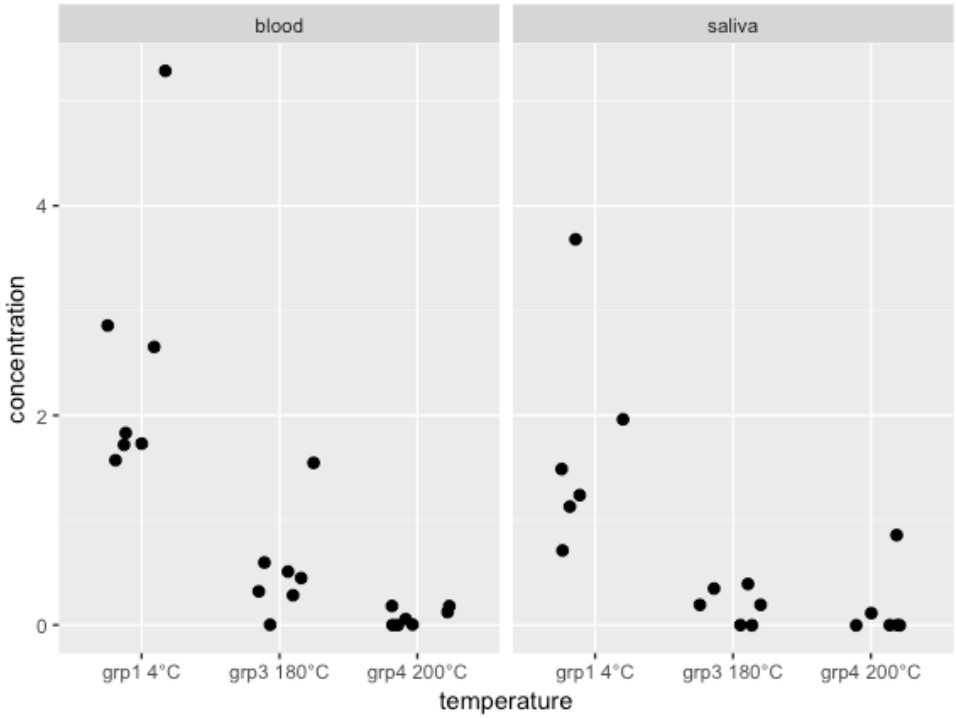

Figure 3.7 Sample concentrations (ng/µL) determined by Qubit® fluorometry.

The Qubit® dsDNA/HS assay was used to quantify the 4 °C (group 1), 180 °C (group 3) and 200 °C (group 4) saliva (n= 6; 30 µL per temperature) and blood (n=7; 30 µL per temperature) stains.

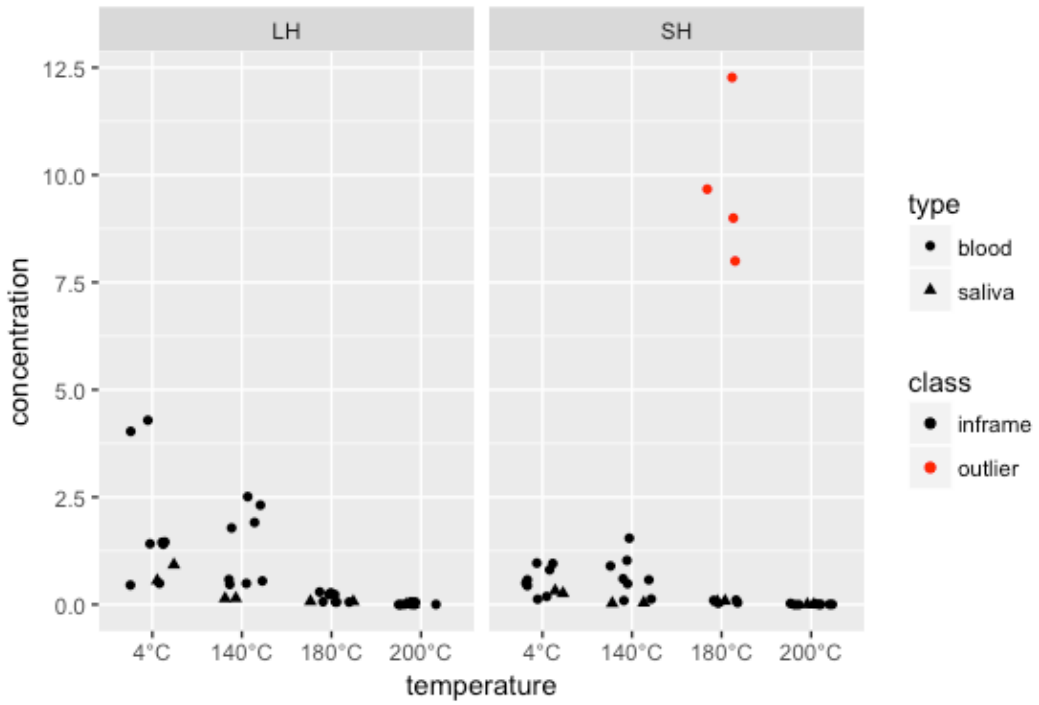

Figure 3.8 DNA concentrations derived from the four stain groups at volume 30 µL.

The Long Human (LH, 214 bp) and Small Human (SH, 80 bp) targets concentration plot, as obtained from the qPCR of blood (30 uL) and saliva (200 uL) stains at 4 °C (n_{blood}=3, n_{saliva}=1), 140 °C (n_{blood}=4, n_{saliva}=1), 180 °C (n_{blood}=3, n_{saliva}=1), and 200 °C (n_{blood}=3, n_{saliva}=1). The rise in SH concentration at 140 °C and 180 °C, compared to the 4 °C, can be explained by the start of degradation of the LH at these temperatures and therefore favouring the amplification of the smaller target. The outliers at 180 °C (SH between 7.5 and 12.5 ng) are from the two blood stains that showed more resistance to degradation, when compared to other stains exposed at the same temperature.

3.4.2 Degradation Assessment

A Degradation Index was computed for each measured concentration by dividing the short qPCR target by the long one:

$$DI = \frac{SH}{LH}$$

The DI logarithmic values were then plotted according to the stains' heat treatment to compare degradation levels between groups (Figure 3.9). All logDI values that are greater than zero (red dots) reflect degradation in a sample (DI>1). Other values (black dots) portray samples where their SH is smaller or equal to their LH are therefore "not degraded" according to this assay. However, the DI test is prone to false negatives

when samples are so degraded that both their LH and their SH are heavily affected: $DI \approx 1$ as in the 180 °C category. Similarly, the fact that SH was almost undetectable in the 200 °C stains ($DI \approx 0$) prevented the log DI analysis.

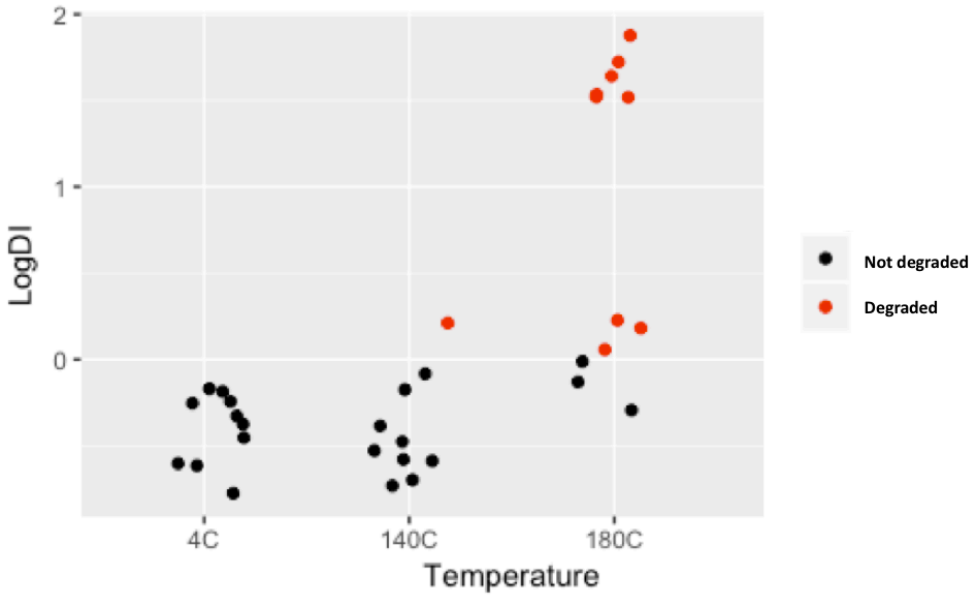

Figure 3.9 Log degradation index of stains at different temperatures.

Degradation Indices (log values) from the qPCR described in a scatter plot for blood (n= 4 stains of 30 µL per temperature) and saliva stains (n=2 stains of 30 µL per temperature) at 4 °C, 140 °C, and 180 °C. The samples that are associated with the highest Degradation Index at 180 °C (logDI = [1.5-2]) are the ones that produced the "outlier" concentrations in Figure 3.8 and the least number of dropouts upon subsequent typing/sequencing. This suggests that, for degraded samples, the Degradation Index values do not necessarily reflect the quantity of dropouts to be expected in typing.

The mtDNA multiplex assay (Figure 3.10) was designed to assess DNA degradation in a rapid and economical manner, before subjecting samples of questioned quality to subsequent high-cost typing/sequencing procedures. The method avoids the false negatives obtained by calculating DIs as it directly assesses the amplifiability of a short (97 bp), intermediate (330 bp) or long (837 bp) DNA fragment (Figure 3.10). The long fragment's loss in the control (4 °C) and 140 °C stains could be explained by a preferential amplification of the shorter targets (intermediate and short) until depletion of most of the PCR reagents. On a closer look however, this large amplicon can be visualised in the 140 °C stains and one of the 4 °C saliva stains. Importantly, this amplicon was lost in many control samples (not degraded) during this project.

However, the intermediate fragment's loss was only seen in the 180 °C and the 200 °C stains, which is consistent with their degraded state as observed in the DI assay. The shortest fragment (97 bp) was also lost in the 200 °C stains - but not in the 180 °C ones - which is consistent with the previous DI experiment that showed that both LH and SH degraded in the 200 °C stains.

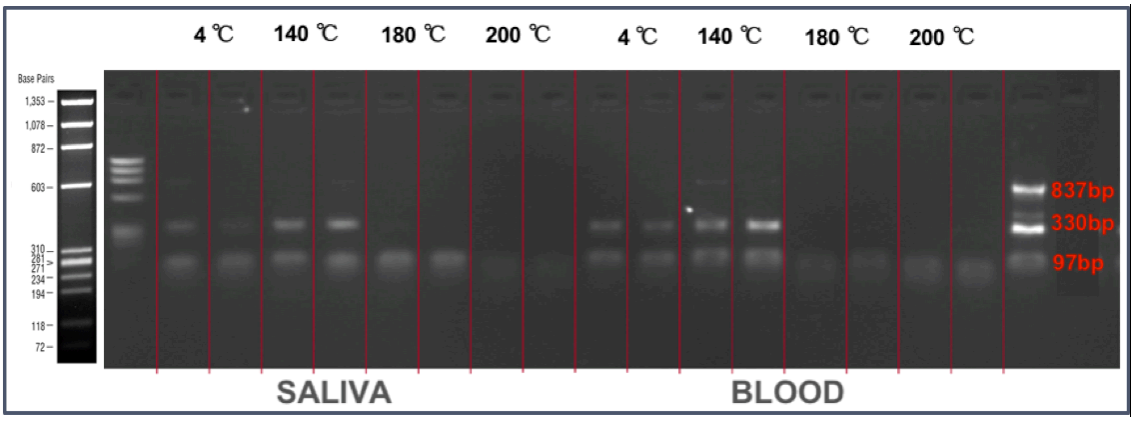

Figure 3.10 Mitochondrial DNA multiplex on stains at different temperatures.

Gel electrophoresis (2% [w/v] agarose) image showing the mtDNA multiplex applied to saliva and blood stains of different temperature treatments. Note the loss of the 330 bp amplicons at 180 °C and both the 330 and 97 bp amplicons at 200 °C.

3.4.3 Typing Results - Biological Stains Temperature Treatments

The measures used to assess how temperature affected the DNA profiles and their signal intensities are Relative Fluorescence Units (RFU) for the CE-based methods and Depth of Coverage (DoC) for the MPS. The amplicons were ordered from shortest to longest, and the signal intensity was divided by two for the homozygous markers for appropriate comparison with the heterozygous markers. The values were then plotted in order of amplicon length and a linear regression was performed to correlate the temperature with amplicon length (data analysis and graph production details in Chapter 2 'Methods').

3.4.3.A Capillary Electrophoresis-Based Techniques

Using NGMSElect® for autosomal-STRs and PowerPlex® Y23 for Y-STRs, full profiles were obtained through typing both the control (4 °C) and the 140 °C stains (Appendix 8.1: Tables 8.1.1 and 8.1.2). All stains within these two treatment groups generated electropherograms that were devoid of any ski-slope patterns or dropouts (Figure 3.15). Although the 140 °C stains' concentration values were lower than that of

their controls', none reached low-template DNA levels (<200 pg/µL). The decrease in RFU with increasing amplicon length is observed in both groups (4 °C and 140 °C) and could be explained by the preferential amplification of shorter fragments ending in a mildly right-tailed data. This phenomenon is more pronounced in the 140 °C stains, indicating a possible beginning of DNA degradation. The correlation between decreasing (RFU) and increasing amplicon size was tested to be statistically significant for the NGMSElect® results - F: 15.23 on 1 and 155 DF, p-value: 0.0001417 for the 4 °C stains; and F: 22.21 on 1 and 92 DF, p-value: 8.658e-06 for the 140 °C stains. The right-tailed pattern was more prominent in the PowerPlex® Y23 analyses with a stronger correlation between the two variables- F: 68.4 on 1 and 274 DF, p-value: 5.856e-15 for the 4 °C stains; and F: 138 on 1 and 44 DF, p-value: 3.708e-15 for the 140 °C.

The right-tailed pattern (or ski-slope effect) is however the most pronounced in the 180 °C stains showing the highest significance between RFU reduction and amplicon length, whether through the PowerPlex® Y23 kit (F: 76.67 on 1 and 258 DF, p-value: 2.716e-16), or through the NGMSElect® (F:197.4 on 1 and 276 DF, p-value: < 2.2e-16). Typing these stains DNA also produced partial profiles due to dropouts (Figure 3.11 and 3.12, green dots). All the 180 °C stains showed dropouts at variable degrees between samples; and these occurred at the higher molecular weight loci when considering each sample's electropherogram separately (Figure 3.13). This is consistent with DNA degradation and was also observed in the Waco disaster partial profiles. Most typed alleles did not exceed 250 bp in length, while the only longer amplicons (>250 bp) come from the two 180 °C blood stains that showed resistance to degradation. False homozygosity occurred when dropouts were limited to a single allele at a heterozygous locus, potentially misleading DNA examiners, while no information was retrievable following the loss of both alleles at a locus (appendix: Tables 11 and 12). Grouped together, these 180 °C stains showed 102 allelic dropouts (AD) out of 266 in total on typing with NGMSElect® (eight stains, 38.3% AD) and 151 AD out of 276 with PowerPlex® Y23 (nine stains, 54.7% AD). The 200 °C typing was the least successful, with no alleles for most stains except for two stains yielding one allele each, slightly above threshold: P02_200 °C (saliva) produced allele X at Amelogenin with rfu=50 and size 100 bp (Figures 3.11); and P22_200 °C (blood) produced allele 11 at DYS391 with rfu=57 and size 105 bp (Figure 3.12).

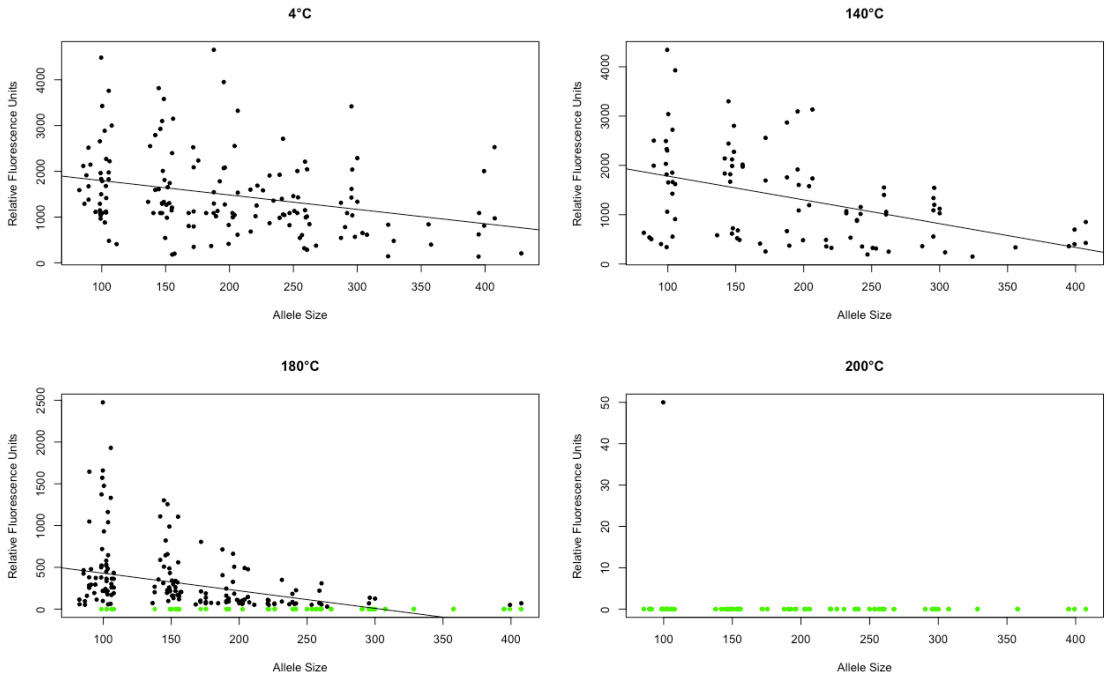

Figure 3.9 The effects of temperature on autosomal STR typing.

Typing results through NGMSElect® of four 4 °C stains and three 140 °C stains, with no dropouts (green dots), eight 180 °C stains that all produced dropouts (102 allelic dropouts out of 266 targeted alleles (38.3%)), and eight 200 °C stains with no profiles.

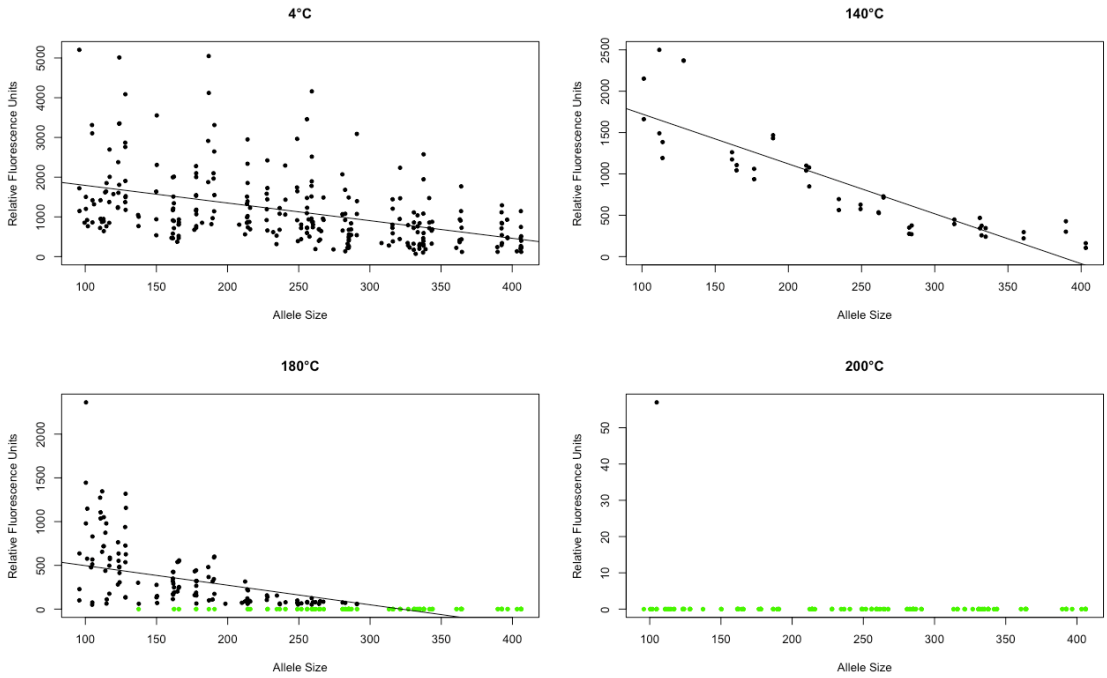

Figure 3.10 The effects of temperature on Y-STR typing.

Typing results through PowerPlex® Y23 of eight 4 °C stains and two 140 °C stains, with no dropouts (green dots), twelve 180 °C stains that all produced dropouts (151 allelic

dropouts out of 278 targeted alleles (54.3%)), and eight 200 °C stains that produced no profiles.

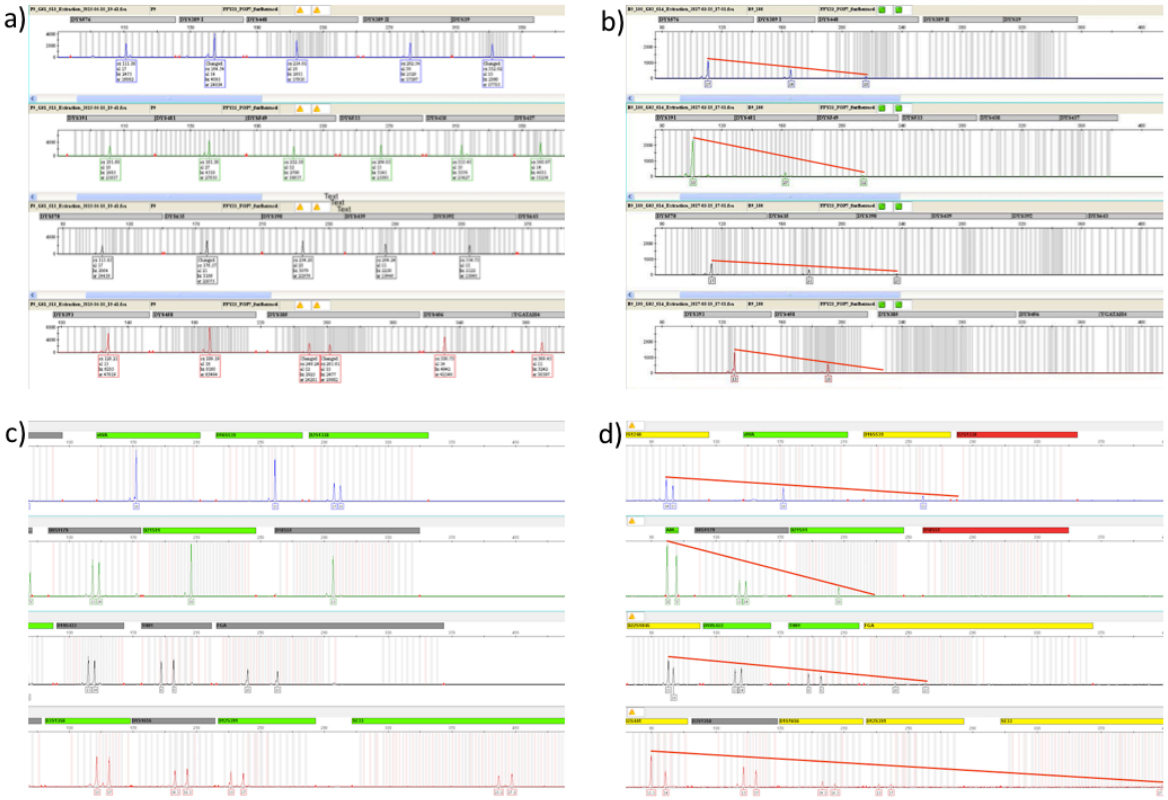

Figure 3.11 Electropherograms after autosomal and Y-STR typing.

Electropherograms obtained through PowerPlex® Y23(top) and NGMSElect® (bottom) analyses from 4 °C stains (left) that generated full profiles and 180 °C stains (right) that manifested the ski-slope pattern (decrease in RFU from left to right) accompanied by dropouts of the longer amplicons.

Similar experiments were carried out on smaller volumes with the intent to study how similar temperature treatments may affect samples with less starting DNA material. Blood stains of respective volumes of 10, five, and two µL were created in triplicates with one kept at 4 °C and two heated at 180 °C for each volume. These had their DNA extracted (section 3.2.2), quantified (section 3.2.3b), and typed using both the NGMSElect® and PowerPlex® Y23 kits. Although the NGMSElect® analysis of the 4 °C stains produced full profiles starting with any of the three tested volumes (Figure 3.14), the PowerPlex® Y23 analysis produced partial profiles (Figure 3.15) starting

with any of these three volumes (2µL: 9 AD per 23 targeted alleles, 39%; 5µL: 6 AD per 23 targeted alleles, 26%; 10µL: 3 AD per 23 targeted alleles, 13%). This has shown retrospectively that such volumes would not have been suitable to produce control profiles.

All the 180 °C stains produced partial profiles with dropouts at the larger molecular weight loci (Figures 3.14 and 3.15), typical of DNA degradation. Through the NGMSElect®, these were counted to be 45, 37 and 65 AD out of 68 targeted alleles in each of the 10, 5 and 2 µL volume category (66%, 54.5% and 95.6% of AD respectively). Allelic dropouts resulting from the PowerPlex® Y23 were counted at 32 for the 10 µL stains, 31 for the 5 µL, and 40 for the 2 µL out of 46 targeted alleles in each volume group (69.6%, 67.4% and 87% of AD respectively). The correlation between the RFU reduction with every amplicon length increase was statistically tested through a Fisher's test resulting in a significant correlation for all three volumes of the 180 °C stain that were typed using NGMSElect® (10 µL stains: F: 55.79 on 1 and 66 DF, p-value: 2.36e-10; 5 µL stains: F: 82.3 on 1 and 66 DF, p-value: 3.242e-13; and 2 µL stains: F: 4.984 on 1 and 66 DF, p-value: 0.02898) and PowerPlex® Y23 (10 µL stains: F: 47.99 on 1 and 44 DF, p-value: 1.46e-08; 5 µL stains: F: 38.76 on 1 and 44 DF, p-value: 1.571e-07; and 2 µL stains: F: 8.663 on 1 and 44 DF, p-value: 0.005168)

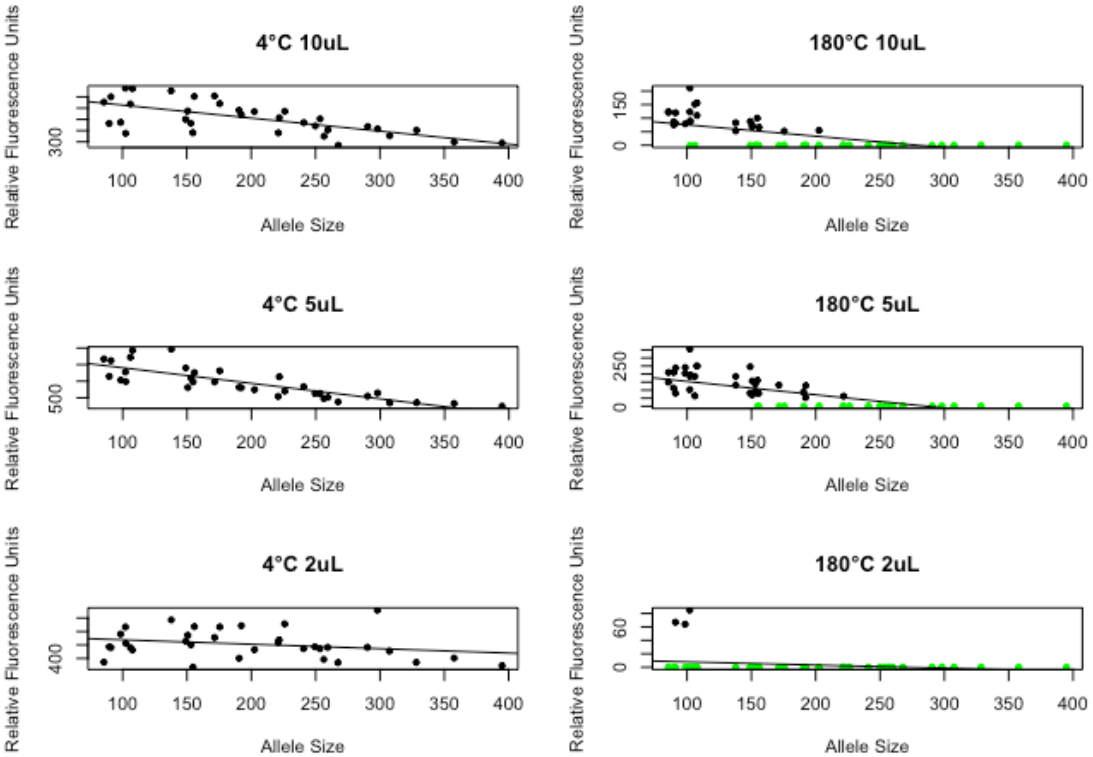

Figure 3.12 The effect of temperature on smaller volumes - autosomal STRs.

Typing results through NGMSElect® of one 4 °C stains (right) and two 180 °C stains (left), of respective volumes 10, 5 and 2 µL (from top to bottom). Dropouts are marked in green and only observable on the 180 °C stains.

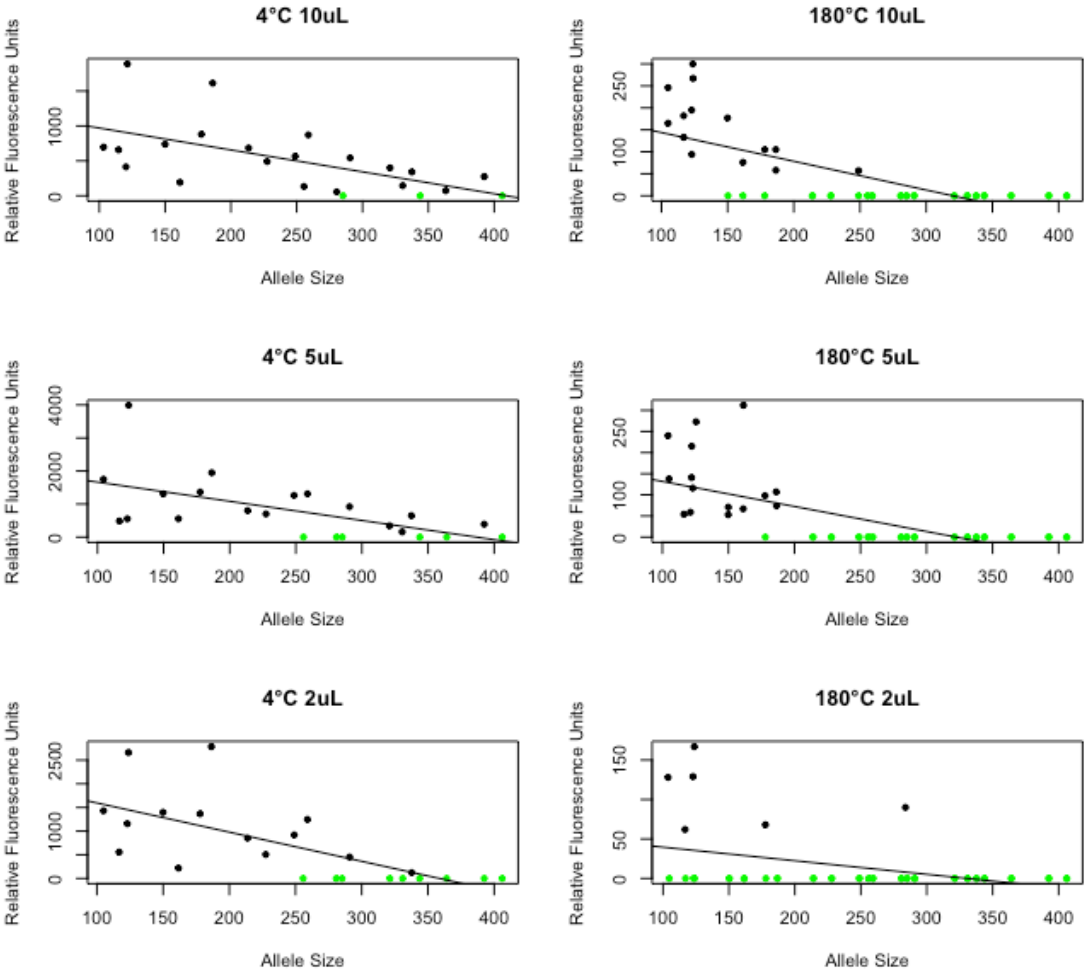

Figure 3.13 The effect of temperature on smaller volumes - Y-STRs.

Typing results through PowerPlex® Y23 of one 4 °C stains (right) and two 180 °C stains (left), of respective volumes 10, 5 and 2 µL (from top to bottom). Dropouts are marked in green and are more pronounced in the 180 °C stains (18 dropouts at 4 °C vs. 103 dropouts at 180 °C).

3.4.4 Massively Parallel Sequencing-Based Technique: Autosomal/Y-STRs and Identity SNPs

3.4.4.A Depth of Coverage affected by high temperatures

The intention of typing DNA from the 4 °C, 180 °C and 200 °C stains through Massively Parallel Sequencing was to assess the technique's performance on heat degraded samples and to compare it with that of CE-based methods. The 140 °C stains were precluded from the MPS since they did not show any dropouts through CE-typing and their concentration values did not reach low-template DNA (concentration ranging from 0.22 to 1.8 ng/µL).

Although the ForenSeq® DNA Signature Prep enabled the simultaneous sequencing of autosomal and Y-STRs as well as iSNPs in a single run, the scatter plots showing the *Depth of Coverage v. amplicon size* were separated into the different target types for comparison with CE-based methods. While the three control stains (4 °C) produced full autosomal (28/28) and Y-STR (24/24) profiles (Figures 3.16 and 3.17), the iSNPs results were less successful as control profiles (Figure 3.18) with 42 locus dropouts out of 282 targeted loci (15%). As with the CE-based tests, all the 180 °C stains produced partial profiles with dropouts varying in number between samples. Altogether, the six 180 °C stains gave rise to 292 out of 314 autosomal STR allelic dropouts (93%), 117 out of 154 Y-STRs' (76%), and 619 out of 680 SNPs' allele dropouts (91%). Most amplicons detected at 180 °C did not exceed 250 bp with the exception of the two blood stains that showed the least degradation when compared to their counterparts, whilst the 200 °C stains did not yield any interpretable alleles. The scatter plots in Figure 3.19 show the loss of amplicons that are longer than 175 bp at 180 °C, mainly affecting the autosomal and Y-STRs. The correlation between the decrease in depth of coverage and the increase in amplicon size was shown through a Fisher's test to be statistically significant for all target types (autosomal and Y-STRs; iSNPs) and in both 4 °C (auto STRs: F: 6.031 on 1 and 205 DF, p-value: 0.01489; Y-STRs: F: 6.031 on 1 and 205 DF, p-value: 0.01489; and SNPs: F: 14.23 on 1 and 474 DF, p-value: 0.0001818) and 180 °C (auto STRs: F: 18.2 on 1 and 312 DF, p-value: 2.642e-05; Y-STRs: F: 18.2 on 1 and 312 DF, p-value: 2.642e-05; and SNPs: F: 39.97 on 1 and 678 DF, p-value: 4.688e-10) stains, although much stronger correlations were obtained with the latter treatment (180 °C).

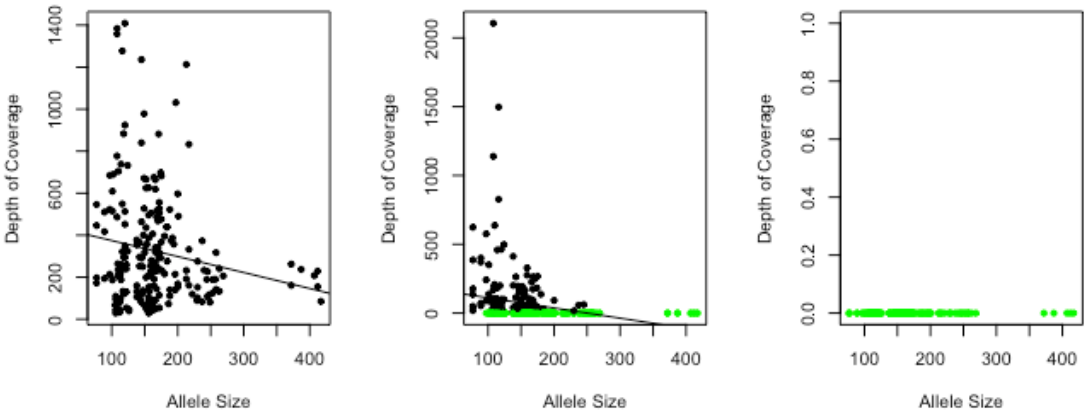

Figure 3.14 Depth of Coverage affected by temperature- autosomal STRs.

Depth of Coverage per autosomal STR amplicon length. The left plot is associated with the 4 °C stains, the middle with the 180 °C, and the right plot with the 200 °C. Dropouts are marked in green.

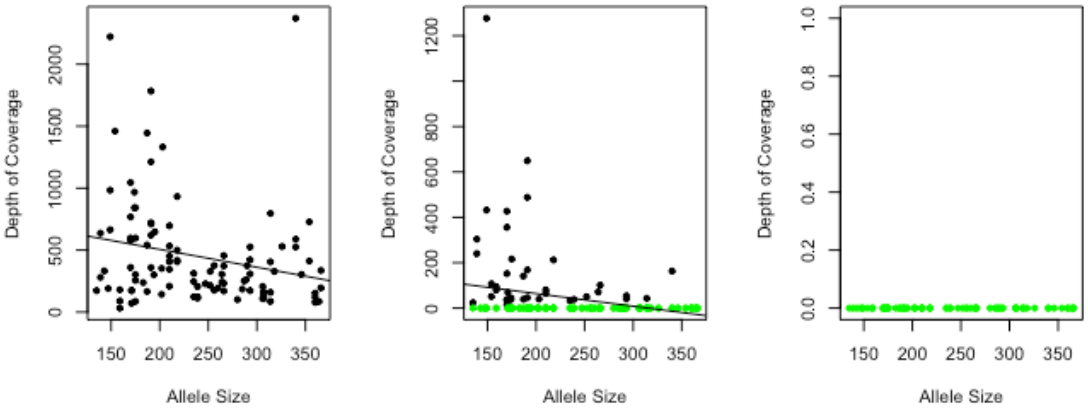

Figure 3.15 Depth of Coverage affected by temperature- Y-STRs.

Depth of Coverage per Y-STR amplicon length. The left plot is associated with the 4 °C stains, the middle with 180 °C, and the right plot with 200 °C. Dropouts are marked in green.

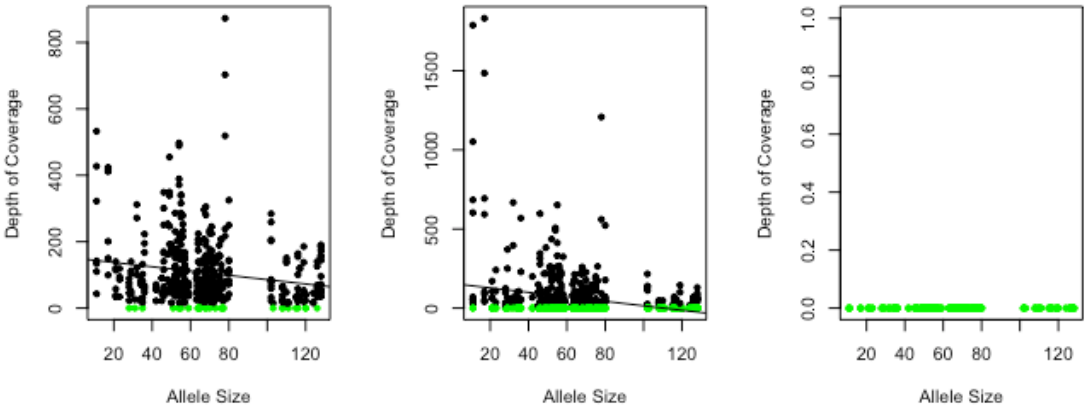

Figure 3.16 Depth of Coverage affected by temperature- iSNPs.

Depth of Coverage per iSNP amplicon length. The left plot is associated with the 4 °C stains, the middle with the 180 °C, and the right plot with the 200 °C. Dropouts are marked in green.

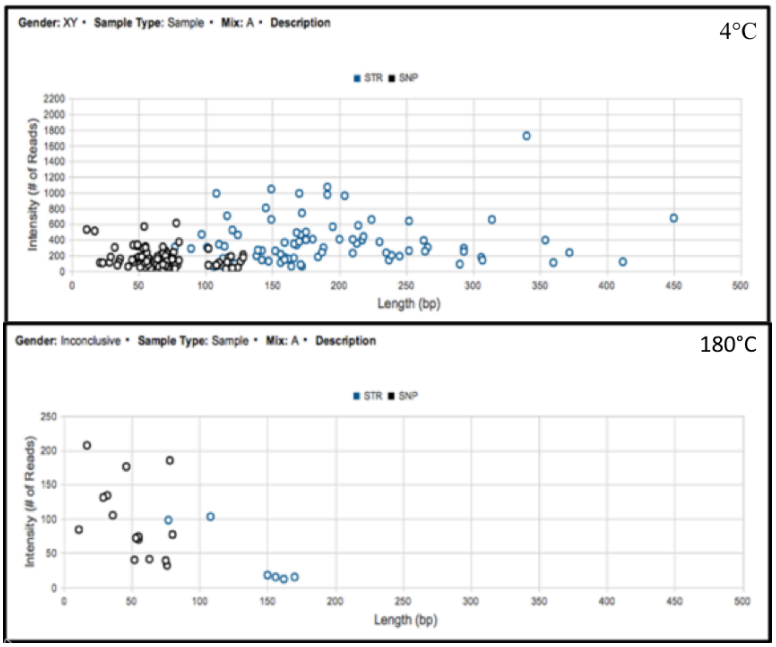

Figure 3.17 4 °C v. 180 °C stains on the Universal Analysis Software (UAS).

Scatter plots given by Verogen's UAS where the Number of Reads (or Depth of Coverage) per amplicon are plotted against the amplicon size. The autosomal and Y-STRs are marked in blue, while the iSNPs are marked in black. The top plot is associated with a 4 °C stain (P22_4 °C), and the bottom one is associated with 180 °C stain (P22_180 °C). Note the lack of amplification of the >175 bp fragments for the 180 °C stain mainly affecting the STRs.

3.5 Discussion

3.5.1 Methodology

3.5.1.A Sample Type

A number of studies referenced in the introduction focused on human remains of significant size (i.e. bones, muscles) in disaster victim identification or old skeletons and mummies inspired by the fields of archaeology, taphonomy and ancient DNA. Others worked with pure DNA or extracts, also known as naked DNA samples (Alongi *et al. 20*15). This work expanded the scope to include substrates that could realistically be found at a contemporary crime or disaster scene where very little remains are detected. Blood and saliva represent commonly found biological stains that may be attributed to both suspects and victims. The choice was made to work with native rather than naked DNA, i.e. biological tissues rather than DNA extracts, to increase the relevance of the tests. In this form, DNA initially remains supercoiled, associated with other cellular components such as nucleosomes, enclosed within the natural cellular membranes and surrounded by the cytoplasm.

Compared to other biological casework items blood and saliva proved to be the most efficient for DNA profiling (Einot et al. 2017) and together with semen and hair, they form the most common types of samples that are collected and analysed from crime scenes (Harbison et al. 2001). Since 1996, DNA profiles from biological stains from unknown contributor(s) cases have been included in European National Databases along with those from suspects and criminal offenders (Schneider and Martin 2001).

3.5.1.B Discrepancy in Damage between Bloodstains

Two of the overall tested bloodstains showed significantly less damage (fewer dropouts, higher detection signal) than others of the same volume that were also heated at 180 °C for 30 minutes. Ambers et al. (2014) observed similar damage discrepancies in bloodstains and proposed a series of possible explanations. Damage was reported to be more consistent in liquid blood compared to dried bloodstains (Nelson and National Institute 2015). This observed difference may warrant future research assessing DNA quality from liquid or dried samples collected from the crime scene. Alternatively, while the same level of damage may have affected all bloodstains, their initial leukocyte DNA content may have been different. This physiological contrast could be

caused by pathology, e.g. infection, or due to an inter-population variability: McKenzie. (2004) reports a higher leukocyte concentration in Caucasians compared to African Americans. The donor of these two stains is Caucasian, which differs from the other two donors (East Asian and Middle Eastern). A third explanation for the difference in damage may be structural. The blood's plasma, which is mainly constituted of ions, proteins, carbohydrates and fats may, in specific quantities and conformations, provide a better or worse thermal insulation to DNA. Finally, the difference could simply be stochastic. The assumption that similar environmental exposure will affect replicate samples in exactly the same way is as yet unproven. Such explanations reinforce the need to consider native DNA samples in research rather than naked DNA extracts.

3.5.1.C Degradation Assessment

The DIs that were derived from the qPCR detected the degraded nature of seven out of 15 tested (x) 180 °C stains (including the stains of different volumes: 2, 5 and 10 µL). Where it failed, it did so because of the heavily degraded DNA that affected both the short and the long qPCR targets. This explains why the 200 °C stains' degraded nature was not assessed via this method. The mtDNA multiplex that was specifically developed for this project offered a faster, more economical and direct degradation assessment method that overcame the DIs false negative problems.

All stains that showed amplification of both the intermediate and small targets, i.e. the 30 microliters 4 °C and 140 °C stains produced full profiles on typing. All those that amplified only the short product (180 °C) produced partial profiles, while those that did not show any amplification with this assay (200 °C) tended to not give any interpretable results through NGMSElect® (autosomal STR), PowerPlex® Y23 (Y-STR) or even the ForenSeq® DNA Signature Prep (Autosomal/Y-STRs/iSNPs). Having produced full profiles through the NGMSElect® assay, the 4 °C stains of respective volumes 10, five and two microliters do not seem to have their DNA degraded, or to contain carry-over salts and other impurities during the extraction process. It also reduces the possibility of a defect in the Capillary Electrophoresis system that was common to both experiments. Another factor that goes reduces the possibilities of degraded DNA is the amplification at several PowerPlex® Y23's largest loci while dropping out at shorter targets for the same profile. The primers' quality at the eight affected loci (DYS19, DYS385, DYS389II, DYS392, DYS437, DYS438,

DYS643, and Y-GATA-H4) could be checked for the specific kit that was used in this experiment. Repeating this experiment could have warranted a clearer explanation for this oddity.

The maximum amplicon size that was obtained through the 180 °C associated-degradation (~250 bp) is slightly larger than what was suggested by (Freire-Aradas et al. 2012) to be the approximate fragment lengths (~200 bp) resulting from the digestion of chromatin by endogenous endonucleases that target the linker DNA between nucleosomes. The authors proposed to target these nucleosome-protected regions through SNP multiplexes that are designed for highly degraded DNA samples.

3.5.2 Significance of results

3.5.2.A Effects of Temperature Exposure

The loss of genetic information due to thermal effects is an accepted phenomenon (Mann et al. 1990; Robins et al. 2001; Smith et al. 2003; Larkin et al. 2010; Allentoft et al. 2012; Matisoo-Smith and Horsburgh 2016), except when the heat exposure contributes to halting a dead organism's decomposition or drying of a liquid biomaterial such as crime scene or swabbed biological fluids. The first tested heat treatment - 140 °C for 30 minutes - had probably started to affect the sample's DNA as reflected by the decrease in concentration and RFUs. The conditions however were insufficient to preclude full profiles with the currently available typing methods.

Increasing the temperature by 40 °C for the same exposure time resulted in partial profiles for every tested sample. Partial profiles represent one of the known complications in forensic genetics as partial matches may mislead the examiner, by introducing false homozygosity through allele dropout, and consequently affect the strength of DNA evidence (Chapter 5). Allele dropout is less potentially misleading in the typing of haploid markers such as the Y-STRs as the few duplicated loci are usually known in advance (i.e. in PowerPlex® Y23). Additionally, the loss pattern observed can suggest degradation rather than insufficient typeable DNA copies. This is reflected by the loss of the larger amplicons rather than the stochastic loss that is observed in LCN analyses (Butler 2009).

The virtually total loss of DNA at 200 °C is consistent with previous studies (Imaizumi et al. 2014) and supports the assumption that dried blood and saliva that initially

contain similar DNA input, are unlikely to produce any interpretable DNA information with the tested chemistries when exposed to 200 °C for 30 minutes. Although partial profiles with a pattern suggestive of DNA degradation were consistently obtained from the 180 °C stains and no profiles were obtained from the 200 °C stains, it remains essential to consider such finding's relevance to casework.

3.5.2.B Relevance to Casework - Real Fires

In his study about 'temperatures in flames and fires' (Babrauskas 2006) estimated the base or any other continuously flaming region of an open fire and flash-overs, using gas burners in a "pool fire" mode burning in oxygen, to reach 900~1000 °C. The flame tips however, were measured to be around 320~400 °C. Such values suggest that fires and potentially other sources of extremely high heat would exceed the temperatures that would destroy DNA within minutes to hours if the biological samples were in direct contact or close proximity to the heat source.

However, there are disasters involving fire or high temperature where a substantial number of victims were genetically identified, as mentioned in the introduction. Such DVI successes could be explained by the temperature's intensity and duration of exposure, the insulating properties of the samples' surrounding, and the initial DNA content. The general rule is that any object's temperature depends on its thermal conductivity, its size, and its density. Despite the bodies' condition, the cardiac blood that served to successfully identify the cable car fire's 155 victims could have been insulated by the bodies' outer layers, clothing items, or surrounding objects. A similar thought process could be applied to the Waco siege soft and hard tissues, as well as the 9/11 attacks and the American Airlines Flight 587 human remains.

In addition to the temperature exposure, several other factors are of importance to the estimation of DNA degradation due to thermal effects: the initial DNA quantity in a sample, the tissue in which DNA is enclosed, the methods and technologies that are available to use, and environmental factors such as the relative humidity and surrounding objects that may protect the sample from the heat source.

Chapter 4 The Effects of Explosions on Forensic DNA Analysis

Figure 4.1 Assassination with Vehicle-Bound Improvised Explosive Device (VB-IED).

Firefighters extinguishing a large fire that resulted from a VB-IED that ripped through the crowded neighbourhood of Ashrafieh in the Lebanese capital, killing top intelligence official Major General Wissam al-Hassan and at least seven other persons; also wounding 78 persons. (West 2017; image from bbc.co.uk/news/in-pictures-20008421).

4.1 Introduction

Explosions, whether they result from accident, disaster or criminal activity, have a major impact on the affected communities and the emergency services. Violent explosions can result in deaths, enduring physical and psychological harm, as well as significant destruction to property.

Their effects can be felt outside of the active zone due to the intense sound, high pressure, and flashlight that it produces and may cause severe thermal, pressure-related, penetrating and blunt physical injuries to multiple victims, depending on their position relative to the blast, the force of the explosion, and the nature of projected materials. Blast-related injuries are traditionally classified into primary, secondary and tertiary categories. Primary injuries mostly affect gas-containing organs such as the

bowels, lungs and ears, and are the products of the explosion's sharp rise in pressure, also referred to as blast overpressure (Wightman and Gladish 2001). While they are not expected to affect the detection of human remains, the wounds and surrounding areas' histological examination showed cellular damage (Argyros 1997; Romolo et al. 2014) and electron microscopy revealed cell death (Brown et al. 1993) which would most probably lead to DNA degradation.

Secondary injuries occur when accelerated objects strike the victim and tertiary ones are caused by the victim being physically thrown by the force. Both may cause dismemberment and significantly reduce the size of detectable human remains to the extent that in some of the most energetic blasts no remains could be detected from those close to the epicentre. To present some examples:

- On October 23th 1983, a truck bomb attacked the US Marine Barracks in Beirut, Lebanon, killing 241 American servicemen and injuring many others. The explosion's intensity was the equivalent of 6 to 9 tons of Trinitrotoluene (TNT), and was described by the US court as the largest non-nuclear explosion ever. The "vaporisation" of victims (Diaz and Newman 2005) as well as that of the perpetrator were reported.
- The Lockerbie disaster occurred of December 21st, 1988 saw the disintegration of Pan-American Flight 103 while flying at 9000 meters following a mid-air bomb blast. Another explosion upon impact with the ground created a 90 m long and nine meters deep crater resulting in the total destruction of a number of houses. Of the 270 victims, 253 were positively identified by analysing 678 fragmentary human remains. The principal method of identification was dactyloscopy[1], together with odontology, documents and personal body characteristics, such as tattoos (Moody and Busuttil 1994). There was no mention of the seventeen remaining victims in the literature.
- The suicide bomber who attacked the Australian Embassy in Jakarta 2004 carried a charge so intense that it reduced his body to small tissue fragments, preventing conventional identification (physical examination, fingerprint and odontology) and necessitating mitochondrial DNA analysis as an alternative to the autosomal STR typing that failed in some instances (Sudoyo et al. 2008) .

[1] Identification through DNA identification was not available in 1988.

- On 14 February 2005, as Lebanese Prime Minister (PM) Rafic Hariri's convoy was driving on one of Beirut's main coastal roads, a moving white Mitsubishi Canter van carrying the equivalent of 2500-3000 kg of TNT was detonated, killing the PM, 21 other persons, and causing injury to 226 persons. As the case is still ongoing, little is known about the suicide bomber's remains. Court reports (Special Tribunal for Lebanon 2013) mentioned that the analysis of small fragmented remains, possibly parts of the bomber's nose (West 2017) originated from an as yet unidentified male. Lebanese expert witnesses that worked on the case mentioned the difficulty of working with the available samples, and that partial DNA profiles were all that could be obtained (Verwiel and Van Der Voort 2014).

In general, the damage of an explosion happens so fast that in physics, it is defined as an injection of energy that occurs faster than dynamic time scales which, in astronomical terms, is a characteristic time for a particular change to take place (Oran and Williams 2012). Explosions can also be defined as rapid expansions of gas or dust particles that result in sudden pressure changes (Martin 2008). The reaction is highly exothermic and expands in the form of "flame propagation" also known as a combustion wave. It can be considered as a finite flow of expanding hot gases whose temperature, velocity and travel distance depend not only on the amount of released work and heat, but also on the system's rear boundary conditions. In this sense, an equal explosive charge would dissipate through a sealed container at higher speeds, temperatures and pressures when compared to an open system (Lee 2008). In other terms, the same chemical energy would be converted to different proportions of kinetic and thermal energy depending on the system's boundaries. Theoretical, experimental, and computational studies of a wide array of explosions led to classification of explosions as deflagrations and detonations.

A deflagration is a type of combustion wave travelling at subsonic speeds (a few meters per second, except for 'turbulent' deflagrations that might go supersonic), burning at temperatures that can reach 3000 °C (Esslinger et al. 2004), and exerting overpressures of less than one bar under ambient pressure conditions (Gonzalez-Nicieza et al. 2014). In deflagration, the products' expansion disturbs the reactants

downstream of the flow, and the sum of the reactants' displacement velocities combined with the burning velocity of the medium determine the overall propagation speed.

A detonation, on the other hand, occurs when enough energy is released in a system that accelerates the wave to supersonic speed (>343 m/s in dry air at ≈20 °C). In addition to an induction zone that is similar to that of a deflagration, a detonation's combustion wave is preceded by a shock front which is so fast that downstream reactants do not react prior to its arrival, as they chemically dissociate into free radicals once in the induction zone; and within which pressure is so intense that it shatters surrounding objects through a phenomenon known as *brisance*. A detonation's propagation is therefore characterised by a closely coupled shock-deflagration complex.

Detonations are faster, hotter and more powerful than deflagrations. They can propagate at 1500–2000 m/s (Mach 6), exert an overpressure of tens of bars at ambient pressure, and reach temperatures up to 5230 °C (Simpson et al. 1999). While the pressure across the reaction front in deflagrations drops, pulling the combustion products in, it increases drastically in detonations, pushing the products away in the direction of the wave's propagation. Such effects should be considered when the aim is to detect and collect biomaterials and other types of evidence after a nearby explosion.

The exposure time of immobile objects located within the reaction zone depends on the wave's speed of propagation (1 to 10^3 m/s), the reaction's thickness (portion of air affected), and the affected object's size. In their *time to explosion* measurements of PVC and galvanised steel pipe bombs, Bors et al. (2014) provided an idea about the duration that an object would be subjected to extreme conditions if placed either inside or close to the pipe's outer surface (Figure 4.2). Still frame photography captured the explosions for 5 to 10 milliseconds after initiation as they aimed to time the containers' total failure, therefore considering the *duration of explosion* starting with the first flash appearance (point of first failure) and ending at the last still frame (the pipe's total failure). The *duration of explosion* is considered to be shorter than the *duration of exposure* (Table 4.1), since heat generation is believed to start before the first flash of light and progress after the final still frames. The authors found that the explosion's time-frame is, for a given charge, dependent on

the container's mechanical properties (elastic modulus, yield strength) which in turn are directly affected by the type of material and its temperature at the time of explosion. In general, steel had a shorter *duration of explosion* than PVC and this discrepancy was more pronounced at lower ambient temperatures.

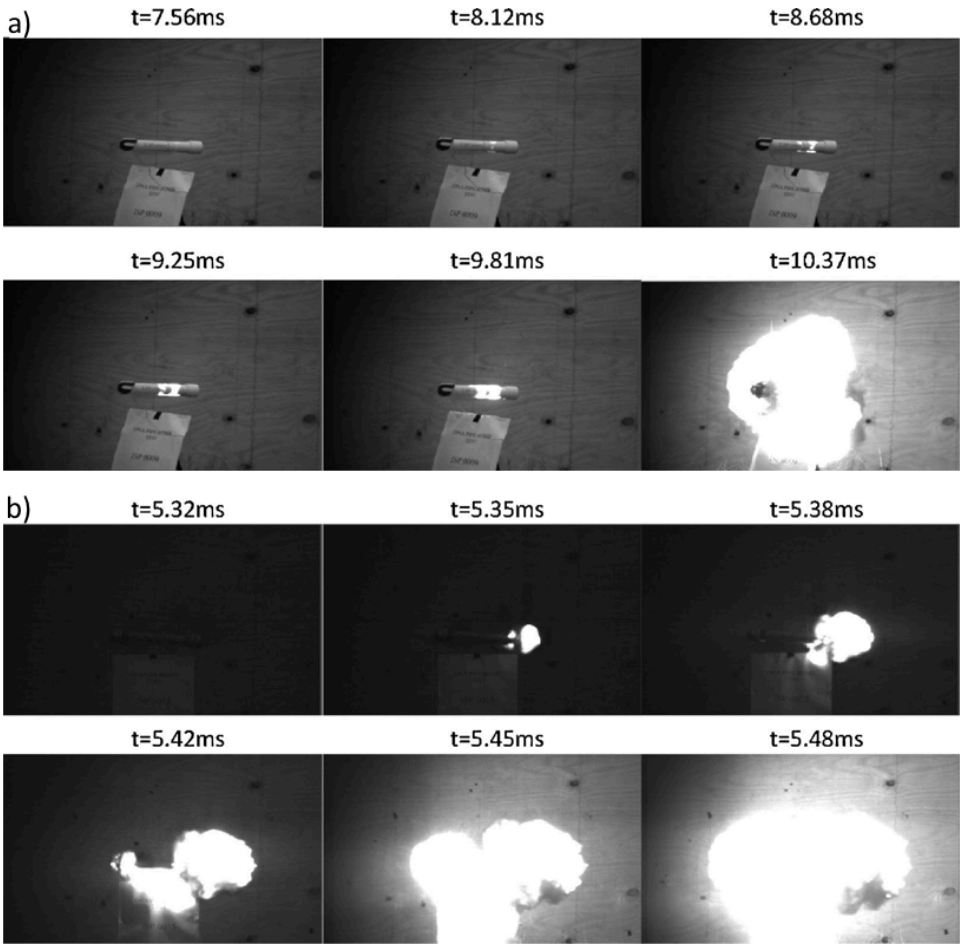

Figure 4.2 Time to explosion and duration.

Stepwise frame images showing the *time to explosion* (appearance of first flash) and the *duration of explosion* (from the first flash until the pipe's complete failure) in a PVC (top) and galvanised steel (bottom) DBSP charged pipe bombs (Bors et al. 2014).

Table 4.1 Duration of exposure to explosions.

Season	Material	Duration of exposure (ms)
Spring	PVC	> 1.5
	Galvanized steel	> 0.5
	Black steel	> 0.5
Winter	PVC	> 2.24
	Galvanized steel	> 0.13
	Black steel	> 0.13

Minimum sample exposure time in milliseconds from DBSP pipe bombs of different materials in spring *v.* winter, derived from the duration of exposure by Bors et al. (2014).

Not all explosions are the product of a deliberate human act. The United States Bomb Data Center, (United States Bomb Data Center, (USBDC) 2016) classifies explosions in three main categories: accidental, undetermined, and bombings. When reactants meet an ignition source in a system that permits, an explosion will occur. It may arise as a consequence of natural phenomena such as some volcanic eruptions and astronomical explosions (Carey and Bursik 2015), as part of human negligence causing a number of explosions in storage facilities (Fu et al. 2016), and accidental explosions of combustible gas or dust (Croft 1980; Li et al. 2016).

Intentional bombing, however, requires the construction of a device that can deliver the force of an explosion. Explosive devices or bombs find a "legitimate" use in industry to demolish and mine, and by governments to militarily attack enemies or defend against them. When access to sophisticated, specialised and accurately performant bombs is restricted, people have improvised their own explosive devices in numerous and mind-boggling ways. The history of Improvised Explosive Devices (IED) may have started[2] with anarchists' dynamite bombs that were used against civilians in the United States from the 1880s until the early 1900s (Farazmand 2014). More than 29 attempts have been made at unifying the definition of IEDs (Gill et al. 2011) and distinguishing them from other types of bombs. Keyes (2005) defined IEDs from a technical point of view as:

[2] Improvised Incendiary Devices are excluded from the historical assessment here, which can be traced back at least to ancient Rome with catapulted lamp oils.

"A main charge, which is attached to a fuse, which is attached to a trigger. In some types of IEDs, these three components are integrated into a single unit. The trigger activates the fuse. The fuse ignites the charge, causing an explosion. The effects of the IED are sometimes worsened by the addition of material, such as scrap iron or ball bearings. Sometimes the trigger is not the only component that activates the fuse; there can also be an anti-handling device that triggers the fuse when the IED is handled or moved." (Keyes 2005).

The main charge, also called the energetic, can either be a low explosive (also called a propellant), which deflagrates in ambient pressure conditions, or a high explosive, which self-sufficiently detonates in normal pressure conditions. In the previously mentioned study (Figure 4.2), Bors et al. (2014) used pipe bombs charged with a Double Base Smokeless Powder (DBSP), the most widely available gunpowder in the USA, which are considered to be most typical of current Improvised Explosive Devices (Oxley et al. 2018) (see Figure 4.3). It is relatively simple to build such devices with affordable material that can be obtained at commercial establishments. Although plastic containers are often encountered, especially where metal detectors are used, metal pipes charged with DBSP remain the most frequently used IED (National Research Council 1998). Like most propellants, with the exception of *triple base* smokeless powders containing Nitroguanidine (8200 m/s) which is used for heavy artillery, DBSP is a low explosive since it deflagrates in ambient pressure conditions. One of its main constituents, however, making it superior to its *single base* predecessor in terms of resistance to moisture, softness, and better performance, is the first discovered high explosive: Nitroglycerine (NG). Other criteria that characterise the propellant's quality include proportions of constituents and the granules' shapes. Smokeless powders can be cut into sheet-shape granules, flakes, cylinders and spheres. They can contain perforations to allow simultaneous burning in and out of each solid granule and are usually coated with deterrents such as flash suppressants and graphite.

Three out of five tested pipe bombs in this work were filled with a commercial ball shaped DBSP. This propellant is considered the most performant DBSP with a burning rate that is optimised by design. A 'dough' of Nitrocellulose, stabilizers and solvents is morphed into small spheres; and as the solvents are extracted, Nitroglycerine is impregnated into the empty spaces before coating some of the granules with deterrents, flash suppressants and graphite. Although this energetic usually deflagrates, it might be induced into detonation when ignited in a sealed environment such as a pipe bomb. As a result, the resulting combustion wave may reach 1000 m/s (Heramb and McCord

2002). Reproducing detonations from low-explosive bombs, in an empirical fashion, is difficult as the reaction speed depends on factors that are as yet out of the operators' control.

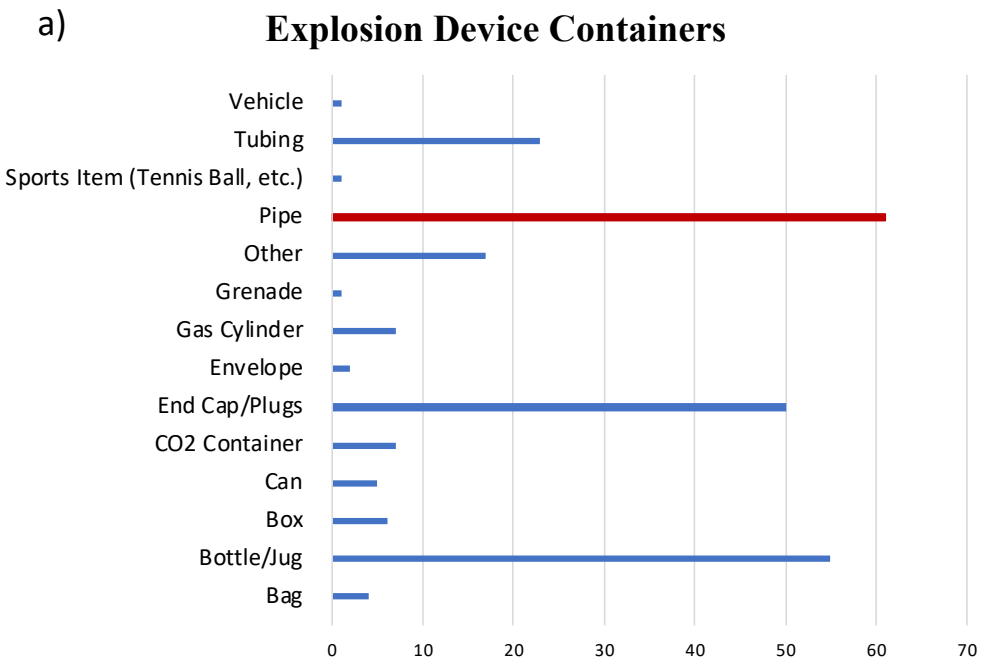

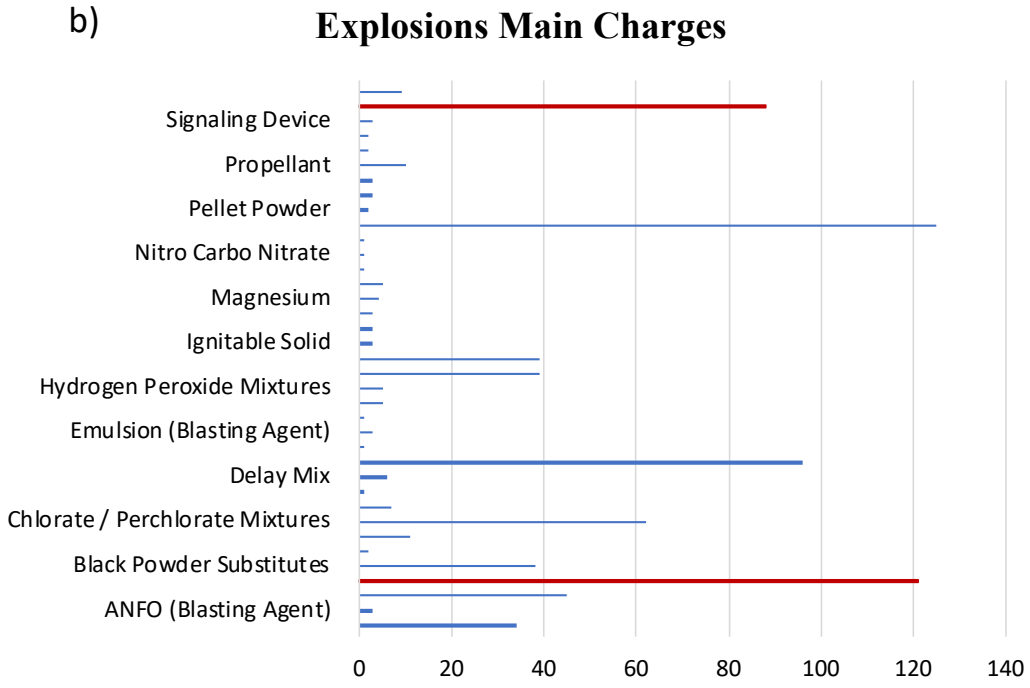

Figure 4.3 Explosive containers and energetic charges - statistics.

Histograms enumerating the use of pipes as explosive device containers on the left, as well as black powder and smokeless powders as the explosions' main charges. Adapted from data available in the National Research Council (1998).

The US National Academy of Engineering and Department of Homeland Security separated legitimate from non-legitimate use of bombs and defined IEDs as virtually

any kind of explosive device that is manufactured or used by non-State groups. Through his Global Terrorism Database (National Consortium for the Study of Terrorism and Responses to Terrorism, (START) 2018), Lafree shows that explosive devices have been the terrorists' worldwide weapons of choice since 1970 (Figure 4.4). The European Counter Terrorism Center at Europol counts approximately 57 out of 142 terrorist attacks in 2016 involving the use of explosives (≈ 40%), with similar numbers for the previous year in 2015. The number of such attacks employing firearms as a weapon of choice dropped dramatically from 57 in 2015 to 6 in 2016 (Europol 2017). In Afghanistan alone, there were around 7500 IED explosions between 2004 and 2009. Another 8000 IEDs were found and cleared in the same period (Rosen 2010).

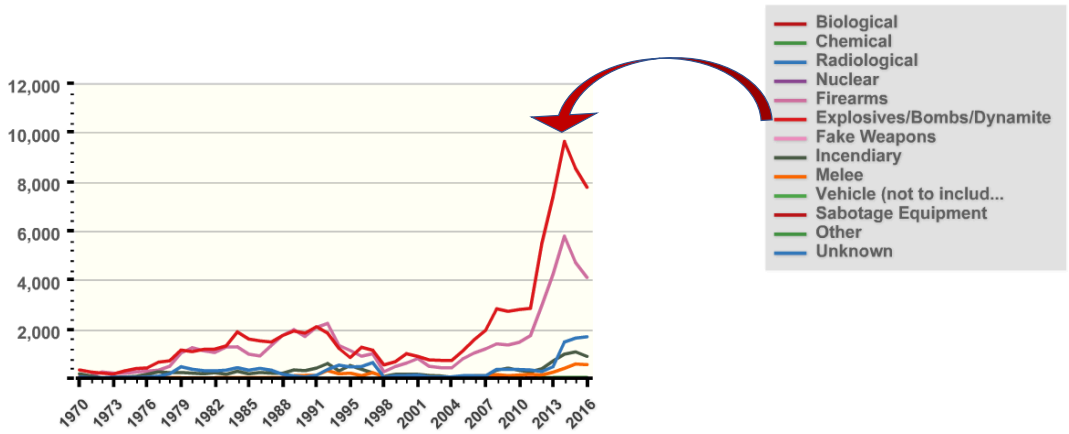

Figure 4.4 Bomb: weapon of choice in terrorism.

Line chart showing the use of each weapon category that was used in terrorist attacks worldwide, from 1970 until 2016 (National Consortium for the Study of Terrorism and Responses to Terrorism, (START) 2018).

Numerous types of IEDs other than DBSP-charged pipe bombs have been used in crime. More powerful explosions that are directed at a specific target can be in the form of a wider container charged with high explosives. Some of these explosives or their precursors, may be easily purchasable in large quantities, at even cheaper prices than DBSP, and prepared at home before the attack. These include the fertilizer Ammonium Nitrate mixed with Fuel Oil (ANFO) as used in the 1995 Oklahoma City bombing (Hinman and Hammond 1997), and triacetone triperoxide (TAPT) produced by the

reaction of acetone and hydrogen peroxide that was used in the 2015 Paris, the 2016 Brussels Airport, and the 2017 Manchester concert bombings (Gomes 2017).

High explosives are classified into primary, secondary and tertiary explosives (Fox 1999). Primary explosives are very sensitive to heat, shock, friction or electrostatic discharge. They include lead azide and mercury fulminate and are usually part of a bomb's initiating system referred to as blasting caps. Secondary explosives require a larger shock to detonate, and include Nitrocellulose, desensitised Nitroglycerine, and pentaerythritol tetranitrate (PETN). Tertiary explosives are the most powerful but are also the safest to handle and transport. They can be referred to as military-grade explosives and include Nitroamine explosives such as RDX and HMX[3]. While DBSP was used for this project as a pipe bomb's low explosive main charge, an RDX containing high explosive referred to as Composite 4[4] (C4) was used as a high explosive. Blasting caps and detonation cords containing PETN were also used in this project as part of the initiation systems.

4.2 Aims and Objectives

This part of the work is destined to explore the effects of explosions on forensic DNA analyses from blood and saliva stains. Designing an experiment involving real explosive devices that are able to carry traceable biological samples was the first objective. It was followed by initiating a collaboration with police forces to enable a legal construction and detonation of the explosives. A post-explosion search and collection of samples was performed after each blast before the subsequent DNA analyses. After DNA extraction, Real-Time PCR quantification served as a primary sample quality check before running through the mitochondrial DNA degradation assessment that was designed in Chapter 3. The next objective was to type DNA and generate profiles constituted of various types of markers (autosomal and Y STRs, autosomal SNPs) employing Capillary Electrophoresis-methods and Massively Parallel Sequencing, followed by a comparison between the two technologies. Finally, the experimental design allowed to evaluate the effects of various explosives-related

[3] RDX stands for Research Department Explosive while HMX's name was speculated to be derived from High Melting Explosive, Her Majesty's Explosive, High-velocity Military Explosive, or High-Molecular-weight RDX (Cooper 1996).
[4] C4 composition: 91% RDX + 5.3% dioctyl sebacate (DOS) or dioctyl adipate (DOA) + 2.1% polyisobutylene (PIB) + 1.6% of a mineral oil.

variables on DNA including the energetic type, the casing material, and the stain's biological nature, location and volume.

4.3 Materials and Methods

4.3.1 Introductory Briefing

Subjecting biological samples to real explosions proved more complex than Chapter 2's stain heating procedure. The Larimer County Sheriff's office in Fort Collins Colorado, was the first law enforcement agency that agreed to collaborate and offered access to their laboratory for sample preparation before assembling and initiating the pipe bombs on site (April 2016). Together with the Colorado State Police bomb squad, they assisted in the post-blast search and recovery process.

About a year later (May 2017), the bomb squad at Penn State University Police agreed to conduct similar experiments under the supervision of the Federal Bureau of Investigation (FBI). Saliva stains were excluded from analysis after showing no significant difference compared to blood[5]. Military-grade high explosive C4 was tested instead of DBSP. The experimental design was an improved version over the first one, especially with relation to the samples' preparation and their documentation.

4.3.2 Sample preparation and bomb assembly

4.3.2.A Colorado Experiment

Blood (30 µL) and saliva (200 µL) stains were tested inside and outside three DBSP-charged pipe bombs (two brass pipes and one copper pipe). The biological fluids were collected from two male donors (P20 and P29) and stored overnight at 4 °C.

Holes were drilled in each end cap to allow for the insertion of the detonation cord and a metallic bolt to firmly hold the end caps in place if necessary. There was no mixing of sample types on a single device as each pipe bomb contained either blood or saliva. Such biological stains were deposited at known locations on the pipes' inner surfaces as well as on auxiliary components that in turn were placed inside and outside each pipe. The samples were left to dry overnight at room temperature before being covered with

[5]Touch DNA were included in the Penn State experiment and a special DNA extraction method that concentrates nucleic acids prior to their elution was employed. Results are still under analysis and more details will be discussed in Chapter 6.

coloured electric tape that protected the samples, served as a substrate, and as a colour coding system to distinguish between samples to trace back the stains' original location after the explosion.

The devices were assembled on site before the explosions. Each pipe was fully filled with a granular shaped DBSP Hodgdon Hornady LEVERevolution© and initiated through wired detonation cord and blasting capsules.

Table 4.2 Dimensions and charge of DBSP-charged pipe bombs in Colorado

	Brass (Pipe 1) - ten 30 µL blood stains	Copper (Pipe 2) - ten 30 µL blood stains	Brass (Pipe 3) - six 200 µL saliva stains
Length (mm)	150	150	150
Inner Diameter (mm)	37	41	37
Wall Thickness (mm)	1	1	1
Charge (g of DBSP)	≈122.5	≈183.5	≈122.5

4.3.2.B Penn State Experiment

Blood was collected from one male donor (P30) and stored overnight at 4 °C. Blood spots (10 and 30 µL) were tested inside and outside two C4-charged pipe bombs (one PVC pipe and one galvanised steel pipe). No holes were drilled in the end caps since the C4 detonation did not require a wired detonation cord; and the two pipes (PVC and galvanised steel) could fit their end caps without the use of a metallic bolt.

Stains were deposited on the electric tapes of different colours (Figure 4.5), left to dry and then the green (15 stains of 10 µL) and yellow (15 stains of 30 µL) samples were mounted on each pipe (Figure 4.6), whilst the white (15 stains of 30 µL) and blue (15 stains of 10 µL) samples were added to the inside of each pipe moments before the detonation. Each pipe was charged with approximately 113.5 g of C4 and detonated through a wireless system using blasting capsules.

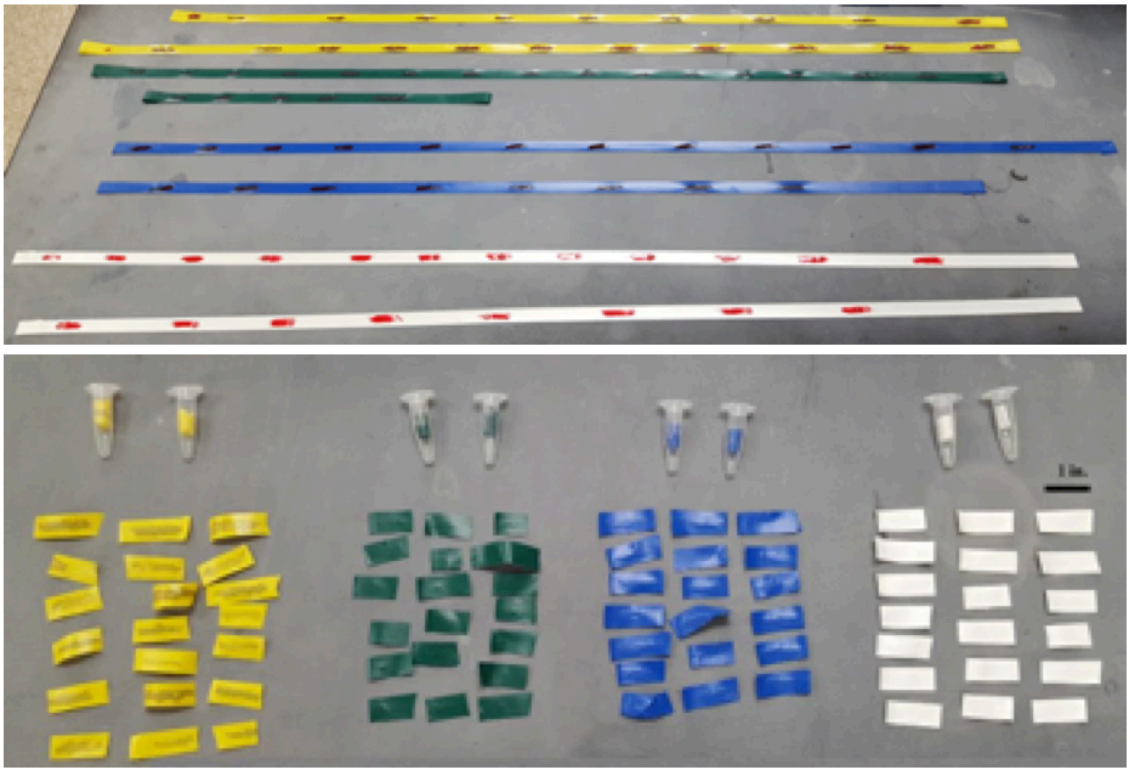

Figure 4.5 Preparing pipe bomb associated samples.

Biological stains were pipetted on the inner surfaces of colour-coded adhesive tape and left to dry before folding them into flaps or rolling them onto the pipes and other bombs components.

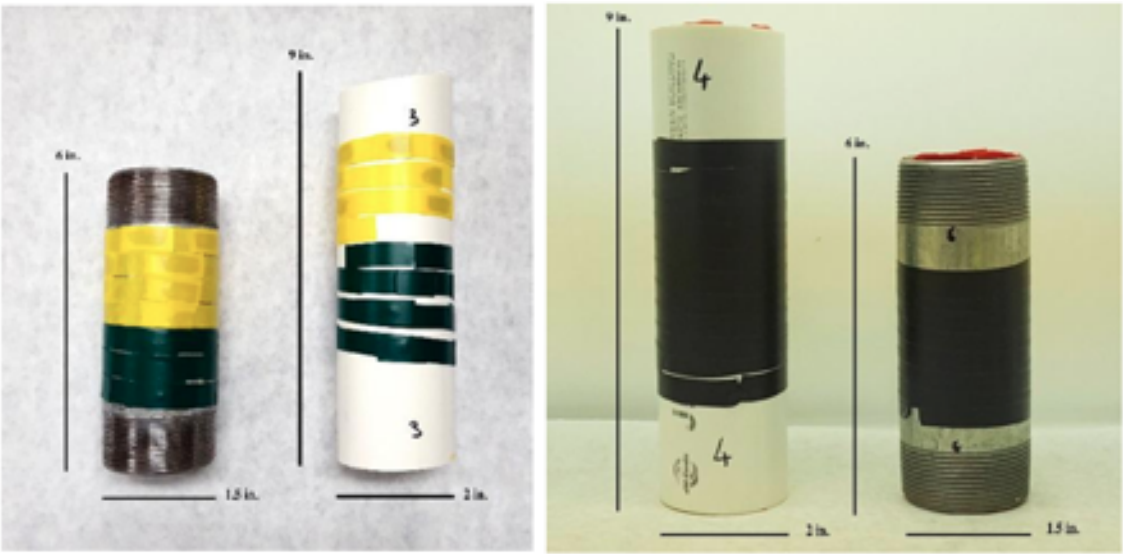

Figure 4.6 Pipes and their associated samples.

Steel (metallic) and PVC (white) pipes that carry tape-protected biological stains. These will be charged then exploded. The different colours aim at coding for different samples, in this case yellow is 30 µL blood stains, green is 10 µL, black is outside stains and red is inside.

Table 4.3 Dimensions and charge of C4 charged pipe bombs in Penn State.

	Galvanised Steel (Pipe 4) -10 and 30 µL blood stains (n=30 each volume)	PVC (Pipe 5) - 10 and 30 µL blood stains (n=30 each volume)
Length (mm)	152	229
Inner Diameter (mm)	36	49
Wall Thickness (mm)	2	1.5
Charge (g of C4)	≈113 g	≈113 g

4.3.2.C Shared Features of Both Experiments

In both experiments, all bomb components were washed with 20% bleach to eliminate DNA from exogenous sources followed by rinsing with DNA free water prior to the addition of the samples.

Controls:

- Positive control pipe: one 30 µL and one 10 µL bloodstain were attached to the pipe and then analysed after transport to and from the test site. This pipe was neither charged nor exploded.
- Negative control pipe 1: no biological samples were deposited on this pipe that was transported to and from the explosion site. This pipe was charged but not exploded. It served as a control for the pipes' cleaning, construction and transportation.
- Negative control pipe 2: no biological samples were deposited on this pipe, which was exploded and had its fragments collected and screened for potential contamination from the explosion and recovery processes.

The forensic negatives were subsequently swabbed and tested.

4.3.3 Detonation and Collection of Items

All bomb handlers wore latex gloves and face masks and provided buccal swabs for elimination purposes in case of contamination. Unattached samples were added to the

system during assembly of the bomb (Figure 4.7). The pipe bombs were placed in a pit (Figure 4.8) and exploded after evacuation of the area. In Colorado, a camera was fixed close to the test site and a metal drum covered the pipe bombs before their explosion in order to contain the debris. After failing to contain debris from a C4-charged pipe bomb in Colorado, and following the officer's recommendations, no metal drum was used in the Penn State experiments. The search and recovery areas - marked in purple in Figure 4.9 - were divided into zones and searched by forensic science students together with members of the bomb squad through the strip method, which consisted of walking in a straight line covering the total area. This was conducted after each explosion.

Figure 4.7 On-site preparation of a DBSP charged pipe bomb.

Figure 4.8 Placing the pipe bomb.

PVC pipe bomb placed in a pit prior to detonation. This pipe carried touch cells (discussed in Chapter 6) during the Penn State experiment and is a reflection of how all pipes were placed before their initiation.

Figure 4.9 Bombs search and recovery areas- USA.

DBSP-charged pipe bombs in Colorado (left) and C4-charged pipe bombs in Penn State (right). The search areas are marked in purple and their dimensions as follows: 388 m perimeter, and 11,216 m^2 of surface area in Colorado; 1433 m perimeter, and 113,502 m^2 of surface area in Penn State.

4.3.4 Extraction

DNA extraction was performed manually in a limited access pre-PCR environment using a silica adsorption method with two washes and a final elution volume in 100 µL (QIAGEN QIAamp® DNA Mini kit, DNA purification from swabs, spin protocol).

4.3.5 Real-Time PCR Quantification

While a subset of samples from the Colorado experiment (n=10) had their DNA quantified through a fluorescence-based assay (Qubit®, dsDNA HS), the majority were analysed by Real-Time PCR. The Colorado samples were quantified using the Quantifiler® Trio whilst Penn State samples were quantified using the Quantifiler® HP kit (available in Penn State). Both kits are from the same manufacturer (Thermo Fisher) and contain identical PCR Reaction Mix, Dilution Buffer and DNA Standard components. They both target the same large (LH=214 bp) and small (SH=80 bp) multi-loci nuclear DNA copies and are specific to primate DNA with high detection sensitivity and a robust performance in the presence of PCR inhibitors and with degraded DNA. The primary difference is that the HP kit does not detect the male target (MH=75 bp) included in the Trio kit. However, validation studies did not show significant differences in DNA quantity as determined by the two kits (Holt *et al* 2016). The Degradation Index and PCR Inhibition were also estimated for each sample.

4.3.6 DNA Typing/Sequencing

4.3.6.A Colorado Experiment

The controls and the DBSP-exploded stains were typed through two Capillary Electrophoresis (CE) based methods using NGMSElect® for 16 autosomal STRs (plus Amelogenin) and PowerPlexY23® for 23 Y-STRs.

4.3.6.B Penn State Experiment

The controls and the C4-exploded stains were typed through a Capillary Electrophoresis (CE) based method using PowerPlex® Fusion 6C (23 autosomal and 3 Y-STRs, and Amelogenin) and by Massively Parallel Sequencing (MPS) using the ForenSeq® DNA Signature Prep kit (Plex A) and sequenced on the MiSeq FGx® machine.

The amplicon sizes in the three PCR/CE based assays ranged from 80bp to 470bp and were separated on an ABI 3130xl Genetic Analyzer. The resulting electropherograms were analysed using GeneMapper® v4 for the PowerPlexY23® kit and GeneMapper® ID-X v1.5 for the NGMSElect® and the PowerPlex® Fusion 6C. The minimum threshold used for reportable alleles was 50 rfu for both heterozygous and homozygous loci.

Regarding the MiSeq FGx® data, the analysis was performed using Illumina's dedicated software (Universal Analysis Software-UAS). The X-STRs were excluded from the project for simplification purposes and comparability with the CE-based methods. The minimum thresholds used for reportable alleles were 29 reads for autosomal and Y- STRs (both homozygous and heterozygous loci), 14 reads for heterozygous identity informative SNPs and 20 reads for homozygous ones.

4.4 Results

4.4.1 Sample Recovery

The fragments collected after the C4 explosions were visibly smaller than those from the DBSP explosions as can be seen by comparing Figures 4.10, 4.11 and 4.12 with Figure 4.13. Additionally, more items were recognisable from the DBSP bombs and the

adhesive tape was still covering the samples in most cases[6]. The body of pipe 1 (Figure 4.12) was the least damaged and showed volume expansion to accommodate the release of hot gases. Some of the items were covered in soot indicating the burning effect. Although similarly charged and composed of the same material, pipe 3 (Figure 4.12) showed more fragmentation than pipe 1 as well as bending of the central metallic bolt which is supposed to be the one of the most blast-resistant items within the bomb. Pipe 2, which is made of copper and contained the largest charge, showed the most severe fragmentation among the DBSP-charged bombs (Figure 4.11), and its fragments looked almost like those from the C4 bombs (Figure 4.13).

With regards to the recovery of samples, all stains were recovered from the DBSP bombs, whereas only 80% of the 30 µL (yellow tape) and 43.35% of the 10 µL (green tape) blood stains located on the pipes' outer surface were recovered from the C4 bombs. The blue and white tapes placed inside could not be found after the explosion.

Figure 4.10 Post-blast recovered items associated with DBSP-pipe 1 (P1- brass).

Five blood stains (30 µL) had been placed inside and five others outside.

[6] Note that images in Figures 4.10, 4.11 and 4.12 were taken after some of the adhesive tape was detached in the laboratory and the stains swabbed from some of the additional items.

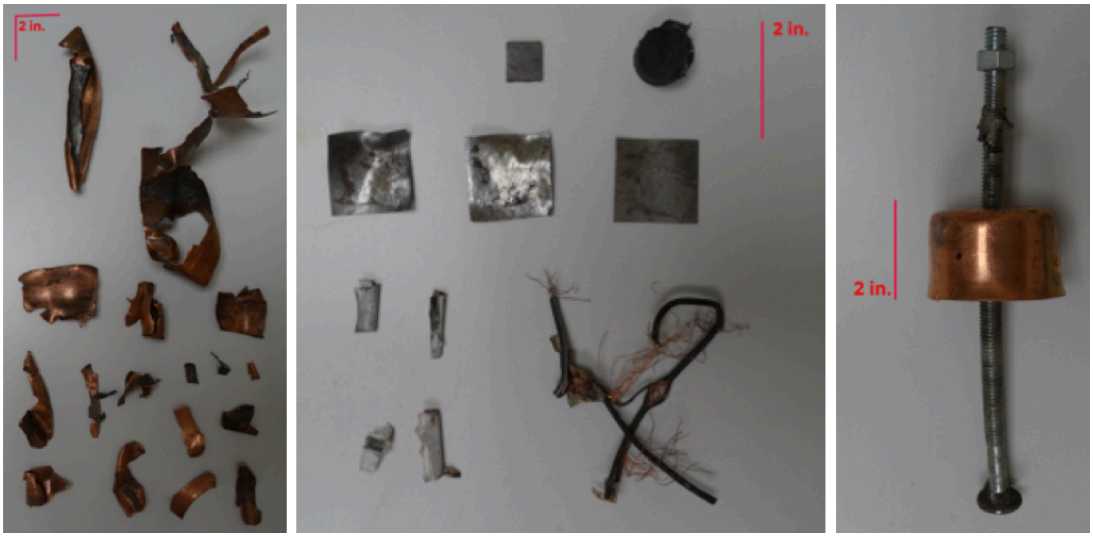

Figure 4.11 Post-recovery items associated with DBSP-pipe 2 (P2-copper).

Five blood stains (30 µL) were placed inside and five others outside.

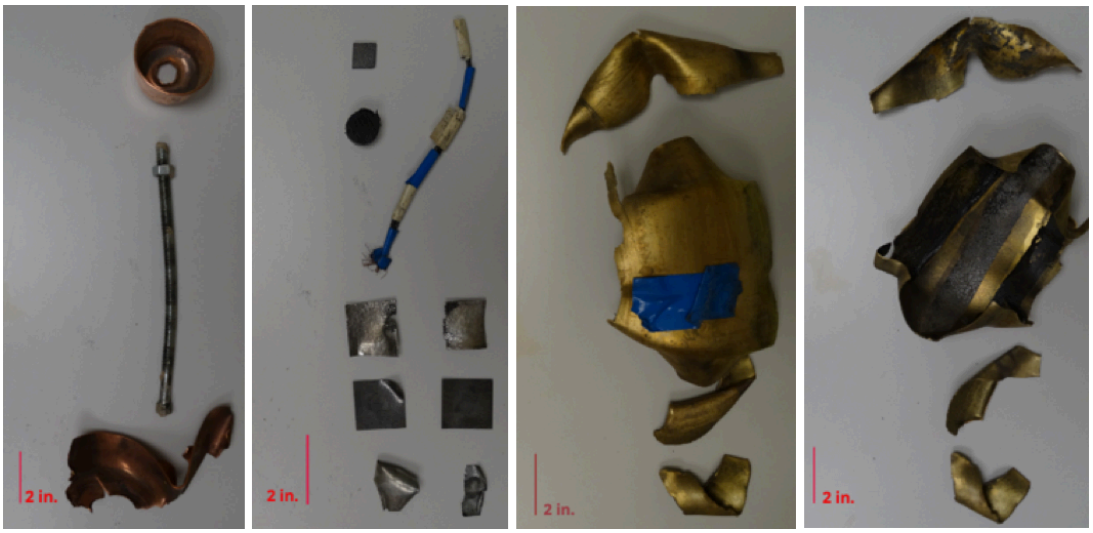

Figure 4.12 Post-recovery items associated with DBSP-pipe 3 (P3-brass).

Three saliva stains (200 µL) were placed inside and three others outside.

Figure 4.13 Post-recovery items associated with C4-pipes four and five.

Table 4.4 Post-blast items recovery- DBSP.

	P1 (Brass) 10 blood stains (30 µL)	P2 (Copper) 10 blood stains (30 µL)	P3 (Brass) 6 saliva stains (200 µL)
30 µL blood stains, outside	5/5 (100%)	5/5 (100%)	NA
30 µL blood stains, inside	5/5 (100%)	5/5 (100%)	NA
200 µL saliva stains, outside	NA	NA	3/3 (100%)
200 µL saliva stains, inside	NA	NA	3/3 (100%)
Total	10/10	10/10	12/12

Post-blast (total, n=26) recovery of saliva and blood stains resulting from the explosions of the three DBSP-pipe bombs in Colorado.

Table 4.5 Post-blast items recovery- C4.

	P4 (Steel) 60 blood stains	P5 (PVC) 60 blood stains
Yellow, 30 µL stains, outside	86.7% (13/15)	73.3% (11/15)
White, 30 µL stains, inside	0% (0/15)	0% (0/15)
Green, 10 µL stains, outside	40% (6/15)	46.7% (7/15)
Blue, 10 µL stains, inside	0% (0/15)	0% (0/15)
Total	19/60	18/60

Post-blast recovery of blood stains (n=39) resulting from the two C4-pipe bombs in Pennsylvania. Partial bloodstains that were shredded by the explosion were counted as half. The tape shredding phenomenon was only seen after the steel pipe explosion, P4.

4.4.2 Quantification Results

The post-blast qPCR concentrations were compared between the experiment's different variables (Figure 4.14). The C4-stains' within comparisons were between different volumes - 10 µL *v.* 30 µL - and different pipe containers - PVC *v.* steel. The DBSP-stains' within comparisons were between sample types - blood *v.* saliva, locations - inside *v.* outside of the pipes, and the different container materials - brass *v.* copper. Finally, both groups were also compared between each other in terms of the type of energetic used: C4 (military-grade explosive, n=39) *v.* DBSP (low explosive, n=26).

The relationship between DNA concentration and these variables (volume, location, type of explosive) was modelled using a multivariate linear regression. Only the type of explosive, C4 *v.* DBSP, and the volume of stain were shown to significantly affect the concentration of recovered DNA. The consequences of eluting the DNA extracted from stains of different sizes into the same volume is self-evident and is not investigated further, the type of explosive affected both the LH (F = 14.92, 54= DF, p-value= 2.845e-08) and SH (F = 13.29, 54= DF, p-value= 1.321e-07) fragment with lower

yields from the DBSP explosive.

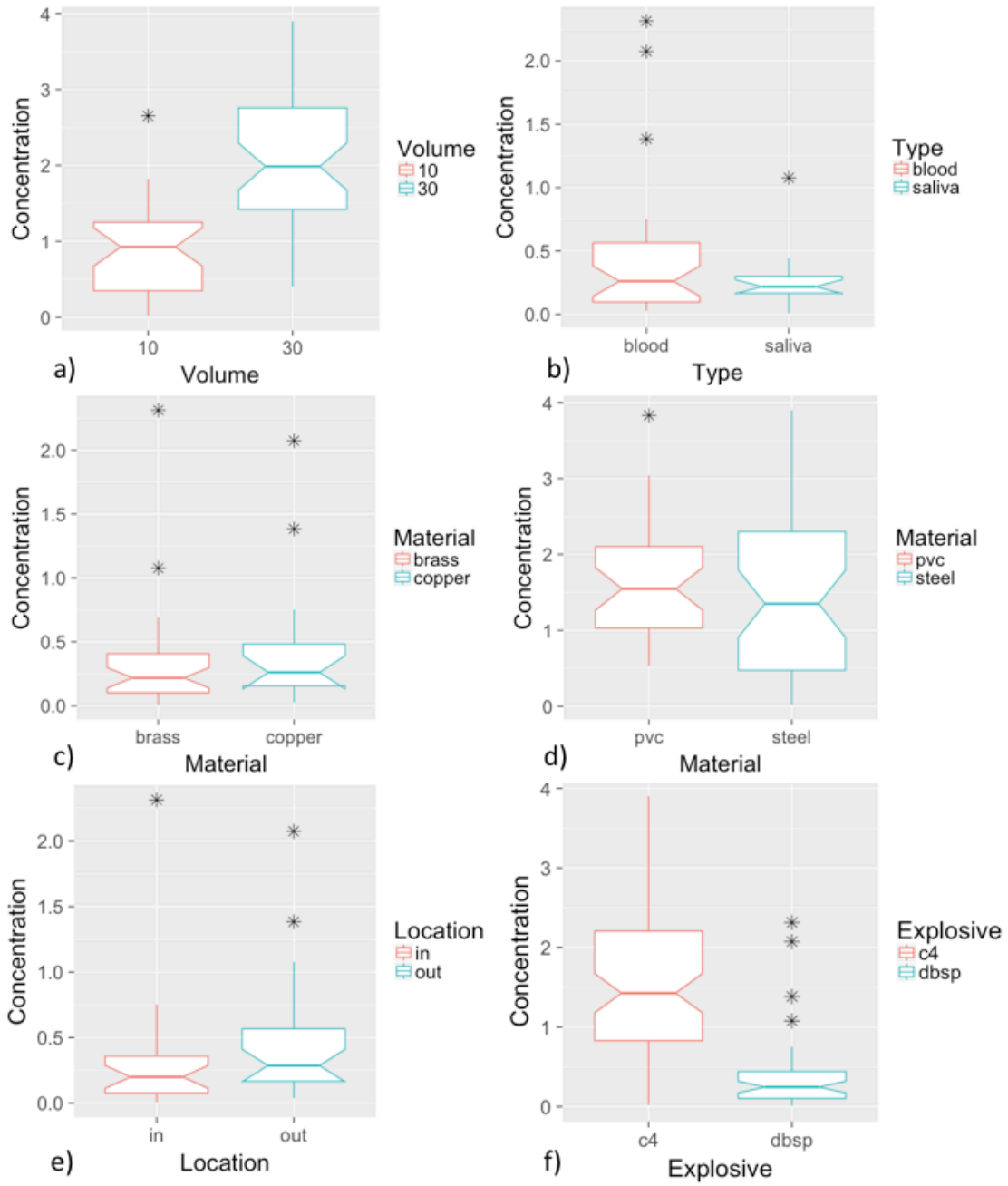

Figure 4.14 RT-PCR DNA concentrations after the explosions.

Post-blast DNA concentrations (determined by qPCR) between the following different variables: a) volume (30 v. 10 µL), b) type (blood v. saliva), c) material (brass v. copper), d) material (PVC v. steel), e) location (in v. out), and f) explosive (DBSP v. C4).

Cost, time and other practicalities limited the comparisons between blood and saliva, and between brass and copper containers to the DBSP; and the comparison of PVC and steel to C4. This created blind spots as to whether such variabilities between

experiments may have affected the DBSP *v.* C4 comparison. However, separate analyses showed that the container material and the sample type (blood or saliva) were not significant to DNA concentrations, unlike the type of explosives (Table 4.6, Figure 4.14).

4.4.2.A Container Type

The hypothesis that the bomb's container type may influence the recovery of DNA (concentration) is refuted with no statistical significance between container type and DNA concentration in both Colorado - brass *v.* copper - and Pennsylvania - PVC v. galvanised steel- experiments (Table 4.6).

Table 4.6 Significance testing between pipe material and DNA concentration.

Experiments	container type	Fisher's test
Colorado	Brass (n= 20)	LH: F = -0.46259, df = 10.454, p-value = 0.6531 SH: F = -1.2601, df = 9.9836, p-value = 0.2363
	Copper (n= 6)	
Pennsylvania	PVC (n= 18)	LH: F = 0.80381, df = 36.408, p-value = 0.4267 SH: F = 0.57294, df = 36.15, p-value = 0.5702
	Steel (n= 19)	

4.4.2.B Sample Type

Comparison of Real-Time PCR quantification results of blood (n=20) and saliva (n=6) from DBSP IEDs was performed using a simulation of 500 random pairings between blood and saliva to alleviate bias from the unequal number of observations. It was concluded that DNA concentrations obtained from exploded blood stains were not significantly different from those obtained from exploded saliva stains, as most pairing's p-values and t-statistics are almost equal to one and zero, respectively (Figure 4.15).

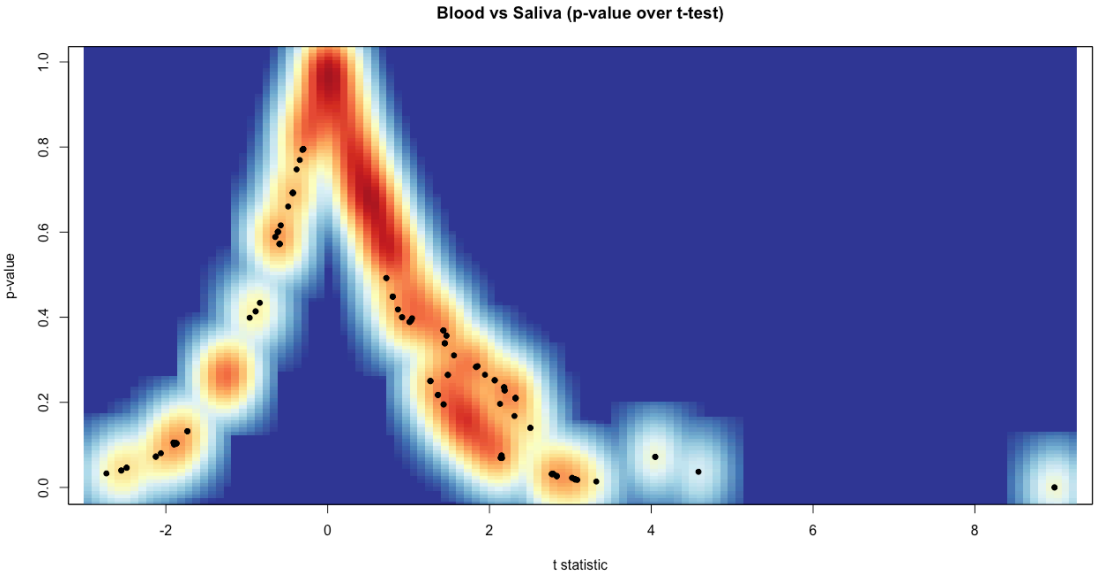

Figure 4.15 Significance testing between sample type and DNA concentration.

Simulation of 500 random pairings between DBSP-exploded blood and saliva stains, showing each paring's p-value plotted against its t-statistic. The area of highest density (dark red) is around t=0 with the highest probability (p-value∼1).

4.4.2.C Additional Data Exploration and Testing for Significance (DBSP v. C4)

The qPCR concentrations estimates were checked for normal distribution. Following the simulation of a normal distribution reference population of similar size, mean and standard deviation (n=65, μ=1.26, sd= 1.1), the data was plotted in the same way through a quantile plot and a histogram. Compared to the bell-shaped normal distribution it showed a negative binomial trend (Figure 4.16).

The data's binomial distribution suggested performing significance tests that are based on ranking and do not assume normality, *i.e.* the Wilcoxon and the Kruskal-Wallis chi-squared tests. Both tests showed a significant difference in DNA concentrations between stains that were exposed to DBSP explosions and those that were exposed to C4 (Wilcoxon = 899, p-value = 2.455e-07; Kruskal-Wallis chi-squared = 23.601, df = 1, p-value = 1.185e-06). While these nonparametric tests are adequate for hypothesis

testing, they lack the statistical power that traditional parametric tests have.

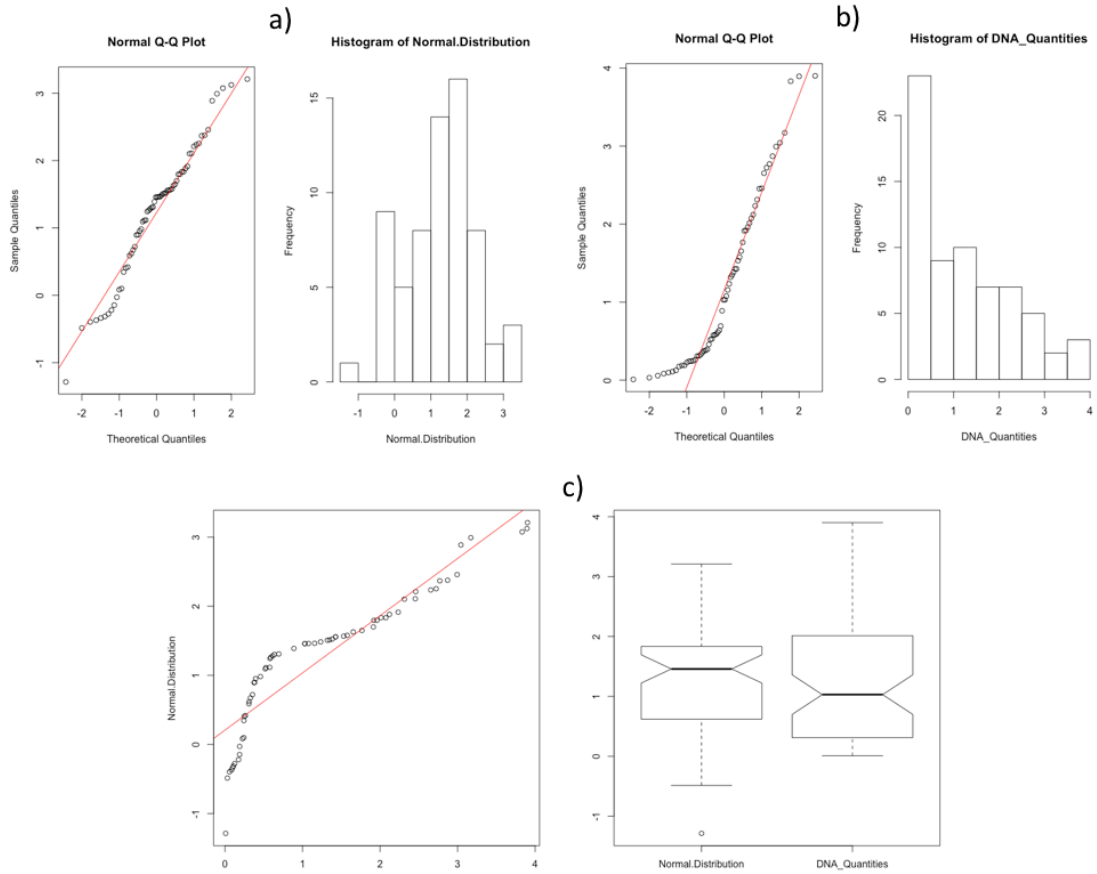

Figure 4.16 Divergence for normal distribution.

A quantile plot and a histogram were generated for the simulated normal distribution (a) and the qPCR data (b) for visual comparison between the two populations. The quantile plot and boxplots (c) further illustrate the qPCR data's divergence from a normal distribution.

4.4.3 Degradation assessment

4.4.3.A Degradation Index

The qPCR derived Degradation Indices (DI) show that both 4 °C stains and those exposed to C4 explosions have DIs that are lower than 1, while a subset of those exposed to DBSP explosions have DIs higher than 1 suggesting degraded DNA (Figure 4.17).

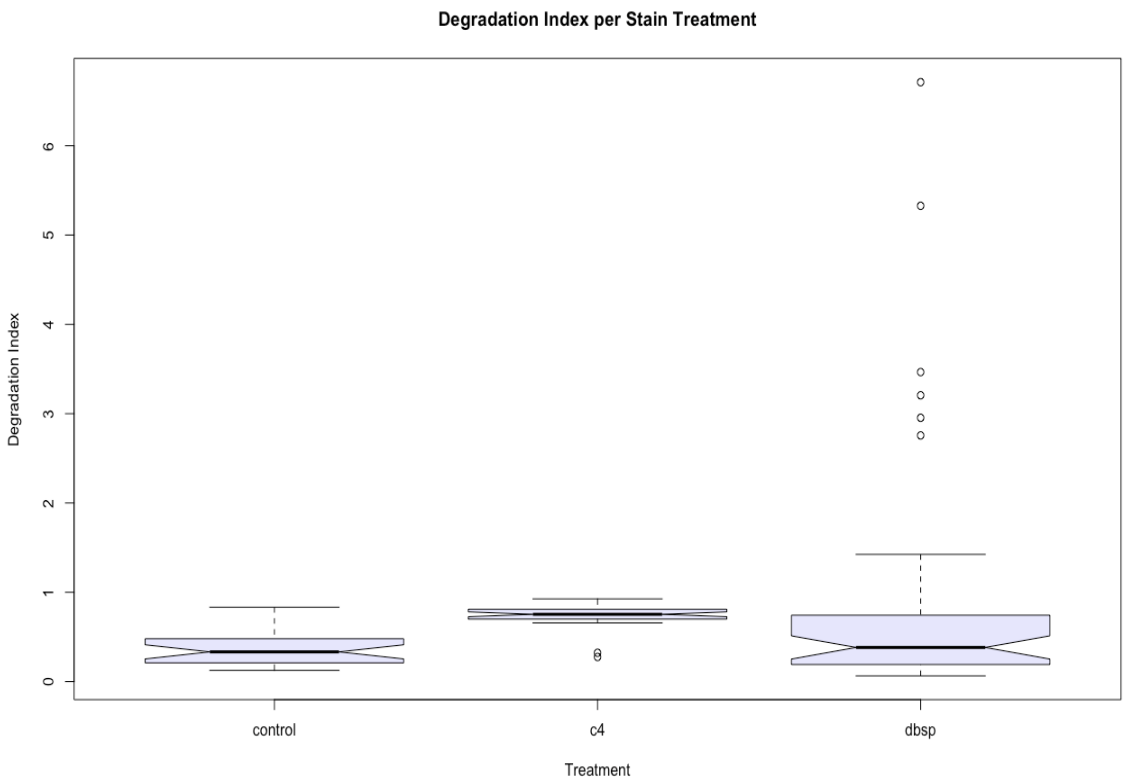

Figure 4.17 Degradation Indices- controls v. exploded stains.

Boxplots comparing the Degradation Index (log values) between 4 ℃ (controls) stains (n=14, left), C4 (n=39, centre), and DBSP -exploded stains (n=26, right).

4.4.3.B Mitochondrial DNA multiplex

The mitochondrial DNA multiplex was used to amplify post-blast stains to further assess their quality prior to typing and sequencing. All tested C4 stains (n=6) showed amplification of at least the small (97 bp) and intermediate (330 bp) targets with four out of six also showing amplification of the long fragment (837 bp) (Figure 4.18). No significant difference could be observed between the 30 µL and 10 µL blood stains. The DBSP stains manifested a pronounced difference in DNA degradation between samples, in both blood and saliva stains, however without significant differences between the two biomaterials (Figure 4.19). The intermediate and small amplicons were amplified in two out of the seven tested blood stains from pipe one (p1) with one of them also exhibiting the large target's amplification, while two out of five indicated the same "non-degraded" nature from pipe two (p2), together two out of three tested saliva stains from pipe three (p3).

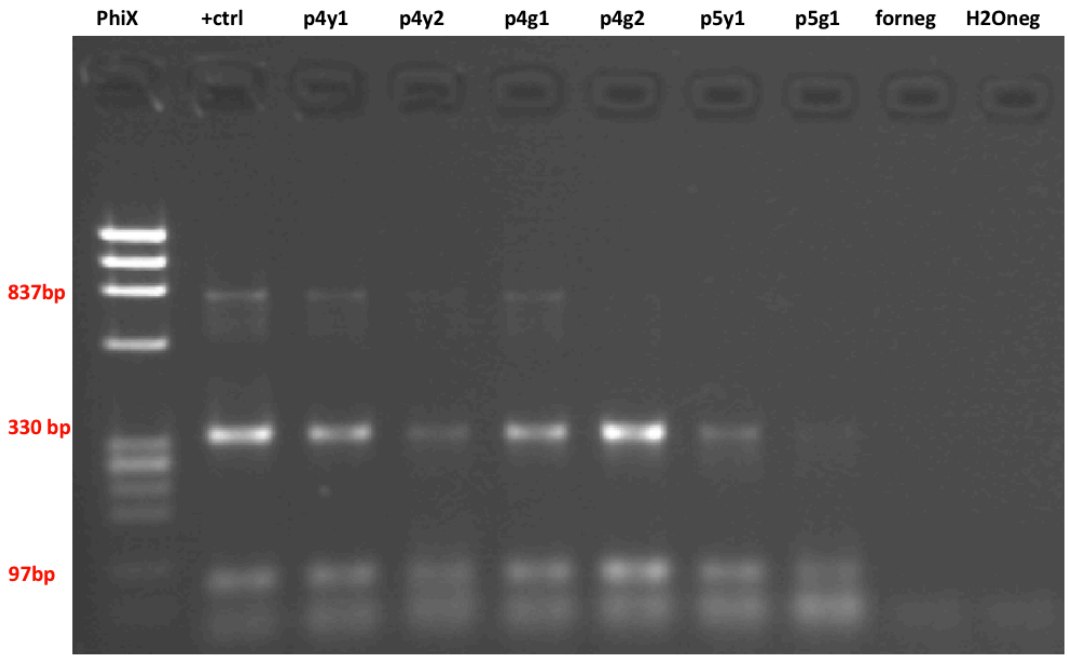

Figure 4.18 mtDNA multiplex results applied to C4-exploded stains.

Gel electrophoresis (2% agarose) image illustrating the mtDNA multiplex results when applied to C4-exploded stains. Letter "p" in the samples' name indicates the pipe followed by its number, while the second letter indicates the stain's volume: "y" for 30 µL and "g" for 10 µL. All stains showed amplification of at least the intermediate and short targets suggesting that any DNA degradation would not preclude DNA typing.

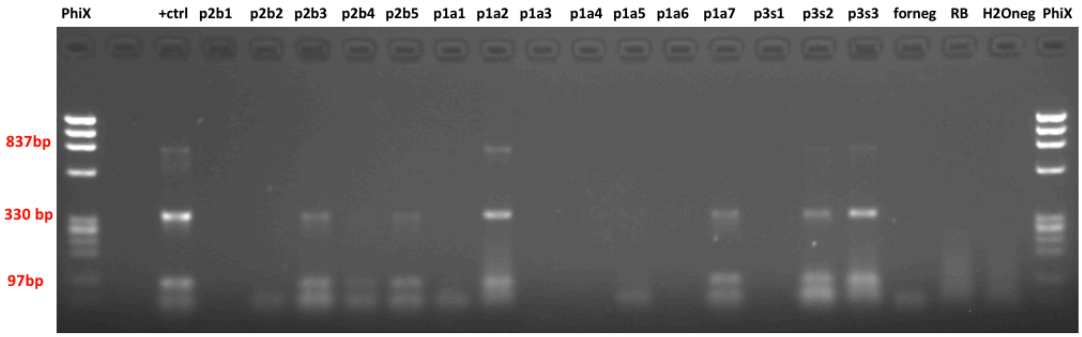

Figure 4.19 mtDNA multiplex results applied to DBSP-exploded stains.

Gel electrophoresis (2% agarose) image illustrating the mtDNA multiplex results when applied to DBSP-exploded stains. Letter "p" in the samples' name indicates the pipe followed by its number, while the second letter indicates the sample type: "a" and "b" for blood stain, "s" for saliva stain. The results show considerable variation in the amplification success for both saliva and blood stains. "Forneg" refers to a forensic negative, which is a control against the presence of a forensic sample on specific surface, and RB to Reagent Blank.

4.4.4 DNA Typing/Sequencing

Stains from both the C4 and DBSP devices were typed using CE-based autosomal and Y STR methods (PowerPlex® Fusion 6C for C4, and NGMSElect® and PowerPlex® Y23 for DBSP). The C4 stains were also sequenced by MPS using the ForenSeq DNA Signature Prep kit.

4.4.4.A Composite.4 (C4) Stains

Full profiles and good quality sequences were obtained from all 39 tested stains through MPS (Figure 4.22), while 37 out of 39 samples generated full profiles through CE such as the one shown in Figure 4.20. The two samples that failed CE typing of are unlikely to have done so due to degradation, as the typical pattern of declining signal strength with increasing molecular weight was not seen and the same samples were successfully typed/sequenced through MPS. The failure is most likely due to operator error. Surprisingly opposing trends of signal intensity to amplicon lengths were observed between CE and MPS. While the PowerPlex® Fusion 6C resulted in lower RFU for larger DNA fragments engendering a tailing off in signal strength towards the right-hand side of the EPG for both the unexploded and exploded stains (Figure 4.21), the ForenSeq DNA Signature Prep resulted in an opposite pattern where the amplification of larger fragments had a higher DoC (Figure 4.23). The correlation between amplicon length and RFU was shown to be statistically significant with the control stains' $F=146$ on 1 and 88 DF, and p-value: $< 2.2e-16$, .and the C4 stains' $F= 366.1$ on 1 and 1662 DF, and p-value: $< 2.2e-16$. With every base pair increase, the RFU seemed to decline 4.4 units for the controls and 3.7 units for the C4 stains. However, the DoC increased by 0.7 reads per additional base pair for the controls ($F=36.39$ on 1 and 762 DF, p-value: 2.515e-09) and by 0.9 for the C4 stains ($F=490.5$ on 1 and 8739 DF, p-value: $< 2.2e-16$): This slight increase in DoC at the larger molecular weight amplicons may be explained by the manufacturer's attempt at countering the bias towards shorter DNA fragments, by dedicating more space for the larger fragments and possibly resulting in a reversed bias.

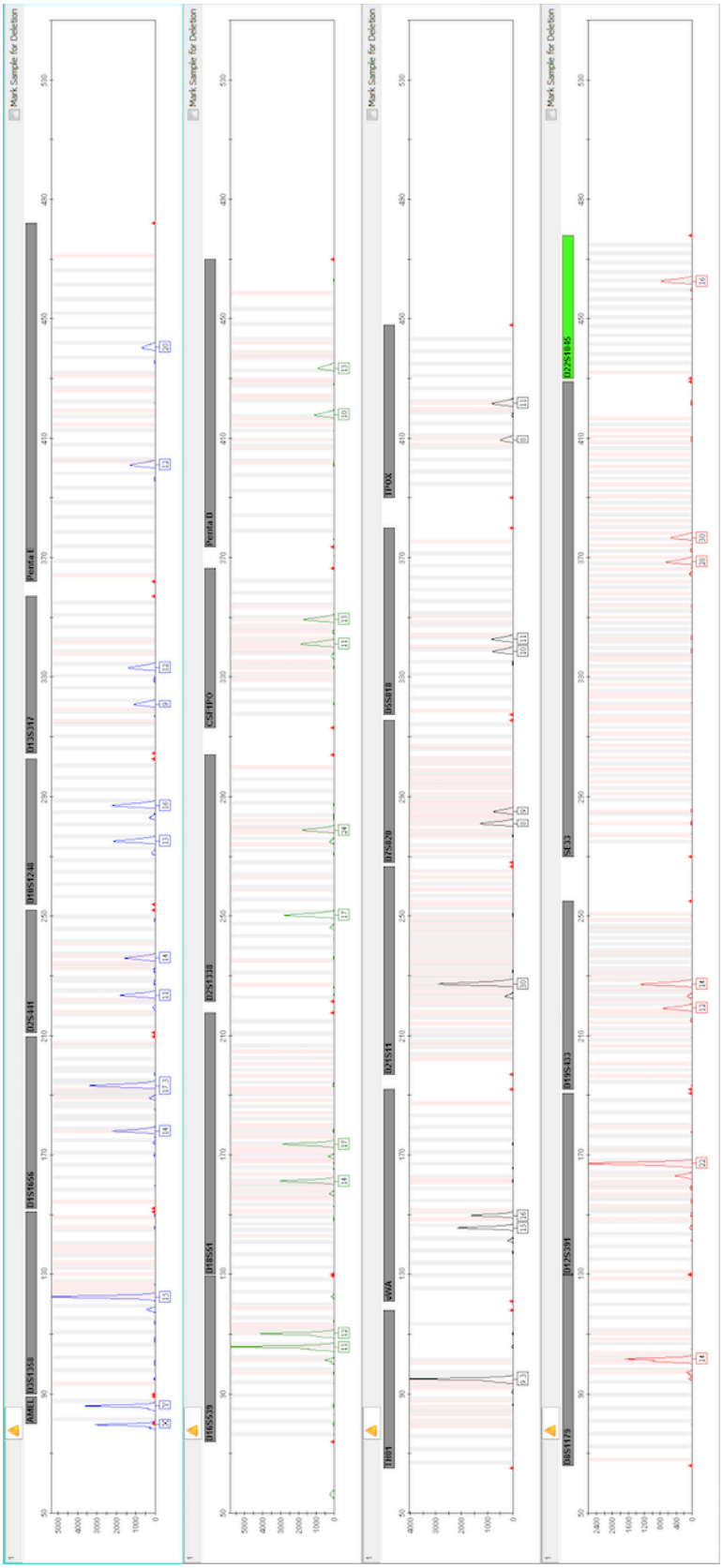

Figure 4.20 Electropherogram- stain exploded with C4 pipe.

Electropherogram (EPG) a fully interpretable STR profile from a 30 µL blood stain that was placed on the outer surface of a C4-charged pipe bomb that was detonated.

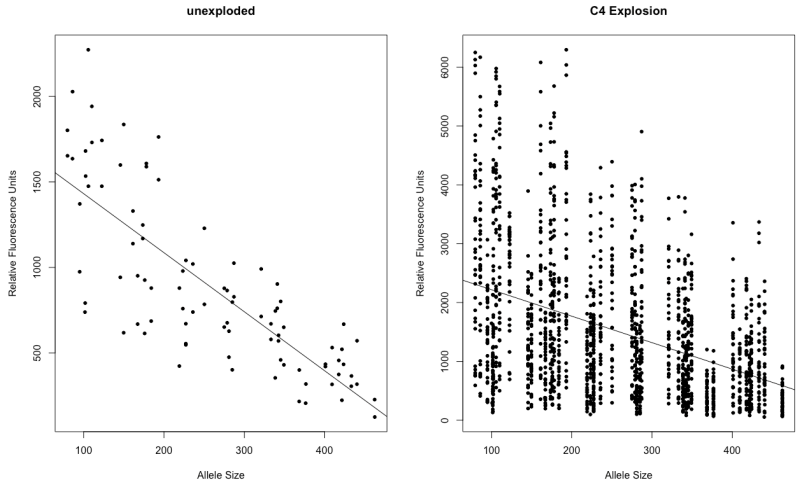

Figure 4.21 The effect of C4 explosions on CE-based STR typing.

Plotting the Relative Fluorescence Unit (RFU) intensities against the amplicon lengths for the control (left, n=2) and the C4 stains (right, n=37) typed using the PowerPlex® Fusion 6C kit.

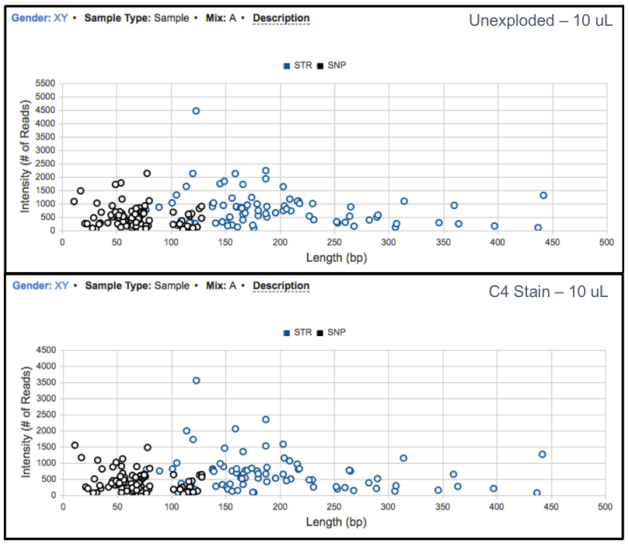

Figure 4.22 Unexploded v. C4 exploded stains on the Universal Analysis Software (UAS).

Scatter plots from Illumina's Universal Analysis Software showing Number of Reads (or Depth of Coverage) per amplicon plotted against amplicon length. The autosomal and Y-STRs are marked in blue, while the iSNPs are marked in black. The top plot is derived from an unexploded 10 µL blood stain (positive control), and the lower one from a similar stain placed on the outer surface of a C4-charged pipe bomb. Both samples were successfully typed indicating that whatever degradation may have occurred was insufficient to affect analysis of the C4 stain.

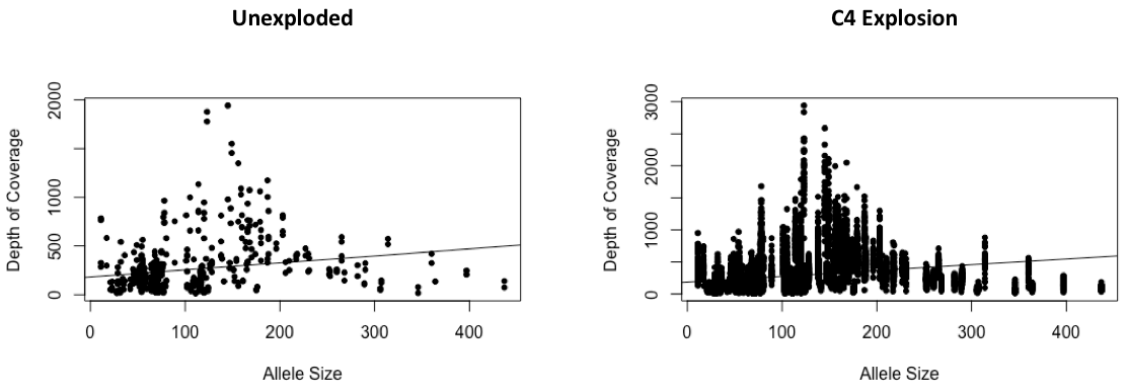

Figure 4.23 The effects of C4 explosions on Massively Parallel Sequencing.

Plotting Depth of Coverage (DoC) against amplicon length for C4 stains (right, n=39) sequenced with the ForenSeq® DNA Signature Prep kit. Two positive controls (left, n=2) were also tested to ensure that a non-exploded sample would result in a full profile.

4.4.4.B Double-Base Smokeless Powder (DBSP) Stains

The blood and saliva stains exposed to DBSP explosions showed DNA degradation with a reduced RFU and dropouts at the higher molecular weight loci, generating partial profiles with a ski-slope pattern (Figure 4.25). Autosomal STR typing with NGMSElect® showed a mean RFU reduction by 4.4 units with each additional base pair and produced 19 allele dropouts out of 866 targeted alleles (2.2% dropout). Among 26 analysed stains, four gave partial profiles while the remaining 22 gave full profiles (Table 4.7, Figure 4.24). PowerPlex® Y23 showed a mean RFU reduction of five units with every base pair increase resulting in 66 dropout alleles out of 621 targeted (10.6% dropout). Of 26 analysed stains, 10 gave partial profiles while the remaining 16 produced full profiles (Table 4.8, Figure 4.24). The null hypothesis H_0 stating no difference in RFU between amplicons of different lengths was rejected through the Fisher's tests that were applied to exploded stains analysed with both the NGMSElect® ($F=208.1$ on 1 and 863 DF, p-value: $< 2.2e-16$) and the PowerPlex® Y23 ($F=234.6$ on 1 and 619 DF, p-value: $< 2.2e-16$).

Post-blast DNA degradation affected 27% of blood and saliva stains recovered from exploded DBSP-charged pipe bombs. Of these, three blood and three saliva were attached to the pipes' outer surfaces, while six blood and one saliva were placed inside the pipe. In terms of dropouts, no significant difference was found between locations

(in v. out), between sample types (blood v. saliva), and between container material (brass v. copper).

Table 4.7 Partial profiles from DBSP exploded stains through autosomal STR typing.

ID[7]	Type	Location	Dropouts
p1abinline1	blood	in	11
p1abferprx	blood	out	1
p3bsinline1	saliva	in	6
p3bswt0	saliva	out	1

[7] ID codes start with the pipe's number followed by letters and digits that respectively designate the donor (a or b), the stain type (b:blood, s:saliva) and location (blttape: tape around steel bolt, inline: on the pipe's inner surface and covered with tape, wt: tape around electric wire, ferprxy: iron proxy covered with tape).

Table 4.8 Partial profiles from DBSP exploded stains through Y-STR typing.

ID	Type	Location	Dropouts
p1abblttape	blood	in	4
p1abinline3	blood	in	3
p1abwt0	blood	out	10
p1abwt5	blood	out	6
p2bblttape	blood	in	1
p2bbinline2	blood	in	16
p2bbinline3	blood	in	4
p3bsinline1	saliva	in	12
p3bswt1	saliva	out	1
p3bswt2	saliva	out	9

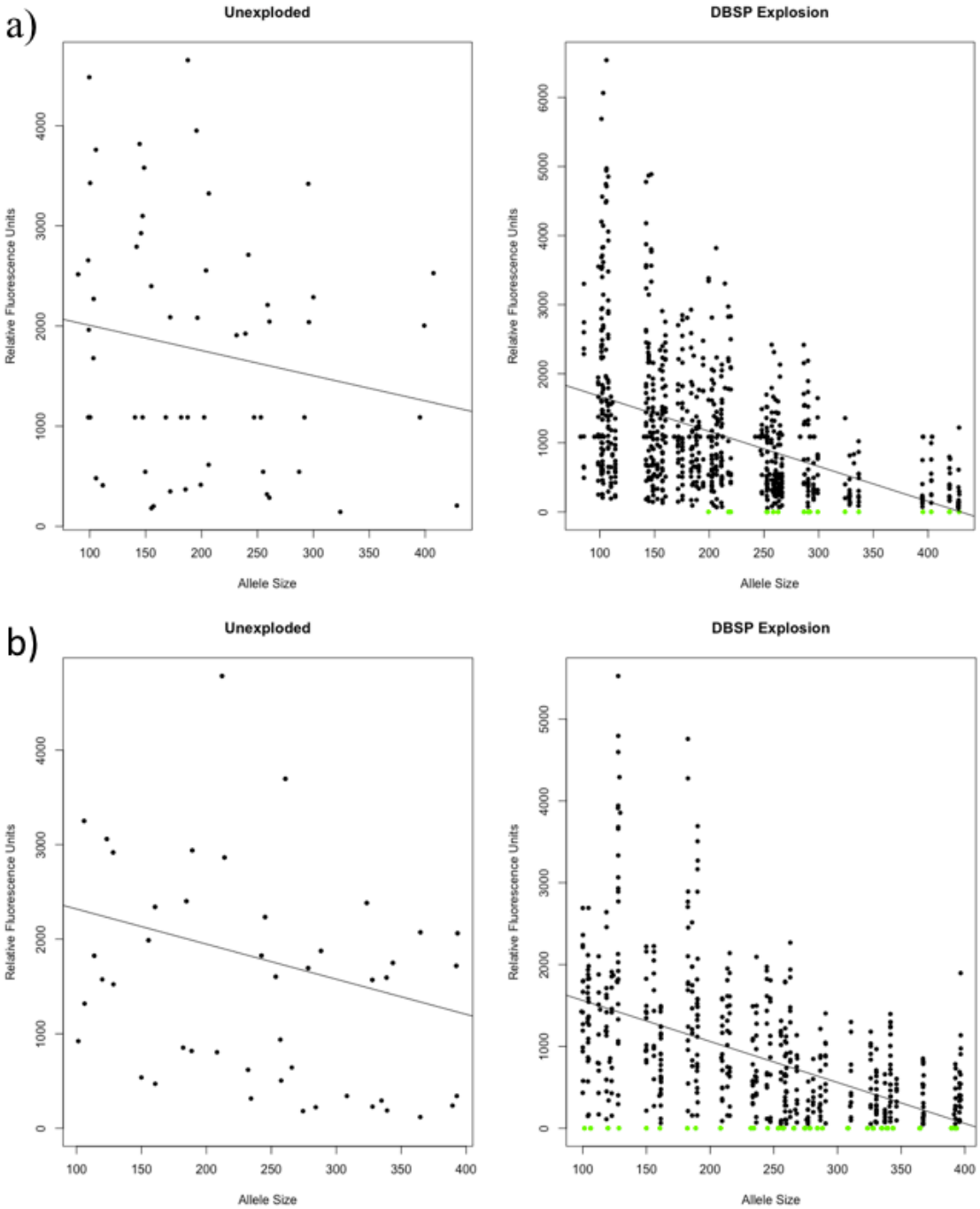

Figure 4.24 The effects of DBSP explosions on CE-based STR typing.

Plotting Relative Fluorescence Units (RFU) against amplicon length for control (left, n=2) and DBSP stains (right, n=26) typed with NGMSElect® (a) and PowerPlex® Y23 (b).

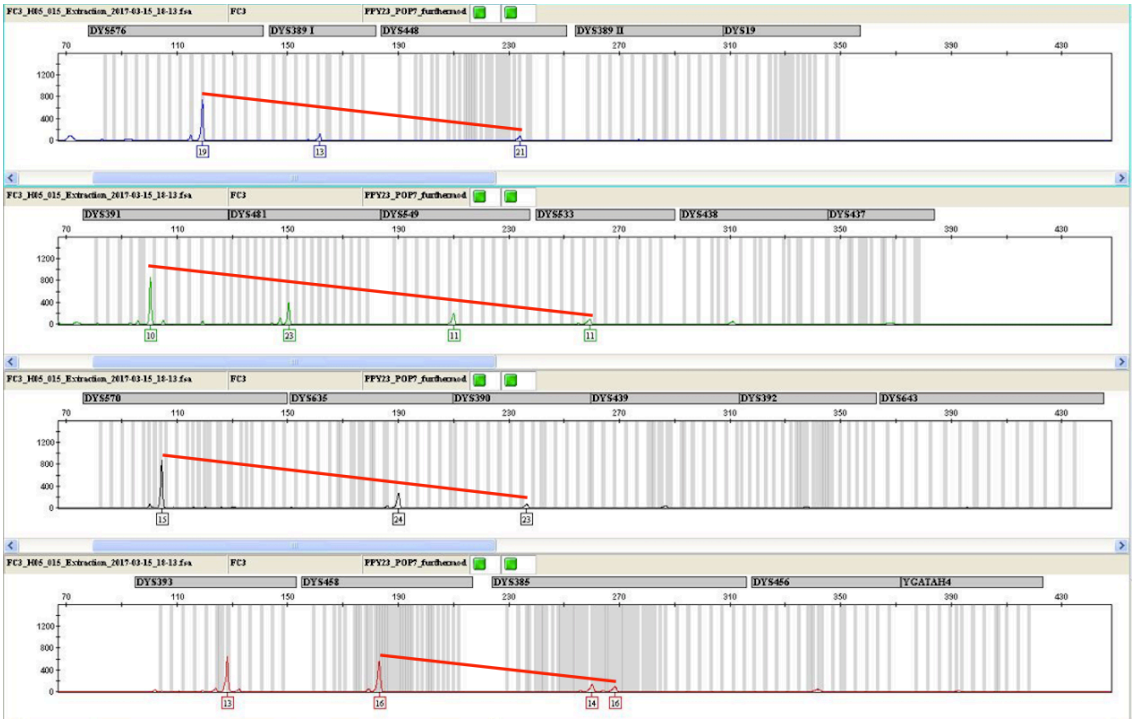

Figure 4.25 Electropherogram - partial Y profile from DBSP exploded stain.

Electropherogram (EPG) showing a partial Y-STR profile from a 200 µL dried saliva stain placed the outer surface of an exploded DBSP-charged pipe bomb. The ski-slope effect with dropouts of the longer amplicons is typical of DNA degradation.

Finally, no presence of human DNA was detected in the negative controls, indicating that the decontamination process was sufficient and that no contamination occurred during the preparation, explosion, collection and analysis processes.

4.5 Discussion

4.5.1 Experimental Design - Strengths and Limitations

Pipe bombs were chosen for this project out of the virtually unlimited spectrum of different types of explosive devices. The primary reason was simplicity of construction which facilitated collaboration with law enforcement agencies as the experimental design is straightforward and did not require sharing of sophisticated and classified ways of building bombs. The simple construction process also reduced the risks of contamination from the bomb maker with less steps that could be done wearing personal protective equipment.

As it would be difficult for members of the public to imagine the exact shape of other more sophisticated bombs, the simplicity of pipe bombs facilitated the scientist's planning of the test samples' placement in advance and simplified communication of the details with the bomb experts. Their design also facilitated the purchase of the pipes, end caps and other materials from local hardware stores. Pipe bombs could also be efficiently decontaminated with bleach and UV irradiation prior to placing the biological stains. Finally, the experimental prototypes reflect today's reality as pipe bombs were reported to be the most frequently used type of bombs according to the *US Explosives Incident Report* (United States Bomb Data Center, (USBDC) 2016) and the FBI (Heramb and McCord 2002).

The materials used in construction were chosen according to their availability at the time and location of the two sets of experiments. The brass and copper pipes, together with copper end caps were purchased by another PhD student from the UK before transporting them to Colorado and using some for their own purposes of detecting post-blast latent fingerprints. A year later in Pennsylvania, PVC and galvanised steel pipes were the most readily available material in the locality. The change of materials introduced another variable that could have had an effect on DNA recovery, although the comparisons between brass *v.* copper and PVC *v.* steel produced non-significant differences. Furthermore, DNA had previously been successfully recovered from copper and brass (Holland et al. 2019), and from PVC and galvanised steel with a similar success rate for DNA profile recovery (Esslinger et al. 2004), which assumed no significant problem with any of the chosen materials was not foreseen. The potential impact of using different stains (blood *v.* saliva) and locations (in *v.* out) with DBSP was unknown prior to the trials but was shown not to have a significant effect.
This study was performed without prior experience working with explosives, consequently the initial experiment in Colorado was guided by literature which discussed a variety of methods to study post-blast DNA recovery. While some earlier studies had access to casework items or human remains (Sudoyo et al. 2008; González-Andrade and Sánchez 2005; Phetpeng et al. 2015), others worked on IED or ammunition substrates without inducing any explosion prior to DNA analysis (Thanakiatkrai et al. 2017; Holland et al. 2019).

Naturally, working with explosives required approval from the relevant law enforcement agencies and access to crucial material to construct an efficient bomb

which is restricted to security services use in the UK and the USA. These materials include the military grade energetics such as the C4 and the detonating systems (detonation cord, fuse capsule, remote detonator, etc.). A more important restriction to respect as civilian scientists is the knowledge about constructing and operating bombs.

The collaboration with law enforcement in this project afforded expertise in pipe bomb construction and their safe deployment once the samples were deposited onto and inside the inert container by the scientist. A number of studies had adopted a similar approach of assembling dedicated explosive devices that were later detonated under 'controlled' conditions (Esslinger et al. 2004; Foran et al. 2009; Tasker et al. 2017). Tested surfaces included cloth, paper, electric circuits, rubber bands, PVC, and different types of metals. While IEDs continue to evolve, some of the latest prototypes are posted online from unconventional warfare zones (Figure 4.26).

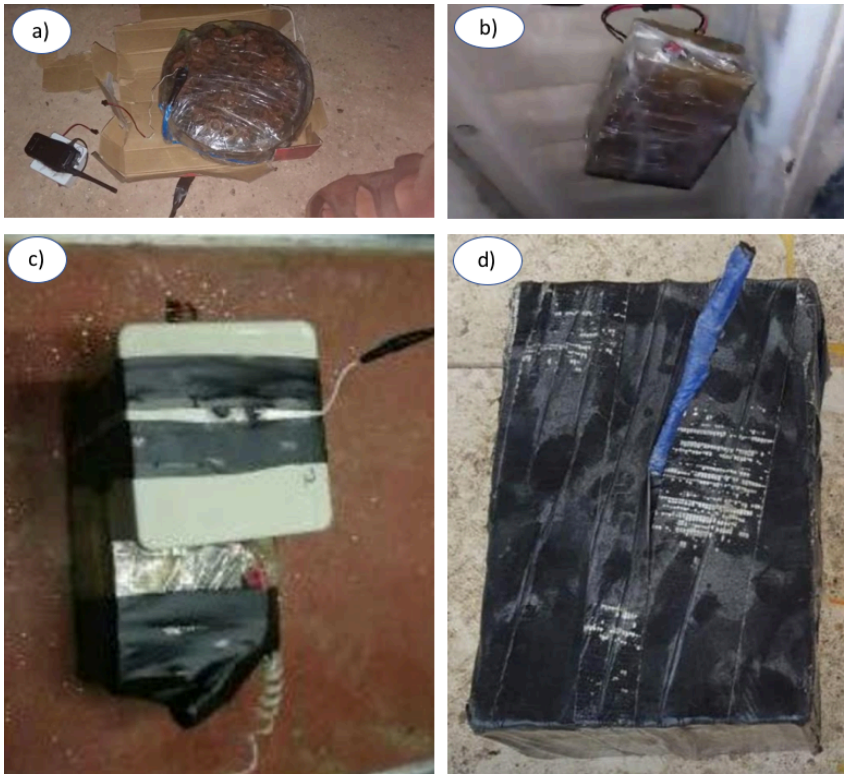

Figure 4.26 Currently used Improvised Explosive Devices.

A series of Improvised Explosive Devices found in rebel held areas in Syria (2018). Note the heavy use of tape and electric wires (Qalaat Al Mudiq 2018). a: remote controlled directional fragmentation IED found in Idlib Syria. b: Vehicle-bound IED planted under an HTS[8] car (January 20th 2019). c: Dismantled IED from Idlib Syria bound to unspecified substrate. d: Neutralised IED in Manbij-city Northern Syria, found under the car of Syrian Democratic Forces.

4.5.2 Distinguishing Between Explosions and Accompanying Fires

Fires and other sources of high temperature are often the cause or the consequence of an explosion. Two high profile examples mentioned in Chapter 4, where forensic DNA identification was hindered by failed or partial profiles were the Texas Waco disaster, and the 9/11 twin tower attack[9]. Other explosions which have challenged forensic DNA analysis are the Jakarta 2004 and the Beirut 2005 Vehicle Bound IED (VBIED) attacks, mentioned in this Chapter's introduction. VBIED attacks often lead to subsequent fires

[8] HTS: Hay'at Tahrir al-Sham or the "Organization for the Liberation of the Levant". Jabhat al-Nusra, HTS's precursor organization, was formed in Syria in 2011 as al-Qaeda's affiliate.

[9] The 9/11 did not involve any device that is made to explode but rather used flying passenger planes as large bombs.

because of the presence of combustible material such as gasoline, motor oil, and other surrounding objects.

The Spitsbergen plane disaster represents a case where accompanying fires, if any, could not be sustained due to the snowy grounds and the extremely low temperatures on the crash's site (Olaisen et al. 1997). In August 1996, a controlled flight into terrain caused Vnukovo Airlines Flight 2801 to crash on the Operafjellet Mountain in Norway, killing all 141 people on board (Figure 4.27). The collected human remains were ready for DNA analysis thirteen days after the incident, and by day twenty, all victims were positively identified. From these, 139 had their autosomal STRs analysed using the quadruplex (plus Amelogenin) as well as five minisatellites (10^3 to 10^4 base pairs in length). All markers were successfully typed and no dropouts were reported. The remaining two victims had been identified at the external examination stage.

Figure 4.27 Vnukovo Airlines Flight 2801 crash.

The flight crashed at the junction between the slope and the plateau of the Opera Mountain (Operafjellet) in snowy terrain. The arrow indicates where the majority of body parts were found (Olaisen et al. 1997).

The examples mentioned above shed light on the uncertainty whether partial profiles or failed amplification might be caused by the explosion itself or by accompanying fires. The pipe bomb experiments described here allowed us to test the effect of an explosion alone on DNA samples that are not in as large a quantity as found in the 1996 Vnukovo Airlines or the 2001 American Airlines Flight 587 crashes, but rather in the form of small biological stains.

4.5.3 Significance of Results

By protecting the stains inside adhesive tape, which in turn was rolled around electrical wires as well as metallic and plastic substrates, the experiments described here focus on

the type of substrates that are targeted in real casework involving bomb attacks. Figure 4.26 shows that tape is abundantly used in contemporary IED construction and provides the best opportunity of finding latent fingerprints and biological samples trapped within the tape folds, or between the tape and the substrate that can be confidently attributed to the bomb maker(s).

The deposition of blood and saliva stains in these locations considerably overestimates the amount of a bomb maker's DNA that is expected to be found on a real device but was intended to provide sufficient DNA to explore the consequences of the damage incurred on subsequent DNA analysis. The current DNA technical leader at the Bureau of Alcohol, Tobacco, Firearms and Explosives (ATF) laboratory stated that over 90% of their evidence samples were from "touch evidence" found on guns, bomb components, and Molotov cocktails (Bille 2014). This project's second batch of experimental devices in Pennsylvania (2017) included touch cells as evidence both inside and outside detonated C4-charged pipe bombs. These experiments and the preliminary results will be discussed in Chapter 6 of this thesis. The priority here was given to the biological fluids since the full profiles that were obtained from the unexploded stains (positive controls) can be adequately compared with post-blast stains allowing the exploration of the explosion's effects without any stochastic effects due to the low-template DNA touch samples. The comparison of controls *v.* exploded/heated touch cells is complicated by the partial profiles that are produced even under normal conditions and the lack of within-same sample reproducibility because of random stochastic effects, or between sample differences because of both within and between donor shedding variability. In addition to the robustness it offers, blood and saliva stains do not necessarily overestimate DNA quantities that would be recovered in the genetic identification of victims of explosions (or fire in Chapter 3), therefore reflecting the reality of both suspect and victim identification scenarios.

4.5.4 Improvements from First to Second Explosion Experiment

The restrictions imposed on the use of explosives precludes the civilian scientists from repeating the experiment, and therefore moving from a pilot trial towards a randomised controlled experiment. A number of questions remained unanswered before and after the first experiment in Colorado. Not being familiar with explosions, the most natural question was whether a sample would disappear after pipe bomb explosions initiated by

different charges. How much of it would remain? And could DNA extraction be performed on the relevant item?

Other questions that followed concerned the initial stains volumes, the type of items to receive such stains, and their locations in relation to the explosion. The decision to keep the same volumes as in the previous chapter for the Colorado experiment - 30 µL of blood and 200 µL of saliva - was backed by the consistent obtention of positive controls with full profiles, and by opening the possibility to compare between the effect of a prolonged exposure to high temperature (Chapter 3) with that of an explosion (Chapter 4). Blood stains of 10 µL that were kept at 4 °C produced partial profile using PowerPlex® Y23.

Whilst knowledge of current forensic practice guided the choice of adhesive tapes, electrical wires and the pipes' metallic surfaces as substrates for sample deposition, placing them inside and outside the pipe bombs was primarily aimed at detecting any significant difference in DNA damage between the two. Van der Voort et al. (2015) reported that the explosion's centre is where peak overpressure and temperature occur before dissipating with distance. The idea was to explore whether biological traces left by the bomb maker inside are more susceptible to destruction than traces left by the bomb handlers, suicide bombers or proximity victims. While the DBSP experiments did not manifest any significant difference in DNA degradation between the two locations, all samples (n=60) that were placed inside the C4-charged pipe bombs could not be detected after the explosion; even after thorough search and recovery efforts conducted by forensic science students and FBI professionals. The recovery area was divided into two zones, which were then searched with the strip method, where the search and recovery personnel would walk in a straight line that combs through the designated area (Maloney et al. 2014). Repeating the experiment indoors or in a Total Containment Vessel[10] (TCV) could confirm if the 60 blood stains that were enclosed in white or blue adhesive tape flaps were pulverised by a quarter pound C4-explosion. This project was granted a second opportunity to work with explosives after communicating the first experiment's details to Pennsylvania Police a year later. The latter accepted to work with pipe bombs this time charged with military grade C4

[10] Total containment vessels (TCVs) are fully enclosed containers designed to safely secure, transport, and test explosive or chemical devices. However, the temperature that is reached by an explosion inside such a structure is significantly higher than that of an outdoor explosion. Caution should therefore be considered when comparing both explosion events.

explosives[11]. A number of improvements were introduced to the original experimental design that was adopted in Colorado:

- The lack of significant differences in DNA concentrations and typing success between 200 µL of saliva and 30 µL blood led to the preference of the latter. Blood was selected for its superior homogeneity in DNA content between stains, its higher resistance to decomposition in ambient conditions due to the lower amounts of bacteria and other microorganisms, and its smaller volume making space for more samples on a single pipe bomb.
- Since all the Colorado samples were protected with adhesive tape prior to their explosions, electrical wires and other additional items that are not part of the bomb's construction were excluded as substrates. This freed up more space for additional samples and facilitated the colour coding to recognise the samples and their locations after their recovery from the blast.
- The extra space allowed for the introduction of a smaller blood volume - the 10 µL stains - as a trial to reduce DNA quantity overestimation when compared to realistic scenarios.

4.5.5 Difference in the effects of High and Low Explosives

Degraded DNA was observed in samples from each of the three DBSP explosions but not in samples that were recovered[12] from the C4- explosions. The two types of explosives were tested at different times - around one year apart - and in different locations - Colorado for the DBSP and Pennsylvania for the C4. Few differences exist between the two experiments such as the covering of the pipes with a metal drum prior to the explosions in Colorado. Additionally, the Colorado samples had to be shipped to the UK before processing at the University of Leicester, while the Pennsylvania samples were analysed in Penn State University during the student's secondment period. Nevertheless, all necessary precautions against DNA damage and contamination were taken to preserve DNA in the dried stains. Packaging and transportation for example was done by storing the items in paper evidence bags and by keeping them in dry and cold conditions throughout their shipment.

---

[11] Penn State Police bomb squad in collaboration with the Federal Bureau of Investigation had a preference in constructing C4 pipe bombs over DBSP as the process required less steps and ensured successful detonations.

[12] Inside samples could not be detected/recovered from C4-charged pipe bombs.

The climatic conditions in both locations, including temperature and pressure, relative humidity, as well as wind speed is described in Table 4.9. It is unlikely that the difference in ambient temperature at the time of the experiments between Colorado and Penn State played a role in the protection of DNA during the C4 explosions which happened at 21 °C, and in the degradation of DNA during the DBSP explosions which happened at three to six degrees Celsius. First, it is expected that C4 explosions would be less influenced by ambient temperatures (Hawk et al. 2004). More importantly, the duration of DBSP explosions was shorter at lower temperatures (Bors et al. 2014) which leads to slightly less heat exposure when compared to DBSP explosions in warmer temperatures.

Table 4.9 Climatic conditions at the time of the bomb experiments.

Date	Location	Temperature	Sea Level Pressure	Relative Humidity	Wind Speed	Number of Tests
27/04/2016	Fort Collins, CO	6 °C	1010 hPa	65%	11 Km/h (E, SE)	3
28/04/2016	Fort Collins, CO	3 °C	1015 hPa	75%	11 Km/h (SE)	2
17/05/2017	Pleasant Gap, PA	21 °C	1015 hPa	56%	8 Km/h (W, SW)	5

If it is assumed that such differences are unlikely to significantly affect the Real-Time PCR quantification and the DNA typing results, one main difference remains to be accounted for between the two experiments: Colorado tested low explosive pipe bombs (DBSP) that deflagrate if the pipe's boundaries did not induce detonation, while Penn State tested high explosive pipe bombs (C4) that detonate at initiation. Since the propagation speed of deflagration is lower than that of the detonation, the DBSP stains may have been subjected to a longer extreme temperature time compared to the C4 stains. Figure 4.28 shows stepwise frame images of one of the exploded DBSP pipe bombs over 1000 milliseconds (ms) with a flash that approximately lasts for 850 ms after the first flash of light. A C4 bomb, that was tested and filmed in Colorado, exploded faster and more violently destroying the metal drum that covered the pipe

(Figure 4.29). The 500 ms long stepwise frame images showed a flame lasting for only 40 ms.

Figure 4.28 Stepwise frames of DBSP explosion.

The double-base smokeless powder (DBSP) charged device exploding over ≈1000ms with a flame duration of ≈850 milliseconds. The flame is seen from the 2nd until at least the 6th frame.

Figure 4.29 Stepwise frames of C4 explosion.

The C4 charged device exploding over ≈500ms with a flame duration ≈ 40ms. The flame is only observed at the second frame and disappears in the third one.

Assuming that the duration of exposure to extremely high temperatures is reflected by the flame duration, the stepwise images (Figures 4.28 and 4.29) showed a 20 fold increase in duration that is subjected by the DBSP explosions when compared to the C4 detonations. This difference in DNA degradation depending on the explosive's speed of decomposition may need to be studied closely, especially that the link can be made by re-visiting a number of previous studies. No post-blast DNA degradation was observed in Rampant (2017) where the high explosive Pentaerythritol tetranitrate (PETN) was used as the main charge of PVC pipe bombs. On the other hand, other studies (Esslinger et al. 2004; Hoffmann et al. 2012) showed DNA degradation from pipe bombs that were charged with low explosives.

Chapter 5 Implications of Degraded DNA on the Weight of Evidence

5.1 Introduction

In the public imagination a DNA match is often associated with extremely strong evidence connecting a crime stain to a potential source. Indeed, a full match obtained through DNA typing using currently available techniques can reach an extremely high power of identification to the extent that some have suggested reporting the result with *reasonable certainty* (Budowle et al. 2000). With kits that include more than ten autosomal STR markers, the random match probability[13] (*RMP*) between profiles from unrelated individuals could be as low as 10^{-30}. For practical reasons related to reporting such numbers to court, Foreman and Evett (2001) recommend setting an upper-bound value of one in a billion to allow for factors such as population substructure that may might limit the discriminatory power of a full profile match, assuming that no non-DNA evidence in favour of the suspect is brought in by the defence. However, the evidential power may be much further reduced when the profile is incomplete due to dropouts, as alleles go undetected as a result of degradation.

The current importance of genetic profiling in forensic identification results from decades of forensic DNA developments, the adoption of a hypothetico-deductive method in forensic science (Jamieson 2004; Houck 2015), and the advent of advanced probabilistic interpretation of the evidence (Evett et al. 2000). However, the evolution of genetic profiling methods has involved trade-offs between discrimination power, sensitivity and versatility. The earliest forensic genetic tests were DNA fingerprints, barcode-like patterns produced when a subset of long (>4 kb) minisatellite regions sharing sufficient sequence similarity were detected by hybridisation with radioactively labelled copies of Alec Jeffreys' Multi-Locus Probes. Comparisons between individuals were based solely on visually matching the patterns of bands, sometimes accompanied by a statistical method that was soon challenged in court (e.g. R v John Henry Bell. in 1993). Interpreting the results became even more problematic where a number of bands

[13] The random match probability is the conditional probability of a match between the suspect's profile and any individual's profile from the population of interest (Steele and Balding 2015).

were not detected due to degradation - which is this work's core interest. These problems were further exacerbated where mixtures were present, or in cases of relatedness between compared individuals because the bands in a DNA fingerprint could not be associated with specific loci. Single Locus (minisatellite) Profiling (SLP) increased the hybridisation stringency such that each probe detected just one hypervariable minisatellite locus. These were used sequentially so that a number of loci could be scored from the same DNA sample.

The *RMP* (random match probability) was obtained by multiplying together the relative frequencies[14] of each SLP profile band both within and between loci, a method known as the product rule. The rule assumes an independent inheritance at each locus and relies on the fact that the hypervariable regions were usually selected on different chromosomes (Weir 1992). Using this method, SLP *RMP*s could reach the order of 10^{-7}, equivalent to the rarity of the profile being one in tens of millions. The Forensic Science Service (FSS) in the United Kingdom worked on a database representing African, Asian, and Caucasian subpopulations, using four SLP probes with frequencies of SLP alleles between five and ten percent.

Berry et al. (1992) and Evett et al. (1993) proposed an improved method of interpreting the evidence through Bayesian reasoning resulting in a Likelihood Ratio (LR) that weighs the evidence (scientific observation) in the light of two opposing and ideally exhaustive hypotheses. The LR is the ratio of the probability of the observed evidence conditional upon the prosecution's hypothesis (Hp), for the numerator, and on the defence's hypothesis (Hd) for the denominator. The following equation ensues:

- $LR = \frac{Pr(E|Hp)}{Pr(E|Hd)}$
    - E: observation of the scientific result (the evidence) - e.g. a DNA match.
    - Hp: the prosecution hypothesis; the suspect is the source of the crime stain.
    - Hd: the defence hypothesis; someone else unrelated to the suspect but within the suspect's population[15] is the source of the crime stain.

[14]SLP *rmps* were based on the relative frequency of binned alleles.
[15] The implications brought by relatedness and the suspect's population will be discussed later in this Chapter.

The numerator, representing in this case the probability of the queried profile matching that of the suspect assuming that the prosecution hypothesis is true, has a maximum value of one (100%). This number can decrease slightly in the case of suspected laboratory errors, mutation events and other practical imperfections. The denominator is the probability of the profiles matching assuming the defence hypothesis is true. In the simplest cases, this is equal to the queried profile's *RMP* in the suspect population.

A major challenge in deriving this probability under Hd is to define the relevant population which ideally (although almost never in practice), is limited to potential criminals fitting the case's circumstances. The assumption often suggests that the crime stain donor shares ethnicity and geography with other suspect individuals. Other circumstances can also delimit the population of interest, with the most extreme example being an event under investigation that happened on an isolated island (Balding and Donnelly 1995). In most cases, however, and because there are no known reasons to narrow the suspect pool, the 'suspect population' is impossible to delineate and a 'database' of individuals from a broad ethnic background (Caucasian, Afro-Caribbean, Hispanic, etc.) relevant to the crime locale is used to provide the profile and allele frequencies from the different subpopulations.

Identifying the differences between the real 'suspects' population and the one represented in the used 'database' is important. The probability of a matching DNA profile given that someone else unrelated to the suspect, is the source of the crime stain ($Pr(E|Hd)$) depends on the database that is in use and which uncertainties in terms of allele frequencies should reflect that of potential suspects. These uncertainties arise from the possibility of relatedness between innocent suspects and the perpetrator, sampling variations, the possibility of apparent homozygotes, from mere assumptions of the Hardy-Weinberg equilibrium, where all alleles are assumed to be equally distributed within a population, and from an assumed independence across loci. Relying on a database that represents a population with less relatedness between individuals - fewer Identical By Descent (IBD) alleles - than that of the suspect population, is anti-conservative and may lead to prosecution bias. For example, suspects that are from a closed population with a prevalence of consanguineous marriages, therefore having an increase of shared alleles between individuals, would be at a disadvantage if a regular DNA database of unrelated individuals is employed to compute $Pr(E|Hd)$.

The coancestry effect may be negligible in many cases; especially if it does not change the LR's order of magnitude. However, it is more consequential for related individuals within the suspect population, for migrant groups that are poorly represented in national databases, and importantly here, in cases of partial profiles (Balding and Nichols 1994). In the event that the 'suspect population' is limited to one subpopulation by ethnicity and geography, then remediating for uncertainties is largely achieved through application of population genetics theory. Nichols and Balding (1991) proposed the inclusion of the parameter Fst (or θ), a measure of inter-population variation in allele frequencies, in the LR calculation to account for the coancestry effect. While θ may vary between loci of the same individual, DNA markers (both STRs and VNTRs) that are analysed for forensic purposes are expected to have similar θ values, mainly determined by the population's history of foundation, growth, and immigration (Balding and Nichols 1994).

Fst:

- *Fst measures the genetic differentiation between populations: the shared ancestry and the variation in sub-population allele frequencies.*
- *Weir and Cockerham (1984) estimate Fst in terms of the ratio between sub-population variability to total genetic variability at a locus.*

Depending on whether a locus is homozygous or heterozygous, Evett and Weir (1998) propose two equations that are applied to diploid markers. They take into account the population structures that were described by Nichols and Balding (1991), assuming that the suspect is from the offender's sub-population and that the two are not closely related:

Homozygous locus:

- *Sampling adjustment:* $(P_A+4)/(n+4)$
- *equation:* $(2\theta + (1-\theta)\,P_{A1})(3\theta + (1-\theta)P_{A2})\,/\,(1+\theta)(1\ +2\theta)$

Heterozygous locus:

- *Sampling adjustment*: $(P_A+2)/(n+4)$
- *Equation:* $2(\,\theta + (1-\theta)\,P_{A1})(\theta + (1-\theta)P_{A2})\,/\,(1+\theta)(1\ +2\theta)$

The sampling adjustment is justified by small sample size data, sampling errors, and undesirable sampling properties introduced by the product rule. It is achieved by adding

both the suspect and the criminal profiles to the database (2 alleles from the stain + 2 alleles from suspect; n+4: adding 4 alleles to the database) (Balding and Nichols 1994). Broader situations where the suspect subpopulation is difficult to define, e.g. a crime in a cosmopolitan city, require a more conservative θ value so as to remain conservative (avoiding favouring the prosecutor). A θ of 0.03 is considered conservative in modern USA and Europe, after encountering the highest θvalue at 0.0286 for Indian Americans (Budowle et al. 2001).

Although adaptable to Single Nucleotide Polymorphisms (SNPs), Y chromosome STRs, and mitochondrial DNA, most previously discussed population genetics concepts were developed by the forensic DNA community for autosomal STR typing. The evolution from SLP analysis to Short Tandem Repeat (STR) analysis both increased the number of analysable markers and decreased their size, allowing simultaneous amplification of a suite of markers through PCR, therefore providing better detection rates with trace and degraded DNA and a higher level of discrimination between individuals. However, it is worth noting that the earliest autosomal STR systems were associated with a considerably smaller *RMP*, which was in the order of 10^{-4} with the quadruplex, for example. The benefits of increased sensitivity, speed and ease of use across a wider range of sample types largely outweighed the loss in discrimination power resulting from the analysis of less variable loci. Whilst the autosomal biparental inheritance and meiotic random assortment contribute to high levels of diversity and thus the rarity the profile it also makes them less susceptible to relatedness effects when compared to haploid markers.

In cases of highly degraded or low template DNA (see Chapter 1), autosomal Single Nucleotide Polymorphism (SNP) analysis can either replace or complement autosomal STRs. They are most easily adopted for Disaster Victim Identification and missing persons cases as these are not dependent upon searching pre-existing (STR) criminal databases. Furthermore, as their mutation rate is typically 100,000 times lower than autosomal STRs, cases of discrepancies between child and alleged parents at one or two rapidly mutating STR loci are unlikely to be mirrored by mismatches at SNP loci (Børsting and Morling 2011).

From an interpretation point of view, the biallelic nature of most SNPs limits their discriminatory power and lowers their heterozygosity when compared to STRs (Jobling and Gill 2004). The analysis of 50 to 150 SNPs with high minor allele frequencies is

therefore required to be comparable to existing STR multiplexes in terms of evidential weight. Gill (2001) proposed an autosomal SNP-related LR equation that assumes Hardy-Weinberg equilibrium:

- $LR_n = \left(\frac{1}{a^2}\right)^{a^2n} . \left(\frac{1}{2ab}\right)^{2abn} . \left(\frac{1}{b^2}\right)^{b^2n}$
    - a: frequency of allele A.
    - b: frequency of allele B.
    - n: number of loci in the assay.
    - possible genotypes are AA, AB or BB with a + b = 1.

Population specific allele frequency data are available for most autosomal SNPs currently analysed in forensics (Sanchez et al. 2006; Churchill et al. 2017).
Where STR evidence is inconclusive, inclusion of autosomal SNP markers can add value through the multiplication of both Likelihood Ratios: $LR_{STRs}.LR_{SNPs}$(Phillips et al. 2008). DNA results involving the combination of different marker types, notably SLPs and STRs, was first presented to court in the 1990s. While each type was presented separately in *R v Shatanawi* (1993), the LRs were multiplied together in *R v Doheny* (1997) (Foreman and Evett 2001).

Other authors proposed an overall LR between autosomal STRs and haploid markers, notably Castella et al. (2006), merging autosomal with mitochondrial: $LR_{STRs}.LR_{mtDNA}$ and Walsh et al. (2008), merging autosomal with Y-STRs: $LR_{autoSTRs}.LR_{Y-STRs}$.

This extension of the product rule assumes independence between the different markers and the different techniques. Such operations acquire a new dimension with the advent of Massively Parallel Sequencing (MPS) in which different DNA types can be analysed in a single assay. Examples include the ForenSeq® DNA Signature Prep kit that includes 27 autosomal STRs, 7 X-STRs, 24 Y-STRs, and 94 identity informative SNPs, and the prototype Promega PowerSeq® System that includes 22 autosomal STRs, 23 Y-STRs and 10 amplicons covering the mitochondrial control region. Data resulting from both technologies are included in this work. Massively parallel sequencing-by-synthesis provides freedom from the need to distinguish loci by size, and the limited number of fluorescent labels that constrains CE-based techniques. Thus, the increased number of analysed markers reveals a high degree of genotype and haplotype polymorphism, and through the possibility of joining LRs of different marker types,

MPS may become the technology of choice in cases where a CE-derived evidence is of limited strength.

This applies not only to partial profiles but also in cases where the analysis of haploid markers is recommended (e.g. Y-STRs in sexual offences, mtDNA in degraded samples). Andersen and Balding (2017) argue that no haploid DNA match that is presented in court on its own is sufficient to establish the source of a DNA sample. Other matching marker types, such as autosomal STRs, SNPs, or additional non-DNA evidence would be required. The haploid markers' interpretation is different from that of diploid ones. They can be interpreted as a single allele, since they are inherited in a single block. Their uniparental[16] inheritance and lack of meiotic recombination[17] affect the strength of evidence, leading to their haplotypes being shared among multiple individuals within the same lineage, and, depending on the haplotype's frequency, among other random individuals.

Nevertheless, matching haplotypes support the association between a crime stain and the suspect, an unidentified body or a lost person. Different haplotypes support the alternative contention. However, mismatches do not automatically lead to an exclusion, following a logic similar to diploid markers, with the interpretation being directly linked to the mutation rate. An exclusion is only warranted in the presence of three or more mismatches between compared haplotypes. A statistical interpretation is indicated in cases of one or two[18] differences to exclude mutations or somatic mosaicism in cases of same donorship. In such cases the LR's numerator decreases and acquires an intermediate value between zero and one. Re-analysis, or the expansion to additional markers - of the same or of different DNA types - may be required if the interpretation results are inconclusive (Caliebe and Krawczak 2018).

The discrimination level of haploid markers is therefore dictated by the mutability of specific regions on the Y chromosome and mtDNA. Current Y-profiling technology

---

[16] MtDNA leakage from the father and recombination with maternal mtDNA were recently reported (Luo *et al.* 2018). We assume strict maternal inheritance for the purposes of forensic interpretation of mtDNA evidence.

[17] With the exception of recombination between X and Y chromosomes in the terminal pseudoautosomal regions (5%). Forensic Y-STRs are usually located on the non-recombining parts (95% of the Y chromosome) (Bradbury 2017)...

[18] While such a number is consensual amongst the scientific community, some would argue that even three differences are also possible between two samples from a same source (or from paternal/maternal descendance).

can detect many STRs with high mutability[19] which helps to distinguish between distantly related males on one hand but complicates the exclusion of patrilineal descendants in historical or cold cases on the other. Andersen and Balding (2017) found that, with currently available kits, tens of meioses are sufficient to eliminate occurrences of matching haplotypes between patrilineal relatives (Figure 5.1). Methods to evaluate Y-STR matches and report them to court are a matter of scientific debate and research. A frequentist approach would require looking for the matching haplotype's *RMP* in a relevant database. The Bayesian reasoning would lead to an LR whose denominator would also require knowledge about this *RMP*. However, database information may be of limited value because of the lack of randomness in population sampling, and the concentration of patrilineal relatives in distinct and small geographic areas, or specific social groups. Counting the number of matches in a database and reporting them to court as such, offers simplicity and provides accurate information for haplotypes that are well represented in a database. However, the risk of prosecution bias is significant for those haplotypes that have not previously been observed in the database, leaving the court with an impression that the strength of evidence is greater than it actually is.

Although Andersen and Balding (2017) support the use of LR in general, they discuss the difficulties applying it to Y profiles because of the previously mentioned problems related to relevant databases, and because the matching probability would be dependent on the number of meioses between queried individuals. They developed a simulation model of Y profile evolution that estimates the number of matching Y profiles taking into account population genetics theory and data. The model, termed MAle Lineage ANalysis (MALAN), mimics different Y lineages by simulating paternal descent in the form of pedigrees. Key parameters include the per-locus mutation rate, the variance in reproductive success (VRS) and the population growth rate. It was shown that the distributions are not significantly affected by changes in these parameters, therefore supporting evidential assessment in cases where VRS and population growth rate cannot be determined, where the number of matching individuals would only vary slightly. The queried contributor would usually be a male individual who belongs to the pedigree's last three generations - or live population - and who matches the crime stain's haplotype. Coancestry, kinship and sampling adjustments are not performed

[19] The sum of mutation rates at each STR locus.

since all matches with related individuals as well as the database's size are included in the simulation. The result could be presented to court in the following manner:

'A Y-chromosome haplotype was generated from the crime stain. The suspect has a matching haplotype and so is not excluded as the source of DNA. Based on population genetics theory and data, the number of males in the population with this haplotype is probably fewer than 20, with a very unlikely chance for it (< 5%) to exceed 40. The individuals ages are distributed over a wide spectrum and their locations are unknown. Since these individuals share paternal-line ancestry with the suspect, that may extend beyond his known relatives, some of them could also share ethnic identity, language, religion, physical appearance and place of residence with the suspect.'

The authors recommend switching back to a match probability approach (*RMP* or LR) in cases of partial profiles, as the number of matches in the suspect population is expected to increase with fewer loci typed. They claim that the resulting matching partial Y profiles do not necessarily belong to the source's closely related individuals and are therefore better estimated from databases.

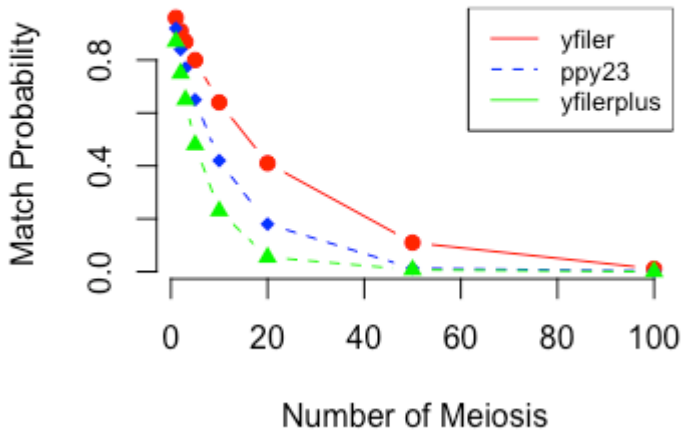

Figure 5.1 Y haplotype matching probability per number of meiosis.

Line chart built with the data provided by Andersen and Balding (2017) and representing the *RMP* between Y-chromosome profiles depending on the number of meiosis.
Mutation rates (μ): 0.044 for Yfiler, 0.083 for PowerPlex® Y23, and 0.135 for Yfiler Plus.

Similarly to their work on the Y-chromosome, Andersen and Balding (2018) simulated a model that counts the number of matching mitochondrial DNA haplotypes (mitogenomes) and investigated its dependence on the model's key parameters: mutation rate, population size and growth rate. Again, the assumption was that matching individuals may not be well-mixed in the population so that database statistics can be an unreliable in determining the real count in a specific population. Their results showed that it was possible to obtain a single occurrence in a large database, while in reality hundreds of individuals may be sharing the queried mitogenome - by contrast to tens of individuals sharing a Y haplotype in a similarly-sized population. Such mitogenomes were shown to belong to related individuals that range up to ~500 meioses apart, as opposed to tens of meioses apart for matching Y haplotypes. This can be explained by the mutation rate for the entire mtDNA genome being an order of magnitude lower than for the set of Y-STRs in current Y profiling kits, leading to much larger sets of matching individuals. Nevertheless, the mtDNA mutation rate is at least an order of magnitude greater than that of nuclear DNA (Khrapko et al. 1997), and mutations have been observed between mother and children (Parsons et al. 1997). Notably (and more positively), the mtDNA's low mutation rate when compared to Y-STRs alleviates the database sampling and relatedness biases, although these still need to be accounted for.

The interpretation of the mtDNA evidence to estimate the strength of a *no exclusion* result is required in cases of exact or near match[20] between a questioned and a reference sample. First, matching mitogenomes (or near matches) have less discriminatory power than matching autosomal profiles or even Y haplotypes (Butler 2014). This is especially true for mitogenomes that are common in the relevant population. On the other hand, a rare haplotype played a crucial role in the identification of King Richard III (King et al. 2014) and a shared heteroplasmy authenticated of the remains of Tsar Nicholas II (Ivanov et al. 1996). In addition to the counting method that is relied upon in Balding and Andersen (2018), both the Bayesian (Tully et al. 2001) and the frequentist (Holland and Parsons 1999) approaches are options that could be applied

[20] A near match of one or two differences would require a statistical interpretation to assess the strength of a *no exclusion* result. There is a general consensus to directly exclude in the advent of three or more differences.

depending on the case circumstances and the type of data that is available, such as relevant databases or site-specific mutation rates (Tully and Wetton 2014).

Independently from the chosen method of interpretation, the strength of evidence depends on the mitogenome's rarity in case of an exact match, but also on the probability of mutation(s) in cases of a near match. When maternal descent is in question, the probability of mutation is directly influenced by the number of meioses that separate the individuals under comparison, and by the tissue from which DNA was extracted (Calloway et al. 2000). Informative data regarding site-specific mutations have been gathered throughout years of research, where phylogenetic analyses have played a major role, and allow a distinction to be made between highly polymorphic bases (hotspots) and the mutational stable positions that allow the distinction between two identical haplotypes (Salas et al. 2007).

Bayesian reasoning will be applied in this chapter to interpret evidence that is related to potential maternal descent between living individuals and the unidentified victim of a murder dating back to 1930. On the morning of November 6 that year, two passers-by noticed a fire near Hardingstone, Northamptonshire, UK. Closer inspection revealed a car in flames that contained a charred human body. This case, known as the "Blazing Car Murder", led to the conviction of Alfred Rouse who was hanged in Bedford Gaol on March 10th, 1931. Apart from knowing his gender, the male victim's remains unidentified to this day. On his grave was marked "In memory of an unknown man". After an appeal to individuals that had lost matrilineal relatives at the same time and in the same geographical region, ten families came forward to verify their familial relatedness with the "Blazing Car Victim". This old case involved a prolonged exposure to fire that is expected to have degraded DNA and represents not only a possible challenging DNA analysis but also interpretation of the evidence.

5.2 Aims and Objectives

This chapter addresses the challenges to interpretation of degraded biological stains caused by exposure to high temperatures. It is divided into three main objectives using three types of data. Partial matches that were obtained after sample exposure to heat (Chapter 3) were interpreted using a Bayesian approach with a first objective to compare the strength of evidence with that of full matches obtained from controls. Secondly, this comparison extended to the type and number of markers that were

targeted through Capillary Electrophoresis and Massively Parallel Sequencing: 17 autosomal STRs (AmpFLSTR NGMSElect®) vs. 27 autosomal STRs vs. 27 autosomal STRs (ForenSeq® DNA Signature) + 94 iSNPs (ForenSeq® DNA Signature). The Bayesian interpretation was also applied to mitochondrial DNA evidence within the context of the Blazing Car Murder, which includes an unidentified and burned male victim dating from 1931. This part of the work aimed at illustrating how the strength of the evidence may be affected in real casework involving fire, where nuclear DNA failed to amplify restricting the possibilities of analysis to mitochondrial DNA only. The third part of this chapter revolved around Y-STRs profiles (23 markers) and was based on counting the number of matches rather than computing Likelihood Ratios. A marker drop-out simulation study that intended to show the effects of partial matches on the power of discrimination was performed using databases constructed at King's College London (n= 3128, and at the University of Leicester (n= 435), and eleven different paternal lineages (n=730) that were simulated via the MAle Lineage ANalysis (MALAN) R package together with partial drop-out of their profiles.

5.3 Materials and Methods

5.3.1 Autosomal STRs and SNPs - Interpretation

5.3.1.A Profiles

Three full and six partial autosomal STR profiles were obtained from blood stains that were respectively exposed to 4 °C and 180 °C for 30 minutes (Chapter 2). DNA typing was performed via the CE-based NGMSElect® kit (16 markers + Amelogenin) and the MPS-based ForenSeq® DNA Signature Prep kit (27 autosomal STRs, 94 identity SNPs).

Table 5.1 Samples used for the autosomal STR and SNP interpretation.

Temperature	Number (n)	Donor
4 °C	3	P2, P9 and P22
180 °C	6	P2 (2x), P9 (2x) and P22 (2x)

5.3.1.B Balding and Nichols Frequency Corrections and Likelihood Ratios

A Likelihood Ratio (LR) expressing the plausibility of a scientific observation (e.g. partial DNA match) in the light of two competing hypotheses was derived for each profile using the following formulae:

5.3.1.C Autosomal STRs (Nichols & Balding 1991)

Homozygous locus:

- *Corrected* P_A*= (initial* P_A*+4)/(n+4)*
- $LR_{locus} = (2\theta + (1-\theta)\,P_{A1})(3\theta + (1-\theta)P_{A2}) \,/\, (1+\theta)(1 + 2\theta)$

Heterozygous locus:

- *Corrected* P_A*= (initial* P_A*+2)/(n+4)*
- $LR_{locus} = 2(\theta + (1-\theta)\,P_{A1})(\theta + (1-\theta)P_{A2}) \,/\, (1+\theta)(1 + 2\theta)$

5.3.1.D Autosomal SNPs (Gill 2001)

Homozygous locus:

- $LR_{locus} = (\frac{1}{a^2})^{a^2 n}\ OR\ (\frac{1}{b^2})^{b^2 n}$

Heterozygous locus:

- $LR_{locus} = (\frac{1}{2ab})^{2abn}$

LRs for each locus were multiplied together, assuming independence between loci, and following the product rule.

5.3.1.E Wording of the Prosecution (Hp) and Defence (Hd) Hypotheses

Hp: The suspect is the source of the Crime Stain
Hd: Someone else unrelated to the suspect is the source of the Crime Stain.

5.3.1.F The numerator for autosomal STRs and SNPs

The probability that full or partial crime scene profile match the suspect's full profile, assuming that Hp is true. Here, this value is considered to be 1.

5.3.1.G The denominator for autosomal STRs and SNPs

The probability that the full or partial crime scene profile matches the suspect's full profile assuming that Hd is true. Promega's revised database v.3[21] comprising a total of 1036 individuals (342 African Americans, 361 Caucasians, 236 Hispanics, and 97

[21] Last revised on July 19 2017.

Asians) was used to provide the autosomal STR allele frequencies. A conservative Fst of 0.03 shared across loci was assumed, reflecting realistic situations where no reliable information about the relevant population is available (EWCA Crim 2439 2010). The database created by Churchill et al. (2017) by sequencing 725 unrelated individuals (167 African Americans 208 USA Caucasians, 189 Southwest Hispanics and 161 Chinese/Asians) using the ForenSeq® kit was used for autosomal SNPs. The average allele frequencies between the four subpopulations from Churchill et al. (2017) were used.

5.3.1.H $\boldsymbol{LR_{STRs}}.\boldsymbol{LR_{SNPs}}$Combination

Information gathered at autosomal STRs and SNPs was assumed to be independent. This implied that their LRs could be multiplied to generate a combined LR.

5.3.2 Haploid Markers

5.3.2.A Y-Chromosome - Dropout Simulations

Two actual genotype datasets were selected with the intent of simulating the effects of degradation-induced dropouts on different levels of haplogroup diversity within a given population - in this case the British Isles.

King's College London Dataset

With the aim of studying the effect of dropouts on resolution between subpopulations, a profile database of 23 Y-STRs from 3128 individuals (1062 White British, 977 Black British, 720 Irish and 369 South Asian British) was used (Aliferi et al. 2018). The dropouts were simulated to occur from the longest locus to the shortest locus.

University of Leicester Dataset

The previous analysis was complemented by studying the effects of dropouts on the number of Y haplotype matches in a database of 435 White British males typed at the University of Leicester. A similarity matrix was constructed in Excel for this purpose. The 435 profiles were inputted in a matrix format with a formula that measures the step-wise number of mutational differences between each of the profiles: a one to one comparison where ‘zero’ represents a full match and in this case ‘61’ represents the highest observed sum of absolute difference values. The loci were arranged from shortest to longest (Figure 5.2), and dropouts were simulated one at a time starting with the longest one so as to mimic situations of DNA degradation. Heatmaps were then

built following the enhanced ‘Heatmaps.2’ function that is available with the ‘gplots’ R package to visualise changes in resolution with the loss of the genetic information.

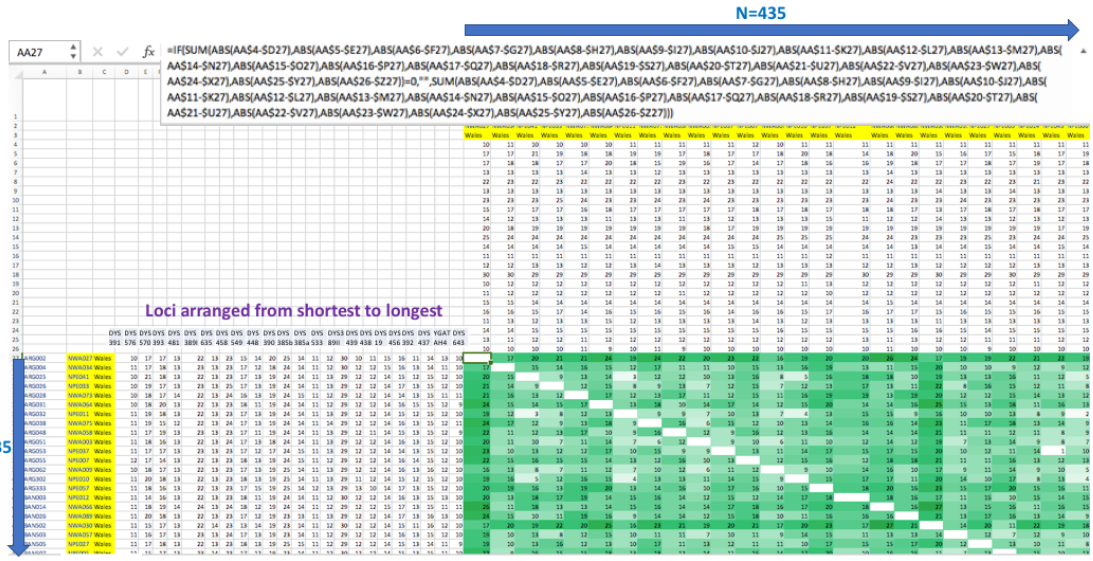

Figure 5.2 Similarity matrix of Y haplotypes.

Screenshot from the first few samples (22 rows, 26 columns) that were compared with each other through a similarity matrix. The loci were dropped one at a time starting from the longest one to the shortest. The formula that was applied to assess differences between haplotypes quantifies them from zero representing a total match to a number representing the sum of stepwise mutational differences between the two profiles. The number of differences is coded through a colour gradient that starts with white and gradually moves towards dark green.

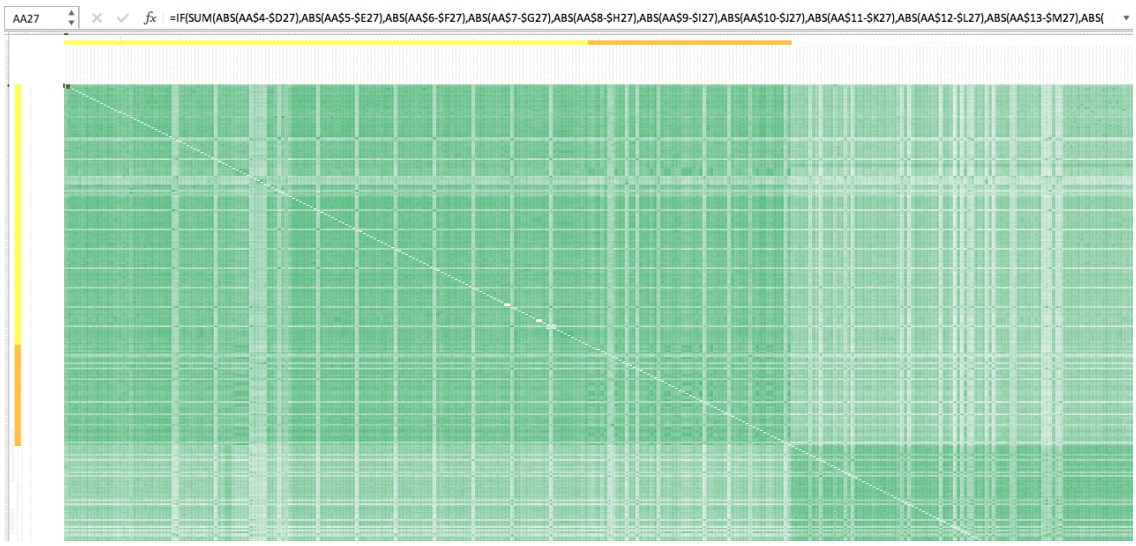

Figure 5.3 Similarity matrix (broader view)-

Screenshot of the same similarity matrix showing more rows and columns for an enhanced visualisation of how it shapes into a heatmap with going from dark green (most different) to white in the direction of full matches.

MAle Lineage ANalysis (MALAN) Model

The open-source MALAN R package was used to construct a partial Y profiles case study to understand the effects of degradation-induced dropouts on proposed model of interpretation. Two different populations were simulated and treated separately. While the first was produced for its small size (N=85), simplicity, and the easy visualisation of matching profiles, the second was designed to reflect a more realistic scenario with a larger population (N= 11,402) stemming from eight different founders. It is reported that the number of matching profiles is insensitive to the population size, provided that the latter is superior to 10^3 (Andersen and Balding 2017).

The first population was simulated starting with 10 individuals at the latest generation and going back 20 generations to reach its single founder. The result was a pedigree representing a male lineage constituted of 85 individuals. The second population started with a thousand individual at the bottom of the pedigree and evolved for 200 generations upwards resulting in eight different pedigrees each containing the following number of individuals:

Pedigree 1: 2740	Pedigree 2: 2464	Pedigree 3: 407	Pedigree 4: 1421
Pedigree 5: 2565	Pedigree 6: 758	Pedigree 7: 736	Pedigree 8: 311

Growth rates and Variability of Reproductive Success (VRS) were kept constant for both populations. The live populations were set to the youngest three generations in each pedigree and amounted to 30 individuals in the first population and 3000 individuals in the second.

Alleles were then filtered out one at a time for all individuals, from the longest locus to the shortest, starting with what would be a full profile that is obtained via the PowerPlex® Y23 kit. Each pedigree was then populated with Y-haplotypes starting with allele 0 at all loci for each founder, and running a neutral, symmetric, single-step mutation process at each locus over the generations. Locus-specific mutation rates were assigned using Table 2 and uncertainty was allowed through a Beta (1.5 200) prior distribution, where the posterior distribution given the count data would be Beta(x + 1.5, y + 200), where x and y are the numbers of meioses in which mutations did and did

not occur on a specific locus. Finally, the number of matching Y-haplotypes was quantified and those matching individuals were marked in orange on their respective pedigree.

Table 5.2 Mutation rates per Y-STR marker - MALAN partial profiles.

Marker	Mutation Probability	Marker	Mutation Probability
DYS438	0.00037	Y-GATA-H4	0.00303
DYS392	0.00052	DYS533	0.00367
DYS393	0.00105	DYS549	0.00375
DYS437	0.00122	DYS389II	0.00412
DYS385a-b	0.00122	DYS456	0.00429
DYS643	0.00135	DYS635	0.00433
DYS448	0.00152	DYS481	0.00502
DYS390	0.00211	DYS439	0.00545
DYS19	0.00224	DYS458	0.00636
DYS391	0.00245	DYS570	0.01335
DYS389I	0.00293	DYS576	0.01472

5.3.2.B Mitochondrial - The Blazing Car Murder

The Victim's Sample

The victim's tissue was collected from the St Bartholomew's Hospital museum and then analysed by an external team at Northumbria University Centre for Forensic Science (NUCFS). It was in the form of a formalin-fixed paraffin embedded (FFPE) prostate tissue section that was linked via archived records back to the victim. Anti-contamination and

cleaning procedures were performed prior to DNA extraction which was performed following Shi et al. (2002) and Gilbert et al. (2007) (organic extraction). The slide's external surfaces were wiped with bleach (10%) followed by DNA–free water rinses.

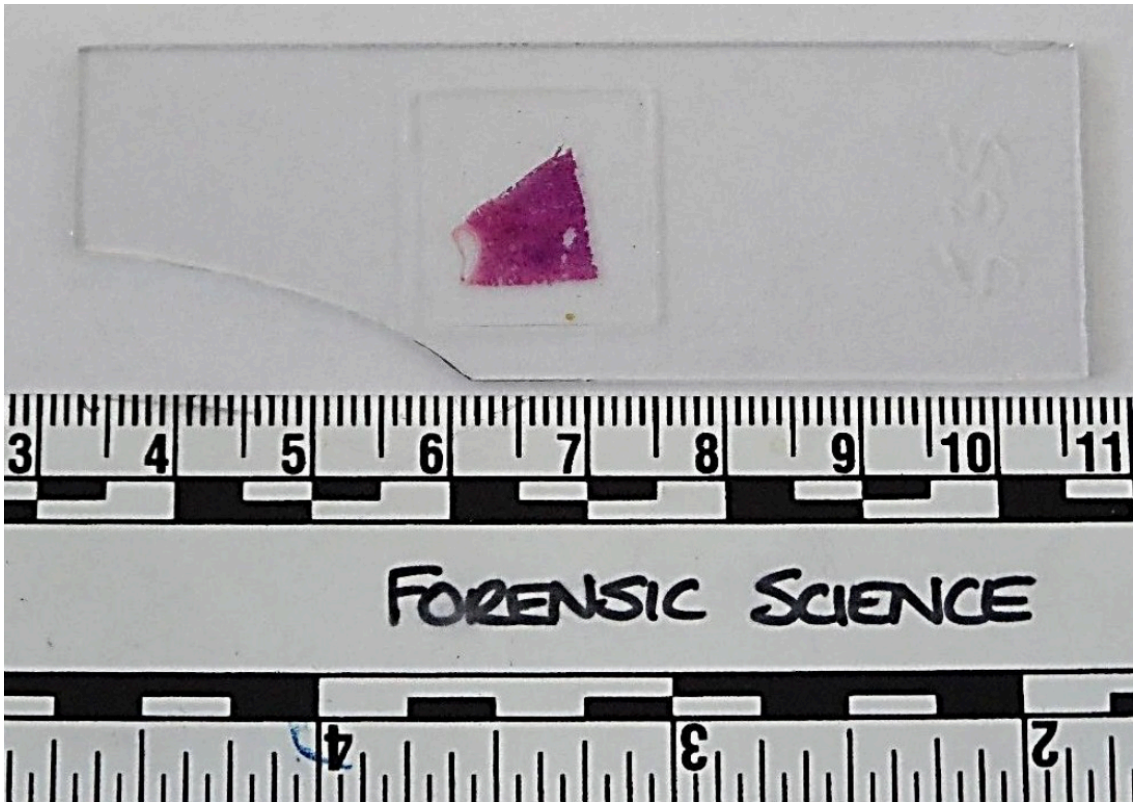

Figure 5.4 Victim's FFPE prostate tissue-

An image of the slide after two portions of the tissue had been removed for DNA extraction.

Autosomal STR typing was performed on the DNA extract from the FFPE tissue using the NGMSElect® multiplex comprising 16 autosomal STRs (plus Amelogenin). The resulting electropherogram (EPG) showed heavy DNA degradation with only eight of the shortest loci containing one or two typed alleles out of 17 loci in total; and a general decrease in rfu from the shortest to longest alleles (Figure 5.5). Allele 16 at locus vWA was the longest amplicon detected at 72 rfu and extending approximately to 175 bp. No alleles beyond this size could be typed.

The hypervariable segment I (HVSI) and hypervariable segment II (HVSII) were sequenced via four short overlapping amplicons for each section of mtDNA. The methodology was based on that described by (Edson et al. 2004) and the sequencing was carried out in both forward and reverse directions so that each base call could be viewed in duplicate for sequence validation.

Only one difference, represented by an A to G transition at position 263 (263G) in HVSII, was observed between the revised Cambridge Reference Sequence (rCRS) and the alleged victim's DNA (Figure 5.6). Two C insertions at position 309 were excluded from subsequent comparisons as they occurred within the less reliable poly-C stretch.

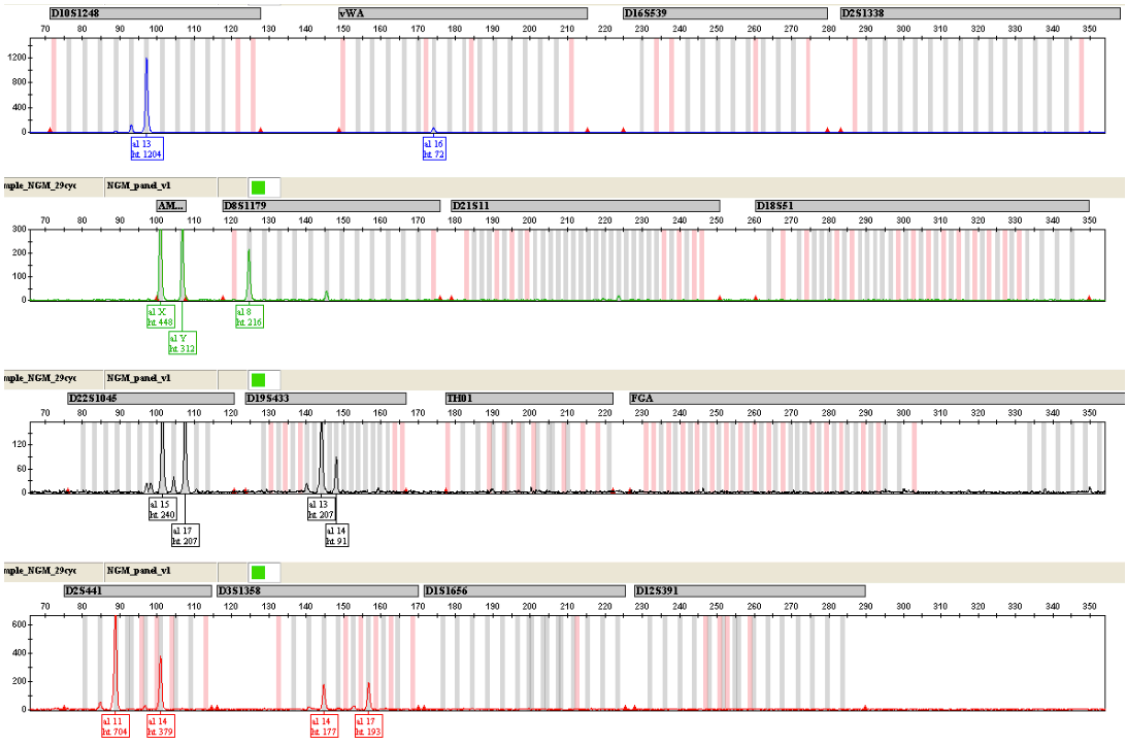

Figure 5.5 Victim's partial NGM profile.

Partial NGM profile generated by the NUCFS from DNA extracted from the first portion of prostate tissue removed from the histological slide.

```
241 ACAATTGAATGTCTGCACAGCCACTTTCCACACAGACATCATAACAAAAAATTTCCACCA
    ACAATTGAA
    ACAATTGAATGTCTGCACAGCCGCTTTCCACACAGACATCATAACAAAAAAT
    ACAATTGAATGTCTGCACAGCCGCTTTCCACACAGACATCATAACAAAAAATTTCCACCA
                GTCTGCACAGCCGCTTTCCACACAGACATCATAACAAAAAATTTCCACCA
```

Figure 5.6 Sanger sequence of the victim's control region.

Parts of the BCV control region sequence (here HVSII) showing an A to G transition at position 263 (A263G) (Graham and Barlow 2013). The text in black indicates the rCRS sequence and each other colour indicates a different amplicon from the prostate tissue samples obtained using overlapping PCR amplicons. Differences between the rCRS and prostate tissue sequence are highlighted in yellow.

Reference Samples

Reception of Samples:

An invitation to members of the public who believed that a maternal line relative had disappeared at the time and in the region of the murder resulted in the delivery to the University of Leicester of 24 sealed (PACE DNA sample mouth swab kit, FSS) buccal swabs coming from 12 donors[22] - two swabs per individual. Each self-sampled mouth swab package was originally labelled with the donors' first and last names but were then coded to preserve their anonymity as follows: 97, 113, 114, 116, 117, 118, 119, 120, 121, 122, 124 and 125.

DNA extraction:

DNA from the buccal samples was extracted using the QIAamp® DNA Mini and Blood Mini kits following the DNA isolation from buccal swabs protocol, into 100 µL of elution buffer.

PCR - Sanger Sequencing:

The entire mitochondrial control region was amplified by use of the primers L15,999 (5′-CAC- CATTAGCACCCAAAGCT-3′) and H409 (5′-CTGTTAAAAGTGCATACCGCC-3′) followed by Sanger sequencing of the PCR products in both directions (Helgason et al. 2000). The products were purified by ExoSAP treatment prior to sequencing.

Interpretation:

<u>Wording of the Hypotheses</u>:

Hp: the buccal swab donor and the victim are from the same maternal lineage.

Hd: the buccal swab donor and the victim are from different maternal lineages.

A Likelihood Ratio (LR) value was calculated for each comparison between the victim and a potential maternal line relative:

- $\frac{Pr(E|Hp)}{Pr(E|Hd)} = \frac{Probability\ of\ the\ evidence|\ Hp}{Probability\ of\ the\ evidence|\ Hd}$

<u>In case of a full match</u>:

The numerator translates into the probability of having matching sequences assuming Hp. Here this value is considered to be one.

The denominator translates into the probability of having matching sequences assuming Hd. This is the random match probability in the European DNA Profiling Group (EDNAP) MtDNA Population Database (EMPOP) (Parson and Dür 2007).

[22] The 12 reference individuals come from ten potentially different maternal lineages, as individuals 116 and 117, as well as 118 and 119, are siblings.

<u>In case of a near match</u>:

The numerator translates into the probability of having mutations at the discordant sites assuming Hp.

- Numerator: $k * u$
    - k: number of generations between queried samples.
    - u: mutation frequency at the specific site(s) (Soares et al. 2009).

The numerator translates into the probability of having these mutations at their specific sites assuming Hd.

- Denominator: the haplotype's frequency using the EMPOP database. Both haplotypes under comparison were included and a Balding and Nichols correction was used (n = 26,127). Homopolymeric C-stretches at common positions (e.g. 309) were excluded as differences from the analysis.

5.4 Results

5.4.1 Heat-Induced Dropouts

5.4.1.A Diploid Markers - Autosomal STRs and identity informative SNPs

LRs were derived from real profiles generated whilst studying the effects of high temperatures on forensic DNA typing using CE-based and MPS technologies (Chapter 3). First, the decrease in evidential value due to the temperature degradation of DNA (4 °C v. 180 °C) was illustrated through a dot plot (Figure 5.7). Worth noting is that the two 180 °C stains that were less degraded than other similarly treated stains (Chapter 3) produced LRs that could still be reported in court with as much confidence as full profile matches. Their respective LR values were 10^{34} and 10^{39} through the CE-based NGMSElect® kit (16 markers, Amelogenin excluded[23]), and 10^{26} and 10^{53} through the MPS-based ForenSeq® DNA Signature Prep kit (26 markers, Amelogenin excluded). The other tested 180 °C stains produced much weaker LRs that would significantly affect the evidential strength in court: 10^{3} and 10^{5} through NGMSElect®, and 10^{2} and 10^{5} through ForenSeq®.

The $LR_{autosomalSTRs}$ comparison between MPS and CE, illustrated in Figure 5.7, shows a clear advantage (higher LRs) in the 4 °C stains but becomes less pronounced in the case of degraded DNA. The full profiles obtained from 4 °C stains analysed by CE generated an average LR of 10^{43}, compared to an average LR of 10^{59} when analysed by MPS. The combined analysis of 27 autosomal STRs and 94 iSNPs (Figure 5.8) that was possible with ForenSeq® elevated the overall evidential value with an average LR of 10^{87} for stains at 4 °C, and 10^{28} for stains at 180 °C, but still left the most heavily degraded stains with low LRs (LRs=10^{3}-10^{5}).

[23] The Amelogenin allele frequencies were assumed to be equal between X and Y (f=0.5) for males and were therefore excluded from the LR computation.

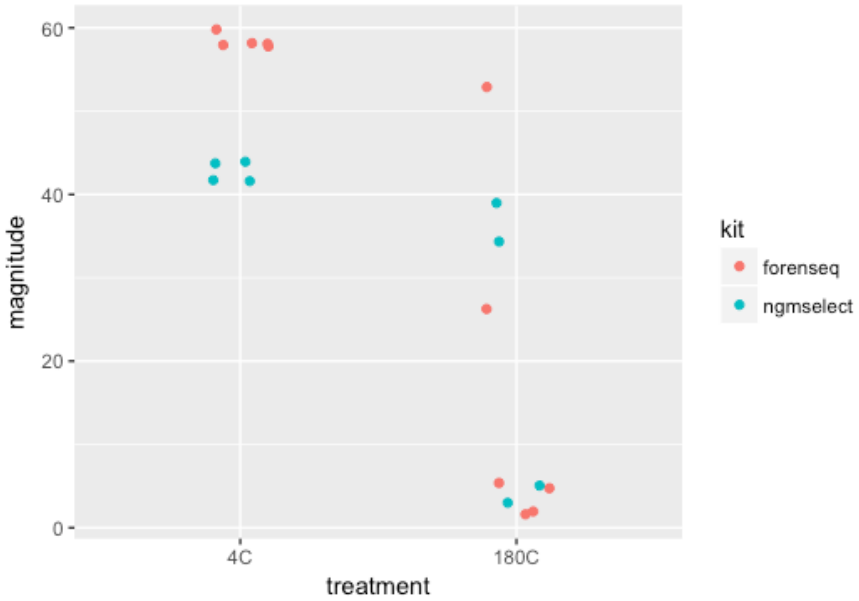

Figure 5.7 LR comparison between CE and MPS.

Comparison of LRs obtained from full (4 ℃) and. partial profiles (180 ℃) generated respectively through ForenSeq® (27 auto-STRs) and NGMSElect® (16 auto-STRs) kits.

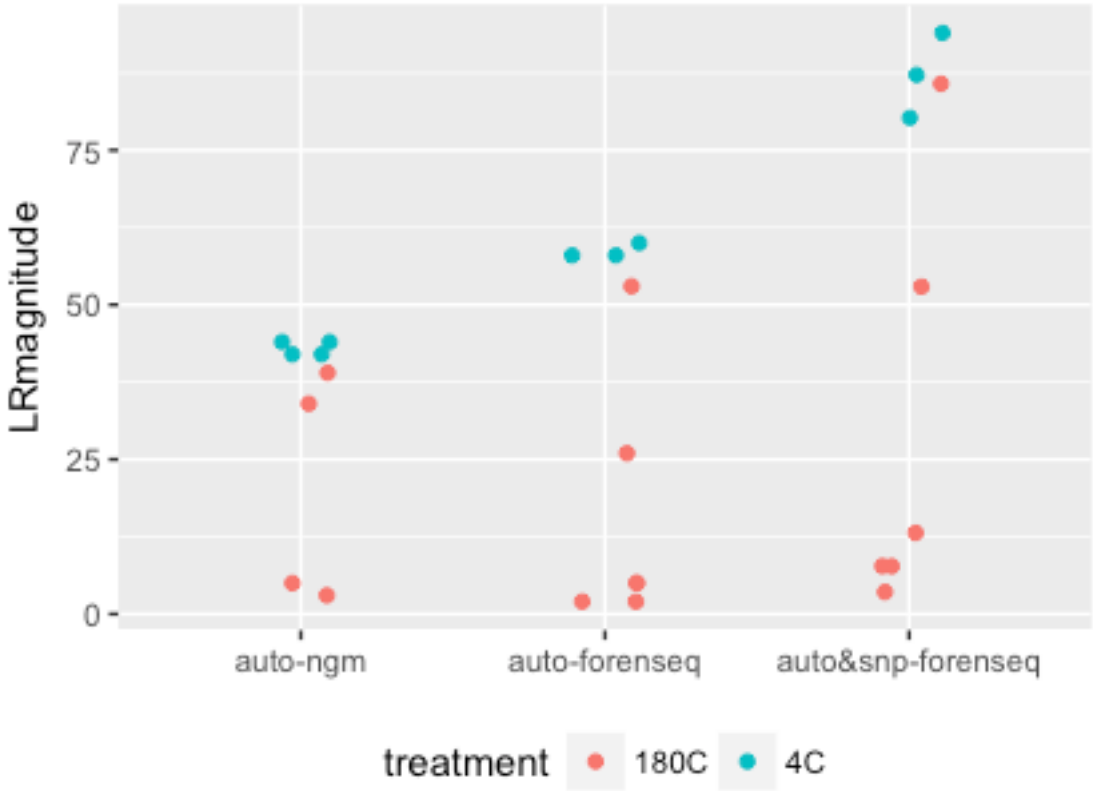

Figure 5.8 Combining the LR from autosomal STRs with that from SNPs.

The effect of adding SNP data on the LRs obtained from full (4 ℃) and partial profiles (180 ℃) generated ForenSeq® (27 auto-STR) and NGMSElect® (16 auto-STR) kits.

5.4.2 Simulated Dropouts

5.4.2.A Y chromosome – Real Datasets (KCL, UoL)

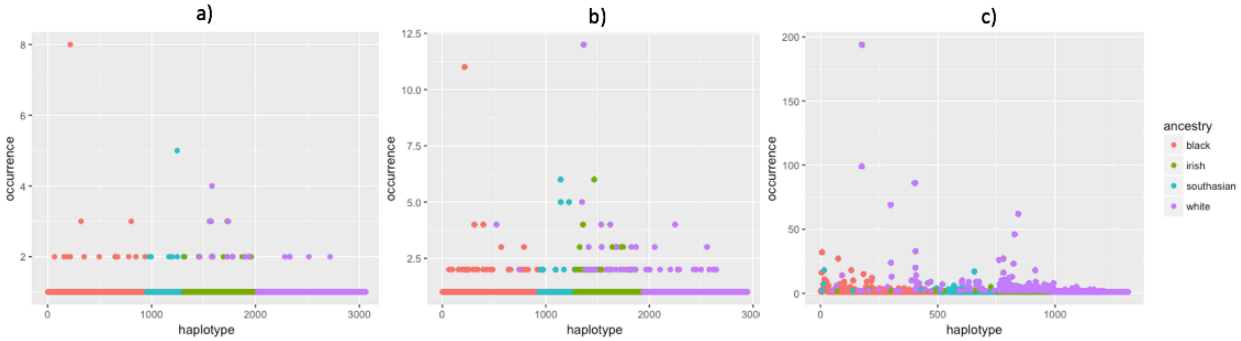

Figure 5.9 Dropouts effects on King's College Database.

The four subpopulations - Black British, White British, South Asians, and Irish PowerPlex® Y23 profiles plotted as per their occurrences in the King's College Database (a). The same data where the four longest loci dropped out are plotted in (b), and where the 15 longest markers are dropped out in (c).

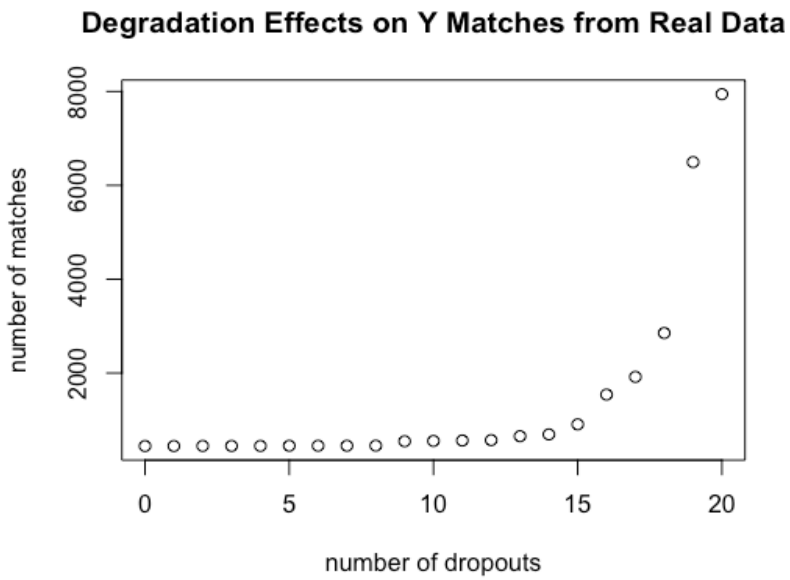

Figure 5.10 Effects of dropouts on UoL's database.

Scatter plot showing the exponential growth in the number of matches, while the number of dropouts increases from the longest to the shortest locus.

Dropouts were simulated to assess two types of database resolutions: distinguishing between subpopulations, and number of matches. Simulating dropouts from the longest to the shortest locus mimicked the loss of genetic information due to DNA degradation, rather than to stochastic losses from low template DNA samples.

The King's College London (KCL) database lost resolution related to distinguishing between the four subpopulations - Black British, White British, South Asians, and Irish - with increasing dropouts as seen by the mixing of colours in Figure 5.9 - where initially each haplotype was unique to a population with the exception of a few shared between the Irish and White British sub-sets. The number of matches also increases as seen on the y-axis with the highest frequency being eight occurrences in the Black population when all 23 markers are typed (Figure 5.9a), moving to 12 occurrences in the Irish/White British population when 19 markers are typed (Figure 5.9b). The number of matches goes up to ≈195 shared across the Irish, Black & White British subpopulations when only 8 markers are typed (Figure 9c).

Similarly, the University of Leicester (UoL) database as well as the MALAN model showed an increasing trend in the number of matching PPY23 profiles, with increasing dropouts (Figures 5.10 and 5.15). This growth was shown to be exponential in the UoL database, as the number of matches was plotted against the number of dropouts (Figure 5.10). The same pattern was also visualised through six heatmaps in Figure 5.11, in cases where 0, 13, 16, 18 20 and 22 dropouts were simulated respectively, with the number of matching profiles colour coded in orange.

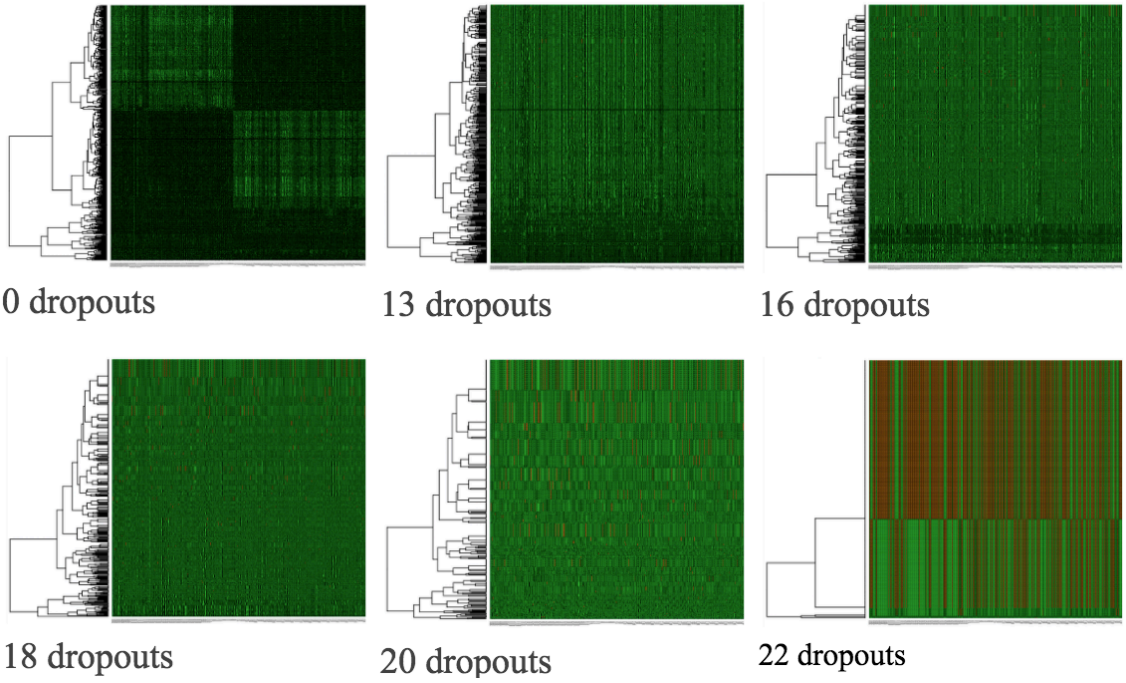

Figure 5.11 Effects of dropouts on the similarity matrix from UoL's database.

Heatmaps generated through R, starting with a similarity matrix in which the 435 Y-STR (23 marker) profiles were compared with each other (n= 189,225 comparisons). The colours represent the degree of similarity between compared profiles going from dark green representing a difference at each of the 23 markers to light orange representing a full match. The more degradation-induced dropouts, the lower the database resolution characterised by an increased number of matching profiles as shown by an increase in the orange colour and simpler dendrograms.

5.4.2.B Y chromosome - MAle Lineage ANalysis (MALAN) Model

The two populations were simulated as planned: dropouts were induced using R's linear filtering function, and the number of matches was counted from a randomly selected queried haplotype after each filtering. The number of matches went from one up to 41 at the first dropout of the largest marker "DYS643" in population one, and from zero matches up to 114 in population two. This spike in matching haplotypes does not necessarily grow linearly as the number of dropouts increases. While 41 matches climb to 70 at the second dropout (Y-GATA-H4) in population one, it dips from 141 matches down to only 11 in population two. This discrepancy in the number of matches growth with increasing dropouts is mainly explained by the chronological order in which the current MALAN model operates with partial profiles:

1. Population simulation;

2. Pedigree building;
3. Filtering of loci (dropout simulation);
4. Haplotyping of individuals according to locus specific mutation rates;
5. Selection of a queried individual;
6. Counting the number of matches.

Being downstream to each dropout simulation and the running of mutations across the remaining loci, the random selection of the queried individual led to differences in the haplotypes' frequencies between each simulation. The general trend however is that of an increasing one although still not showing statistical significance for population one (Figure 5.12).

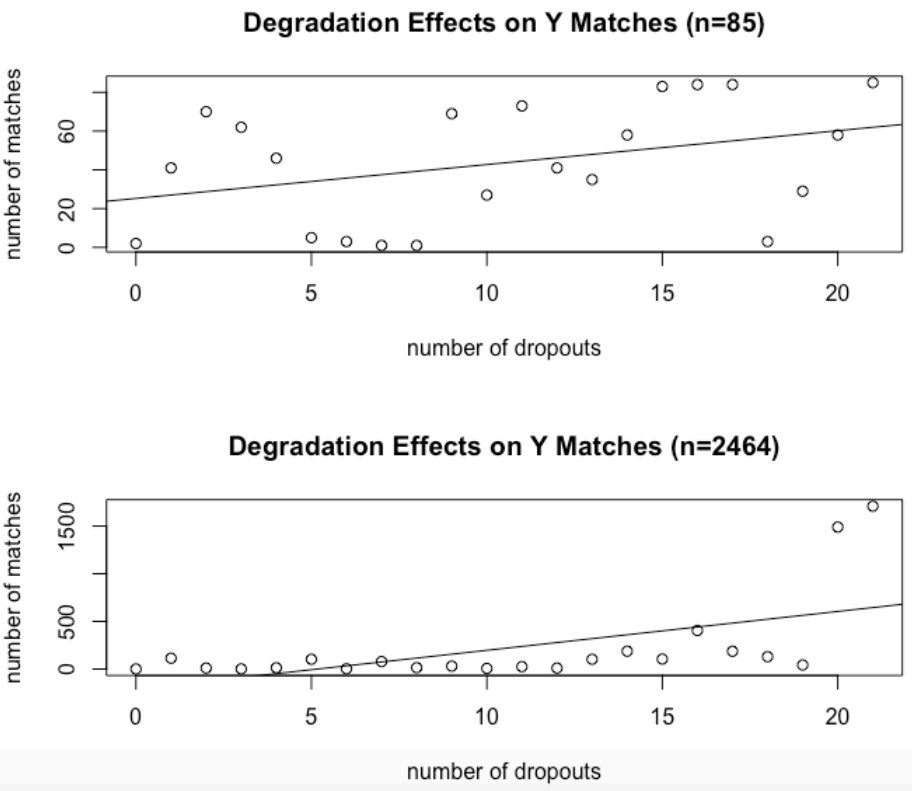

Figure 5.12 Effects of dropouts on the MALAN simulated population.

Plot showing the overall increase in the Y haplotype matches with an increase in locus dropout. The loci were simulated to drop out from the longest to the shortest (in base pairs).

The increasing number of matches with more dropouts was visualised on their corresponding pedigrees by selecting a subset of dropout simulation (Figures 5.13 and 5.14), assuming that increasing the number of simulations would smoothen the correlation between dropouts and the number of matches. Population one that started

with the queried individual's haplotype matching only that of his father and differing from all other individuals in the pedigree (Figure 5.13a), ended in a fully matching pedigree in the extreme case of 22 allelic dropouts (Figure 5.13d). To get there it reached tens of matching haplotypes at several dropout combinations. Dropping out three of the longest markers resulted in 70 matching haplotypes. While a number of dropout combinations diminished the number of matching haplotypes down to one, notably where all seven or eight of the longest markers (DYS643, Y-GATA-H4, DYS437, DYS392, DYS456, DYS19, DYS438, and DYS439) were filtered, most other partial profiles produced between 27 and 85 matching haplotypes (16 out of 21 dropout combinations). When four of the longest markers were dropped, the queried individual matched with 46 other individuals in the pedigree (Figure 5.13b), while 11 dropouts resulted in 73 matches (Figure 5.13c), and 21 dropouts resulted in all the pedigree's 85 individuals matching (Figure 5.13d).

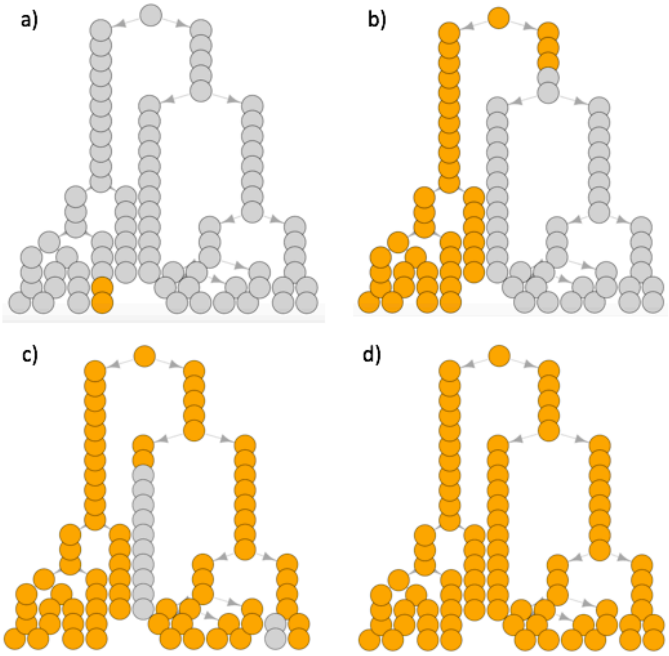

Figure 5.13 Pedigree illustration of population one- number of matches.

Pedigree comprising 85 male individuals over 20 generations, with matching individuals coloured in orange. Only the queried individual's father matches where a full 22 marker profile is obtained (a). Filtering out the four longest markers from the analysis increases the number of matches to 46 (b), then to 73 at the exclusion of the 11 longest markers (c), until all the matching of all the pedigree's 85 individuals at the dropout of all but one marker (d).

Population two started with a unique queried individual's haplotype differing from all other individuals in the pedigree (Figure 5.14a) and ended with 1490 matches out of 2464 individuals at the dropout of 20 markers (Figure 5.14d). When five of the longest markers were dropped, the queried individual matched with 103 other individuals in the pedigree (Figure 5.14b), while 15 dropouts resulted in 405 matches (Figure 5.14c). Although population two comprises eight different pedigrees, the matching profiles did not show on any of the remaining seven pedigrees. This is consistent with the fact that Y haplotypes are usually shared down the same paternal lineage, and it would not be surprising that all individuals of a specific pedigree would match between each other before this haplotype is observed in another founding lineage. Interestingly, pedigree two of population two (Figure 5.14) did not saturate with matching profiles even where only one marker was available for typing, with 21 dropouts resulting in 1709 matching haplotypes out of 2464 individuals in the pedigree. Balding and Andersen (2017) found that only tens of matches would be obtained with their tested Y-STR typing kits (Yfiler®, PowerPlex® Y23, and Yfiler® Plus) irrespectively of the population size.

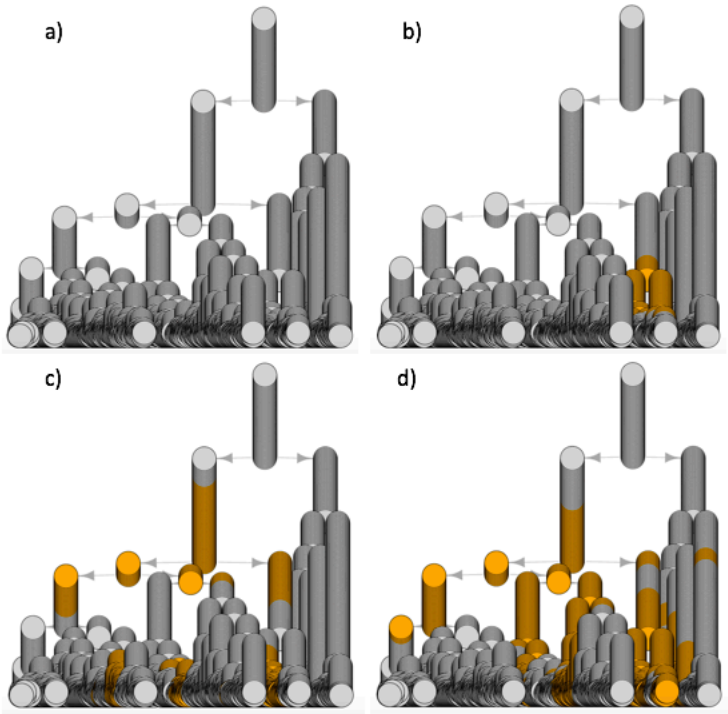

Figure 5.14 Pedigree illustration of population two- number of matches.

Pedigree comprising 2464 male individuals over 200 generations, with matching individuals coloured in orange. The second pedigree out of the eight that were simulated as part of population two. No individual matched the queried individual where a full 22-marker profile was obtained (a). The number of matches jumped to 103 with five of the longest markers dropped out (b), 405 matching individuals at 15 dropouts (c), and 1490 matching individuals when 20 markers were dropped (d).

Our two simulations show that, while full profiles resulted in one and zero number of matches respectively, 16 out of 21 partial profiles from population one and 18 out of 21 partial profiles from population two produced more than ten matching haplotypes. In population two, this number grew to hundreds with the dropping out of five, 13, 14, 15, 16, 17, and 18 of the longest markers, and reached thousands of matches with the dropping out of 20 and 21 of the longest markers.

Through these tasks, MALAN's R package revealed a limitation in its capacity to colour in orange all individuals of a pedigree if the digits that are used to designate the matching individuals exceed 4024 digits. As a consequence, the 1709 matches resulting from the dropping out of the longest 21 markers in population two could only be visualised in two pedigrees instead of one (Figure 5.15a and 5.15b). However, courtrooms would usually be interested in the last three generations (living suspects)

which reduces the number of matching haplotypes down to 464 at 21 dropouts, able to be visualised in one pedigree (Figure 5.15c).

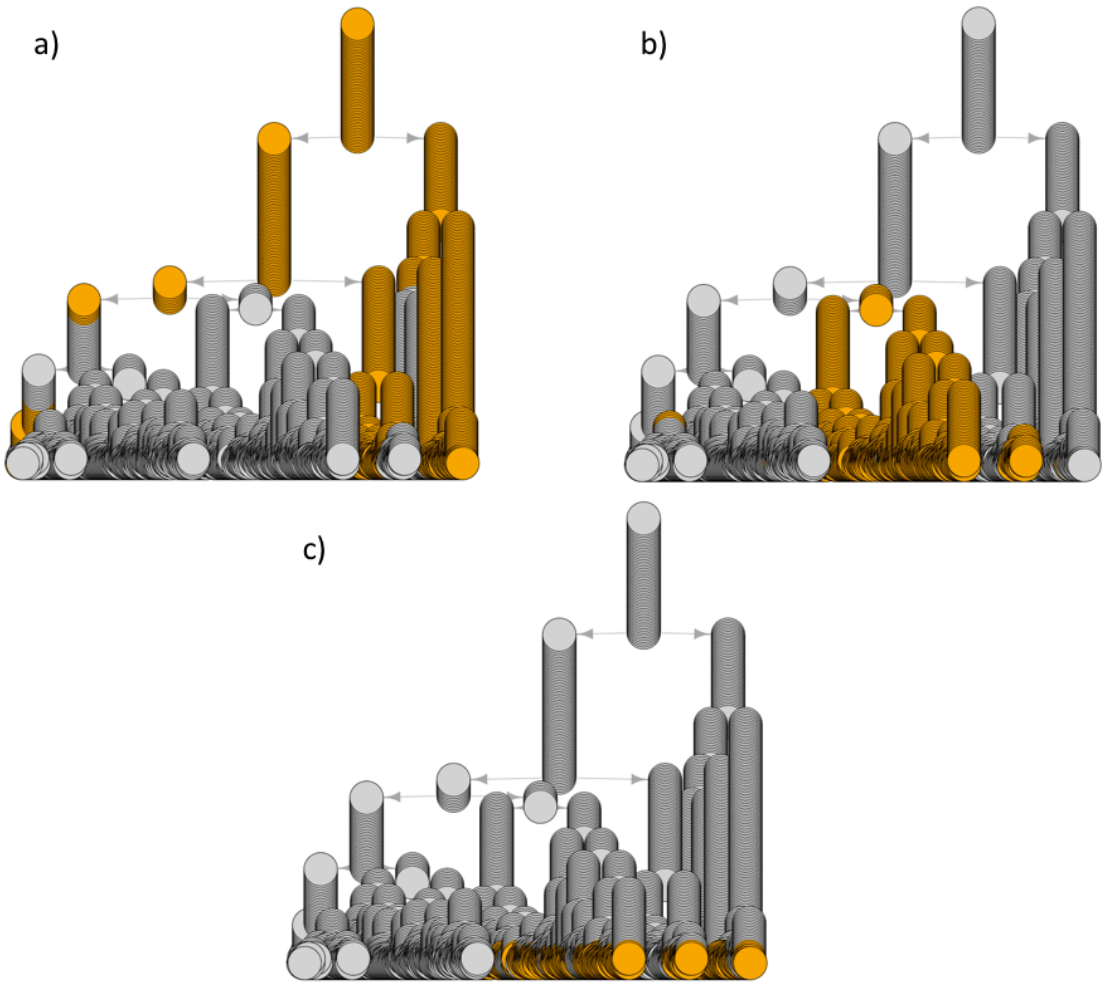

Figure 5.15 Matches in the pedigree v. matches in the live population.

The second pedigree out of the eight that were simulated as part of population two (comprising 2464 male individuals over 200 generations, with matching individuals coloured in orange). 1709 individuals of this same pedigree matched at the dropping out of 21 markers. However, they could only be visualised in two parts (a and b) due to a computing limitation in the current MALAN's R package. However, all 464 matches could be visualised at once (c) if the interest is limited to showing the live population (the last three generations) instead of the complete genealogy.

5.4.3 Mitochondrial - The Blazing Car Murder

The victim's HVSI and HVSII sequences were compared with the same regions in each of the 12 donors. All comparison samples showed one or two differences from the victim's mitotype except for individual 124, who could be directly excluded at this

stage with nine differences (Table 5.3). The LRs that were obtained for all individuals with two differences compared to the victim's mitotype were in favour of an exclusion with an LR less than one. The remaining two individuals who showed only one difference (097 and 114) could not be excluded as their associated LRs were between approximately 10. According to the Association of Forensic Science Providers (2009), the following can be concluded with these LR values:

The comparison between the donor and victim's haplotypes show **moderate** support for a common maternal lineage between the victim and the queried individual.

Table 5.3 Blazing car victim's mtDNA results.

Sample ID	Differences With victim	Number of differences	Haplotype frequency (corrected)	Generations	Mutation frequency	LR	Conclusion
097	16129A	1	2.37E-03	3	8.05E-03	1.02E+01	Moderate support Hp
113	16239T 16519C	2	2.95E-03	3	1.65E-05	1.68E-02	Excluded
114	16189C	1	2.37E-03	3	8.42E-03	1.07E+01	Moderate support Hp
116	16354T 16526A	2	2.33E-03	3	3.42E-07	4.39E-04	Excluded
117	16354T 16526A	2	2.33E-03	3	3.42E-07	4.39E-04	Excluded
118	16311C 16519C	2	4.02E-03	3	2.20E-04	1.64E-01	Excluded
119	16311C 16519C	2	4.02E-03	3	2.20E-04	1.64E-01	Excluded
120	16278T 16519C	2	2.53E-03	3	7.87E-05	9.35E-02	Excluded
121	152C 16311C	2	3.10E-03	3	1.65E-04	1.60E-01	Excluded
122	72C 16298C	2	5.36E-03	3	6.83E-07	3.83E-04	Excluded
124	73G 152C 195C 16126C 16163G 16186C 16189C 16294T 16519C	9 (excluded)	2.30E-03	NA	NA	NA	Excluded
125	16239T 16519C	2	2.95E-03	2	1.65E-05	1.68E-02	Excluded

Comparisons between the victim's mtDNA control region and those of living donors.

5.5 Discussion

5.5.1 The Likelihood Ratio in Forensic Science

A shift from the expert's confident opinion, that is solely based on experience or on a traditionally set of quantifiable criteria, towards a statistical evaluation of the forensic evidence was called for in the early nineties (Evett 1996; Foreman and Evett 2001; Polski et al. 2010). Statistics play a key role in ensuring the scientific foundations of forensic science. They are mostly involved in analysing data, in addressing the examiners' cognitive biases, and, most importantly here, in assessing the strength of the evidence (President's Council of Advisors on Science and Technology, (US) 2016; National Research Council 2009).

Methods of assessing the strength of evidence and reporting it to court are far from being agreed upon internationally. A vast number of expert reports are still being categorical in their conclusion and fail to weigh the evidence in question in terms of alternative hypotheses. Others contain a frequency estimate that intends to support a vague opinion. Courts have rejected evidence because it was probative and therefore not definitive enough for the judge to form an opinion. Other courts ruled the evidence out on the basis that the scientist overpassed her responsibility and did too much (Robertson et al. 2016).

Until recently, frequentist statistics were often used in the interpretation of the evidence. Frequencies, which are essentially defined as outcomes in a series of trials, were often attacked by the forensic science community as they simply reject or accept a hypothesis rather than weigh the strength of the evidence in the light of two competing hypotheses. The Bayesian approach is the current best practice as it avoids the *fall-off the-cliff*[24] effect, and accounts for all available information around a case before making a decision in the forensic context. The earliest known Bayesianists in forensic science may have been Poincaré, Darboux and Appel in their 1904 commentary about the relevance of statistical data associated with scientific evidence in court (Taroni et al. 1999). Their report criticised the frequentist approach and exposed *transposing the*

[24] The *fall-off-the-cliff* effect is the risk that is carried by the frequentist approach where a hypothesis (match) and its alternative (non-match) are illogically separated by a very small value.

conditional[25] as a methodological error: instead of comparing the likelihood of a criminal action committed by the suspect with that of the suspect's innocence, forensic science strictly only expresses the probability of the observed scientific result in the light of two carefully designed hypotheses.

When the Bayesian approach was first adopted for the interpretation of DNA evidence, the Single Locus Probe (SLP) technique was being used to type DNA. Restriction enzymes target the DNA at specific sites, resulting in fragments of different lengths between individuals. Berry et al. (1992) proposed a method that takes account the DNA fragment's lengths measurements errors and that circumvents the issue of between-probe independence. Evett et al. (1993) advocated for both Hardy Weinberg Equilibrium (HWE) and between-probe independence assumptions.

The logical strength of the LR in a forensic context is that it expresses the probability of the scientific observation [what concerns the expert] in the light of the prosecution *v.* defence hypotheses, taking into account other known circumstantial information. Unfortunately, its use has not expanded beyond a few world-leading institutions since it first entered the forensic interpretation arena. Reluctance in adopting the LR is still observed in law enforcement agencies, the judiciary (Berger et al. 2011a), and academic institutions (Morrison 2012). This sometimes extends to straightforward opposition where Lund and Iyer (2017), for example, argued that the LR does not apply to the transfer of information from an expert to a separate decision maker. Despite the criticism, which was readily responded to by exposing the *straw man arguments* and other logical fallacies committed by the critics, a Bayesianist approach using the LR is considered to be the current best practice (Morrison 2017; Aitken et al. 2018; Gittelson et al. 2018).

5.5.2 The Different Types of Markers

5.5.2.A Diploid Markers

Single Nucleotide Polymorphism (SNP) typing showed its potential in defining lineage markers haplogroups which helps in restricting the number of suspects and tracing back

[25] *The fallacy of the transposed conditional, also called the prosecutor's fallacy is when the interpretation addresses the probability of one of the hypotheses assuming the scientific observation (posterior probability) - P(H\|E) - rather than the probability of the scientific observation assuming one of the hypotheses- P(E\|H).*

the geographical origin of samples. Autosomal SNPs are also subject of interest to forensic researchers with advantages that were first observed in paternity testing due to their relatively low mutation rates, and most importantly in the analysis of degraded samples as they provide the possibility to work with short amplicons (Sobrino et al. 2005). Although four to six SNPs could be less informative than a single STR locus, they are the most abundant type of polymorphic markers and they can be readily typed in large volumes. Other advantages include lack of stutter peaks since it usually does not involve repetitive sequences (Balding and Steele 2015).

This project involved Identity-testing SNPs that are used for the same purpose as the forensically selected STR loci: differentiate individuals and exclude suspects that cannot be the source of a biological sample. While current autosomal STR kits include markers for which independence has been verified, and while the coancestry effects were accounted for through theta adjustment (Balding and Nichols 1994), the two assumptions - independence between loci and Hardy Weinberg's Equilibrium (HWE) - were made in this work's calculations of the autosomal SNP LRs. Ideally, a locus-specific Fst should be applied in real casework since the SNPs' mode of inheritance does not differ from that of autosomal STRs. However, it is also expected that identity-testing SNPs are carefully chosen to be thousands of bases apart, increasing the possibility of independence between markers, and with a low coancestry factor (F_{ST} <0.01) (Budowle and Van Daal 2008).However, as the genetic variation may differ from locus to locus, and most of our information on human populations comes from more conventional genetic markers there is a need for an updated exploration of genetic differentiation among human sub-populations for each SNP marker that is included in currently available technologies. With regards to the 94 identity-testing SNPs that were typed in this work, Churchill et al. (2017) tested for HWE and identified eight loci (rs1493232, rs2111980, rs1490413, rs159606, rs729172, rs7041158, rs214955, and rs9905977), five loci (rs1382387, rs1335873, rs993934, rs6811238, and rs321198), six loci (rs2269355, rs2342747, rs917118, rs993934, rs4606077, and rs9905977), and one locus (rs2920816) in the Asian, African, Caucasian, and Hispanic populations, respectively, that deviated from expectations ($p < 0.05$). Locus specific F_{ST} ranged from 0.00231 for rs321198, to 0.24149 for rs1335873.

SNPs also carry considerable disadvantages that may hinder their widespread utilisation or them even replacing STRs. These include complicated mixture analysis due to the

SNPs biallelic (sometimes tri-allelic) nature, the lack of compatibility with long established national STRs databases, and the requirement of large DNA quantities relatively to STRs (Balding and Steele 2015). Here, the autosomal STR and SNP markers were assumed to be independent of each other which would permit the combination of both LRs by multiplication. This is sometimes known as a Naïve Bayes fusion (Morrison 2012) and should be applied with caution in real casework.

5.5.2.B Lineage Markers

The literature also mentioned the combination by multiplication of autosomal STR and lineage marker LRs (Castella et al. 2006; Walsh et al. 2008). Further research into how to adequately combine LRs of different DNA markers may become highly relevant with the introduction of MPS technology into the forensic arena resulting in markers with different modes of inheritance being routinely typed together. Few adjustments were recommended for the multiplication of autosomal and Y STRs LRs: Walsh et al. (2008) suggested raising the θ to 0.04 when estimating the autosomal profile's *RMP* , since the probability of close-relatedness between two individuals sharing the same Y haplotype is high, or directing the defence hypothesis (Hd) against relatedness bias: e.g. 'some other man, who is not a descendant of the father of the suspect, is the donor of the crime stain' (De Zoete et al. 2014).

The best method to interpret a Y-haplotype match (or near match) is still the subject of scientific evaluation. Currently proposed are three ways to report the results: the counting, the frequentist and the Bayesian approaches. While the limitations related to reporting frequencies in a forensic context were discussed previously, Roewer et al. (2000) suggested a Bayesian approach which estimates a posterior distribution of haplotype *RMPs*. King's College London and the University of Leicester are two institutes amongst others in the UK, that have established their own regional but also international Y-STR haplotype databases, and a subset of these was used in this work to simulate dropouts. Also available are open-source multi-regional databases such as YHRD (Willuweit et al. 2007) and Promega (Thompson et al. 2013).

Although worth exploring for comparison purposes, this work did not apply the Bayesian approach in the Y-chromosome interpretation. This was mainly to assess the effects of dropouts on the counting method, recommended by Andersen and Balding (2017), after exploring this effect on LRs from autosomal STRs and SNPs. The premise

was that while the counting method based on a well thought of simulation model may be today's most appropriate method to report the evidential value of a Y haplotype match, dropout events would affect this rule. This part of the work intended to test Andersen and Balding's (2017) with regards to interpreting partial profiles:

> "When only a few loci generate usable results due to poor sample quality, it may be appropriate to use a standard match probability approach. This is because there will be many matching individuals in the population ..."

First, the simulation of population dynamics is considered to be a relevant exploratory tool in the field of forensic DNA (Lanes 2016), and the usefulness of well-developed simulated data was shown to provide real predictions (Andersen et al. 2013). Caution should however be made in transferring such results to real data, especially as artificially designed populations do not necessarily reflect the dynamics of a case-specific relevant population. Two populations of different sizes (N_1=85, N_2=11,402) were simulated using The MALAN system where a symmetric single-step mutation that is based on marker specific mutation rates was run to digitally populate each individual with a haplotype that would be similar to those obtained by the PowerPlex® Y23 kit. Both populations showed a majority of partial profiles combinations resulting in more than ten matches, while a full profile had resulted in one and zero matches respectively. Additionally, a positive correlation was found between the number of dropouts and that of matching haplotypes in population two, which is more representative in size.

However, the trend was not linear in both populations meaning that the number of matches does not increase, and may even diminish, at every additional dropout. The phenomenon could be considered realistic as prior knowledge about the queried individual's profile frequency is usually not available upstream of the investigation. Like in real life, the MALAN's series of functions may choose a relatively frequent haplotype at five dropouts, resulting in an increased number of matches, then pick a rare profile at six dropouts resulting in a low number of matches. This inconsistency is also accentuated by the marker-specific mutation rates, where, for example, short markers with high mutability (e.g. μ_{DYS570}= 0.01 and μ_{DYS576}= 0.015) contribute more in diversifying the population than long ones that would have been dropped out first. It is arguably more consistent to avoid such discrepancies when determining the effects of DNA degradation (loss of the larger markers) on the evidential value of Y haplotypes.

One solution could be in the development of a function that allows to filter markers after the selection of a fixed queried individual. Another option is to extract all the population's haplotypes (in .csv format), manually erase markers from the longest to the shortest, while counting the number of matches after each dropout.

5.5.2.C Mitochondrial DNA - The Blazing Car Murder

The benefit of combining autosomal, Y, and mtDNA LRs declares itself after obtaining weak evidence in the favour of a common maternal lineage between the victim and two of the living donors. This is especially true with the development of autosomal/Y/mitochondrial MPS systems like the prototype Promega PowerSeq® system. In the event that the autosomal and Y STR analyses did not provide more information than the CE (Figure 5.5), whole mtDNA sequencing could provide more information.

Before discussing the interpretation of mtDNA further, the victim's sample requires special attention. First, the sample's authenticity is in question, as it was allegedly found within the archives of the St Bartholomew's Hospital museum and then handled for analysis at the NUCFS. The partial STR profile that was obtained showed a degradation pattern (ski-slope and dropouts) that is in line with the sample's nature (FFPE) and age (1930). With regards to contamination, the microscope slide is expected to have been handled by numerous individuals over the years, therefore leading to human DNA contamination on its surface. Whilst the bleach-water treatment performed by NUCFS should have avoided contaminant carry-over from the external slide surfaces to the embedded tissue prior to DNA extraction, it is likely that the technician who prepared the original biopsy material in the 1930s took no precautions to limit the amount of their own or environmental DNA deposited directly onto the biopsy material during preparation, as disposable surgical gloves first became available more than 30 years later. 'Forensic negatives' were also collected after cleaning to detect the presence of any extraneous DNA which may still have been present. These negative controls were processed in parallel with the victim's tissue. Finally, the DNA extract's small volume limited the possibilities of analysing it further at the University of Leicester.

With regards to the interpretation of mtDNA comparisons between the victim and the 11 non-excluded donors, the Bayesian approach was preferred over the frequentist or

the counting methods. For the numerator ($k * \mu$), the number of generations k was assumed to be *three* for all individuals but should change in case any information about the relatedness of the compared individuals is provided. A minimum of three steps was assumed with one separating the victim from his mother, another one from his mother to his sister, and a third one from his sister to any surviving individual. This assumes that mtDNA is unlikely to change 100% in a single generation as it is most likely to transition through a heteroplasmic state, which in this case was not observed.

The site-specific mutation rate μ was derived from (Soares et al. 2009) data which was based on a worldwide phylogeny of more than 2000 complete mtDNA genomes. They used an empirical approach to estimate the level of variation at any time depth within the tree. One should note however, that inferring from phylogenetic studies may be biased if paternal mtDNA inheritance and recombination is shown to occur at appreciable rates. While other studies mentioned that segregation of mutations occurred at different rates in different tissues (Wilson et al. 1997; Calloway et al. 2000), none has yet estimated a quantifiable difference between prostate and buccal tissue which are both rich in epithelial cells. Consequently, no factor that accounts for the difference in mtDNA polymorphism between the two compared tissue types was included in the numerator.

For the denominator, the EMPOP database was used to determine the mitotypes' *RMP*, as recommended during the ISFG meeting (Prieto et al. 2008). The alternative method of deriving the mitotypes frequencies from the upper 95% confidence interval method ($p = 1- \alpha^{1/n}$) was avoided as it would be of limited value when the frequency estimate p is small (Holland and Parson 1999). Finally, the two donors that were not-excluded from being maternal descendant of the victim fell into the third out of the four possible situations that Tully and Wetton (2014) proposed as possibly encountered when a match- or a single difference- is observed between a known and a questioned sample:

> ***A single base differs between the known and questioned sample. The mutation was previously reported but does not seem to be on a "hotspot". The known sample's haplotype was observed once in the database together with other near matches but excluding the queried sample's haplotype. The findings may be inconclusive depending on the substitution's mutation rate or frequency.***

Chapter 6 Discussion and Future Directions

Heat generated by exothermic reactions is an issue in many types of forensic investigation. This project explored heat- and explosion-induced DNA degradation, developed a simple and robust method that detects this degradation prior to typing DNA using currently available Capillary Electrophoresis (CE) and Massively Parallel Sequencing (MPS)-based techniques, and studied how this may affect the strength of evidence in court.

While it may require days to years for ambient temperatures to degrade DNA (Ambers et al. 2014), extremely high temperatures that are reached by live fires (320 - 1000 °C) (Babrauskas 2006) and during an explosion (>1000 °C) (Esslinger et al. 2004) were shown here as capable of degrading DNA in fractions of seconds, in the case of low explosives, to minutes, in the case of controlled temperatures inside an oven. The investigations of numerous high-profile cases involving live fires were hampered by the quality of the associated biological samples. However, the belief that combustion destroys DNA is still being debated in the scientific community. In their simulated arson experiments, Abrams et al. (2008) found that the degree to which samples were burnt did impact upon the recovery of full DNA typing profiles, while Tontarski et al. (2009) found no effects on the recovery of DNA at temperatures lower than 800 °C. This work subjected dried biological stains to different temperature treatments and found that exposure to 180 °C for 30 minutes consistently reduced the amplification of the set of larger target amplicons (>300 bp) within currently available STR multiplex kits. Exceptions came from two blood stains that showed more resilience through the amplification of ≈400 bp autosomal STRs with the CE-based NGMSElect® kit and ≈300-350 bp Y-STRs with the MPS-based ForenSeq® DNA Signature Prep kit (initial DNA concentration: ≈ 2-4 ng/µL). The same duration of exposure at the higher temperature of 200 °C was associated with a failure to recover any interpretable DNA information.

Unlike the prolonged heat treatments of Chapter 3 (140 °C, 180 °C and 200 °C for 30 minutes), the biological samples in Chapter 4 were placed on the surface and inside pipe bombs that were then detonated. The chapter addressed the converging interests of academics and practitioners seeking to understand whether the effects of an explosion

that are characterised by a sudden combustion wave lasting for only a few milliseconds but reaching thousands of degrees Celsius, would interfere with current DNA analyses aimed at identifying victims and suspects of an explosion event. US law enforcement agencies agreed to construct and deploy the bombs while supervising the experiments. They provided skilled personnel, military material (Composite 4 explosive and advanced initiation systems), as well as time and an outdoor test range to conduct the explosions. The experiments consisted of exploding pipe bombs carrying biological samples inside - in direct contact with the filler- and around the pipes' outer surface. The choice of IEDs was influenced by their frequent criminal use, their confinement properties, and their relatively safe and simple construction. The pipe's simplicity of design allowed for testing multiple investigative scenarios including the bomb maker's identification from the samples within the interior of the device, and that of the bomb handlers or victims from the outside samples.

Klein et al. 2018 conducted arson experiments using a flashover simulator that reached 'near-explosion temperatures (>1000 °C); a seldomly examined subject in the literature. Sixty percent of their samples generated full profiles while the remainder were divided between partial profiles and no interpretable genetic information. Their results were consistent with tests of low-level Double Base Smokeless Powder (DBSP) explosions in this study where 27% of samples showed DNA degradation through partial profiles characterised by the loss of the larger amplicons. While no DNA degradation was observed in samples that were placed on the outer surface of C4-charged pipe bombs, none of stains in this study that were deposited inside the same bombs could be detected after the blast. One side avenue would be to investigate the conditions that may induce a total disintegration of evidentiary samples after an explosion. Reproducing the C4 related experiments inside Total Containment Vessels (TVC), which are normally used to transport explosive materials safely, could serve this purpose. However, it remains to be noted that the explosion temperature may increase significantly in such a case.

Chapter 5 explored how DNA degradation affected the strength of DNA evidence by lowering the Likelihood Ratio and by increasing the number of random matches in a database. The combination of real and simulated data provided the opportunity to work with realistic scenarios on one hand, and to control not only the extent of degradation

but also other parameters which affect evidential strength such as population size and diversity.

6.1 Sample Type Choice

This work intended to explore how extreme temperatures could affect the confidence in identifying disaster victims from events including plane crashes, fires and explosions; and the identification of offenders such as arsonists, bomb makers, and crime concealers. While the discussion focusses mainly on the work performed on biological stains, human bones that were heated in a furnace and touch cells that were exposed to C4 explosions were also tested (work in progress).

6.1.1 Identification of Victims

Post-mortem samples that are intended for a victim's identification usually include cardiac blood, blood clots, and other internal tissues or body fluids (Dinis-Oliveira et al. 2016). However, disasters often cause the dismemberment, co-mingling, and skeletonization of the human remains (de Boer et al. 2018). Clayton et al. (1995) argue that skeletonized material represents a common sample in cases of fire or explosions. While there are numerous methods of victim identification, these are expected to be practical under field conditions, performed in a timely manner, and admissible by the courts as well as the scientific community. The International Criminal Police Organization prioritises friction ridge analysis (dactyloscopy), comparative dental analysis (odontology) and DNA analysis (INTERPOL 2018). Another identifier that is reliable is the unique serial number found on medical implants such as pacemakers (when present). Secondary methods of identification are usually combined with other means and include photographs, personal descriptions, tattoos, medical findings and going through the victim's personal effects.

Cases of fire or explosion may obstruct visual examinations. Forensic odontologists would then compare the antemortem (AM) dental records with the teeth of the deceased person. In case these are lost, broken, or AM records unavailable, dactyloscopists may compare the deceased fingerprints with existing databases. Fingers may also be absent in cases of dismemberment; they may be burned or decomposed beyond recognition, or database information may also be unavailable. Odontology and dactyloscopy could not be performed in the less common events of a body's total disappearance, such as where extreme means were employed to conceal the victim's body either by burning (Groen et

al. 2015) or in other as yet unrevealed ways (Hathaway et al. 2019). Research showed the complete incineration of a human body takes about 2–3 hours at 670 to 810 °C (Bohnert et al. 1998).

Violent explosions can also cause the complete destruction of body parts as well as possible dismemberment into much smaller burned human remains (Macko et al. 2009; Schyma et al. 2011). The victim's total sublimation by an explosion is conceivable as missing persons have been reported in mass fatality incidents (Moody and Busuttil 1994). The mechanism through which visible human remains are not recoverable after an explosion requires further research. Byard and Payne-James (2015), recommend sampling areas that are thought to have been in direct contact with the victim(s). It is common practice in forensic archaeology to bag the soil around a totally decomposed person, and search for fragments of teeth and other bones (Figure 6.1). In this sense, DNA technology offers considerable advantages as it can be recovered from almost any biological material including microscopic traces (Goodwin *et al.* 1999; Holland *et al.* 2003; Budowle *et al.* 2005; Graham 2006) and, in case of unavailable databases, compare it with that of the deceased's direct or indirect references[26].

[26] Direct reference is usually obtained from the queried individual's personal objects such as their toothbrush, while indirect DNA references are their relative's profiles or sequences.

Figure 6.1 Skeletal decomposition.

The excavation of an ancient burial chamber in Beirut, Lebanon, carried out by the Lebanese General Directorate of Antiquities including this work's author. The site was dated back to approximately 300 AD and shows the complete decomposition of skeleton for at least three individuals as marked by the copper ankle rings (green rings) and the underneath decomposition soil (darker in colour).

6.1.2 Identification of Perpetrators

The perpetrator's biomaterial is usually *ex vivo* - outside of the living body - in the form of biological fluids, hairs, or skin cells. Consequently, a perpetrator's mark on a crime scene is often more subtle than that of a victim. Additionally, heat or explosions are expected to limit further access to genetic information in the form of biological traces left by the perpetrator. It is therefore unlikely to recover significant amounts of human tissue from the actors of such disasters, except in special cases of suicide bombings (Sudoyo et al. 2008), and intentional plane crashes (Vuorio et al. 2015).

What really happened at fire scenes may be concealed by burnt evidence. Criminals often attempt to erase their marks by setting places and items on fire and the ability to recovery DNA in such situations would bring significant advantages in resolving crimes. The identification of a victim inside a burnt house for example, may not tell the

complete story if not accompanied by collection of cigarette butts, chewing gums, pop cans, and used kitchen items that might indicate the presence of someone else, or without detecting signs of violence in the form of blood patterns on the walls, the floor, and items that could have been used as the weapon in a crime. Even arsonist's biological evidence may include blood and saliva stains that are similar to the ones tested in this project. In their case report of arson at a restaurant which exploded and then caught fire, Spitsen et al. (2004) discuss a trail of blood drops that started at the crime scene and ended where the suspect sought medical treatment. Similarly, saliva is expected to be present on used cans and bottles as well as on cigarette butts (ENFSI 2017).

Although saliva may also be detected on wiring where a bomb maker has stripped the insulation with their teeth, touch DNA remains the most common (90%) type of biological evidence that is left on explosive devices (Bille 2014). However, working with heavy DNA samples - blood and saliva - ensured robustness and reproducibility of the experiments. Samples of DNA concentrations varying from 0.1 to 4 ng/µL could be repeatedly deposited in different scenarios to accurately determine the relative degree of damage inflicted by different temperatures and duration of exposure. As seen previously, working with touch DNA as the sole biomaterial would lead to unreliable deposition of cells from one handling activity to another (Lowe et al. 2002), and is expected to result in partial profiles from untreated samples (positive controls). Additionally, saliva samples are themselves composed of sloughed off epithelial cells in suspension. Rather than working with extracted (naked) DNA, this work employed native DNA samples - human tissues or cells - which represent the reality of the biological evidence that is expected to be found on the crime scene. Their dried state displayed scenarios where operatives would arrive sometime after the investigated event had happened. In terms of initial quantity, the stains' relatively small volumes (2 - 200 µL) sit at the junction of a perpetrator's biological mark, and a lost victim's human remains.

6.2 Explaining the Damage

Previous studies showed a number of techniques that can degrade DNA artificially. Selecting the method of artificial degradation depends on the sample type, which in turn reflects the study's aim and the material's availability. Non-specific DNA

fragmentation in aqueous solution can be realised through ultrasonication via cavitation and mechanical/thermal effects. Hydrogen bonds are first disrupted at mild intensities (< 2 W/cm^2), followed by single-strand ruptures due to the creation of free radical at higher strengths (Elsner and Lindblad 1989). As previously discussed in DNA "fingerprinting", specific fragmentation in aqueous solution may be performed using restriction enzymes (Nathans and Smith 1975). These are a type of endonucleases that bind to specific sequences of nucleotides and cleave the sugar-phosphate backbone. However, dry-state native DNA such as this work's main sample set requires a different approach to DNA fragmentation. If heat is considered, and is viewed in terms of energy transfer, it becomes essential to consider the temperature's intensity, the time of exposure, the sample's initial temperature, and the presence of other heat absorbing elements around and within the sample.

A controllable oven with measurable temperatures - for prolonged heating - and explosions of real pipe bombs - for flash heating - were the selected extreme conditions. The realistic sample/treatment complex - native DNA/real sources of heat - formed an experimental design that meets similar conditions that would otherwise be felt in real disasters involving fires or explosions. Marrone (2009) found that when exposed to heat, aqueous DNA degrades faster than dry DNA. However, both states have similar activation energies as well as damage-related chemical reactions: base hydrolysis, base modifications, and strand breaks. Characterised by deamination and by the base loss from the 2´- deoxyribose backbone, base hydrolysis will eventually lead to a strand break. However, measurements of glycosidic bond cleavage and strand breaks concluded that base loss alone did not correlate with the extent of DNA fragmentation detected, but that heat also seems to exert a mechanistic strain on the bonds forming the backbone. This is consistent with Alongi et al. (2015) statement that C-N sugar-base (293 kJ/mol) and the PO-C sugar-phosphate (358 kJ/mol) are the weakest bonds in DNA.

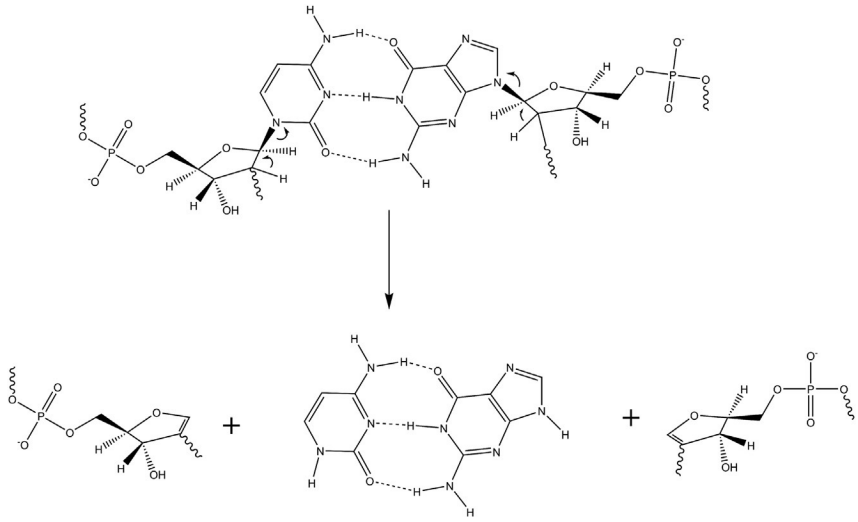

Figure 6.2 Thermal scission of the C-N sugar base bonds.

Illustrating the thermal scission of C-N sugar-bases single bonds from cytosine-guanine paired nucleotides. Image from Alongi et al. (2015).

Once the effects of sustainable heat on DNA typing were determined, this project addressed the effects of explosions, which are characterised by a flash exposure of extremely high temperature, accompanied by violent changes in pressure that may lead to a brisance effect in case of a detonation. The main questions revolved around current capabilities of identifying bomb makers, bomb handlers, and victims of explosions, and the possibility of distinguishing between their traces after the explosion. Both queries require studying the cause of explosion-induced DNA damage on one hand, and the ability to collect recognisable bomb fragments post-explosion on the other.

The samples placed inside pipes before the explosion represent biomaterials that could potentially have been deposited by the constructor of the bomb and samples placed outside the pipes represent a handler's biological traces or those of victims that were near the explosion's epicentre. Unsurprisingly, C4-induced explosions (high explosives) resulted in greater fragmentation than the DBSP (low explosives) explosions. As a consequence, this lessened the ability to recognize potential sample locations that could subsequently be used to distinguish between constructor, handler, or victim. Whilst the sample's location, its biological type (blood or saliva), and the container's material did not influence the level of DNA degradation, the types of explosives did, with obvious signs of DNA degradation after DBSP explosions as opposed to detonation of C4 following which full profiles were obtained.

This result was consistent with the literature that involved comparable experimental designs: biological samples mounted on pipe bombs. Partial profiles were reported in studies that employed single base smokeless gunpowder (IMR powder SR 4756) as the main charge (Esslinger 2004; Foran 2009). One out of the 20 handled pipe bombs produced a full autosomal STR profile (AmpFlSTR® Profiler Plus™) in Esslinger (2004). Three of them returned partial profiles, eight returned correct allelic signals that were below the reportable threshold, whereas no alleles were detected in the last eight pipes. It is essential however to note that the cause of this study's dropouts was not particularly linked to either DNA degradation or to stochastic effects from low-template touch DNA samples. Additionally, there was no mention of which loci dropped out or whether there was any particular pattern indicating DNA degradation. In the study by Foran et al. (2009), pipe bombs were assembled by volunteers who handled steel end caps for 30 seconds each before the explosions. The mitochondrial DNA HVI and HVII regions were then sequenced, resulting in 15 of the 38 samples for HV1-1 (first part of the HV1), five of 38 samples forHV1-2 (second part of the HV1), and no samples for HV2. The study showed the benefit of assaying shorter overlapping mtDNA fragments in post-blast degraded samples, otherwise known as nested PCR. Signs of DNA degradation appeared in the higher sequencing success rate for HV1 (256 bp) that was amplified in two separate fragments, compared to HV2 (283 bp) that was amplified as a single fragment.

On the other hand, studies that used high explosives did not show DNA degradation. Rampant (2017) charged Polyvinyl Chloride (PVC) pipes bombs with Pentaerythritol tetranitrate (PETN) and found no significant difference in DNA concentration, amplifiability, and degradation indices between pre- and post-blast diluted blood samples. Tasker et al. (2017) filled PVC pipes with Tannerite, a binary high explosive and typed post-blast DNA with GlobalFiler® PCR Amplification Kit (Thermo Fisher Scientific). Although 34 out of 44 quantifiable samples (>0.0002 ng/µL) resulted in partial profiles and eight did not show any interpretable alleles, the loci affected by dropouts and the electropherograms' patterns were reportedly associated with stochastic losses from low-template DNA. In fact, this study used only around 30 suspended epithelial cells per sample that were later spiked on the pipe bomb's outer surface without any protection before the blast.

6.3 Future Directions

6.3.1 Overcoming Real Casework Difficulties

The controlled experiments that were performed as part of chapters 3 and 4 differ from real case scenarios in that DNA mixtures and drop-ins were avoided through rigorous decontamination precautions or sample protection (with adhesive tape) in outdoor locations. More importantly, these samples were from known contributors who were included in this project's initial database and whose DNA profiles were generated from buccal swabs as well as from refrigerated blood stains.

In real casework however, many profiles from low-template samples are also DNA mixtures. Minor contaminants that otherwise would not be detected or considered in the presence of high true allele signal complicate the interpretation of such profiles. The improved sensitivity of recently developed kits amplifies this phenomenon and therefore increases the likelihood of obtaining mixed DNA profiles. This would decrease confidence in attributing the source of a crime stain by affecting the statistical interpretation and raising uncertainty about the designation of artefacts or potential drop-ins. In any case, the deconvolution of mixed STR profiles starts by listing the possible genotype combinations; a task that may require multiple angles of approach, including the use of elimination databases, and other algebraic solutions.

Taking into account peak areas or height was proposed by Bright et al. (2010) where excessive differences, above heterozygous balance thresholds for example (peak height ratio outside the range of 0.6 to 1.66), are an indication of an additional contributor. While the exclusion probability, which equates to the probability that a random person would be excluded as a contributor to the observed DNA mixture, was widely used on the basis of its simplicity, it came under heavy criticism on the basis that the number of possible contributors is ignored from the equation which could form in some cases a prosecution bias (Weir et al. 1997). The use of a Likelihood Ratio has been proposed as a viable alternative (Buckleton et al. 2007) but is often faced with uncertainty concerning the number of contributors that is accentuated by allelic dropouts and artefacts that are often present in low template profiles. Related contributors bring an additional complication due to an increased masking effect on the number of alleles.

Where algebraic solutions are complicated, the use of Bayesian networks through Hugin (Mortera et al. 2003) or R functions called GRAPPA (Green 2005) are options.

Such networks have the dual ability to represent a complex problem graphically and enable inferences to be made about the effect of the scientific evidence (E) on the possibilities of the relevant propositions (Hp or Hd). Importantly, MPS technologies provide powerful tools to resolve mixtures by decoupling isometric alleles through identifying differences in their sequences (Xavier and Parson 2017).

6.3.2 Miscoding Lesions and DNA Repair

Determining the nature and the extent of DNA damage may allow reverse engineering by revealing the extreme conditions that the biological sample was subjected to and therefore potentially elucidating unknowns about the criminal event. It also enables the implementation of protocols to bypass the impact of the damage and repair it when necessary. The samples used in this project provided an opportunity to directly compare the effect on different marker types and potentially the nature of the damage imposed. The latter could be investigated through the use of DNA repair enzymes and sequence analysis from the MPS data to look for distinctive damage patterns (work in progress). The focus of Chapters 3 and 4 was on treatments that obstructed PCR amplification, probably by strand breakage or through the creation of abasic sites. Scatter plots with linear regressions were used to measure the relationship between temperature treatments and the sizes and signal intensity (RFU/DoC) of amplicons, with the assumption that longer amplicons would be affected first by DNA degradation.
For those amplicons that could still be amplified, MPS data opened new research directions where deeper analyses would serve to identify lower levels of DNA damage. For example, a study of the error rate would be instructive regarding other types of DNA damage affecting individual bases where sequence changes might have altered the fidelity of PCR replication and subsequent sequencing. DNA amplification is not always inhibited by DNA damage, and oxidative damage for example may introduce miscoding lesions. The ability to recognize where this has happened is crucial for a correct interpretation of a DNA sequence, and not doing so may have drastic consequences in both casework and research. These low-level damage lesions may be caused by deamination, depurination, and oxidative damage.

Cytosine (C) bases are particularly susceptible to deamination and are consequently converted to uracil (U), a base that is analogous to thymine (T). Alternatively, adenine is deaminated into hypoxanthine (HX) which is analogous to guanine (G). Because U pairs with A and HX pairs with C, two types of complementary transitions - “type 1”

(A-G/T-C) and “type 2” (C-T/G-A) – may result from deamination with a preference to “type 2” transitions. Both types of transitions may also result from G depurination leading to type 2 transitions, and that of A, leading to type 1 transitions. Deamination and depurination events are facilitated by hydrolysis, which occurs frequently in aqueous environment (Rathbun et al. 2017).

Recent findings showed that oxidative damage was frequently observed in the MPS analysis of touch cells collected from unexploded copper and brass ammunition (Holland et al. 2019). Copper ions facilitate oxidative damage through reactive oxygen species, notably hydroxyl (OH·) and superoxide ($O2^{-}$). This in turn induces the production of a common DNA lesion called 8-Oxoguanine (8-oxoG). 8-oxoG has a potential to pair not only with C, but also with other bases– A, T, and G. PCR replications however are biased towards the incorporation of A, resulting in a G to T transversion. While such damages cannot be metabolically repaired *ex vivo* or post-mortem, many attempts at repairing them enzymatically at a pre-PCR stage were carried out (Nelson 2009; Nelson and National Institute 2015), and still represent a worthwhile future research avenue. Currently available pre-PCR repair mixes contain a polymerase, a ligase, endonucleases, and glycosylases. The mix was developed to repair DNA nicks, oxidised guanine and pyrimidines, deaminated cytosine, thymidine dimers, blocked 3′ ends and abasic sites. However, it does not repair DNA fragmentation (Robertson et al. 2014). The interest in repairing heat-induced dry state DNA was further increased after it manifested abasic sites in Marrone (2009) and strand breaks that would not occur spontaneously but rather mechanistically with a half-life of 24 ± 2 days.

Studying the effects of extreme conditions on forensic DNA analyses, and developing methods to detect and assess DNA damage, have a bilateral impact potential. On one hand, the extent and the nature of DNA damage in a biological sample would determine the strategy of analysis and its limitations. On the other, and since the sample’s condition is a direct consequence of what happened to it, it may be helpful in the reconstruction of an investigated event (e.g. approximate temperatures reached and duration of exposure) and to distinguish DNA deposited before the event from post-event contamination. In conclusion, this study has shown the characteristic effects that heat has on the quality of both CE and emerging MPS forensic solutions. Both technologies yielded comparable results in terms of their chemistries on DNA

typeability. It emphasizes the potential benefits of the latter which allow the simultaneous typing of large numbers of short amplicon markers (mini-STRs & SNPs) that are more likely to survive in an amplifiable state after heat damage and therefore provide a discriminating profile that can be used for identification purposes. It also shows that interpretation methods that can cope with the complex patterns of allelic dropout and low-level post-event contamination will be key to the successful analysis of this sample type that has great significance in the investigation of the most serious of today's crimes.

7 Bibliography

Abdul-Karim N, Morgan R, Binions R, Temple T, Harrison K (2013) The Spatial Distribution of Post-blast RDX Residue: Forensic Implications. Journal of Forensic Sciences 58:365-371.

Abrams S, Reusse A, Ward A, Lacapra J (2008) A simulated arson experiment and its effect on the recovery of DNA. Canadian Society of Forensic Science Journal 41:53-60.

Aitken C, Nordgaard A, Taroni F, Biedermann A (2018) Commentary: Likelihood Ratio as Weight of Forensic Evidence: A Closer Look. Frontiers in Genetics 9:224.

Aitken C, Roberts P, Jackson G (2010) Fundamentals of probability and statistical evidence in criminal proceedings: guidance for judges, lawyers, forensic scientists and expert witnesses, Royal Statistical Society.

Alaeddini R (2012) Forensic implications of PCR inhibition—a review. Forensic Science International: Genetics 6:297-305.

Aliferi A, Thomson J, McDonald A, Paynter VM, Ferguson S, Vanhinsbergh D, Syndercombe Court D, Ballard D (2018) UK and Irish Y-STR population data—A catalogue of variant alleles. Forensic Science International: Genetics 34:e1-e6.

Al-Kandari NM, Singh J, Sangar VC (2016) Time-Dependent Effects of Temperature and Humidity on Quantity of DNA in Samples of Human Saliva, Blood and Semen in Kuwait. International Journal of Pharmaceutical Sciences and Research 7:2852-2873.

Allentoft ME, Collins M, Harker D, Haile J, Oskam CL, Hale ML, Campos PF, Samaniego JA, Gilbert MT, Willerslev E, Zhang G, Scofield RP, Holdaway RN, Bunce M (2012) The half-life of DNA in bone: measuring decay kinetics in 158 dated fossils. Proc Biol Sci. *279*, pp.4724-4733.

Alongi J, Di Blasio A, Milnes J, Malucelli G, Bourbigot S, Kandola B, Camino G (2015) Thermal degradation of DNA, an all-in-one natural intumescent flame retardant. Polym Degrad Stab 113:110-118.

Aloraer D, Hassan NH, Albarzinji B, Goodwin W (2015) Collection protocols for the recovery of biological samples. Forensic Science International: Genetics Supplement Series, *5*, pp.e207-e209.

Ambers A, Turnbough M, Benjamin R, King J, Budowle B (2014) Assessment of the role of DNA repair in damaged forensic samples, International Journal of Legal Medicine, *128*, pp.913-921.

Andersen MM, Balding DJ (2017) How Convincing Is A Matching Y-Chromosome Profile? *PLoS Genetics*, *13*(11), p.e1007028.

Andersen MM, Balding DJ (2018) How many individuals share a mitochondrial genome? *PLoS Genetics*, *14*(11), p.e1007774.

Andersen MM, Caliebe A, Jochens A, Willuweit S, Krawczak M (2013) Estimating trace-suspect match probabilities for singleton Y-STR haplotypes using coalescent theory. Forensic Science International: Genetics 7:264-271.

Argyros GJ (1997) Management of primary blast injury. Toxicology 121:105-115.

Association of Forensic Science Providers, (2009) Standards for the formulation of evaluative forensic science expert opinion. Science & Justice 49:161-164.

Babrauskas V (2006) Temperatures in flames and fires. Fire Science and Technology Inc, 18, 369-374.

Balding DJ, Donnelly P (1995) Inference in forensic identification. Journal of the Royal Statistical Society: Series A (Statistics in Society) 158:21-40.

Balding DJ, Nichols RA (1994) DNA profile match probability calculation: how to allow for population stratification, relatedness, database selection and single bands. Forensic Science International 64:125-140.

Bär W, Kratzer A, Mächler M, Schmid W (1988) Postmortem stability of DNA. Forensic Science International 39:59-70.

Barash M, Reshef A, Brauner P (2010) The use of adhesive tape for recovery of DNA from crime scene items. Journal of Forensic Sciences 55:1058-1064.

Berger CE, Buckleton J, Champod C, Evett IW, Jackson G (2011) Evidence evaluation: a response to the court of appeal judgment in R v T. Science & Justice 51:43-49.

Berger CE, Buckleton J, Champod C, Evett IW, Jackson G (2011a) Evidence evaluation: a response to the court of appeal judgment in R v T. Science & Justice 51:43-49.

Berger CE, Buckleton J, Champod C, Evett IW, Jackson G (2011b) Expressing evaluative opinions: a position statement. Science & Justice 51:1-2.

Berry DA, Evett IW, Pinchin R (1992) Statistical inference in crime investigations using deoxyribonucleic acid profiling. Applied Statistics: 499-531.

Bille TW (2014) Moving to Probabilistic Genotyping [Powerpoint slides], Bureau of Alcohol, Tobacco, Firearms and Explosives Laboratory. Accessed January 21 2019.

Bleka Ø, Benschop CC, Storvik G, Gill P (2016) A comparative study of qualitative and quantitative models used to interpret complex STR DNA profiles. Forensic Science International: Genetics 25:85-96.

Bobev K (1995) Fingerprints and factors affecting their condition. J Forensic Ident 45:176-183.

Bohnert M, Rost T, Pollak S (1998) The degree of destruction of human bodies in relation to the duration of the fire. Forensic Science International 95:11-21.

Bors D, Cummins J, Goodpaster J (2014) The Anatomy of a Pipe Bomb Explosion: Measuring the Mass and Velocity Distributions of Container Fragments. Journal of forensic sciences 59:42-51.

Børsting C, Morling N (2011) Mutations and/or close relatives? Six case work examples where 49 autosomal SNPs were used as supplementary markers. Forensic Science International: Genetics 5:236-241.

Børsting C, Morling N (2015) Next generation sequencing and its applications in forensic genetics. Forensic Science International: Genetics 18:78-89.

Bradbury NA (2017) All Cells Have a Sex: Studies of Sex Chromosome Function at the Cellular Level. In Principles of Gender-Specific Medicine (pp. 269-290). Academic Press.

Bradshaw R, Rao W, Wolstenholme R, Clench MR, Bleay S, Francese S (2012) Separation of overlapping fingermarks by matrix assisted laser desorption ionisation mass spectrometry imaging. Forensic Science International 222:318-326.

Bright J, Turkington J, Buckleton J (2010) Examination of the variability in mixed DNA profile parameters for the Identifiler™ multiplex. Forensic Science International: Genetics 4:111-114.

Brown RF, Cooper GJ, Maynard RL (1993) The ultrastructure of rat lung following acute primary blast injury. International Journal of Experimental Pathology 74:151-162.

Buckleton JS, Curran JM, Gill P (2007) Towards understanding the effect of uncertainty in the number of contributors to DNA stains. Forensic Science International: Genetics 1:20-28.

Budowle B, Bieber FR, Eisenberg AJ (2005) Forensic aspects of mass disasters: Strategic considerations for DNA-based human identification. Legal Medicine 7:230-243.

Budowle B, Chakraborty R, Scientist S, Carmody G, Monson K (2000) Source Attribution of a Forensic DNA Profile. Forensic Science Communications, 2.

Budowle B, Eisenberg AJ, Daal Av (2009) Validity of low copy number typing and applications to forensic science. Croatian Medical Journal 50:207-217.

Budowle B, Hobson DL, Smerick JB, Smith J (2001) Low copy number—consideration and caution 2001. In Twelfth International Symposium on Human Identification (pp. 9-12). Promega Corporation.

Budowle B, Shea B, Niezgoda S, Chakraborty R (2001) CODIS STR loci data from 41 sample populations. Journal of Forensic Science 46:453-489.

Butler JM (2011) Advanced Topics in Forensic DNA Typing: Methodology. Elsevier Science.

Butler JM (2014) Advanced Topics in Forensic DNA typing: interpretation. Academic Press.

Byard R, Payne-James J (2015) Encyclopedia of Forensic and Legal Medicine. Elsevier Science.

Caddy B, Taylor GR, Linacre A (2008) A review of the science of low template DNA analysis. Office of the Forensic Regulator :23-24.

Cadet J, Sage E, Douki T (2005) Ultraviolet radiation-mediated damage to cellular DNA. Mutation Research/Fundamental and Molecular Mechanisms of Mutagenesis 571:3-17.

Caliebe A, Krawczak M (2018) Match probabilities for Y-chromosomal profiles: A paradigm shift. Forensic Science International: Genetics 37:200-203.

Calloway CD, Reynolds RL, Herrin Jr GL, Anderson WW (2000) The frequency of heteroplasmy in the HVII region of mtDNA differs across tissue types and increases with age. The American Journal of Human Genetics 66:1384-1397.

Caragine T, Mikulasovich R, Tamariz J, Bajda E, Sebestyen J, Baum H, Prinz M (2009) Validation of Testing and Interpretation Protocols for Low Template DNA Samples Using AmpFl STR® Identifiler™. Croatian Medical Journal 50:250-267.

Carey S, Bursik M (2015) Chapter 32 - Volcanic Plumes. The Encyclopedia of Volcanoes (Second Edition) :571-585.

Castella V, Dimo-Simonin N, Brandt-Casadevall C, Robinson N, Saugy M, Taroni F, Mangin P (2006) Forensic identification of urine samples: a comparison between

nuclear and mitochondrial DNA markers. International Journal of Legal Medicine 120:67-72.

Castella V, Mangin P (2008) DNA profiling success and relevance of 1739 contact stains from caseworks. Forensic Science International: Genetics Supplement Series 1:405-407.

Cătălin M, Andrei A, Mitraşca O (2011) Modern methods of collection and preservation of biological evidence for human identification by DNA analysis. Abacus Diagnostics.

Champod C, Lennard CJ, Margot P, Stoilovic M (2004) Fingerprints and other ridge skin impressions. CRC Press.

Churchill JD, Novroski NMM, King JL, Seah LH, Budowle B (2017) Population and performance analyses of four major populations with Illumina's FGx Forensic Genomics System. Forensic Science International: Genetics 30:81-92.

Cina SJ, Gelven PL, Gittinger CK, Re GG, Self SE (1994) Flow cytometry: a screening tool for high molecular weight DNA. Journal of Forensic Science 39:1168-1174.

Clayton TM, Whitaker JP, Maguire CN (1995) Identification of bodies from the scene of a mass disaster using DNA amplification of short tandem repeat (STR) loci. Forensic Science International 76:7-15.

Cooper PW (1996) Explosives engineering. Wiley-VCH.

Coquoz R, Taroni F (2013) Preuve par l'ADN: la génétique au service de la justice.

Croft WM (1980) Fires involving explosions - a literature review. Fire Safety Journal 3:3-24.

Davoren J, Vanek D, Konjhodzić R, Crews J, Huffine E, Parsons TJ (2007) Highly effective DNA extraction method for nuclear short tandem repeat testing of skeletal remains from mass graves. Croatian Medical Journal 48:478.

De Boer HH, Blau S, Delabarde T, Hackman L (2018) The role of forensic anthropology in disaster victim identification (DVI): recent developments and future prospects. Forensic Sciences Research: 1-13.

De Zoete J, Sjerps M, Meester R, Cator E (2014) The combined evidential value of autosomal and Y-chromosomal DNA profiles obtained from the same sample. International Journal of Legal Medicine, 128, pp.897-904.

Diaz T, Newman B (2005) Lightning Out of Lebanon: Hezbollah Terrorists on American Soil. Random House Publishing Group.

DiMaio D, DiMaio VJM (2001) Forensic Pathology, Second Edition. CRC Press.

Dinis-Oliveira R, Vieira DN, Magalhães T (2016) Guidelines for Collection of Biological Samples for Clinical and Forensic Toxicological Analysis. Forensic Sciences Research 1:42-51.

Edson SM, Ross JP, Coble MD, Parson TJ, Barritt, SM (2004) Naming the dead-confronting the realities of the rapid identification of degraded skeletal remains. Forensic Science Review, 16(1), 63-88.

Edwards A, Civitello A, Hammond HA, Caskey CT (1991) DNA typing and genetic mapping with trimeric and tetrameric tandem repeats. American Journal of Human Genetics 49:746-756.

Einot N, Shpitzen M, Voskoboinik L, Roth J, Feine I, Gafny R (2017) Reducing the Workload: Analysis of DNA Profiling Efficiency of Case Work Items. Forensic Science Policy & Management: An International Journal 8:13-21.

Elsner HI, Lindblad EB (1989) Ultrasonic degradation of DNA. DNA 8:697-701.

Esslinger K, Siegel J, Spillane H, Stallworth S (2004) Using STR Analysis to Detect Human DNA from Exploded Pipe Bomb Devices. Journal of Forensic Science, 49, pp.JFS2003127-4.

Europol (2017) European Union Terrorism Situation and Trend Report (TESAT).

Evett IW (1996) Expert evidence and forensic misconceptions of the nature of exact science. Science & Justice 36:118-122.

Evett IW, Jackson G, Lambert JA, McCrossan S (2000) The impact of the principles of evidence interpretation on the structure and content of statements. Science & Justice 40:233-239.

Evett IW, Scranage J, Pinchin R (1993) An illustration of the advantages of efficient statistical methods for RFLP analysis in forensic science. American Journal of Human Genetics 52: 498.

Evett IW, Weir BS (1998) Interpreting DNA evidence: statistical genetics for forensic scientists. Sinauer Associates Sunderland, MA.

EWCA Crim 2439 (2010) Redacted judgement (Approved by the court for handing down) for the case R.v.T.

Fabre A, Luis A, Colotte M, Tuffet S, Bonnet J (2017) High DNA stability in white blood cells and buffy coat lysates stored at ambient temperature under anoxic and anhydrous atmosphere. PLOS ONE, 12, p.e0188547.

Farazmand A (2014) Crisis and Emergency Management: Theory and Practice, Second Edition. Taylor & Francis.

Ferreira MT, Vicente R, Navega D, Gonçalves D, Curate F, Cunha E (2014) A new forensic collection housed at the University of Coimbra, Portugal: The 21st century identified skeletal collection. Forensic Science International 245:202.e5.

Foran DR, Gehring ME, Stallworth SE (2009) The Recovery and Analysis of Mitochondrial DNA from Exploded Pipe Bombs. Journal of Forensic Sciences 54:90-94.

Foreman LA, Evett IW (2001) Statistical analyses to support forensic interpretation for a new ten-locus STR profiling system. International Journal of Legal Medicine 114:147-155.

Fox MA (1999) Initiating Explosives. In: Fox MA (ed) Glossary for the Worldwide Transportation of Dangerous Goods and Hazardous Materials Springer Berlin Heidelberg, Berlin, Heidelberg, pp 119-127.

Freese E, Cashel M (1964) Crosslinking of deoxyribonucleic acid by exposure to low pH. Biochimica et Biophysica Acta (BBA)-Specialized Section on Nucleic Acids and Related Subjects 91:67-77.

Freire-Aradas A, Fondevila M, Kriegel A-, Phillips C, Gill P, Prieto L, Schneider PM, Carracedo Á, Lareu MV (2012) A new SNP assay for identification of highly degraded human DNA. Forensic Science International: Genetics 6:341-349.

Fu G, Wang J, Yan M (2016) Anatomy of Tianjin Port fire and explosion: Process and causes. Process Safety Progress 35:216-220.

Galton F (1892) Finger Prints. Macmillan and Company.

Gashi B, Edwards MR, Sermon PA, Courtney L, Harrison D, Xu Y (2010) Measurement of 9 mm cartridge case external temperatures and its forensic application. Forensic Science International 200:21-27.

Gilbert MT, Haselkorn T, Bunce M, Sanchez JJ, Lucas SB, Jewell LD, Marck EV, Worobey M (2007) The Isolation of Nucleic Acids from Fixed, Paraffin-Embedded Tissues–Which Methods Are Useful When?. PLOS ONE, 2, p.e537.

Gill P (2001) An assessment of the utility of single nucleotide polymorphisms (SNPs) for forensic purposes. International Journal of Legal Medicine, 114, pp.204-210.

Gill P, Brinkmann B, d'Aloja E, Andersen J, Bar W, Carracedo A, Dupuy B, Eriksen B, Jangblad M, Johnsson V (1997) Considerations from the European DNA Profiling Group (EDNAP) concerning STR nomenclature. Forensic Science International 87:185-192.

Gill P, Fereday L, Morling N, Schneider PM (2006) The evolution of DNA databases—recommendations for new European STR loci. Forensic Science International 156:242-244.

Gill P, Horgan J, Lovelace J (2011) Improvised Explosive Device: The Problem of Definition. Studies in Conflict & Terrorism 34:732-748.

Gill P, Jeffreys AJ, Werrett DJ (1985) Forensic application of DNA 'fingerprints'. Nature 318:577-579.

Gill P, Werrett DJ, Budowle B, Guerrieri R (2004) Correspondence. Science & Justice 44:51-53.

Gittelson S, Berger CEH, Jackson G, Evett IW, Champod C, Robertson B, Curran JM, Taylor D, Weir BS, Coble MD, Buckleton JS (2018) A response to “Likelihood ratio as weight of evidence: A closer look” by Lund and Iyer. Forensic Science International 288:e19.

Goldfeder RL, Wall DP, Khoury MJ, Ioannidis JP, Ashley EA (2017) Human genome sequencing at the population scale: a primer on high-throughput DNA sequencing and analysis. American Journal of Epidemiology 186:1000-1009.

Gomes N (2017) Trace Detection of TATP Vapors Using a Low-Mass Thermodynamic Sensor. Open Access Master's Theses. Paper 1067.

González-Andrade F, Sánchez D (2005) DNA typing from skeletal remains following an explosion in a military fort—first experience in Ecuador (South-America). Legal Medicine 7:314-318.

Gonzalez-Nicieza C, Alvarez-Fernandez R, Alvarez-Fernandez MI, Lopez-Gayarre F, Fabian-Alvarez V (2014) Forensic analysis of a methane gas explosion in a block of apartments. Engineering Failure Analysis 36:243-252.

Goodwin W, Linacre A, Vanezis P (1999) The use of mitochondrial DNA and short tandem repeat typing in the identification of air crash victims. Electrophoresis 20:1707-1711.

Graham EA (2006) Disaster victim identification. Forensic Science, Medicine, and Pathology 2:203-207.

Graham EAM, Barlow V (2013) Report on DNA analysis carried out in relation to the ‘Blazing car murder’ 5th / 6th November 1930, Northamptonshire.

Green PJ (2005) GRAPPA: R Functions for Probability Propagation 287.

Green RE, Krause J, Briggs AW, Maricic T, Stenzel U, Kircher M, Patterson N, Pääbo S (2010) A draft sequence of the Neandertal genome. Science 328:710-722.

Greenhalgh MJ, Allard JE (1992) Experiences with a Computerised Database of DNA Profiles in Forensic Casework:298-300.

Groen WJM, Márquez-Grant N, Janaway R (2015) Forensic Archaeology: A Global Perspective. John Wiley & Sons.

Haglund WD, Sorg MH (1997) Forensic taphonomy. The post-mortem fate of human remains. (pp. 201-222). Boca Raton, FL: CRC press.

Hall RD (2001) The forensic entomologist as expert witness. Forensic entomology. The Utility of Arthropods in Legal Investigations: 379-400.

Harbison SA, Hamilton JF, Walsh SJ (2001) The New Zealand DNA databank: its development and significance as a crime solving tool. Science & Justice 41:33-37.

Hathaway O, Francis A, Haviland A, Kethireddy SR, Yamamoto A (2019) International Human Rights and Humanitarian Law. American Journal of International Law, Volume 113.

Hawk JR, Wander JD, Dinan RJ, Trawinski E (2004) Detonation Blast Pressures of TNT and C4 at-100 degrees C. Applied Research Associates Inc Tyndallafb FL.

Hedman J, Ågren J, Ansell R (2015) Crime scene DNA sampling by wet-vacuum applying M-Vac. Forensic Science International: Genetics Supplement Series, 5, e89-e90.

Helgason A, Siguroardóttir S, Gulcher JR, Ward R, Stefánsson K (2000) mtDNA and the origin of the Icelanders: deciphering signals of recent population history. American Journal of Human Genetics 66:999-1016.

Heramb RM, McCord BR (2002) Manufacture of Smokeless Powders and their Forensic Analysis: A Brief Review, Forensic Science Communications, 4.

Higgins D, Austin JJ (2013) Teeth as a source of DNA for forensic identification of human remains: a review. Science & Justice 53:433-441.

Hinman EE, Hammond DJ (1997) Lessons from the Oklahoma City bombing: Defensive design techniques. American Society of Civil Engineers.

Hoffmann SG, Stallworth SE, Foran DR (2012) Investigative studies into the recovery of DNA from improvised explosive device containers. Journal of Forensic Sciences 57:602-609.

Hofreiter M, Serre D, Poinar HN, Kuch M, Pääbo S (2001) ancient DNA. Nature Reviews Genetics 2:353.

Holland MM, Bonds RM, Holland CA, McElhoe JA (2019) Recovery of mtDNA from unfired metallic ammunition components with an assessment of sequence profile quality and DNA damage through MPS analysis. Forensic Science International: Genetics 39:86-96.

Holland MM, Cave CA, Holland CA, Bille TW (2003) Development of a quality, high throughput DNA analysis procedure for skeletal samples to assist with the identification of victims from the World Trade Center attacks. Croatian Medical Journal 44:264-272.

Holland MM, Pack ED, McElhoe JA (2017) Evaluation of GeneMarker® HTS for improved alignment of mtDNA MPS data, haplotype determination, and heteroplasmy assessment. Forensic Science International: Genetics 28:90-98.

Holland MM, Parsons TJ (1999) Mitochondrial DNA sequence analysis-validation and use for forensic casework. Forensic Science Review 11:21-50.

Holt A, Wootton SC, Mulero JJ, Brzoska PM, Langit E, Green RL (2016) Developmental validation of the Quantifiler® HP and Trio Kits for human DNA quantification in forensic samples. Forensic Science International: Genetics 21:145-157.

Hoss M, Jaruga P, Zastawny TH, Dizdaroglu M, Paabo S (1996) DNA damage and DNA sequence retrieval from ancient tissues. Nucleic Acids Research 24:1304-1307.

Houck MM (2015) Professional Issues in Forensic Science. Elsevier Science.

Hronešová J (2018) Bones and Recognition: Compensating Families of Missing Persons in Post-War Bosnia and Herzegovina. Journal of Peacebuilding & Development 13:47-60.

Hummel S, Herrmann B (1994) General aspects of sample preparation Ancient DNA Springer, pp 59-68.

Imaizumi K, Taniguchi K, Ogawa Y (2014) DNA survival and physical and histological properties of heat-induced alterations in burnt bones. International Journal of Legal Medicine 128:439-446.

INTERPOL (2018) Disaster Victim Identification Guide. p.18

Irizarry R, Love M (2014) Biological Versus Technical Variability. https://genomicsclass.github.io/book/pages/biological_versus_technical_var.html. Accessed September 30, 2019.

Ivanov PL, Wadhams MJ, Roby RK, Holland MM, Weedn VW, Parsons TJ (1996) Mitochondrial DNA sequence heteroplasmy in the Grand Duke of Russia Georgij Romanov establishes the authenticity of the remains of Tsar Nicholas II. Nature Genetics 12:417.

Jamieson A (2004) A rational approach to the principles and practice of crime scene investigation: I. Principles. Science & Justice 44:3-7.

Jeffreys AJ, Wilson V, Thein SL (1985) Individual-specific fingerprints™ of human DNA. Nature 316:76.

Jobling MA, Gill P (2004) Encoded evidence: DNA in forensic analysis. Nature Reviews Genetics 5:739-751.

Jobling MA, Hollox EJ, Hurles ME, Kivisild T, Tyler-Smith C: Human Evolutionary Genetics, 2nd edn. New York and London: Garland Science; 2014.

Keyes DC (2005) Medical response to terrorism: preparedness and clinical practice. Lippincott Williams & Wilkins.

Khrapko K, Coller HA, André PC, Li X, Hanekamp JS, Thilly WG (1997) Mitochondrial mutational spectra in human cells and tissues. Proceedings of the National Academy of Sciences 94:13798-13803.

Kimpton CP, Gill P, Walton A, Urquhart A, Millican ES, Adams M (1993) Automated DNA profiling employing multiplex amplification of short tandem repeat loci. Genome Research 3:13-22.

Kind SS (1987) The scientific investigation of crime. Forensic Science Services.

King TE, Fortes GG, Balaresque P, Thomas MG, Balding D, Delser PM, Neumann R, Parson W, Knapp M, Walsh S (2014) Identification of the remains of King Richard III. Nature communications 5:5631.

Kirk PL (1963) The ontogeny of criminalistics. The Journal of Criminal Law, Criminology, and Police Science :235-238.

Klein A, Krebs O, Gehl A, Morgner J, Reeger L, Augustin C, Edler C (2018) Detection of blood and DNA traces after thermal exposure. International Journal of Legal Medicine, 132(4), 1025-1033.

Kloosterman AD, Kersbergen P (2003) Efficacy and limits of genotyping low copy number DNA samples by multiplex PCR of STR loci 1239:795-798.

Landsteiner K (1900) Zur Kenntnis der antifermentativen, lytischen und agglutinierenden Wirkungen des Blutserums und der Lymphe. Zentralblatt für Bakteriologie 27:357-362.

Lanes D (2016) Statistical methods for match probabilities with applications to Y chromosome data. Master's Thesis. Norwegian University of Life Sciences, Ås.

Larkin B, Iaschi S, Dadour I, Tay GK (2010) Using accumulated degree-days to estimate postmortem interval from the DNA yield of porcine skeletal muscle. Forensic Sci Med Pathol 6:83-92.

Lee JHS (2008) The Detonation Phenomenon. Cambridge University Press, Cambridge.

Li G, Yang H-, Yuan C-, Eckhoff RK (2016) A catastrophic aluminium-alloy dust explosion in China. Journal of Loss Prevention in the Process Industries 39:121-130.

Lindahl T (1993) Instability and decay of the primary structure of DNA. Nature 362:709-715.

Lindahl T, Andersson A (1972) Rate of chain breakage at apurinic sites in double-stranded deoxyribonucleic acid. Biochemistry 11:3618-3623.

Lindahl T, Nyberg B (1972) Rate of depurination of native deoxyribonucleic acid. Biochemistry (NY) 11:3610-3618.

Locard E (1920) L'enquête criminelle et les méthodes scientifiques. Flammarion.

Lowe A, Murray C, Whitaker J, Tully G, Gill P (2002) The propensity of individuals to deposit DNA and secondary transfer of low level DNA from individuals to inert surfaces. Forensic Science International 129:25-34.

Lund SP, Iyer H (2017) Likelihood Ratio as Weight of Forensic Evidence:

A Closer Look. Journal of Research of National Institute of Standards and Technology 122.

M Edson S, P Ross J, Coble M, Parsons T, M Barritt S (2004) Naming the Dead - Confronting the Realities of Rapid Identification of Degraded Skeletal Remains. Forensic Science Review, 16, 63-88.

Maciejewska A, Jakubowska J, Pawłowski R (2012) Whole genome amplification of degraded and nondegraded DNA for forensic purposes. International Journal of Legal Medicine 127:309-319.

Macko V, Straka L, Krajcovic J (2009) C-13 explosion victims – peculiarities of autopsy findings. Legal Medicine 11:S509.

Maloney MS, Housman D, Gardner RM (2014) Crime Scene Investigation Procedural Guide. Taylor & Francis.

Mann RW, Bass WM, Meadows L (1990) Time since death and decomposition of the human body: variables and observations in case and experimental field studies. Journal of Forensic Science 35:103-111.

Marrone, A. (2009) The biochemical reactions of dry state DNA. University of Central Florida. Doctoral Dissertation (Open Access).

Martin J (2008) Incendies et explosions d'atmosphère. PPUR Presses Polytechniques.

Martin PD, Schmitter H, Schneider PM (2001) A brief history of the formation of DNA databases in forensic science within Europe. Forensic Science International 119:225-231.

Matisoo-Smith E, Horsburgh KA (2016) DNA for Archaeologists. Taylor & Francis.

McKenzie, S B, Williams, J L, Landis-Piwowar, K (2004). Clinical laboratory hematology (Vol. 1). Pearson/Prentice Hall.

McNally L, Shaler R, Baird M, Balazs I, Forest P, Kobilinsky L (1989) Evaluation of Deoxyribonucleic Acid (DNA) Isolated from Human Bloodstains Exposed to Ultraviolet Light, Heat, Humidity, and Soil Contamination. Journal of Forensic Science, 34, 1059-1069.

McNevin D, Wilson-Wilde L, Robertson J, Kyd J, Lennard C (2005) Short tandem repeat (STR) genotyping of keratinised hair: Part 1. Review of current status and knowledge gaps. Forensic Science International 153:237-246.

Meyer HJ (2003) The Kaprun cable car fire disaster—aspects of forensic organisation following a mass fatality with 155 victims. Forensic Science International 138:1-7.

Montpetit S, O'Donnell P (2015) An optimized procedure for obtaining DNA from fired and unfired ammunition. Forensic Science International: Genetics 17:70-74.

Moody GH, Busuttil A (1994) Identification in the Lockerbie Air Disaster. The American Journal of Forensic Medicine and Pathology, 15, 63-69.

Morrison G (2012) The Likelihood-Ratio Framework and Forensic Evidence in Court: A Response to R v T. The International Journal of Evidence & Proof, 16, 1-29.

Morrison G (2017) A Response to: 'NIST Experts Urge Caution in Use of Courtroom Evidence Presentation Method'. arXiv preprint arXiv:1710.05878.

Mortera J, Dawid AP, Lauritzen SL (2003) Probabilistic expert systems for DNA mixture profiling. Theoretical Population Biology 63:191-205.

Nathans D, Smith HO (1975) Restriction endonucleases in the analysis and restructuring of DNA molecules. Annual Review of Biochemistry 44:273-293.

National Consortium for the Study of Terrorism and Responses to Terrorism, (START) (2018) Global Terrorism Database. Retrieved from https://www.start.umd.edu/gtd.

National Research Council (1998) Black and Smokeless Powders: Technologies for Finding Bombs and the Bomb Makers. The National Academies Press, Washington, DC.

National Research Council (2009) Strengthening forensic science in the United States: a path forward. National Academies Press.

Nelson J (2009) Repair of damaged DNA for forensic analysis. BiblioGov.

Nelson J, National Institute of Justice (2015) Repair of Damaged DNA for Forensic Analysis - Scholar's Choice Edition.

Neumann C, Evett IW, Skerrett JE, Mateos-Garcia I (2012) Quantitative assessment of evidential weight for a fingerprint comparison. Part II: A generalisation to take account of the general pattern. Forensic Science International 214:195-199.

Nichols RA, Balding DJ (1991) Effects of population structure on DNA fingerprint analysis in forensic science. Heredity 66:297.

Office for National Statistics (2017a) The nature of violent crime in England and Wales: year ending March 2017. London: Office for National Statistics.

Office for National Statistics (2017b) Sexual offences in England and Wales: year ending March 2017. London: Office for National Statistics.

Olaisen B, Stenersen M, Mevag B (1997) Identification by DNA analysis of the victims of the August 1996 Spitsbergen civil aircraft disaster. Nature Genetics 15:402.

Olsen RD (1978) Scott's fingerprint mechanics. Thomas (pp. 289-290).

Oran ES, Williams FA (2012) The physics, chemistry and dynamics of explosions. Philosophical Transactions of the Royal Society A: Mathematical, Physical and Engineering Sciences 370:534-543.

Oxley JC, Smith JL, Bernier ET, Sandstrom F, Weiss GG, Recht GW, Schatzer D (2018) Characterizing the Performance of Pipe Bombs. Journal of forensic sciences 63:86-101.

Pääbo S (1989) Ancient DNA: extraction, characterization, molecular cloning, and enzymatic amplification. Proceedings of the National Academy of Sciences of the United States of America 86:1939.

Pang B, Cheung B (2007) Double swab technique for collecting touched evidence. Legal Medicine 9:181-184.

Parsons TJ, Muniec DS, Sullivan K, Woodyatt N, Alliston-Greiner R, Wilson MR, Berry DL, Holland KA, Weedn VW, Gill P, Holland MM (1997) A high observed substitution rate in the human mitochondrial DNA control region. Nature Genetics 15:363.

Parsons TJ, Weedn VW (1997) Preservation and recovery of DNA in postmortem specimens and trace samples. Forensic taphonomy: the postmortem fate of human remains: 109-138.

Pfeiffer H, Hühne J, Ortmann C, Waterkamp K, Brinkmann B (1999) Mitochondrial DNA typing from human axillary, pubic and head hair shafts–success rates and sequence comparisons. International Journal of Legal Medicine 112:287-290.

Phetpeng S, Kitpipit T, Thanakiatkrai P (2015) Systematic study for DNA recovery and profiling from common IED substrates: from laboratory to casework. Forensic Science International: Genetics 17:53-60.

Phillips C, Fondevila M, García-Magariños M, Rodriguez A, Salas A, Carracedo Á, Lareu MV (2008) Resolving relationship tests that show ambiguous STR results using autosomal SNPs as supplementary markers. Forensic Science International: Genetics 2:198-204.

Phillips C, Lareu V, Salas A, Carracedo A (2004) Nonbinary single-nucleotide polymorphism markers 1261:27-29.

Polski J, Smith R, Garrett R (2010) The report of the international association for identification. Standardization II Committee.

President's Council of Advisors on Science and Technology, (US) (2016) Report to the President, Forensic Science in Criminal Courts: Ensuring Scientific Validity of Feature-comparison Methods. Executive Office of the President of the United States, President's Council of Advisors on Science and Technology.

Prieto L, Alonso A, Alves C, Crespillo M, Montesino M, Picornell A, Brehm A, Ramírez JL, Whittle MR, Salas A (2008) 2006 GEP-ISFG collaborative exercise on mtDNA: reflections about interpretation, artefacts, and DNA mixtures. Forensic Science International: Genetics 2:126-133.

Prinz M, Sansone M (2001) Y chromosome-specific short tandem repeats in forensic casework. Croatian Medical Journal 42:288-291.

Purps J, Siegert S, Willuweit S, Nagy M, Alves C, Salazar R, Angustia SM, Santos LH, Anslinger K, Bayer B (2014) A global analysis of Y-chromosomal haplotype diversity for 23 STR loci. Forensic Science International: Genetics 12:12-23.

Qalaat Al Mudiq (2018) Syria: more IEDs recently dismantled in Greater Idlib [Twitter post]. https://twitter.com/QalaatAlMudiq/status/1005411561039679489. Accessed January 21, 2019.

R Core Team (2013) R: A language and environment for statistical computing. R Foundation for Statistical Computing, Vienna, Austria.

R v Hoey (2007) Judgement, The Crown Court Sitting in Northern Ireland 49:20.

Rampant S (2017) The effects of a detonation explosion on the recovery of DNA from fragments of an improvised explosive device. Dissertation/Thesis. Murdoch University.

Rathbun MM, McElhoe JA, Parson W, Holland MM (2017) Considering DNA damage when interpreting mtDNA heteroplasmy in deep sequencing data. Forensic Science International: Genetics 26:1-11.

Raymond JJ, van Oorschot RA, Gunn PR, Walsh SJ, Roux C (2009) Trace evidence characteristics of DNA: a preliminary investigation of the persistence of DNA at crime scenes. Forensic Science International: Genetics 4:26-33.

Rehm HL, Bale SJ, Bayrak-Toydemir P, Berg JS, Brown KK, Deignan JL, Friez MJ, Funke BH, Hegde MR, Lyon E (2013) ACMG clinical laboratory standards for next-generation sequencing. Genetics in Medicine 15:733-747.

Robertson B, Vignaux GA, Berger CEH (2016) Interpreting Evidence: Evaluating Forensic Science in the Courtroom. Wiley.

Robins JH, Matisoo-Smith E, Furey L (2001) Hit or miss? Factors affecting DNA preservation in Pacific archaeological material 5:295-305.

Roewer L, Kayser M, de Knijff P, Anslinger K, Betz A, Caglia A, Corach D, Füredi S, Henke L, Hidding M (2000) A new method for the evaluation of matches in non-recombining genomes: application to Y-chromosomal short tandem repeat (STR) haplotypes in European males. Forensic Science International 114:31-43.

Romolo FS, Aromatario M, Bottoni E, Cappelletti S, Fiore PA, Ciallella C (2014) Accidental death involving professional fireworks. Forensic Science International 234:e9.

Rosen J (2010) The Afghanistan War Logs Released by Wikileaks, the World's First Stateless News Organization. PressThink: Ghost of Democracy in the Media Machine.

Şakalar E, Abasiyanik MF, Bektik E, Tayyrov A (2012) Effect of Heat Processing on DNA Quantification of Meat Species. Journal of Food Science 77:N44.

Salas A, Bandelt H, Macaulay V, Richards MB (2007) Phylogeographic investigations: the role of trees in forensic genetics. Forensic Science International 168:1-13.

Sanchez JJ, Phillips C, Børsting C, Balogh K, Bogus M, Fondevila M, Harrison CD, Musgrave-Brown E, Salas A, Syndercombe-Court D (2006) A multiplex assay with 52

single nucleotide polymorphisms for human identification. Electrophoresis 27:1713-1724.

Sato M, Sato K (2012) Maternal inheritance of mitochondrial DNA: Degradation of paternal mitochondria by allogeneic organelle autophagy, allophagy. Autophagy 8:424-425.

Schiffner LA, Bajda EJ, Prinz M, Sebestyen J, Shaler R, Caragine TA (2005) Optimization of a simple, automatable extraction method to recover sufficient DNA from low copy number DNA samples for generation of short tandem repeat profiles. Croatian Medical Journal 46:578-586.

Schneider PM, Martin PD (2001) Criminal DNA databases: the European situation. Forensic Science International 119:232-238.

Schultz E, Wintenberger E, Shepherd J (1999) Investigation of deflagration to detonation transition for application to pulse detonation engine ignition systems:175-202.

Schyma C, Hagemeier L, Madea B (2011) Suicide by head explosion: unusual blast wave injuries to the cardiovascular system. International Journal of Legal Medicine 125:473-478.

Scientific Working Group on DNA Analysis Methods (SWGDAM) (2015) Interpretation Guidelines for Mitochondrial DNA Analysis by Forensic DNA Testing Laboratories. http://www.swgdam.org/publications/. Accessed October 12, 2019.

Sewell J, Quinones I, Ames C, Multaney B, Curtis S, Seeboruth H, Moore S, Daniel B (2008) Recovery of DNA and fingerprints from touched documents. Forensic Science International: Genetics 2:281-285.

Shen Z, Qu W, Wang W, Lu Y, Wu Y, Li Z, Hang X, Wang X, Zhao D, Zhang C (2010) MPprimer: a program for reliable multiplex PCR primer design. BioMed Central Bioinformatics 11:143.

Shi S, Cote RJ, Wu L, Liu C, Datar R, Shi Y, Liu D, Lim H, Taylor CR (2002) DNA extraction from archival formalin-fixed, paraffin-embedded tissue sections based on the antigen retrieval principle: heating under the influence of pH. Journal of Histochemistry & Cytochemistry 50:1005-1011.

Simpson R, Fried L, Ree F, Reaugh J (1999) Unraveling the Mystery of Detonation. https://str.llnl.gov/str/Simpson99.html. Accessed April 24, 2018.

Smith CI, Chamberlain AT, Riley MS, Stringer C, Collins MJ (2003) The thermal history of human fossils and the likelihood of successful DNA amplification. Journal of Human Evolution 45:203-217.

Soares P, Ermini L, Thomson N, Mormina M, Rito T, Röhl A, Salas A, Oppenheimer S, Macaulay V, Richards MB (2009) Correcting for purifying selection: an improved human mitochondrial molecular clock. American Journal of Human Genetics 84:740-759.

Sobrino B, Brión M, Carracedo A (2005) SNPs in forensic genetics: a review on SNP typing methodologies. Forensic Science International 154:181-194.

Special Tribunal for Lebanon (2013) The Prosecutor v. Salim Jamil Ayyash, Salim Jamil Ayyash, Mustafa Amine Badreddine, Hussein Hassan Oneissi, Assad Hassan Sabra :43-45.

Spitsen M, Argaman U, Chaikovsky A, Shelef R (2004) The Burned Palm. Journal of Forensic Identification 54:321.

Sudoyo H, Widodo PT, Suryadi H, Lie YS, Safari D, Widjajanto A, Kadarmo DA, Hidayat S, Marzuki S (2008) DNA analysis in perpetrator identification of terrorism-related disaster: Suicide bombing of the Australian Embassy in Jakarta 2004. Forensic Science International: Genetics 2:231-237.

Sullivan G, Edmondson C (2008) Heat and temperature. Continuing Education in Anaesthesia Critical Care & Pain 8:104-107.

Sweet D, Hildebrand D (1999) Saliva from cheese bite yields DNA profile of burglar: a case report. International Journal of Legal Medicine 112:201-203.

Taroni F, Champod C, Margot PA (1999) Forerunners of Bayesianism in early forensic science. Journal of Forensic Identification 49:285.

Tasker E, LaRue B, Beherec C, Gangitano D, Hughes-Stamm S (2017) Analysis of DNA from post-blast pipe bomb fragments for identification and determination of ancestry. Forensic Science International: Genetics 28:195-202.

Technical Working Group on Crime Scene Investigation, United States of America (2012) Crime Scene Investigation: A Guide for Law Enforcement.

Templeton JE, Linacre A (2014) DNA profiles from fingermarks. BioTechniques: the International Journal of Life Science Methods 57:259-266.

Thanakiatkrai P, Phetpeng S, Sotthibandhu S, Asawutmangkul W, Piwpankaew Y, Foong JE, Koo J, Kitpipit T (2017) Performance comparison of MiSeq forensic genomics system and STR-CE using control and mock IED samples. Forensic Science International: Genetics Supplement Series 6:e321.

The European Network of Forensic Science Institutes (ENFSI) (2017) Best Practice Manual for the Investigation of Fire Scenes:52-53.

Thermo Fisher Scientific Inc (2016) Application Note: Comparison of Quant-iT and Qubit DNA quantitation assays for accuracy and precision. thermofisher.com/qubit.

Thompson JM, Ewing MM, Frank WE, Pogemiller JJ, Nolde CA, Koehler DJ, Shaffer AM, Rabbach DR, Fulmer PM, Sprecher CJ (2013) Developmental validation of the PowerPlex® Y23 System: a single multiplex Y-STR analysis system for casework and database samples. Forensic Science International: Genetics 7:240-250.

Tontarski KL, Hoskins KA, Watkins TG, Brun-Conti L, Michaud AL (2009) Chemical enhancement techniques of bloodstain patterns and DNA recovery after fire exposure. Journal of Forensic Sciences 54:37-48.

Tsuchimochi T, Iwasa M, Maeno Y, Koyama H, Inoue H, Isobe I, Matoba R, Yokoi M, Nagao M (2002) Chelating resin-based extraction of DNA from dental pulp and sex determination from incinerated teeth with Y-chromosomal alphoid repeat and short tandem repeats. The American journal of forensic medicine and pathology 23:268-271.

Tully G, Bär W, Brinkmann B, Carracedo A, Gill P, Morling N, Parson W, Schneider P (2001) Considerations by the European DNA profiling (EDNAP) group on the working practices, nomenclature and interpretation of mitochondrial DNA profiles. Forensic Science International 124:83-91.

Tully G, Wetton J (2014) Interpretation of Mitochondrial DNA Evidence. Wiley Encyclopedia of Forensic Science, 1-10.

United States Bomb Data Center, (USBDC) (2016) Explosives Incident Report (EIR).

Urquhart A, Kimpton CP, Downes TJ, Gill P (1994) Variation in short tandem repeat sequences—a survey of twelve microsatellite loci for use as forensic identification markers. International Journal of Legal Medicine 107:13-20.

Van der Voort, M. M., van Wees, R. M. M., Brouwer SD, van der Jagt-Deutekom, M. J., Verreault J (2015) Forensic analysis of explosions: Inverse calculation of the charge mass. Forensic Science International 252:11-21.

Van Oorschot RA, Ballantyne KN, Mitchell RJ (2010) Forensic trace DNA: a review. Investigative Genetics 1:14.

Vergnaud G, Denoeud F (2000) Minisatellites: mutability and genome architecture. Genome Research 10:899-907.

Verwiel AM, Van Der Voort K (2014) Special Tribunal for Lebanon Blog. https://lebanontribunal.blogspot.com/2014/07/first-week-of-july-experts-in-human.html. Accessed January 22, 2019.

Votrubova J, Ambers A, Budowle B, Vanek D (2017) Comparison of standard capillary electrophoresis based genotyping method and ForenSeq DNA Signature Prep kit (Illumina) on a set of challenging samples. Forensic Science International: Genetics Supplement Series 6:e142.

Vuorio A, Laukkala T, Pooshan N, Budowle B, Eyre A, Sajantila A (2015) On doctors' accountability and flight deck safety. Croatian Medical Journal 56:385.

Walsh B, Redd AJ, Hammer MF (2008) Joint match probabilities for Y chromosomal and autosomal markers. Forensic Science International 174:234-238.

Warshauer DH, King JL, Budowle B (2015) STRait Razor v2. 0: the improved STR allele identification tool– Razor. Forensic Science International: Genetics 14:182-186.

Weir BS (1992) Independence of VNTR alleles defined as fixed bins. Genetics 130:873-887.

Weir BS, Cockerham CC (1984) Estimating F-statistics for the analysis of population structure. Evolution 38:1358-1370.

Weir BS, Triggs CM, Starling L, Stowell LI, Walsh K, Buckleton J (1997) Interpreting DNA mixtures. Journal of Forensic Science 42:213-222.

West N (2017) Encyclopedia of Political Assassinations. Rowman & Littlefield Publishers.

Wetton JH, Lee-Edghill J, Archer E, Tucker VC, Hopwood AJ, Whitaker J, Tully G (2011) Analysis and interpretation of mixed profiles generated by 34 cycle SGM Plus® amplification. Forensic Science International: Genetics 5:376-380.

Weyermann C, Ribaux O (2012) Situating forensic traces in time. Science & Justice 52:68-75.

Whitaker JP, Clayton TM, Urquhart AJ, Millican ES, Downes TJ, Kimpton CP, Gill P (1995) Short tandem repeat typing of bodies from a mass disaster: high success rate and characteristic amplification patterns in highly degraded samples. BioTechniques: the International Journal of Life Science Methods 18:670-677.

Wightman JM, Gladish SL (2001) Explosions and blast injuries. Annals of Emergency Medicine 37:664-678.

Willuweit S, Roewer L, International Forensic Y Chromosome User Group (2007) Y chromosome haplotype reference database (YHRD): update. Forensic Science International: Genetics 1:83-87.

Wilson IG (1997) Inhibition and facilitation of nucleic acid amplification. Applied and Environmental Microbiology 63:3741-3751.

Wilson MR, Polanskey D, Replogle J, Dizinno JA, Budowle B (1997) A family exhibiting heteroplasmy in the human mitochondrial DNA control region reveals both somatic mosaicism and pronounced segregation of mitotypes. Human Genetics 100:167-171.

Wittwer CT (2009) High-resolution DNA melting analysis: advancements and limitations. Human Mutation 30:857-859.

Xavier C, Parson W (2017) Evaluation of the Illumina ForenSeq™ DNA Signature Prep Kit – MPS forensic application for the MiSeq FGx™ benchtop sequencer. Forensic Science International: Genetics 28:188-194.

Yang DY, Eng B, Waye JS, Dudar JC, Saunders SR (1998) Improved DNA extraction from ancient bones using silica-based spin columns. American Journal of Physical Anthropology: The Official Publication of the American Association of Physical Anthropologists 105:539-543.

Zeng X, King JL, Stoljarova M, Warshauer DH, LaRue BL, Sajantila A, Patel J, Storts DR, Budowle B (2015) High sensitivity multiplex short tandem repeat loci analyses with massively parallel sequencing. Forensic Science International: Genetics 16:38-47.

Web Resources

thermofisher.com/order/catalog/product/4457889#/4457889. Accessed September 30, 2019.

8 Appendix

8.1 Implications of Heat Induced Dropouts

AmpFLSTR NGMSElect®- ABI 3130xl Genetic Analyzer				
Samples	Homozygous	Heterozygous	False homozygosity	Locus dropout
P02_4 °C (a)	0	17	0	0
P02_4 °C (b)	0	17	0	0
P02_140 °C (a)	0	17	0	0
P02_140 °C (b)	0	17	0	0
P02_180 °C (a)	0	3	4	10
P02_180 °C (b)	0	1	2	14
P09_4 °C (a)	4	13	0	0
P09_4 °C (b)	4	13	0	0
P09_140 °C (a)	4	13	0	0
P09_140 °C (b)	4	13	0	0
P09_180 °C (a)	4	12	1	0
P09_180 °C (b)	3	11	1	2

Table 8.1.1 - 3 per locus between treated and control stains analysed by NGMSElect® (autosomal STRs).

ForenSeq® DNA Signature Prep - Autosomal STR				
Samples	Homozygous	Heterozygous	False homozygosity	Locus dropout
P2 4 °C	1	27	0	0
P2a 180 °C	1	2	8	17
P2b 180 °C	0	3	6	19
P9 4 °C	6	22	0	0
P9a 180 °C	6	20	1	1
P9b 180 °C	3	11	4	10
P22 4 °C	7	21	0	0
P22a 180 °C	4	3	4	17
P22b 180 °C	1	1	2	24
P22_Touch	5	7	10	6

Table 8.1.2 - Profile characteristics per locus between treated and control stains analysed by ForenSeq® (autosomal STRs).

ForenSeq® DNA Signature Prep - Identity Single Nucleotide Polymorphism (SNPs)				
Samples	Homozygous	Heterozygous	False homozygosity	Locus dropout
P2 4 °C	50	39	0	5
P2a 180 °C	12	3	7	72
P2b 180 °C	6	0	1	87
P9 4 °C	48	44	0	2
P9a 180 °C	42	42	2	8
P9b 180 °C	33	32	6	23
P22 4 °C	41	17	1	35
P22a 180 °C	3	0	1	90
P22b 180 °C	8	4	3	79
P22_Touch	9	0	4	81

Table 8.1.3 - Profile characteristics per locus between treated and control stains analysed by ForenSeq® (iSNPs).

8.2 Electropherograms Examples

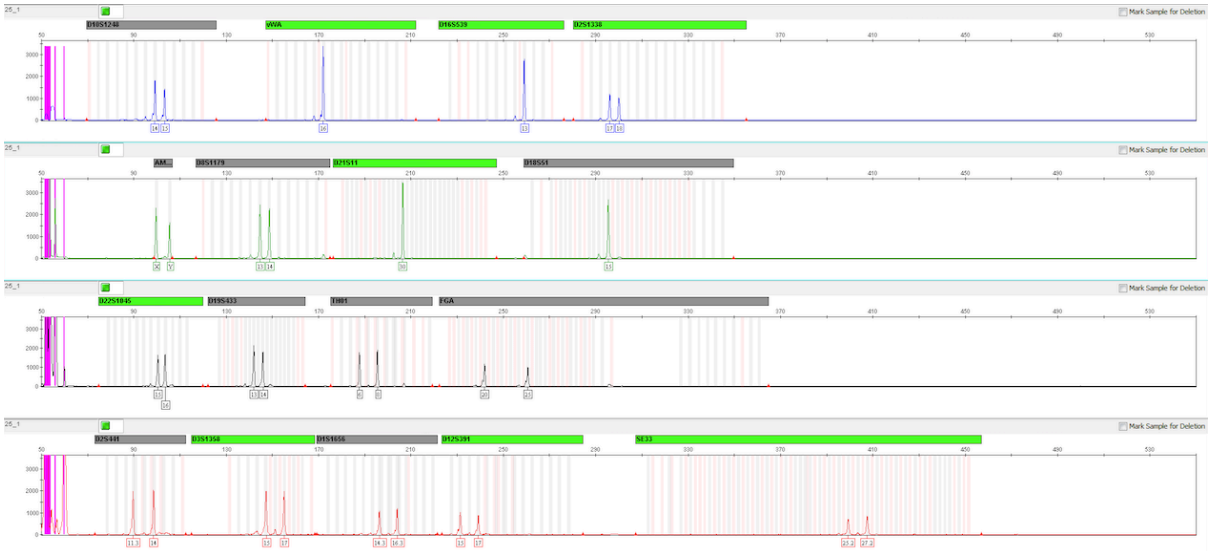

Figure 8.1 NGMSElect® electropherogram for a blood stain at 4 °C.

Full profile of a good quality with all 17 markers successfully typed.

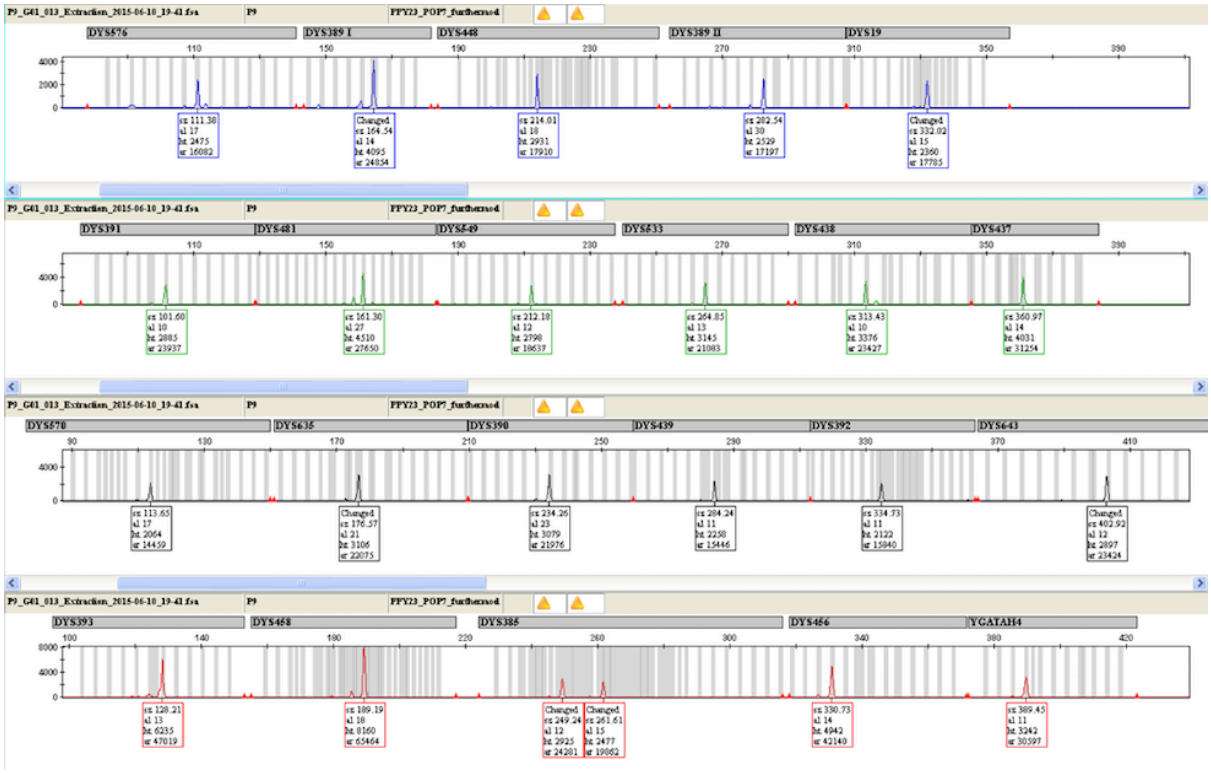

Figure 8.2 PowerPlex® Y23 electropherogram for a blood stain at 4 °C.

Full profile of a good quality with all 22 markers successfully typed.

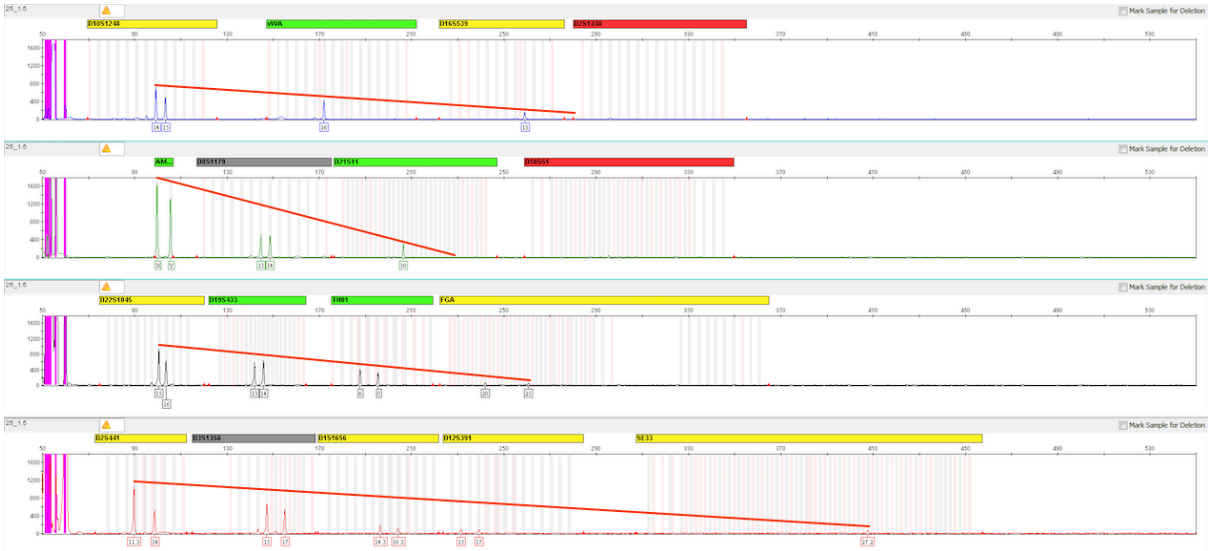

Figure 8.3 NGMSElect® electropherogram for a blood stain at 180 °C.

Partial profile with a ski-slope pattern as the largest loci tend to drop out.

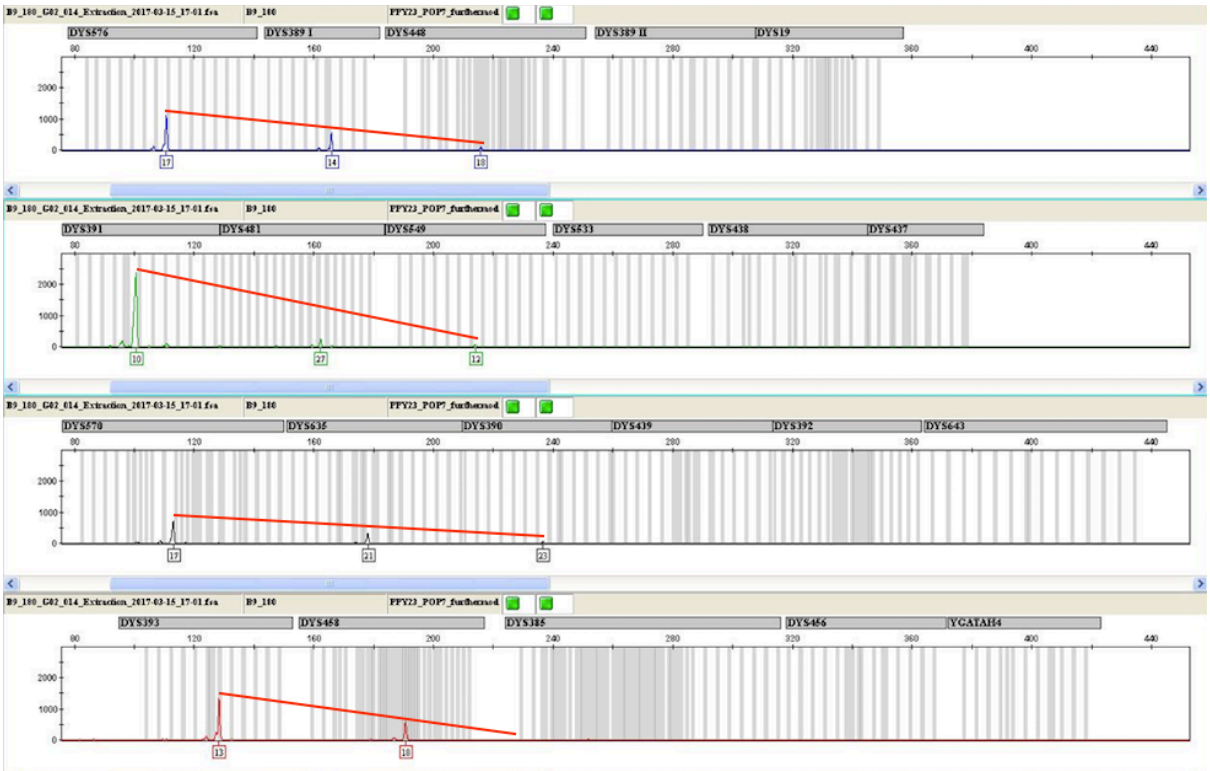

Figure 8.4 PowerPlex® Y23 Electropherogram for a blood stain at 180 °C.

Partial profile with a ski-slope pattern as the largest loci tend to drop out.

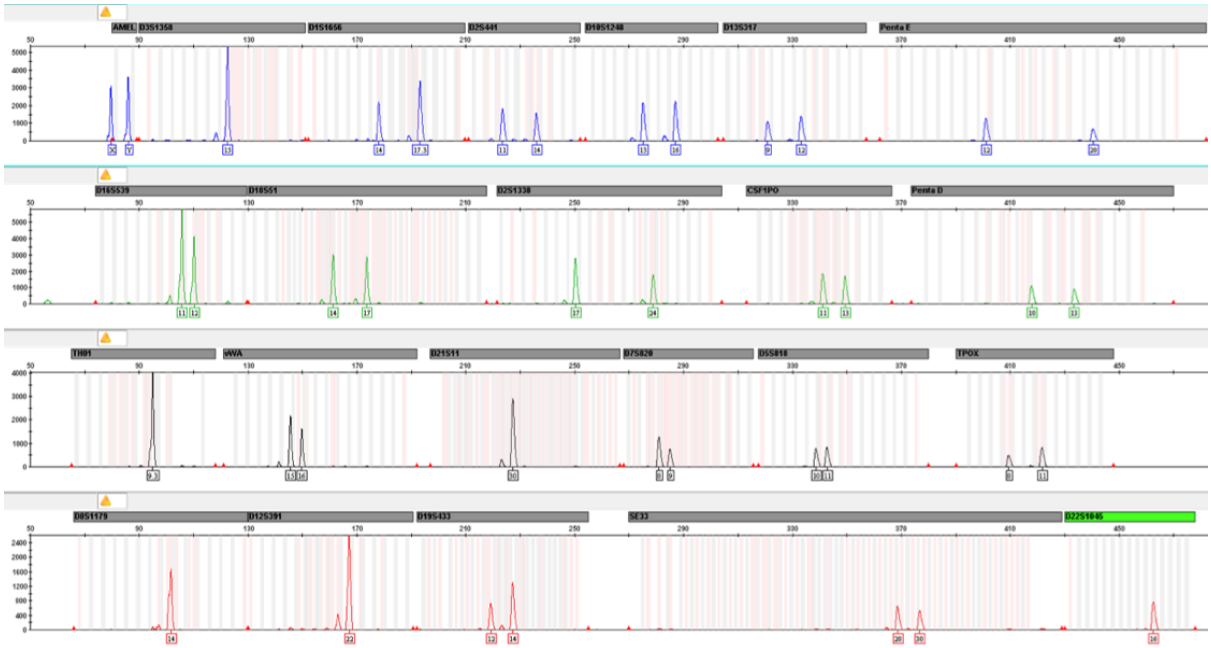

Figure 8.5 PowerPlex® Fusion 6C Electropherogram for a blood stain exposed to a C4 explosion.

Full profile of good quality with all 23 markers successfully typed.

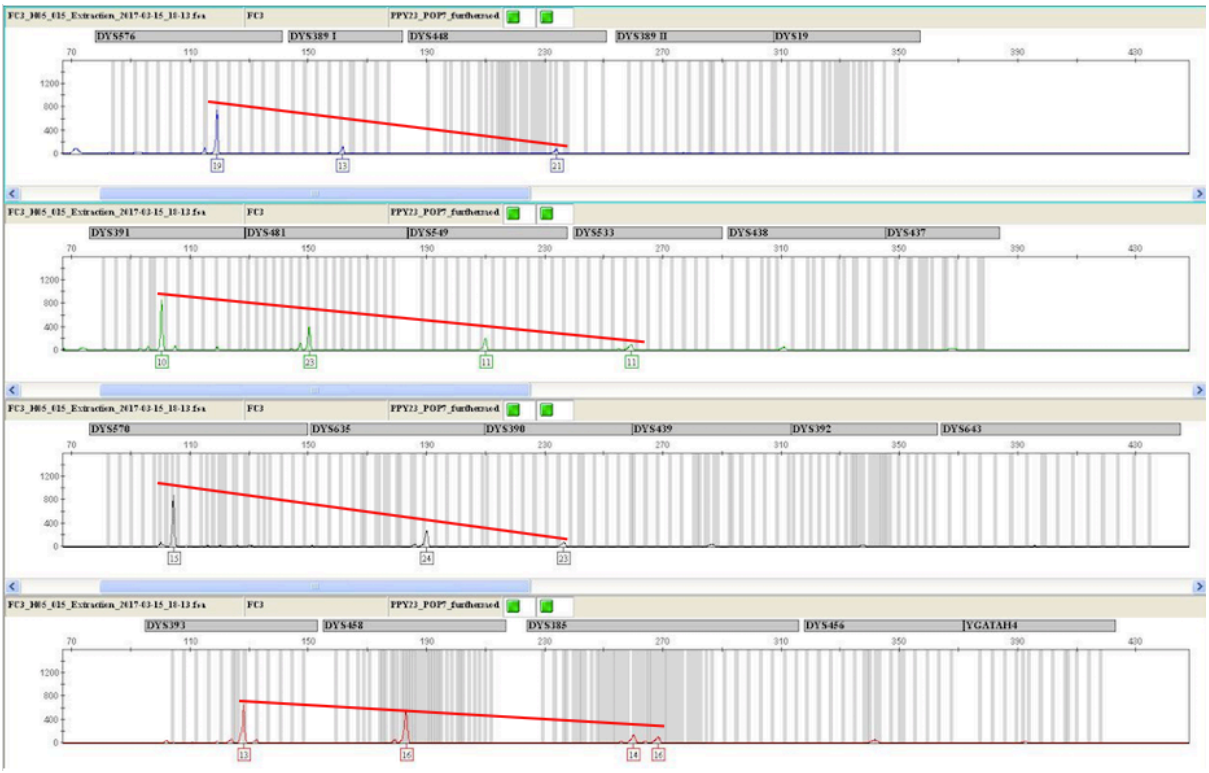

Figure 8.6 PowerPlex® Y23 Electropherogram for a blood stain that was exposed to a DBSP explosion.

Partial profile with a ski-slope pattern as the largest loci tend to drop out.

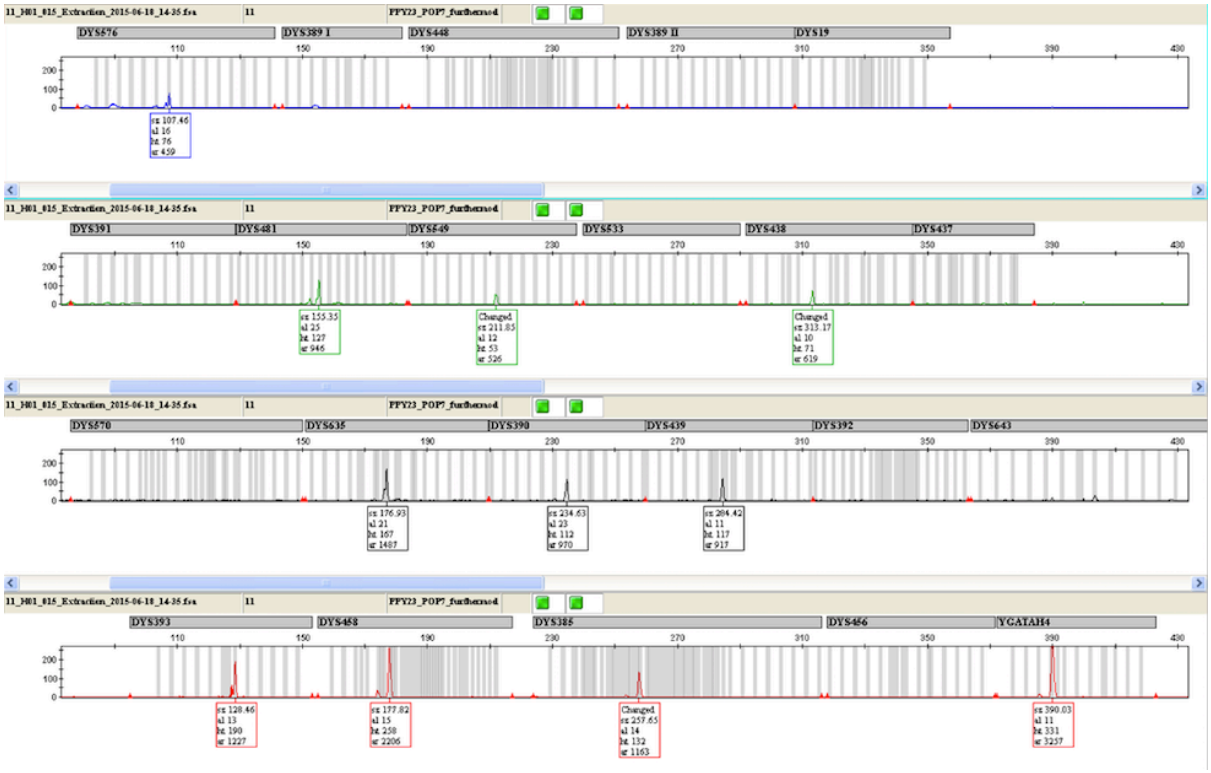

Figure 8.7 PowerPlex® Y23 Electropherogram for a touch DNA sample.

Partial profile with dropouts at random loci without a particular pattern.